Julius-Maximilians-Universität

Würzburg

New Avenues in the Reactivity of Borylene Complexes

Dissertation zur Erlangung des naturwissenschaftlichen Doktorgrades

Siyuan Liu

Würzburg 2019

New Avenues in the Reactivity of Borylene Complexes

Dissertation zur Erlangung des
naturwissenschaftlichen Doktorgrades der
Julius-Maximilians-Universität Würzburg

vorgelegt von
Siyuan Liu
aus Changchun, China

Würzburg 2019

Eingereicht bei der Fakultät für Chemie und Pharmazie am .....

Gutachter der schriftlichen Arbeit:

1. Gutachter: Prof. Dr. Holger Braunschweig
2. Gutachter: Prof. Dr. Maik Finze

Prüfer des öffentlichen Promotionskolloquiums:

1. Prüfer: Prof. Dr. Holger Braunschweig
2. Prüfer: Prof. Dr. Maik Finze
3. Prüfer: Prof. Dr. .....

Datum des öffentlichen Promotionskolloquiums: .....

Doktorurkunde ausgehändigt am: .....

Meiner Familie

„Was mich nicht umbringt, macht mich nur härter.“

Friedrich Nietzsche

Die Experimente zur vorliegenden Arbeit wurden in der Zeit von Oktober 2014 bis Jun 2019 am Institut für Anorganische Chemie der Julius-Maximilians-Universität Würzburg unter der Anleitung von Prof. Dr. Holger Braunschweig durchgeführt.

Die vorliegende Arbeit wurde auszugsweise veröffentlicht unter:

The First Boron-Tellurium Double Bond: Direct Insertion of Heavy Chalcogens into a Mn=B Double Bond

S. Liu, M.-A. Légaré, D. Auerhammer, A. Hofmann, H. Braunschweig*, Angew. Chem. Int. Ed.* **2017**, *56*, 15760–15763.

A Boradiselenirane and a Boraditellurirane: Isolable Heavy Analogs of Dioxiranes and Dithiiranes

S. Liu, M.-A. Légaré, A. Hofmann, H. Braunschweig, *J. Am. Chem. Soc.* **2018**, *140*, 11223–11226.

Synthesis of unsymmetrical B_2E_2 and B_2E_3 heterocycles by borylene insertion into boradichalcogeniranes

S. Liu, M.-A. Légaré, A. Hofmann, A. Rempel, S. Hagspiel, H. Braunschweig, *Chem. Sci.*, **2019**, *10*, 4662-4666.

Acknowledgements

First and foremost, my thanks to Professor Dr. Holger Braunschweig for the great opportunity that he provided me to pursue my dream of doing doctoral research here in Würzburg. Not only did he offer a perfect research environment but also helped me with patient discussions, great ideas and useful suggestions. During the past four years, he has been an incredible role model of a diligent and independent researcher.

I would like to give my thanks to China Scholarship Council (CSC) and the Chinese government for their kind and generous financial support of my studies in Germany. I also thank the staff members of CSC and the Generalkonsulat der Volksrepublik China in Frankfurt am Main who offered me a lot of help for applying for this scholarship and during my time in Germany.

My great thanks to three postdoctoral researchers (Prof. Dr. Rong Shang, Dr. Marc-André Légaré) who were of immense help regarding the research of my borylene project. The former, Dr. Rong Shang, also my old lab mate, introduced me to the project and taught me all necessary techniques with her years of experience. Dr. Marc-André Légaré helped me with all the manuscripts for publications and presentations with a lot of patience and provided me with some great ideas on my projects. Thanks to senior scientist Dr. Rian Dewhurst, who is always very kind and helpful, also helped me a lot with all my paperwork. Their help is one of the most important reasons that I was able to accomplish my research successfully. Furthermore, I would like to thank all the people who have contributed as coauthors on the publications reported in this thesis. In particular, discussions with Dr. Dominic Auerhammer have led to great ideas and to the discovery of new chemistry in the boron chalcogen project.

For technical help, I would like to thank all members of the Institut für Anorganische

Chemie, especially Dr. Rüdiger Bertermann and Marie-Luise Schäfer for their aid in NMR spectroscopy. I would also like to especially thank Dr. Krzysztof Radacki and Alexander Hofmann for their help in X-ray diffraction analysis. Moreover, I want to present my thanks to all the technicians (Kai Hammond, Sascha Stellwag-Konertz and Marcel Müller) in Braunschweig group for their hard and careful work during the time I spent in this group. I also warmly thank our administrative assistants (Birgit Zepke, Sabine Timmroth and Cornelia Walter). Lastly, I would like to thank the senior scientists (Drs. Justin Wolf and Carsten Kollann) for their useful suggestions during my studies.

To all my laboratory colleagues (Prof. Dr. Rong Shang, Dr. Johannes Brand, Dr. Jens Seufert, Stephan Hagspiel, Fabian Schorr and Alexander Okorn) who have worked in lab 209: thank you for the great time spent there. They shared their wonderful minds with me and made academic life a lot of fun. Even though I am a total stranger in this place, their warm and friendly manner enlightened every day I have spent here. To my computer room fellows (Dr. Alex Hofmann, Dr. Jonas Müssig and Carsten Lenczyk), thanks to you guys for offering a very relaxed environment for writing my thesis and help me a lot during this period of time.

To all my Chinese friends, I want to thank you graciously for making me feel like at home in this foreign country. I would like to thank Prof. Dr. Zhaojie Wang from China University of Petroleum, a former colleague and my best friend, who treated me as a real little brother and supported me with great care and patience. To Prof. Dr. Xiaoning Guo, Prof. Dr. Rong Shang, Prof. Dr. Qing Ye, Dr. Liang Zhou, Dr. Mo Zhu, Ruiqi Liu, Kun Peng, Xiaocui Liu, and Shitong Du, I want to thank you for inviting me home from time to time for dinner especially during traditional Chinese holidays. To Dr. Dongren Wang, a senior researcher at Stuttgart University, thank you for giving me much useful advice on doing good research. I want to thank all the members (past and present) of the Würzburg Chinese Soccer team for bringing so much joy and playing together every week. All of you are like my family and provide me great

strength to move on from any difficulty and loneliness.

Finally, I would like to take some time to thank the members of my family, as they were and will always be the greatest source of power in my life. To my mom (Mingzhi Chen), the most outstanding and toughest woman in the world, no words can be used to express my thanks to you for the support you have given me through the years I have been abroad. To my uncle and aunt (Dejiu Xin and Li Liu), I want to thank you for your care and support over the past four years.

Abbreviations

2c–2e	two-center-two-electron
atm	atmosphere (pressure)
Ar	aryl
Ar^f_4	3,5-bis(trifluromethyl)phenyl
BCat	catecholatoboryl-, (1,3,2-benzodioxaborol-3-yl)
bipy	bipyridyl
Br-bipy	5,5’-dibromo-2,2’-bipyridyl
bs	broad singlet
Bu	butyl
cAAC	1-(2,6-di*i*sopropylphenyl)-3,3,5,5-tetramethyl pyrrolidine-2-ylidene
COD	1,5-cyclooctadiene
COF	covalent organic framework
Cp	cyclopentadienyl
Cp*	pentamethylcyclopentadienyl
Cy	cyclohexyl
δ	chemical shift
d	doublet
h, min	hour, minute
DCC	*N*,*N*'-dicyclohexylcarbodiimide
DFT	density functional theory
Dipp	2,6-di*i*sopropylphenyl
Dur	2,3,5,6-tetramethylphenyl
equiv.	molar equivalents
Et	ethyl
Fc	ferrocenyl
$h\upsilon$	photolysis
HOMO	highest occupied molecular orbital
HRMS	high-resolution mass spectrometry

IMe	*N*,*N*′-dimethylimidazol-2-ylidene
*i*Pr	isopropyl
IR	infrared
J	coupling constant
L	ligand
LUMO	lowest unoccupied molecular orbital
m	multiplet
M	metal
Me	methyl
Mes	2,4,6-trimethylphenyl
Mes*	supermesityl
mt	2-sulfanyl-1-methylimidazolyl
NBO	natural bond order
NHC	N-heterocyclic carbene
NICS	nucleus-independent chemical shift
NMR	nuclear magnetic resonance
Ph	phenyl
pip	piperidine
RT	room temperature
s	singlet
t	triplet
*t*Bu	*tert*-butyl
Tbt	2,4,6-tris[bis(trimethylsilyl)methyl]phenyl
THF	tetrahydrofuran
UV-vis	ultraviolet-visible spectroscopy
WBI	Wiberg bond index

Table of Contents

1. Introduction

1.1 General overview of transition-metal complexes of boron

The second half of the 20th century saw a rapidly growing interest in the isolation of transition metal complexes of boron. Starting in the early 1960s, important milestones were reached in terms of the synthesis of species that possess M-B interactions.[1] The very first compound proposed to be a M-B-bonded compound was reported in 1963 and was later classified as a metal boryl complex.[2] Since then, several examples containing different transition metals and bonding motifs with boron have been identified. It was not until 1990, however, that the structural characterization of M-B bonds was achieved, by the groups of Marder[3] and Merola,[4] who were studying iridium-boron complexes (**Figure 1**). During the same period, the importance of transition metal complexes of boron in organic synthesis became increasingly prominent, with the discovery of reactions such as the borylation of C-H bonds and the Suzuki-Miyaura cross coupling.[5-7] For this reason, a growing interest has been focused on boron complexes of transition metals, and their unique properties have been extensively studied by chemists all over the world. The main applications of such organometallic species are in the field of catalysis, such as transition-metal-catalyzed hydroboration, C-H bond activation reactions, C-X (X= F, Cl, Br, and I) bond activations, and others.[8-22] Additionally, applications in sensor devices or optoelectronics have also been proposed.[23-25]

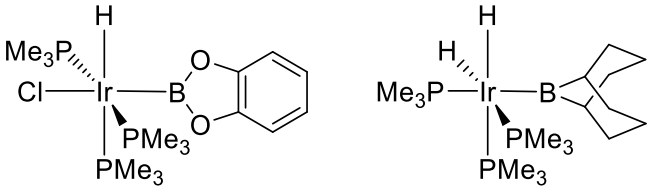

1 **2**

Figure 1. The first fully characterized transition metal complexes featuring a M-B bond, as reported by the groups of Marder and Merola in 1990.

With the development of this branch of chemistry, transition metal complexes of boron are classified in most research reports into the following categories according to the type and number of metal-boron bonds and the coordination number of the boron atom: borane (**I**), boryl (**II**) and bridging (**III**) and terminal (**IV**) borylene complexes (**Figure 2**). Additionally, due to the high Lewis acidity of the boron center, there also exists Lewis-base-stabilized derivatives of these classes of compounds (**IIa, IIIa, IVa**) (**Figure 2**).[26]

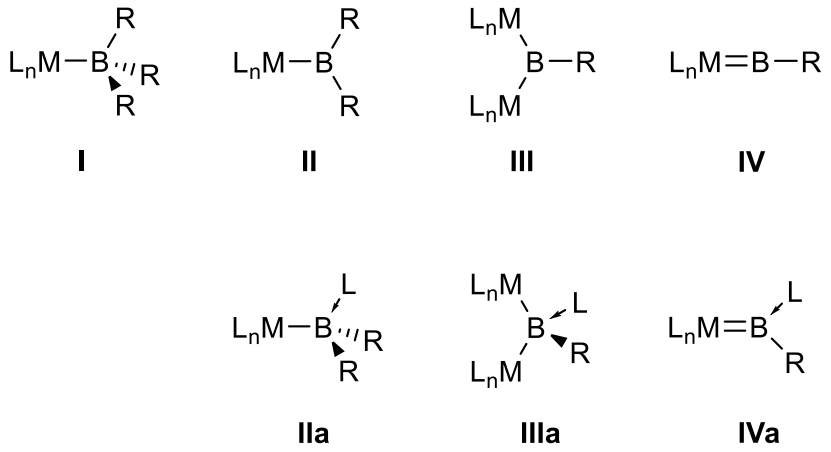

Figure 2. Classification of transition metal-boron complexes according to the number of metal-boron bonds and the coordination number of the boron atom.

The different bonding situation of these complexes reveals a vastly different role of the transition metal center in the interaction. In the case of borane complexes, for example, the metal center behaves as a Lewis base, forming a dative interaction to the borane.[27-28] In this type of coordination mode, the boron-containing moiety is a typical Z-type ligand, with both bonding electrons being provided by the metal. Interestingly, this kind of M-B interaction has only been observed in the case of boron-containing polydentate ligands such as boratranes, and the characterization of an untethered metal borane complex remains elusive.[29] Boryl complexes possess a tricoordinate boron center which features a covalent σ bond with the transition metal and are described as X-type ligands.[30-31] Finally, the metal-boron bond of transition metal borylene complexes is generally recognized to be formed by the two electrons

of the singlet borylene ligand (:BR) donating into the d_z^2 orbital of transition metal together with π backdonation from the d_{xz} and d_{yz} orbital of the transition metal into the two p orbitals of boron.[32-36] The properties of borylene ligands have been studied through computational calculations and reveal a similar bonding pattern and coordination mode to their isoelectronic analogues CO and N_2. Moreover, the existence of base-stabilized transition metal boron complexes shows that the boron atoms in many of these complexes are still Lewis acidic and can be attacked by Lewis bases.[37-46]

1.2 Borane complexes

In 1963, the first transition metal borane complex was proposed by Shriver.[47-48] In his investigation, he reported a reaction between $[Cp_2WH_2]$ and BF_3, which led to the formation of the first borane complex $[Cp_2WH_2(BF_3)]$. However, the assignment of a direct M-BF_3 interaction was later disproved on the basis of single-crystal X-ray diffraction analysis and NMR spectroscopy. Indeed, instead of the metal borane structure proposed by Shriver, the ionic complex $[Cp_2WH_3][BF_4]$ was structurally characterized. A similar reaction was also carried out with *t*$BuBCl_2$ and resulted in the formation of the zwitterionic complex $[\{\eta^5\text{-}C_5H_4(t\text{BuBCl}_2)\}CpWH_3]$ (**Figure 3**).[49-51]

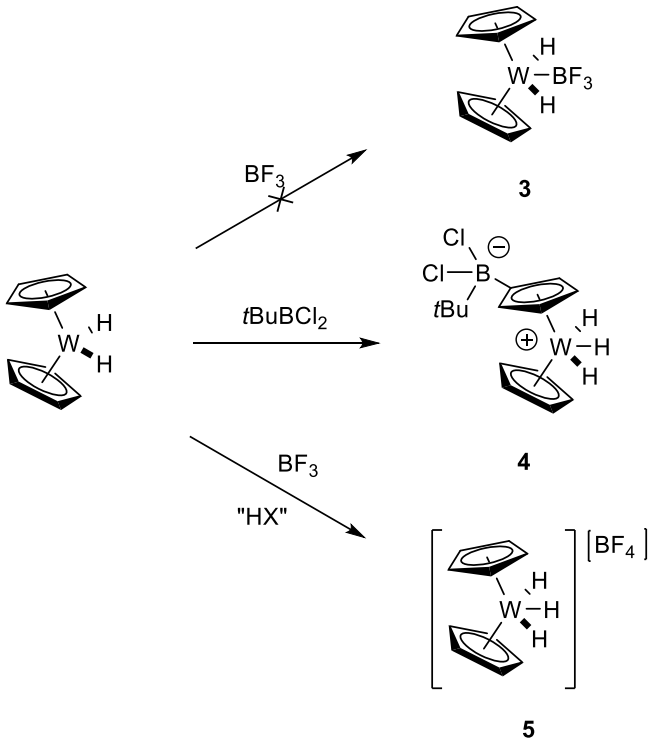

Figure 3. Shriver's proposed borane complex and the actual products: ionic complex $[Cp_2WH_3][BF_4]$ and $[\{\eta^5\text{-}C_5H_4(t\text{BuBCl}_2)\}CpWH_3]$.

Since Shriver's first proposal, several metal borane complexes, such as $Na[H_3BRe(CO)_4]$, $Na[H_3BMn(CO)_3PPh_3]$, $Na[H_3BCo(CO)_4]$,[52] $[(Me_2PC_2Me_2BMe_2)_2Rh(CO)Cl]$ and $[X_3BRh(PPh_3)_2(CO)X]$ (X=Cl, Br),[53] have been proposed. However, no conclusive proof of a direct metal-borane interaction has been

presented. In 1999, however, the first structural evidence of a metal boratrane complex, [(Ph$_3$P)Ru(CO){B(mt)$_3$}] (mt = 2-sulfanyl-1-methylimidazole) (**6**), containing a metal-to-boron dative bond was provided by Hill and coworkers (**Figure 4**).[54] The solid state structure of **6** showed a tetrahedrally coordinated boron and octahedral ruthenium atom connected through a relatively short B-Ru distance (2.16 Å), which confirmed the rather strong B-Ru interaction. After several years, an analogous complex of osmium was synthesized.[28, 55-56]

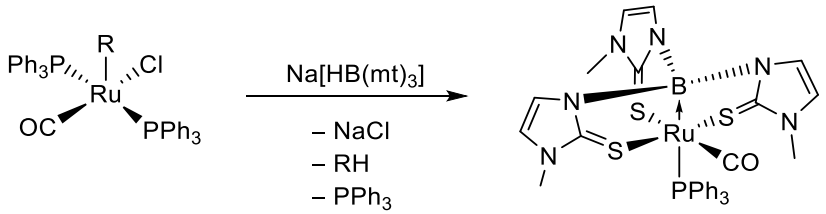

6

mt = 2-sulfanyl-1-methylimidazole

Figure 4. The first structural evidence of a transition metal borane complex [(Ph$_3$P)Ru(CO){B(mt)$_3$}] reported by Hill and coworkers.

During the past 20 years, a growing number of transition metal borane complexes have been synthesized thanks to the development of novel chelating ligands such as the tris(mercaptoimidazolyl)borate (Tm^R) and bis(mercaptoimidazolyl)borate (Bm^R).[57] The family of transition metal borane complexes has since been broadened to many other transition metals including Group 9 (Co,[58] Rh,[59] Ir[60]), Group 10 (Ni, Pd, Pt)[57] and Group 11 (Cu, Ag, Au)[57]. One of the most prominent reports in this field was disclosed in 2008, and contained a rigorous evaluation of the coordinative properties of these ligands, allowing a comparison between six different transition metals from group 10 and group 11.[57] This report further confirmed the ability of boron to act as a σ acceptor ligand towards transition metals.

1.3 Boryl complexes

Among all transition metal-boron compounds, boryl complexes are the most common. The metal-boron bond in boryl complexes is a typical two-center-two-electron (2c2e) covalent bond. The tricoordinate boron atom of the boryl moiety acts as an X-type ligand towards the metal center. As mentioned above, the first two fully characterized boryl complexes (**1**, **2**) were synthesized in 1990 (**Figure 1**). In early investigations, the boron atom of most boryl complexes usually was bound to a substituent bearing a lone electron pair that was able to stabilize the empty p_z orbital at boron. It is also believed that the metal center of a boryl complex can provide a degree of π-backdonation into the vacant p_z orbital. This feature of boryl complexes has recently been experimentally confirmed by addition of 4-methylpyridine to $[(Cp)Fe(CO)_2BCl_2]$, which leads to the elongation of the B-Fe bond upon coordination of the boron atom (1.94 Å to 2.13 Å) (**Figure 5**).[61-62] This study also noted that the base-stabilized compound **8** showed carbonyl stretching bands at lower frequencies (1976, 1916 cm^{-1}) than those of compound **7**, further evidence of a decreased Fe-B π interaction.

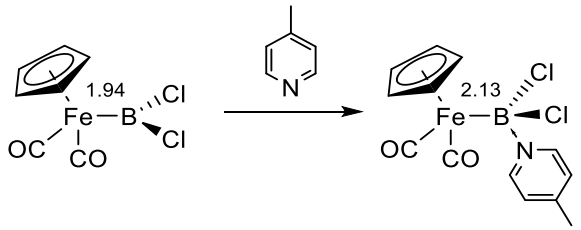

7 **8**

Figure 5. Experimental evidence of iron-boron π-backdonation from the elongation of the Fe-B bond (1.94 Å to 2.13 Å) upon coordination of **7** by a Lewis base to give **8**.

The main method for the synthesis of transition metal boryl compounds is through oxidative addition of B-B,[63-65] B-H[64-66] or B-E (E = other main group elements such as Sn[67] or Cl[68]) bonds to low-valent transition metal complexes, and a great number of boryl complexes have been synthesized in this way (**Figure 6**). Another important

method to obtain boryl complexes is through salt elimination, which normally takes place between an anionic transition metal complex and a suitable boron halide.

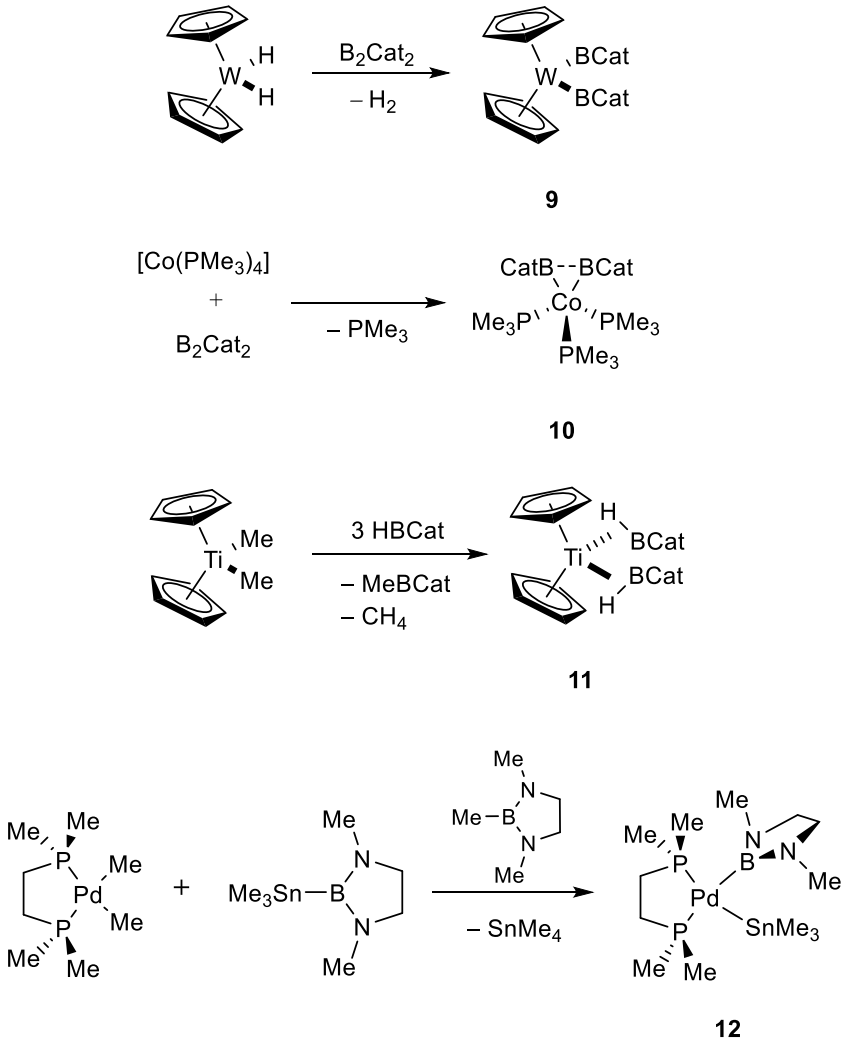

Figure 6. Synthesis of boryl compounds by oxidative addition.

In addition, Yamashita, Nozaki and coworkers successfully synthesized boryllithium and borylmagnesium species.[69-71] By using these species as precursors, transition metal boryl complexes can be prepared by nucleophilic substitution to metal centers. Since then, the first boryl complexes of group 11 (Cu, Ag, Au) and group 4 (Ti, Hf) metals have been successfully synthesized (**Figure 7**).[72-74]

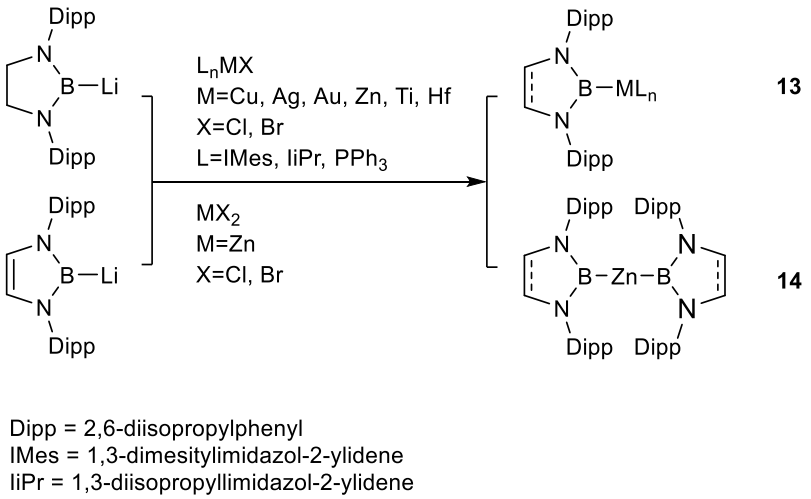

Dipp = 2,6-diisopropylphenyl
IMes = 1,3-dimesitylimidazol-2-ylidene
IiPr = 1,3-diisopropyllimidazol-2-ylidene

Figure 7. Synthesis of boryl complexes by nucleophilic attack towards the metal centers using boryllithium species.

Most recently, the group of Braunschweig reported the synthesis of a series of platinum boryl complexes by oxidative addition of haloboranes to Pt(0) complexes (**Figure 8**).[75-79] With spontaneous halosilane elimination, linear Pt-B-E (E = O, NR, CR_2)-containing complexes featuring B-E multiple bonding character were synthesized. Among them, $[(Me_3P)_2BrPt(BO)]$ (**15**) is the first compound reported to contain a B≡O triple bond.[79] Compared to the complexes containing B=O double bonds, which normally undergo oligomerization, **15** shows remarkable stability. A solution of **15** could be kept at room temperature for 24 h and showed no sign of oligomerization or decomposition.

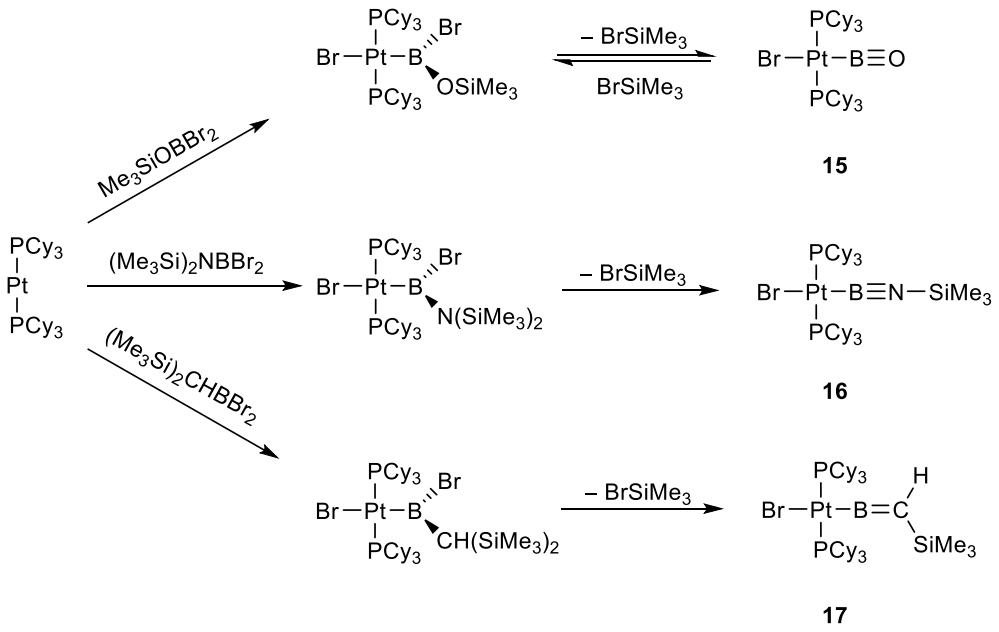

Figure 8. Synthesis of a series of platinum boryl complexes by oxidative addition of haloboranes to [Pt(PCy_3)$_2$].

Among the transition metal complexes of boron, metal boryl complexes have the most well-developed applications. Indeed, they are regarded as the key reagents in catalytic reactions such as diboration, C-H and C-F bond activation.[15-18, 80-81] From this point of view, these compounds provide great possibilities and convenience in the field of organic synthesis.

1.4 Borylene complexes

Subvalent main group complexes have attracted much attention for several decades, in particular the family of hypovalent carbon compounds known as carbenes. The importance of their applications in many aspects of modern chemistry is difficult to overstate.[82] The boron analogue of this class of species, borylene ligands, was first discovered in 1967,[83] and monovalent borylenes of the form [:B-R] featuring boron in its +1 oxidation state have been investigated computationally.[37-45] Similar to carbenes, free borylenes are very reactive species that bear a lone electron pair.[84] In contrast to carbenes, borylenes have only one substituent and two empty p orbitals (LUMO, LUMO+1) while the non-bonding lone electron pair (HOMO) is located at an sp-hybridized boron center. Compared to the parent BH molecule, the HOMO energy of borylenes tends to decrease when electron-withdrawing R groups such as F, Cl, and CF_3 are substituted, and the energy of the LUMO increases with electron-donating substituents. On the other hand, carbenes have a singlet or triplet ground state depending on their substitution pattern, while theoretical studies show that borylenes have a singlet ground state. According to a recent investigation of Bettinger and coworkers,[85-86] the smallest singlet-triplet gap was calculated for :$BSiMe_3$ (8.2 Kcal/mol) and the largest one was for :BF (78.7 Kcal/mol).

In contrast to carbenes, free monovalent borylenes [:BR] have thus far never been isolated due to their highly reactive character. Even though they can be spectroscopically observed through matrix isolation experiments, examples remain scarce. Only a few examples, such as BH and BX (X = F, Cl, Br or I), have been observed by microwave spectroscopy,[83, 87-88] while other examples[89-91] (aminoboylene, ethynylborylene, and phenylborylene) have been observed by infrared spectroscopy in inert gas matrices. On the other hand, the indirect proof of the formation of borylene has been provided through chemical trapping experiments.[92-95] Although free borylenes have never been isolated, borylenes coordinated by one[96-97] or two Lewis bases[98-103] have been successfully synthesized in recent years. On the

other hand, transition metal borylene complexes in which the borylene ligand binds to the metal in a terminal or bridging bonding mode have been well investigated in recent years.[56, 104-109]

The properties of borylenes as ligands for transition metals have been investigated by theoretical studies.[36-45] These studies showed that the bonding properties of the borylene ligand B-F are closely related to those of the isoelectronic ligands N_2 and CO, and the comparison was also expanded to BNH_2 and BO^-. All these A-E type ligands have a σ-symmetry HOMO with a sp lobe occupied by a lone electron pair and two degenerate π* LUMOs except for BNH_2. The HOMOs of these ligands can participate in metal-ligand bonding through σ-electron donation to the empty d_{z^2} orbital of the metal. On the other hand, the two π* LUMOs can accept π backdonation from the d_{xz} and d_{yz} hybrid orbitals of the metal center (**Figure 9**). Calculations[38] show that the HOMO energies of these ligands increase in the order of N_2<CO<BF<BNH_2<BO^-, indicating that the latter have a stronger σ donating ability. On the other hand, the LUMO energies decrease from N_2 to BF. For BNH_2, the $2b_1$ LUMO has a slightly higher energy than the $2b_2$ LUMO (**Figure 9**) because the latter is stabilized through a bonding interaction with combination of the two hydrogen 1s atom orbitals. **Figure 9** shows a large increase of the LUMO energy from BNH_2 to BO^- owing to the negative charge, thus making BO^- a poor π acceptor. Despite the BO^- example, borylene ligands are, in general, very good σ donors and relatively good π acceptors. In agreement with this, computational studies have provided theoretical evidence that upon bonding to a metal (M=B-R),[41, 110-111] the boron atom in the borylene ligand becomes positively charged and the σ-bonding is slightly polarized towards boron while the π-bonding is highly polarized towards the metal center. This polarization, together with the low coordination number at boron, leads to an observed trend of nucleophilic attack at the boron center and thus to kinetic instability. This can be prevented by steric protection using bulky substitution or electronic stabilization.[104-106, 112] Overall, the nature of different borylene ligands give these transition-metal borylene complexes a handful of interesting reactivity

patterns that have been investigated over the past 30 years.

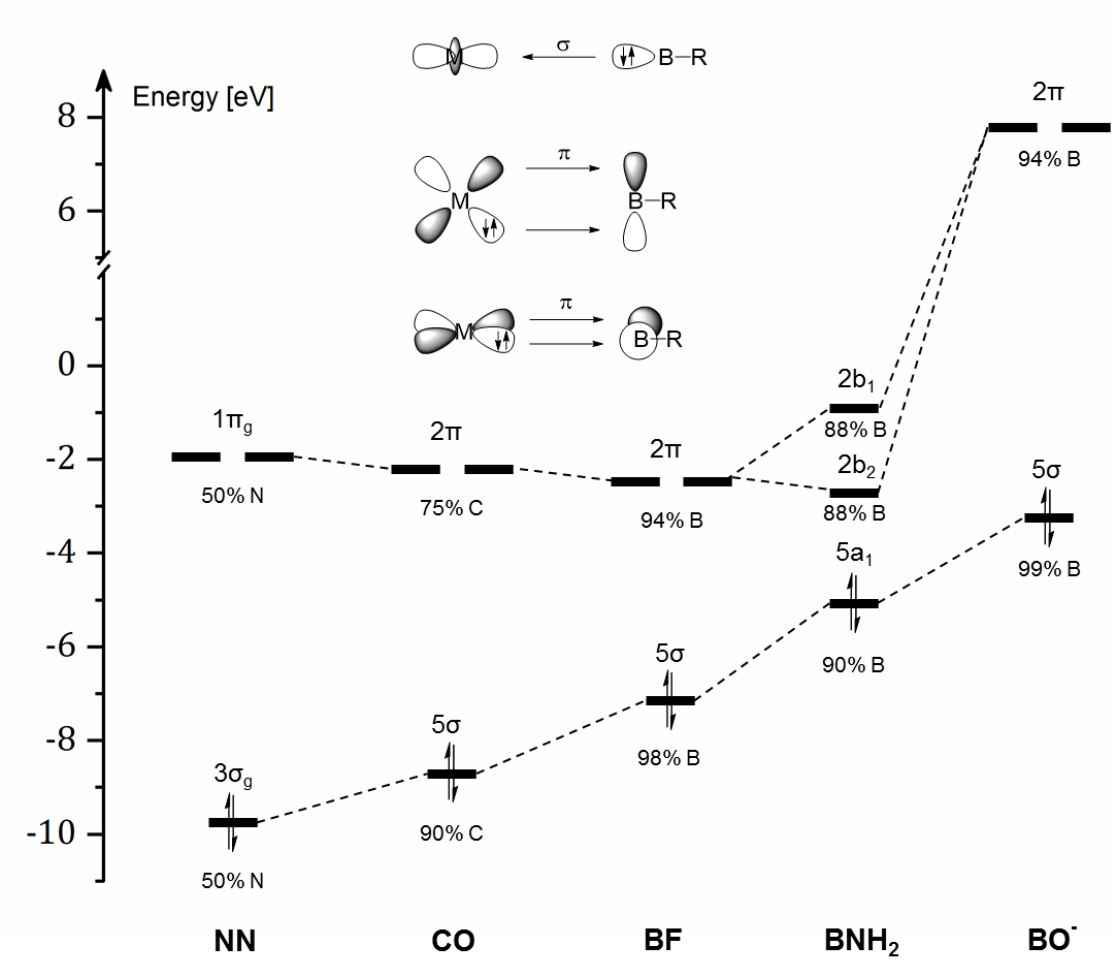

Figure 9. Valence orbital energies (eV) of the AE systems N_2, CO, BF, BNH_2 and BO^- and localization of the MOs on the electropositive atom (%).[39]

1.4.1 Synthetic routes to transition metal borylene complexes

Transition metal borylene complexes can be divided to two categories: bridging and terminal. The former bear a boron moiety connected to two or more metal centers, while the latter has only one metal center bound to the boron moiety with a metal boron double bond arising from M-to-B backbonding (**Figure 2**). Salt elimination is the most commonly used method to synthesize transition metal borylenes. The first stable bridging borylene complex was reported by Braunschweig and coworkers in

1995 through a salt elimination reaction between a cationic manganese compound [K_2{(Cp)Mn(CO)$_2$(SiPh$_2$Me)}] and [$B_2(NMe_2)_2Cl_2$] (**Figure 10**).[107] The solid state structure showed that the borylene moiety was connected to two manganese centers and the ^{11}B NMR spectrum showed a peak at δ_B = 103 (**Figure 10**). In 1998, the first terminal borylene complex was made by Cowley and coworkers[108] from the salt elimination between $K_2[Fe(CO)_4]$ and the dichloroborane Cl_2BCp^* (**Figure 10**). In this study, the :BCp* ligand is bound to the 16-electron $Fe(CO)_4$ fragment in a terminal fashion, which is analogous to that of a BF ligand.[109] In this case the compound can be described as an iron borylene species. However, the structural analysis showed a rather long Fe-B bond length (2.101(3) Å) falling between those of reported iron-boryl complexes (1.959(6) Å – 2.028(7) Å), and thus corresponding to a B-Fe single bond. On the other hand, computational calculations indicated that no π backbonding was found between iron and boron. Therefore, the author referred to this as a Cp*B→$Fe(OC)_4$ bonding mode. In 1998, Braunschweig and coworkers reported terminal borylene complexes of group 6 transition metals by salt elimination reactions between $Na_2[M(OC)_5]$ and [$Cl_2BN(SiMe_3)_2$] (**Figure 10**).[106] Most recently, Figueroa and coworkers reported the synthesis of the first transition metal borylene featuring a terminal BF ligand.[109]

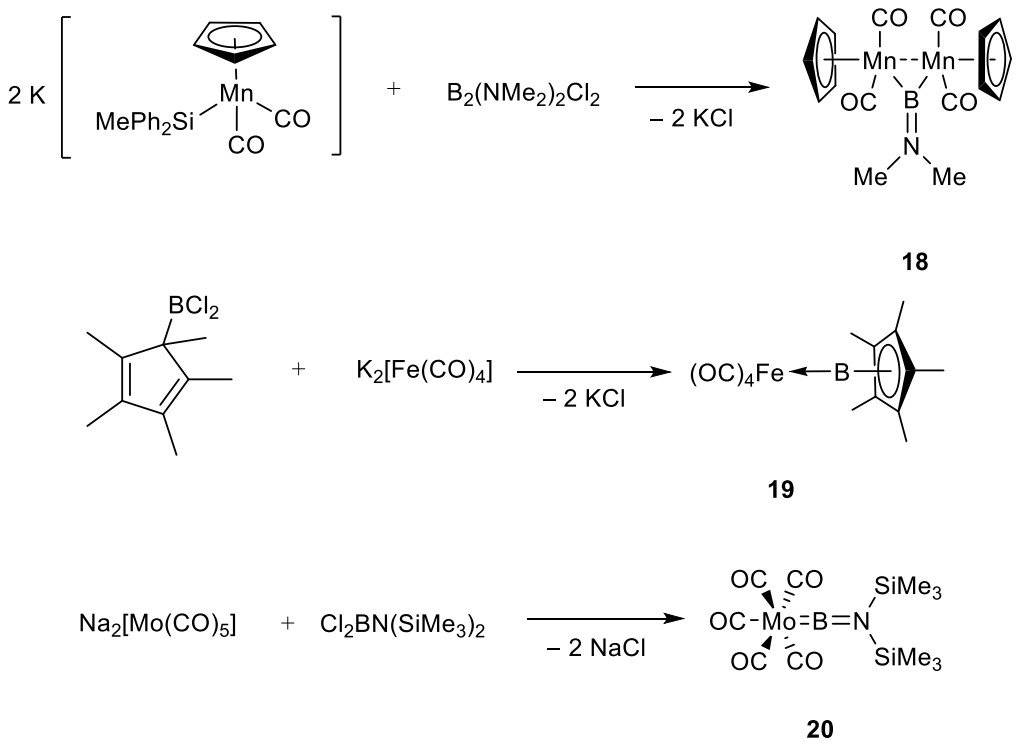

Figure 10. Synthesis of transition metal borylene complexes through salt elimination reactions.

The same strategy was also used to synthesize other terminal borylenes such as the "hypersilyl" (-Si(SiMe$_3$)$_3$)-substituted borylene **21**,[104] terphenylborylene **22**,[105, 113] and iron borylene **23**.[112] These compounds exhibit low-field shifted ^{11}B NMR resonances (**21**: δ_B = 204, **22**: δ_B = 150, **23**: δ_B = 144) compared to the aminoborylene complex **20** (δ = 90). More interestingly, a recent work from the group of Braunschweig showed the synthesis of the first examples of imidazol-2-ylidene-stabilized aminoborylenes acting as ligands to transition metals via salt elimination reaction.[114] These species showed unique robustness and the boron-metal interaction is a purely B→M σ-donation according to a theoretical study. The result revealed an interesting bonding situation of a borylene ligand towards transition metals.

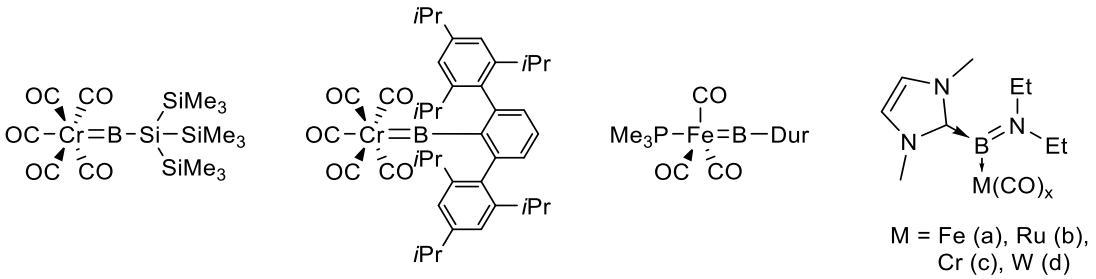

Figure 11. Structures of terminal borylene complexes **21**, **22**, **23, 24a-d**.

Another important method to synthesize transition metal borylene complexes is by borylene transfer from isolated borylene complexes to transition metal carbonyl complexes. Most of these syntheses are carried out with group 6 transition metal borylene complexes under photolytic or thermal conditions. In this way, a series of novel borylene compounds featuring group 5,[115] group 7[116] and group 9[117-119] transition metals were prepared **(Figure 12**).

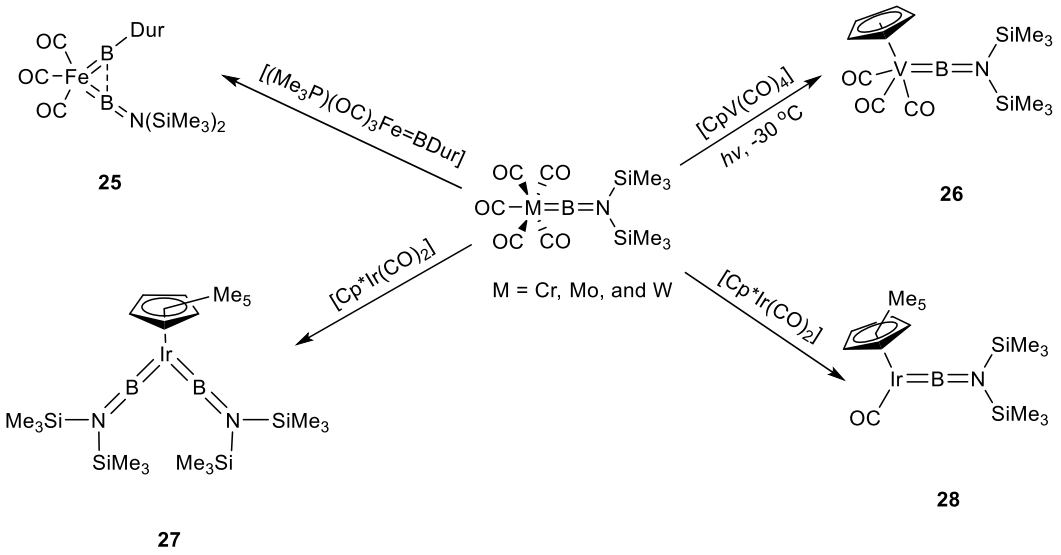

Figure 12. Synthesis of second generation borylene complexes by borylene transfer from group 6 borylene complexes $[(OC)_5M{=}BN(SiMe_3)_2]$.

Moreover, the first heterobimetallic bridging borylene complex was also formed in this way (**Figure 13**). Interestingly, this complex gradually loses the $[W(CO)_5]$ moiety and provides a terminal borylene complex of cobalt, which then slowly undergoes a

self-borylene-transfer reaction, forming a homodinuclear bridging borylene (**Figure 13**). Moreover, this borylene transfer strategy also provides a route to synthesize the first bis-borylene complexes containing two identical ([(Cp*)Ir{BN(SiMe$_3$)$_2$}$_2$])[120] or two different ([(OC)$_3$Fe{BN(SiMe$_3$)$_2$}{BDur}]) borylene moieties (**Figure 12**).[121]

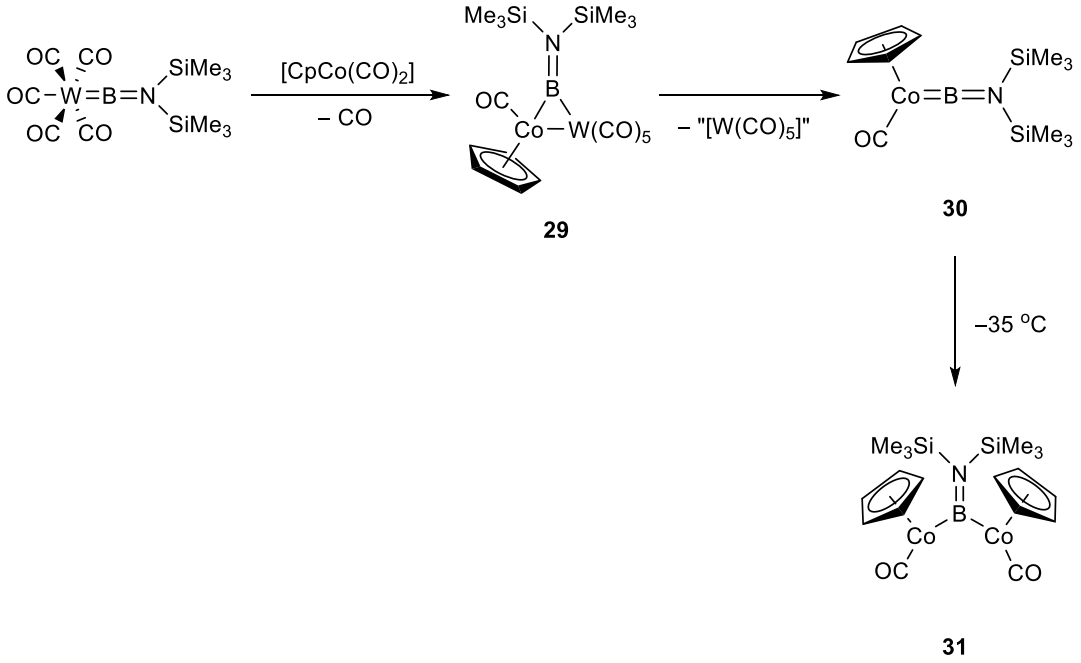

Figure 13. The synthesis of the first heterodinuclear bridging borylene containing cobalt and tungsten.

There are also a few examples of cationic borylene complexes synthesized by halide abstraction from boryl complexes with Na[BAr$^f_4$]. In 2003, Aldridge and coworkers reported the preparation of the first cationic borylene complex [{(Cp*)Fe(CO)$_2$}(BMes)][BAr$^f_4$] (**Figure 14**) by abstraction of the chloride from the boron atom of [{(Cp*)Fe(CO)$_2$}{B(Mes)Cl}].[122] Following this report, other examples of cationic borylene complexes containing group 8 transition metals were prepared using the same method.[123-125]

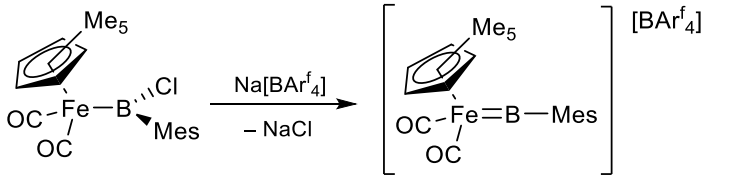

Ar^f = 3,5-bis(trifluromethyl)phenyl

32

Figure 14. Synthesis of the first cationic borylene complex [{(Cp*)Fe(CO)$_2$}(BMes)][BAr^f_4] (**32**) by halide abstraction reported by Aldridge and coworkers in 2003.

Shortly afterwards, Braunschweig and coworkers successfully managed the synthesis of cationic borylene complexes of a group 10 metal (platinum) using a similar strategy. However, in this case, the presence of halide substituents on both the platinum center and the boryl ligand in the precursor led to diverging reaction pathways for the halide abstraction. Indeed, competition between the abstraction of a halide from boron or platinum can take place in these systems. In most cases, a halide could be first abstracted from the platinum center, resulting in a T-shaped cationic boryl intermediate, one example of which was successfully isolated and characterized.[126] In this case, subsequent addition of a Lewis base could force the boron-bound halide to migrate to the metal center, providing base-stabilized borylene complexes (**Figure 15**).[78, 126-127] Alternatively, in the case of a bulky substituent (Mes) on boron, halide abstraction spontaneously occurs at boron, leading to a cationic terminal borylene complex (**Figure 15** (bottom)).[128]

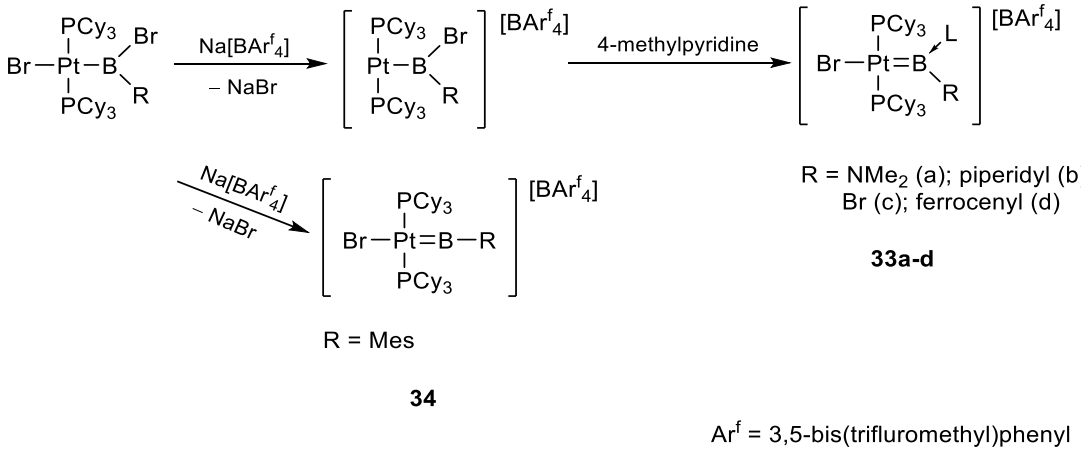

Figure 15. Synthesis of platinum borylene complexes by halide abstraction as reported by Braunschweig and coworkers.

In addition to the aforementioned methods for the synthesis of borylene complexes, a unique case of borylene preparation through hydrogen elimination was reported by Sabo-Etienne and coworkers in 2008.[129] In this case a ruthenium dihydride complex reacts with a dihydroborane to afford a ruthenium borylene complex under vacuum and the dihydrogen release can be reversed under an atmosphere of H_2 (**Figure 16**). The ^{11}B NMR spectrum of **35** revealed a broad signal at δ_B = 106, which indicated the presence of a borylene species and the solid state structure of the product showed a very short Ru-B distance (1.780(4) Å), confirming the double bond character of the Ru-B interaction. Furthermore, computational studies indicated that the Ru-B bond order is 1.49, which further suggested the Ru=B double bond nature of this compound.

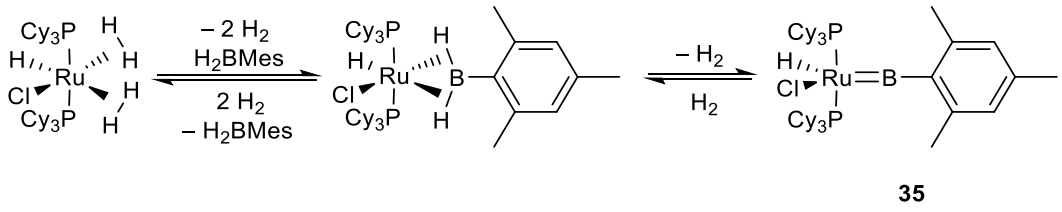

Figure 16. Synthesis of a ruthenium borylene by hydrogen elimination by Sabo-Etienne and coworkers.

1.4.2 Reactivity of transition metal borylene complexes

1. Borylene transfer to organic substrates

As described above, a borylene moiety can be transferred from a transition metal complex to another to form second generation borylenes. Alternatively, transition metal borylene complexes can transfer their borylene ligands to organic substrates such as alkynes, in this case leading to borirenes.[23, 25, 130-134] These species are of great interest to organic chemists as they are the smallest neutral aromatic systems containing 2π-aromatic electrons.[135] Even though several synthetic entries into these molecules have been reported since 1968, most of them were carried out in extreme conditions and each route were severely limited in scope.[136-139] In the case of borylene transfer from Group 6 complexes, however, the synthesis of borirenes proved to be a general method to obtain these interesting compounds (**Figure 17**). Furthermore, the reactions were carried out under mild conditions such as photolysis or at relatively low temperatures.[23, 25, 130-134]

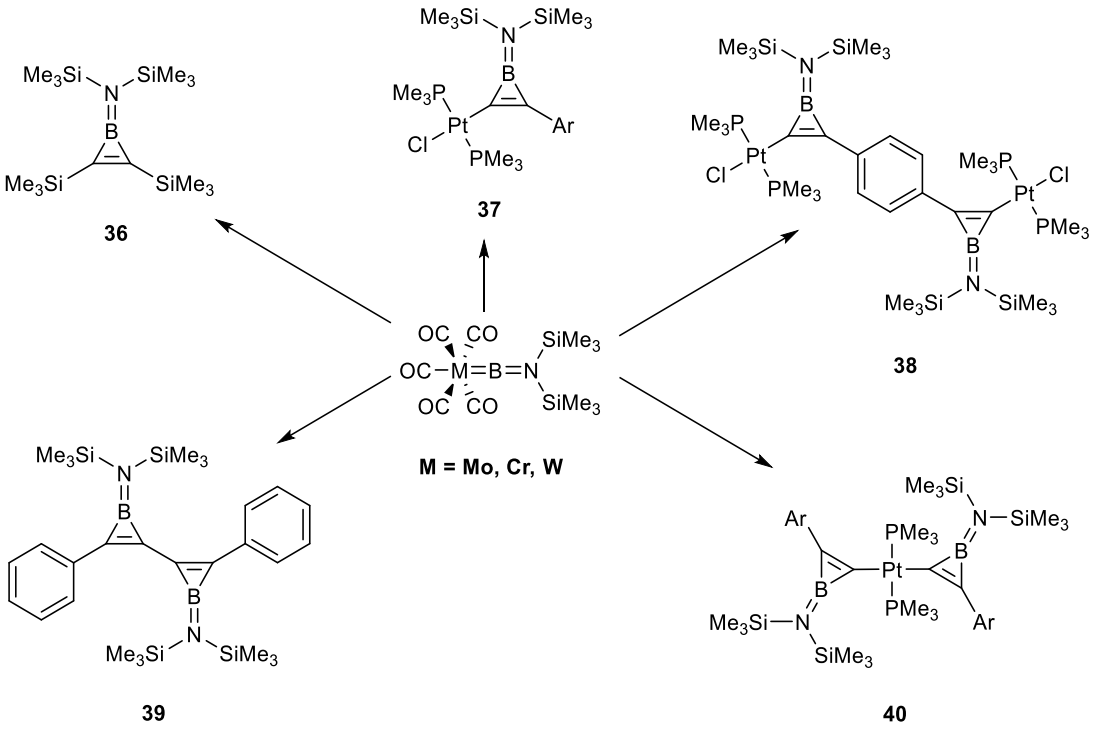

Figure 17. Synthesis of borirenes by borylene transfer from transition metal complexes.

2. Metathesis reactions

It has been revealed by computational studies that borylene ligands on transition metals have strong σ donor and comparable π acceptor abilities compared to their isoelectronic ligands such as CO or N_2 (**Figure 9**). Several contributions have demonstrated that that these complexes have reactivity that mirrors that of carbene complexes, including the fact that they can undergo metathesis reactions.[140-142]

Some borylene complexes were found to readily react with organic molecules that contain unsaturated polar bonds through metathesis reactions. In 2005, Aldridge and coworkers reported the reaction of the cationic borylene complex $[(Cp)Fe(CO)_2(BNiPr_2)]^+(BAr^f_4)^-$ with $Ph_3P{=}S$ (**41**) and $Ph_3As{=}O$ (**42**).[124] The reactions occur through a two-step process in which the chalcogen atoms are first coordinated to boron center and subsequently metathesized, resulting in the formation of an iron phosphine complex and boron-chalcogen heterocycles.(**Figure 18**)

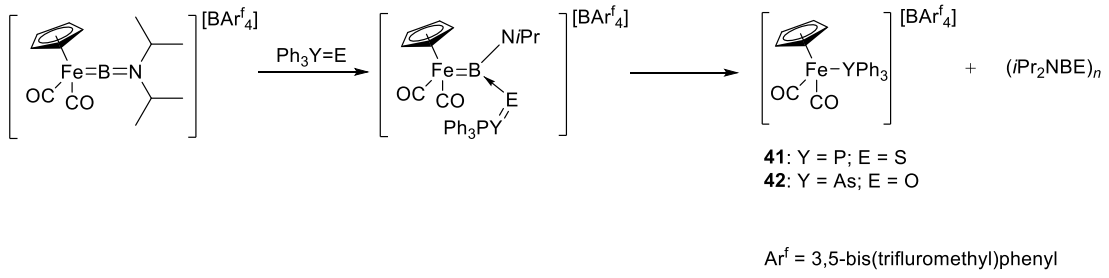

Figure 18. Metathesis reactivity of cationic borylene complex $[(Cp)Fe(CO)_2(BN{\it i}Pr_2)]^+(BAr^f_4)^-$ with $Ph_3P{=}S$ (**41**) and $Ph_3As{=}O$ (**42**).

Soon after this work, Braunschweig et al. reported metathesis reactions of a manganese borylene complex, $[(Cp)(OC)_2Mn{=}B{\it t}Bu]$ with various ketones and N,N'-dicyclohexylcarbodiimide (DCC). The process is postulated to occur through a [2+2] cycloaddition mechanism.[141] Contrary to the work of Aldridge, no E-B (E = O or N) coordination intermediates could be observed in this instance. Instead, the reaction led directly to the isolation of products that feature a Mn-B-X-C (X = O, NR)

four-membered ring (**Figure 19**). Furthermore, the formation of a Fischer-type carbene complex of manganese was proposed as an end product on the basis of NMR spectroscopy. Several years later, the reaction pattern was extended to other ketones and transition metal borylenes.[114] In the meantime, the same group was able to fully characterize the Fisher-type carbene products by single-crystal X-ray diffraction analysis and yielded a variety of interesting transition metal carbene complexes, including the first adamantylidene complex (**Figure 19**).[140]

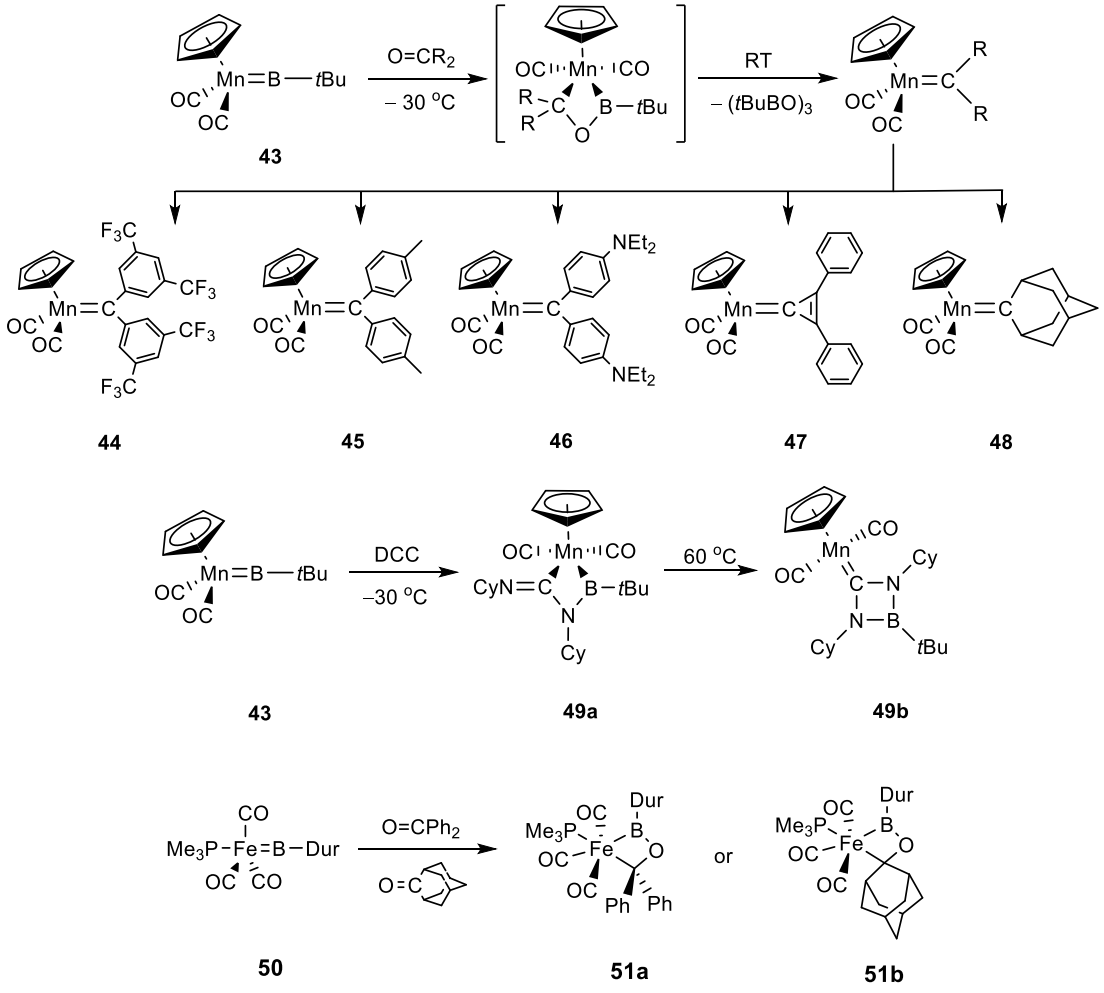

Figure 19. Metathesis reactions of manganese borylene complex [(Cp)(OC)$_2$Mn=B*t*Bu] with ketones and DCC (N,N'-dicyclohexylcarbodiimide) according to a [2+2] cycloaddition procedure by Braunschweig and coworkers.

More recently, it has been discovered that M=B/C=N bond metathesis reactions can lead to the formation of stable iminoboranes (**53**) and other cycloaddition products (**54**) (**Figure 20**).[143] In this research, chromium borylenes with bulky substituents (**22** and its isopropyl analogue) have been used to react with carbodiimides (RN=C=NR) and resulted in full bond metathesis. Computational calculations showed that in this case the formation of the iminoborane is more energetically favored (through a metathesis reaction) than the potential pathway of carbodiimide inserting into Cr=B bond.

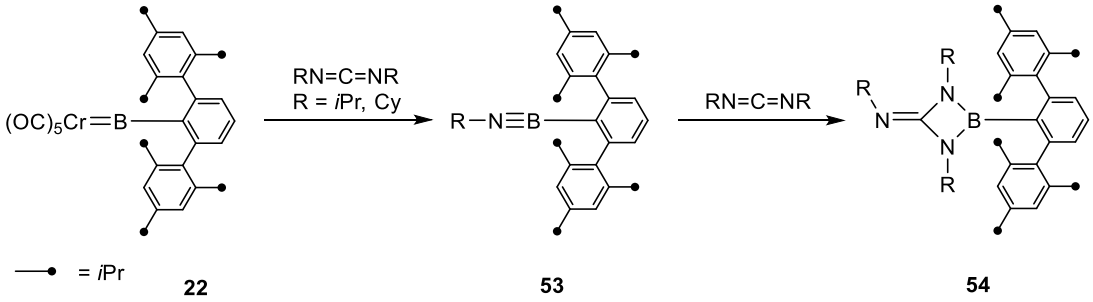

Figure 20. M=B/C=N bond metathesis reactions can lead to the formation of stable iminoboranes and further cycloaddition products.

3. B-C bond formation via borylene ligand coupling

As early as 1970s, an intramolecular CO-CR coupling had been reported by Kreissl et al.[144] from reaction of a metal carbyne complex [(η^5-C_5H_5)$(OC)_2$W≡C-R] (R = C_6H_5, $C_6H_4CH_3$, $C_6H_4OCH_3$, $C_5H_4FeC_5H_5$, and $C_6H_2(CH_3)_3$) with two equivalents of PMe_3 to form complexes of the form [(η^5-C_5H_5)$(OC)_2(Me_3P)_2$W-C(R)=C=O], which contain ketenyl ligands. This reaction motivated researchers to investigate whether similar reactivity of transition metal borylene complexes could be achieved, presumably leading to the formation of new complexes with boron-carbon bonds. In 2013, Braunschweig and coworkers reported the first intramolecular coupling of a Group 7 metal borylene ([(Cp)$(OC)_2$Mn=B*t*Bu]) (**43**) with one of its carbonyl ligands (**Figure 21**).[145] In this study, two equivalents of supermesityl isonitrile (CNMes*, Mes* = 2,4,6-tBu$_3$(C_6H_2)) were reacted with the borylene complex **43** and B-C coupling was achieved. More interestingly, the complex can lose both isonitrile

ligands and convert back to the starting material upon treatment with a strong Lewis base.[142] In the same year, another borylene-CO coupling reaction was discovered, which occurred through the reduction of a bulky substituted chromium borylene [(OC)$_5$Cr=BAr'] (Ar' = 2,6-(2,4,6-*i*Pr$_3$C$_6$H$_2$)$_2$C$_6$H) (**22**) with KC$_8$.[105] The product was a cyclic cationic complex containing two bridging carbonyl ligands (**Figure 21**). Later that year, similar reactivity was observed from an unsymmetrical bisborylene complex [(OC)$_3$Fe{BDur}{BN(SiMe$_3$)$_2$}] (**24**) triggered by addition of PMe$_3$. As a result, an iron-coordinated OC-B(Dur)-B(N(SiMe$_3$)$_2$) unit was formed in the first step and a catenated OC-B-B-CO chain was obtained upon addition of PMe$_3$ to the reaction mixture (**Figure 21**).[146] In addition to the intramolecular coupling, the bisborylene compound **24** was reported to couple with alkynes to form 1,4-dibora-1,3-butadiene and 1,4-diboracyclohexadiene complexes.[147]

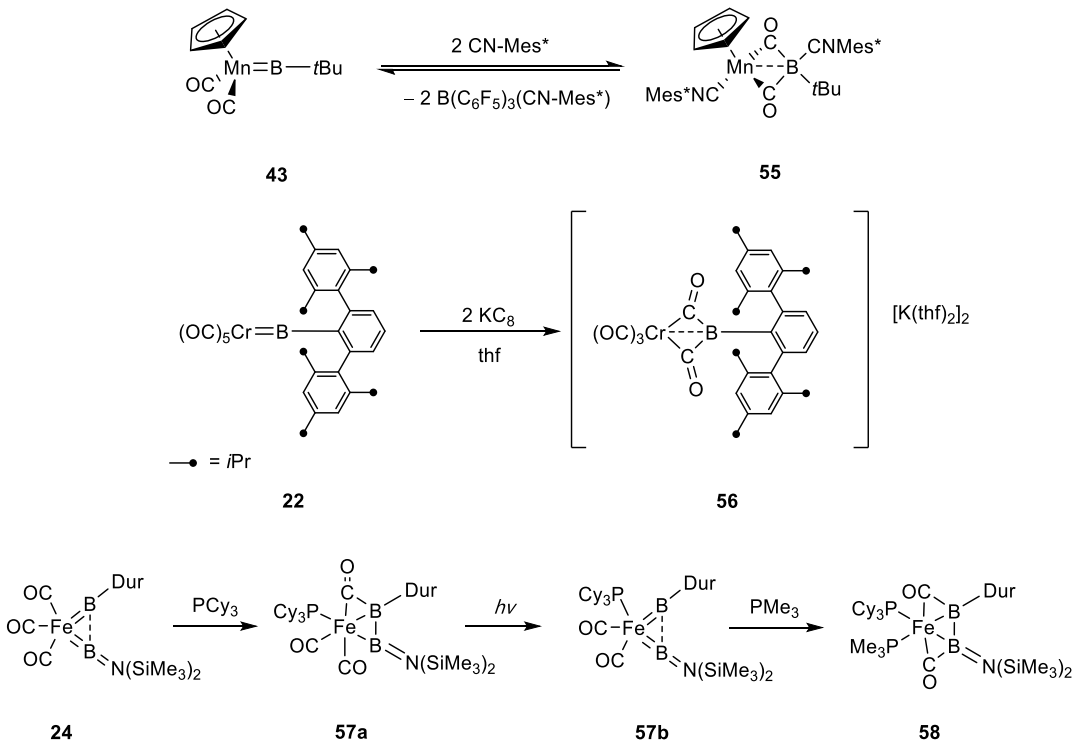

Figure 21. B-C bond formation via borylene-ligand coupling.

4. Activation of C-H bonds

The activation of carbon-hydrogen bonds has attracted considerable attention for

decades because of its importance in the field of organic synthesis. Currently, metal-catalyzed borylation is one of the most efficient and commonly used methods to achieve C-H functionalization.[8-12, 14, 17, 19, 148] Interestingly, transition metal borylene complexes also provide a few C-H functionalization methods. In 2008, Braunschweig and coworkers reported the activation of a C-H bond of 3,3-dimethyl-1-butene using chromium borylene complex $[(OC)_5Cr{=}BN(TMS)_2]$ under photolytic conditions (**Figure 22**).[149] Later, the same group reported a stepwise reaction containing borylene ligand insertion into a sp^3 C-H bond of a tricyclohexylphosphine ligand (**Figure 22**).[150] Most recently, the same group reported a three-step reaction of a manganese borylene in which the boron moiety inserts into a C-H bond of a cyclopentadienyl ligand (**Figure 22**).[151]

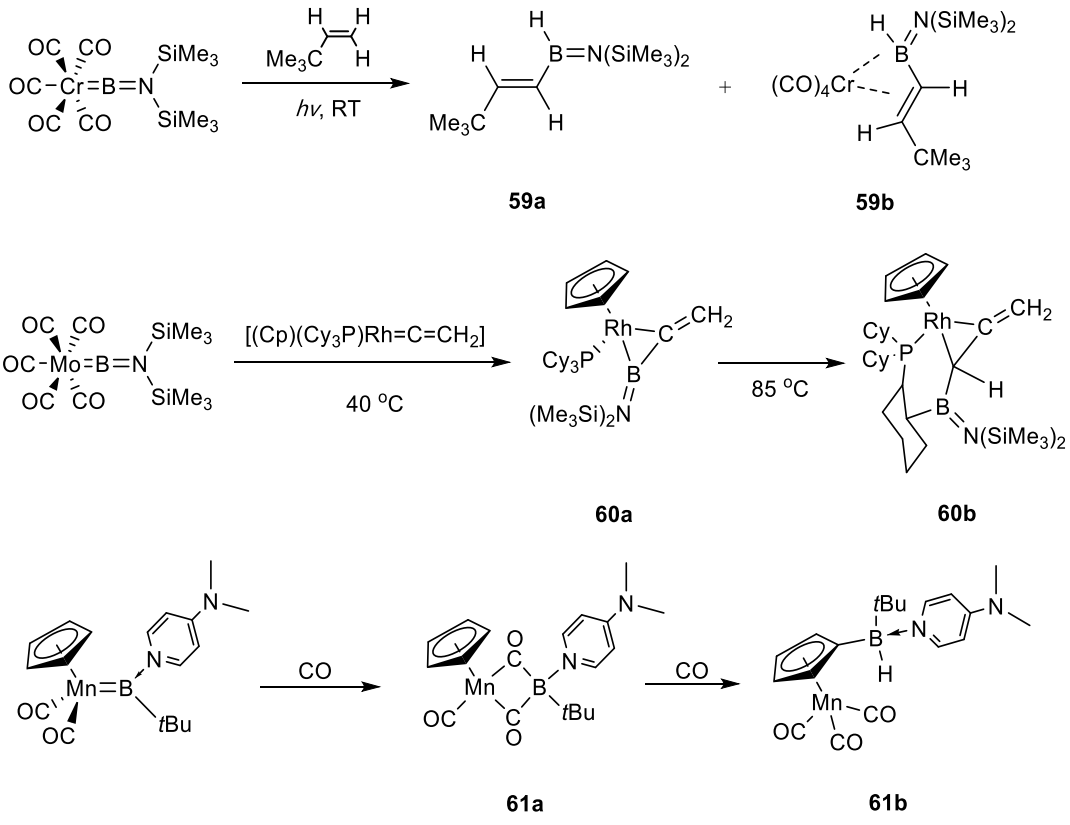

Figure 22. Activation of C-H bonds by transition metal borylene complexes.

5. Reactions with Lewis bases

The boron atoms in some transition metal borylene complexes bear a relatively

unoccupied p orbital or orbitals[100, 105, 124-125, 142, 146-147] and are thus reactive towards Lewis bases. Previous investigations[124-125, 145] showed that direct adduct formation could take place upon the addition of one equivalent of Lewis base and lead to the formation of a base-stabilized transition metal borylene complex of the form [L_nM=B(L')R]. However, in the case of manganese borylene [(Cp)$(OC)_2$Mn=B*t*Bu] (**43**),[145] an extra addition of CO to the resulting adduct formation products [(Cp)$(OC)_2$Mn=B(L)*t*Bu] (L = DMAP or IMe) would lead to the liberation of the boron moiety from the manganese center and afford CO coupling products [(Cp)(OC)Mn{κ^2-C,C'-C(O)B(*t*Bu)(L)C(O)}] (**Figure 23**). In some other cases,[100, 147] the direct adduct formation is not observed, and base-stabilized metal-free borylenes can be isolated instead (**Figure 23**).

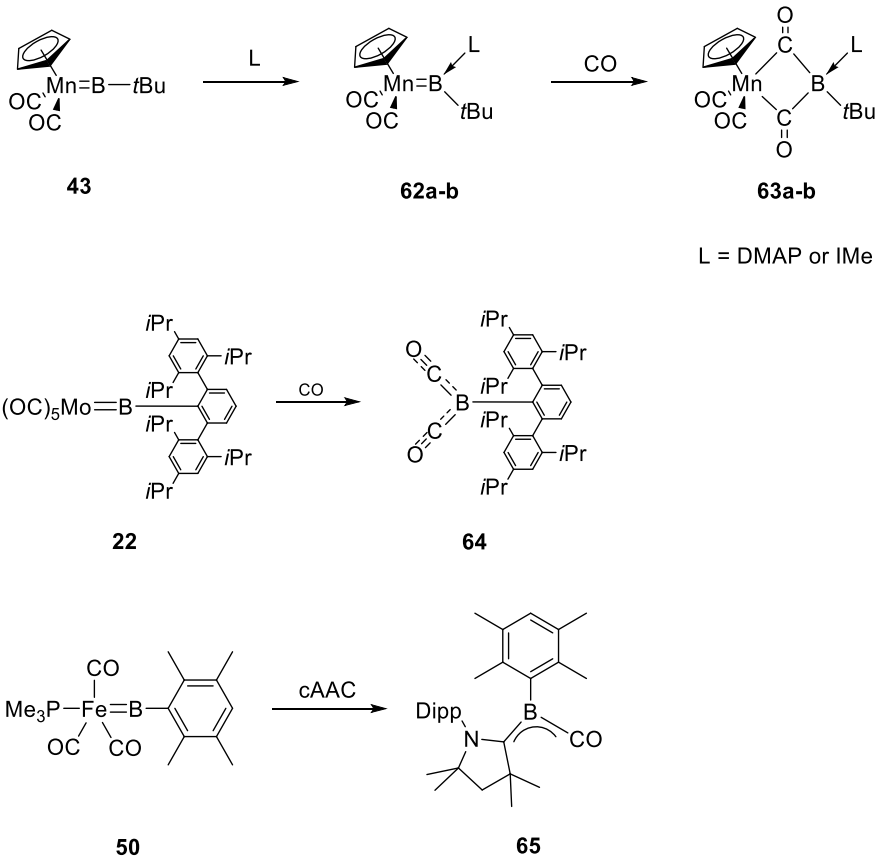

Figure 23. Various products arising from reactions of Lewis bases with borylene complexes.

6. Other reactivities of borylene complexes

Apart from the above-mentioned reactions, borylene complexes have other modes of reactivity that cannot be easily classified in the previous categories. In 2016, Braunschweig and coworkers have reported a reaction between [(Cp)(OC)$_2$Mn=B*t*Bu] and P-chloro(supermesityl)imino-phosphane [ClPNMes*] (Mes* = 2,4,6-*t*Bu$_3$(C$_6$H$_2$)), which yielded the first stable terminal phosphinidene complex of manganese (**Figure 24**).[151] Though related to metathesis reactions, the mechanism for this reaction is strikingly unique and nontrivial. Computational studies showed that the reaction starts with the nucleophilic attack of the phosphorus atom of the iminophosphane towards the metal center of the borylene complex. The final phosphinidene product is then formed from the rearrangement of the B(*t*Bu)Cl moiety.

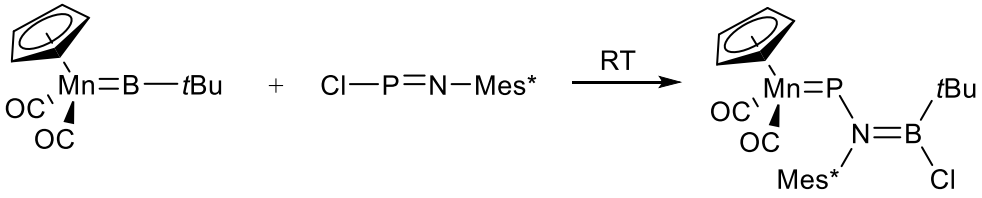

65

Mes* = 2,4,6-tBu$_3$(C$_6$H$_2$)

Figure 24. Reaction of [(Cp)(OC)$_2$Mn=B*t*Bu] and P-chloro(supermesityl)-iminophosphane [ClPNMes*].

Another unprecedented reaction involving borylene complexes is the intramolecular cleavage of the C-O bond of a carbonyl ligand of bisborylene **24**.[152] In the study, a cyclic (alkyl)(amino)carbene (cAAC) was used to react with the borylene and resulted in a highly unusual compound **66** (**Figure 25**).

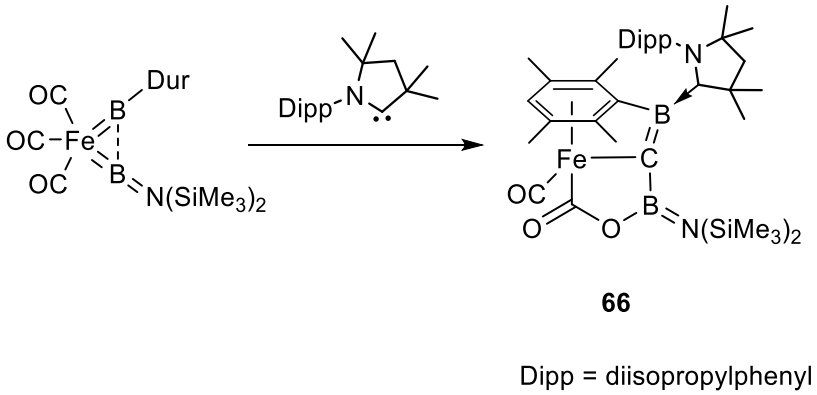

66

Dipp = diisopropylphenyl

Figure 25. Reaction of bisborylene **24** with cAAC.

1.5 Boron chalcogenide complexes

1.5.1 Chalcogen-containing boracycles

The history of boroxines can be traced back to the first half of the 20th century. The synthesis of these species is normally achieved by the dehydration of boronic acids. As early as 1938, Snyder and coworkers proposed a direct formation of boroxines from dehydration of 1-butaneboronic acid with $SOCl_2$.[153] Later, a number of investigations focused on either their fundamental interest or their applications (lithium-ion battery materials,[154-156] flame retardants[157-158] etc.). In 2005, a seminal work from Yaghi and coworkers[159] described the synthesis and characterization of the first crystalline boroxine-based covalent organic framework (COF). This work opened undeveloped areas of the design and synthesis of extended organic structures consisting of building blocks linked by strong covalent bonds. Since that time, COFs have been developed into materials that can be utilized in the fields of gas storage, photonics and catalysis.[160]

Though boroxines are well studied, their heavier analogues based on the other chalcogens, such as sulfur and selenium, have not received as much attention. There are only a few examples of B-E (E = S, Se) cyclic complexes, most of which were reported in the 20th century. The first isolated five-membered heterocyclic boron chalcogenides $R_2B_2S_3$ (**Figure 27**) dated back to 1964 by Schmidt and Siebert.[161] In 1986, Nöth and Rattay reported the preparation of a phenyl-substituted B-S-B-S four-membered ring (**Figure 27**).[162] In the case of selenium, a few examples that feature four or five-membered boron-containing rings have been reported. The first cyclic B_2Se_2 (**Figure 27**) was isolated in 1985 by Nöth and coworkers.[198] Most recently, Braunschweig and coworkers reported the synthesis of a B_2E_2 (E = S, Se) four-membered rings by reacting a cyanoborylene complex with elemental chalcogens.[163] Furthermore, the chemistry of boron with tellurium remains for the most part unknown at the moment.

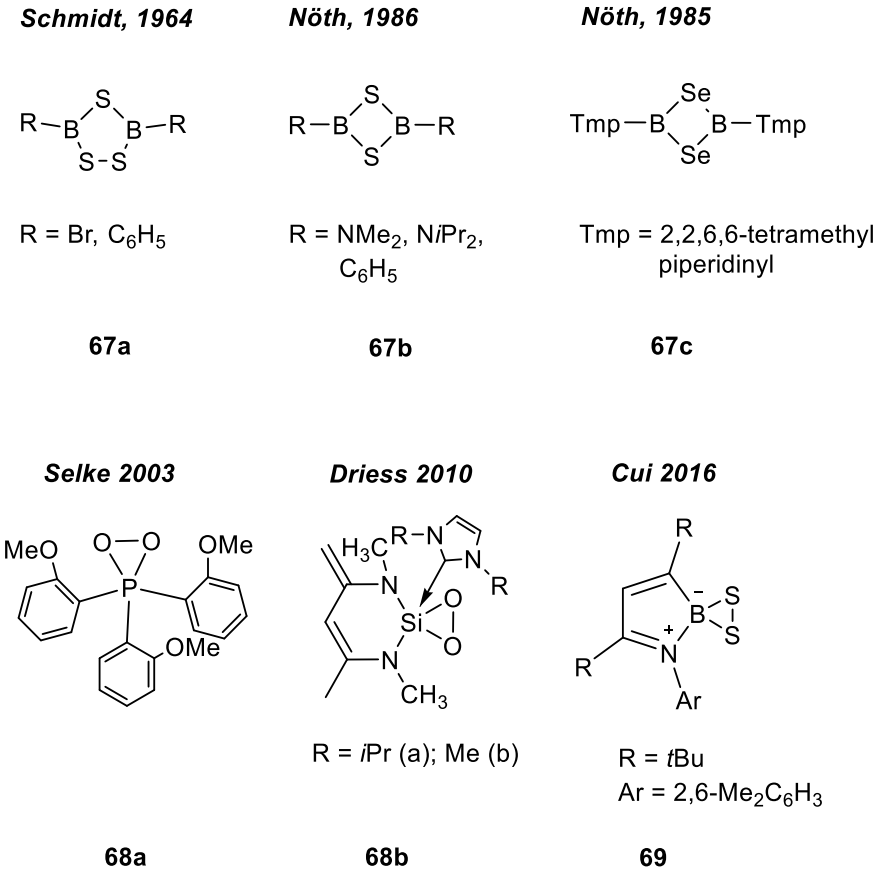

Figure 27. Examples of cyclic dichalcogenides of main group elements.

1.5.2 Boron dichalcogenides

Small cyclic molecules such as cyclopropane or cyclobutene usually feature significant ring strain, which makes them reactive and important intermediates and reagents in synthetic chemistry. Among small three-membered rings, dioxiranes and dithiiranes are very reactive oxygen and sulfur sources for chalcogen transfer and oxidation reactions.[164-166] Owing to their importance as reagents and intermediates in organic reactions, the properties and reactivities of organic dioxirane and dithiirane compounds have been extensively studied. The identification and isolation of inorganic analogues of these compounds, especially by direct reaction of elemental oxygen and sulfur with main-group species, has generated considerable interest in recent years as a platform to study intermediates in biological oxidation reactions. However, this has been hampered by the high reactivity of these species. As a result,

the number of cyclic peroxides and persulfides of the non-carbon *p*-block elements remains extremely limited.

The first phosphadioxirane was experimentally isolated and published by Selke and coworkers in 2003.[167] Through the reaction of $^1O_2$ and tris(*o*-methoxyphenyl) phosphine at –80 ºC the authors successfully observed a cyclic phosphine peroxide. In 2010, Driess and coworkers synthesized the first base-stabilized silicon peroxide under mild conditions.[168] Very recently, the first boron persulfide LB(η^2-S_2) (**69**) has been reported by Cui's group (**Figure 27**).[169] While dioxiranes and dithiiranes are relatively common in organic chemistry, there is only one example of their heavy isosteres based on selenium[170] and examples with tellurium remain completely unknown to this day.

1.5.3 Complexes featuring boron-chalcogen multiple bonds

Studies of low-valent group 13 compounds have attracted much attention in recent years, especially those featuring multiple bond character.[33-34, 171-172] It was first reported by Okazaki in 1996 that (Tbt)B=S (Tbt: 2,4,6-tris[bis(trimethylsiyl)methyl]phenyl) could exist as an intermediate during the formation of a B-S-S-Sn four-membered ring.[173] However, the first experimentally isolated compound containing a boron-chalcogen multiple bond was reported by Cowley and co-workers in 2005.[174] In the following years, compounds that featured B≡O, B=S, and B=Se character were successfully obtained and described.[48, 79]

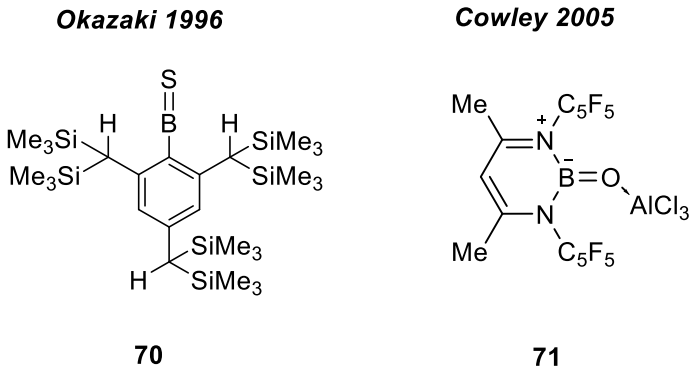

Figure 28. Compounds that feature boron-chalcogen multiple bonding.

Most of these species tend to be labile and are prone to spontaneous oligomerization processes, forming ring systems. To prevent this, electronic stabilization or steric protection are often used. The first B=O compound was synthesized by Cowley using C_6F_5-substituted *β*-diketiminate $[HC(CMe)_2(NC_6F_5)_2]^-$ (L^-) as the supporting ligand for boron. Moreover, to balance the electron density between boron and oxygen, the authors used $AlCl_3$ as Lewis acid to stabilize the product (**Figure 28**). As a result, the compound was stable at room temperature without the need for further protection from oligomerization even in solution. DFT calculations showed that the B-O bond becomes only slightly shorter upon the removal of $AlCl_3$ (1.292 Å), compared to that of the observed product (1.316 Å), suggesting a double bond character of the B=O separation of **71**.[174]

In 2011, Cui and coworkers reported similar structures with B-O double bonds using a Dipp (2,6-di*i*sopropylphenyl) substituted *β*-diketiminate as the ligand to stabilize boron (**Figure 29**).[175] Hydrogen bond donors, weak Brønsted acid or strong Lewis acids ($B(C_6F_5)_3$, BCl_3) were used to quench the Lewis basicity of the oxygen atom. The B-O bond distances are all shorter than the above-mentioned compounds, which are in the range of boron-oxygen double bonds. Several complexes featuring B=O double bond character have since been synthesized,[176-181] but none of them exist in the absence of a stabilizing component. The only example that features a naked oxygen atom so far is a platinum complex with a B≡O triple bond that was reported

by Braunschweig in 2010 and is described above (**Figure 8**, **Chapter 1.3**).[79]

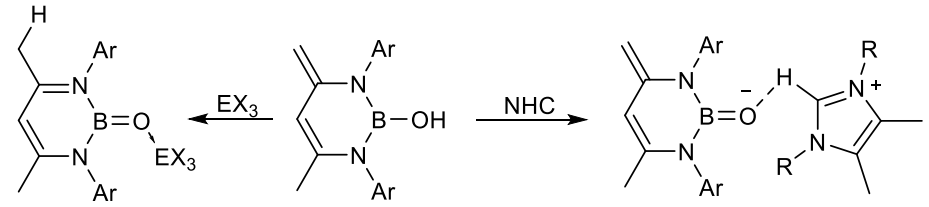

72a,b **73a,b**

Figure 29. Complexes containing B=O double bonds reported by Cui's group.

Similarly, there are few examples of compounds of boron multiply bonded to heavier chalcogens. The first compound containing a B=S double bond can be dated back to 1996, when Tokitoh and coworkers reported that an intermediate of the reaction between dithiastannaboretane and 1,3-dienes at elevated temperature featured B=S double bonds.[173] In this work, they proposed that the dithiastannaboretane would release the B=S compound when it was heated to 120 ºC, and that the compound could be captured by the 1,3-diene (**Figure 28**). However, the researchers could never isolate the intermediate in question in order to provide structural evidence for its existence. In 2010, Cui and coworkers reported the first fully characterized complexes containing B=S or B=Se double bonds (**Figure 30**). They used similar β-diketiminate ligands shown in **Figure 27** to stabilize the boron center.[48] Interestingly, unlike the B=O compounds, these analogues no longer need stabilization from a Lewis acid in order to prevent oligomerization. Experimental evidence also indicated that the complexes are stable in solution at room temperature. The boron-chalcogen bond lengths for these compounds are shorter (B=S: 1.741(2) Å; B=Se: 1.896(4) Å) than those with boron-chalcogen single bonds (B-S: 1.77-1.805 Å; B-Se: 1.960-2.13 Å).[48]

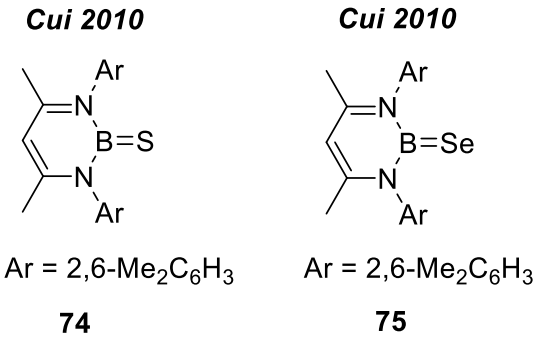

Figure 30. The first fully characterized complexes containing B=S or B=Se double bonds.

In 2013, the group of Braunschweig reported a rare example containing a boron-sulfur double bond [S=B-*t*Bu] as an intermediate.[140] The intermediate was observed by ^{11}B NMR spectroscopy in the reaction between a manganese borylene **43** and triphenylphosphorane sulfide (**Figure 31**), giving rise to a broad resonance at $\delta_B = 88.6$. Computational modelling provided a tentative structure for this intermediate. However, **76** was never isolated.

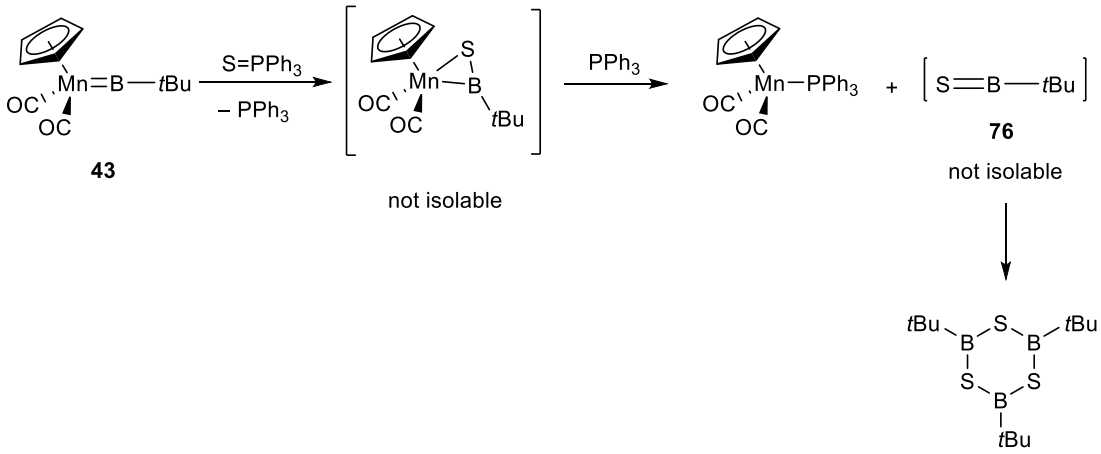

Figure 31 An intermediate (**76**) containing a B=S interaction from the reaction of [(Cp)(OC)$_2$Mn=B*t*Bu] (**43**) and S=PPh$_3$.

More recently, a few more examples of B=E (E = S or Se) complexes have been reported. One example worth mentioning is a complex synthesized by Cui and coworkers which was obtained by the reaction of a boron disulfide complex and

triphenylphosphine (**Figure 32**).[169] Even though there is no structural proof of the proposed compound, the ^{11}B NMR spectrum showed a resonance at $\delta_B = 50.3$ which suggests a decrease of the coordination number of boron relative to its precursor ($\delta_B = -4.86$). The study showed a direct way to lower the coordination number of the boron dichalcogenide to form a B=S species.

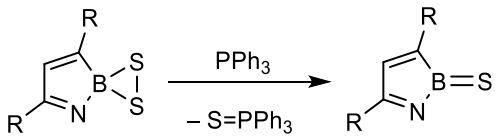

77 **78**

Figure 32. The reaction of a boron disulfide complex with triphenylphosphine.

2. Results and discussion

2.1 Reactivity of borylene complexes with bipyridine species

2,2'-bipyridines have a rich chemistry and have served as chelating ligands for synthesizing organometallic complexes used in many fields. They have also been used in the synthesis of compounds containing boron since the late 1950s when boronium complexes bearing a bipyridine ligand $[(bipy)BR_2]^+$ were first discovered in 1959; these compounds can be described as analogues of photochromic viologens and diquat wherein the carbon atom of the C-N unit is replaced by boron. Later, neutral radicals of the form $[(bipy)BR_2]^{\cdot}$ generated by reduction of bipyridine-boronium salts have been investigated.[182-184] Recently, Russell and coworkers reported similar compounds with lower oxidation states [(bipy)BX] (X = Cl or Ph) (**Figure 33**) which showed different character from the two species mentioned above.[185] The complexes were prepared by reaction of Li_2[bipy] with $[Cl_2BX]$. The products were isolated as red crystalline solids and the ^{11}B NMR spectrum of **80** displayed a resonance at δ_B = 20.7. Attempts to describe the compound as a bipyridine-stabilized B(I) species failed due to the short B-N distances (1.419(2) to 1.444(2) Å), which are in the typical range of B-N interactions (1.414 to 1.440 Å[185-186]). Therefore, the experimental data implies a boron atom in its +3 oxidation state. In addition, through NICS-1 (nucleus-independent chemical shift) calculations the authors discovered an interesting fact about these compounds. The data showed that the NICS-1 values of the central C-N-B-N-C ring in the compounds were higher than the corresponding ring of the fluorenyl anion calculated using the same method,[187] which indicated that these five-membered rings display a strong aromaticity.

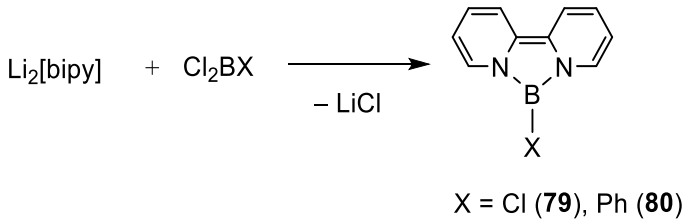

Figure 33. [(bipy)BX] (X = Cl or Ph) heterocycles prepared from the reaction between Li_2[bipy] and [Cl_2BX].

Reactions between Lewis bases and borylene species have been extensively studied in the past decade (**Figure 23**). In some cases, with more than two equivalents of a base, the boron moiety can be released from the metal center and lead to the formation of base-stabilized metal-free borylene compounds.[100, 147] Bipyridine ligands are strong electron donors with chelating properties. For these reasons, we hypothesized that they would possess tremendous potential for the stabilization of borylene moieties and may lead to the formation of novel bipyridine-stabilized borylenes.

2.1.1 Reaction of [(OC)$_5$Mo=BN(SiMe$_3$)$_2$] (20) with 2,2'-bipyridine (81)

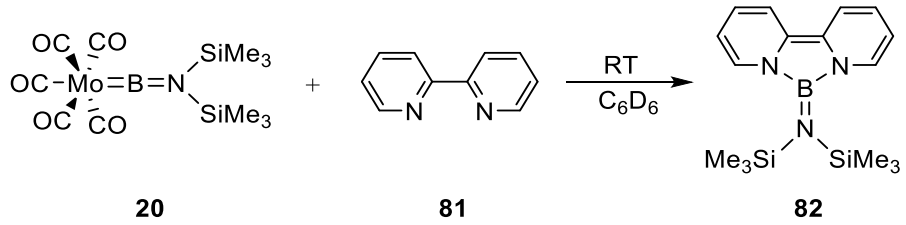

20 **81** **82**

Figure 34. The synthesis of **82** from [(OC)$_5$Mo=BN(SiMe$_3$)$_2$] (20) and 2,2'-bipyridine (**81**)

Hence, C_6D_6 solutions of [(OC)$_5$Mo=BN(SiMe$_3$)$_2$] (**20**) and 2,2'-bipyridine (**81**) (1:1 ratio) were added to a Young NMR tube at room temperature and the resulting mixture immediately turned deep red (**Figure 34**). The ^{11}B NMR spectrum showed a new resonance at δ_B = 20 which was significantly higher shifted than the borylene starting material (δ_B = 91) and was in same range as compounds **79** and **80**, suggesting the formation of an analogous tricyclic species. The reaction was monitored by NMR spectroscopy. After 6 h at room temperature, the ^{11}B NMR spectrum clearly showed residual **20**, which indicated that the reaction was not complete. Therefore, another equivalent of bipyridine was added to the solution, thus leading to the disappearance of the resonance at δ_B = 91. After work up, an air and moisture sensitive red oil was obtained, which could be characterized by ^{1}H, ^{13}C and ^{11}B NMR as pure [(bipy)BN(SiMe$_3$)$_2$] (**82**). ^{1}H NMR spectrum revealed a new signal at δ_H = 0.07 for the protons of the SiMe$_3$ groups, at a different frequency from that of **20** (δ_H = 0.13). Additionally, the aromatic resonances at δ_H = 7.51 (dt), 7.11 (dt), 6.11 (ddd) and 5.99 (ddd) correspond to the protons on the 2(2'), 5(5'), 4(4'), and 3(3') carbon atoms of the bipyridyl unit, respectively, indicating the formation of a new symmetrical species. Compound **82** has a good solubility in nearly all organic solvents (benzene, toluene, pentane, THF, etc.). The constitution was confirmed by ^{1}H, ^{13}C and ^{11}B spectra and elemental analysis as $C_{16}H_{26}BN_3Si_2$, indicating the migration of the boron moiety to the bipyridine ligand and full liberation from the metal center. Thus far, all attempts to crystallize the product by using different solvents (pentane,

benzene, toluene, THF) or different techniques have been unsuccessful. Therefore, no single crystals suitable for X-ray diffraction analysis could be obtained. Hence, no structural evidence could be given to confirm the solid state structure of **82**.

2.1.2 Reaction of $[(OC)_5Mo{=}BN(SiMe_3)_2]$ (20) with 5,5'-dibromo-2,2'-bipyridine (83)

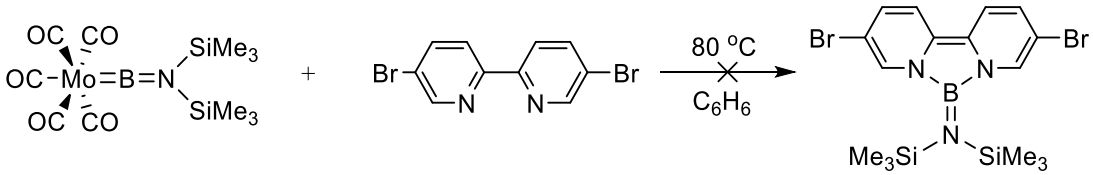

20 **83**

Figure 35. Reaction of $[(OC)_5Mo{=}BN(SiMe_3)_2]$ (**20**) with 5,5'-dibromo-2,2'-bipyridine (**83**).

To probe the versatility of the synthetic method and to acquire structural proof for these species, other bipyridine species treated with **20** at room temperature. To this end, 5,5'-dibromo-2,2'-bipyridine (**83**) was treated with one equivalent of the molybdenum borylene **20** under the same conditions as for the synthesis of compound $[(bipy)BN(SiMe_3)_2]$ (**82**) (**Figure 35**). The reaction was monitored by multinuclear NMR spectroscopy and no change could be observed after 24 h at room temperature. The solution was then heated to 80 °C, at which point a small peak was observed at $\delta_B = 20$ in the ^{11}B NMR spectrum after 48 h, which is in the same range as **82**. However, the resonance of the starting material ($\delta_B = 91$) remained as the main peak. The reaction was kept at this temperature for a week until it showed a new resonance at $\delta_B = 32$, which indicated the decomposition of **20**. All attempts to isolate the product that corresponds to the ^{11}B NMR peak at $\delta_B = 20$ were unsuccessful. Repeating the reaction in other solvents, such as toluene or THF, resulted in a mixture of several products displaying different ^{11}B NMR resonances from which no isolable component could be obtained.

2.1.3 Reaction of $[(OC)_5Mo=BN(SiMe_3)_2]$ (20) with 5,5'-bis[(trimethylsilyl)ethynyl]-2,2'-bipyridine (85)

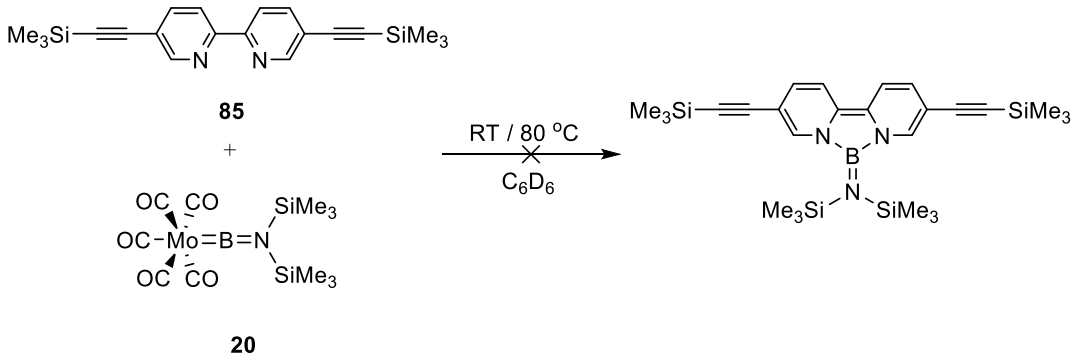

Figure 36. Reaction of with 5,5'-bis[(trimethylsilyl)ethynyl]-2,2'-bipyridine (**85**) with $[(OC)_5Mo=BN(SiMe_3)_2]$ (**20**).

To further study the influence of substituted bipyridine ligands on the reaction, 5,5'-bis[(trimethylsilyl)ethynyl]-2,2'-bipyridine (**85**) was synthesized and treated with compound **20**. Equimolar amounts of the two starting materials were dissolved in C_6D_6 in a Young NMR tube and the reaction was monitored by multinuclear NMR spectroscopy. After the solution had been kept at room temperature for 48 h, the solution had turned red and a small peak at δ_B = 20.9 had appeared in the ^{11}B NMR spectrum, which was similar to the situation in **2.1.2**. The solution was then heated to 60 °C for 24 h to drive the reaction to completion. However, only the decomposition product of the molybdenum borylene **20** could be identified from the ^{11}B NMR spectrum and all attempts to isolate any analytically pure products were unsuccessful.

2.1.4 Reaction of [(Me3P)(OC)3Fe=BDur] (50) with 2,2'-bipyridine (81)

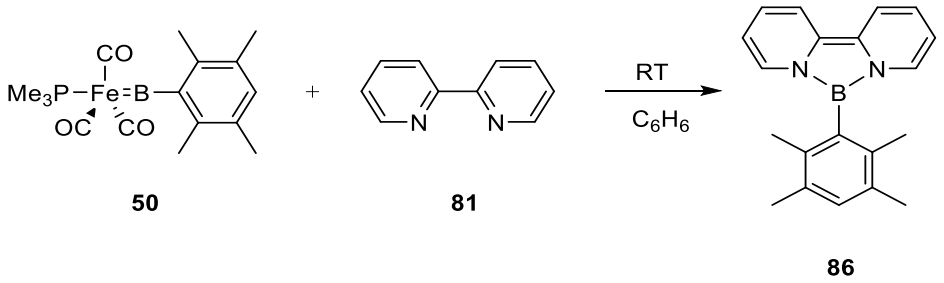

Figure 37. Synthesis of **86** from [(Me$_3$P)(OC)$_3$Fe=BDur] (**50**) and 2,2'-bipyridine (**81**).

To extend this reactivity to other borylenes, an iron borylene [(Me$_3$P)(OC)$_3$Fe=BDur)] (**50**) substituted with 2,3,5,6-trimethylphenyl (Dur) group was treated with one equivalent of 2,2'-bipyridine (**81**) (**Figure 37**). The two reactants were dissolved in C_6D_6 and the reaction was monitored by multinuclear NMR spectroscopy. After being kept at room temperature for 12 h, the ^{11}B NMR spectrum of the dark red mixture displayed a new resonance at δ_B = 23 which completely replaced that of the iron borylene **50** (δ_B = 130). After workup, the air and moisture sensitive red solid [(bipy)BDur] (**86**) was obtained in moderate yield (43%). ^{1}H, ^{13}C and ^{11}B spectra of **86** display all corresponding signals in the expected range for the predicted structure displayed in **Figure 37**. The constitution was further confirmed by elemental analysis.

Single crystals suitable for X-ray diffraction analysis were obtained from a pentane solution of the product at –30 ºC. The molecule crystallizes in the monoclinic space group P2(1)/c (**Figure 38**). The geometry of **86** shows several interesting features compared to that of 2,2'-bipyridine. The C-C bond connecting the two pyridyl groups is relatively short (C1-C2 = 1.387(3) Å versus 1.488 Å in free bipy[188]), which implies a double bond character in the C1-C2 interaction. Compared to free bipyridine (116.26°),[188] the two rings in the bipyridyl ligand are slightly bent towards the boron, which is reflected by the angles N1-C1-C2: 107.9(2)° and N2-C2-C1: 107.6(2)°. The B-N bond distances of **86** (1.435(3) Å and 1.436(3) Å) are in the range of B=N interactions shown in literature.[149] The bond length analysis clearly indicates that the

boron of this molecule is in its +3 oxidation state rather than the expected base-stabilized borylene. Furthermore, compared to the analogous complex [(bipy)BPh] (**79**) reported by Russell and coworkers (**Figure 33**),[185] the lengths of the bridging C1-C2 bond of bipyridine moiety and the two B-N bonds are almost the same as those of **79** (C-C: 1.380(2) Å, B-N: 1.443(2) Å and 1.442(2) Å) which indicates a similar geometry. Therefore, **86** can also be described as a boron-nitrogen analogue of the fluorenyl anion.

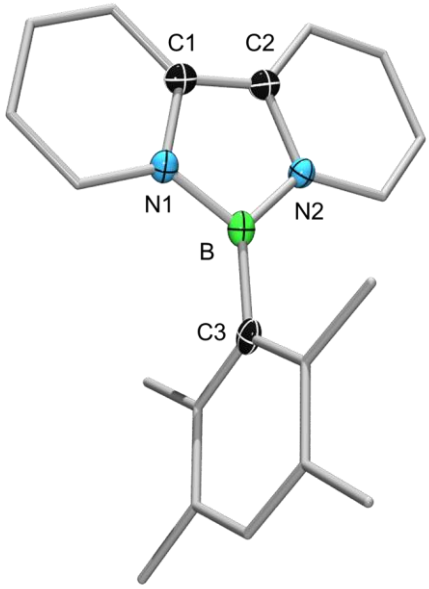

Figure 38. Molecular structure of **86**. Ellipsoids drawn at the 50% probability level. Hydrogen atoms and the ellipsoids of some carbon atoms are not shown for clarity. Relevant bond lengths [Å] and angles [º]: C1-C2: 1.387(3), B-N1: 1.436(3), B-N2: 1.435(3), B-C3: 1.567(4), N1-C1-C2: 107.9(2) N2-C2-C1: 107.6(2).

2.1.5 Reaction of [(Me$_3$P)(OC)$_3$Fe=BDur] (50) with bipyridine (83)

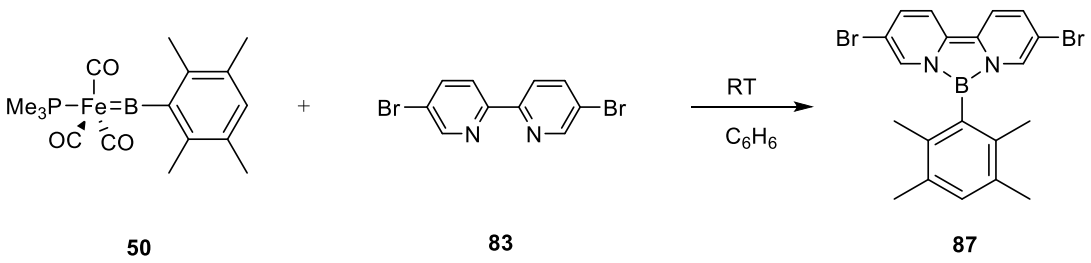

50 **83** **87**

Figure 39. Synthesis of **87** from 5,5'-dibromo-2,2'-bipyridine (**83**) and [(Me$_3$P)(OC)$_3$Fe=BDur] (50).

Given the successful borylene transfer from **50** to bipyridine, other bipyridine substrates were used to probe the generality of the synthetic method. To this end, the reaction of equimolar amounts of [(Me$_3$P)(OC)$_3$Fe=BDur] (**50**) and 5,5'-dibromo-2,2'-bipyridine (**83**) was carried out under same conditions as the reaction described in **2.1.4**. A similar resonance at δ_B = 22 in the ^{11}B NMR spectrum indicated the formation of a similar species. Red crystals were obtained from a saturated toluene/pentane solution of the crude product at –35 ºC. After workup, a few red crystals of [(Br$_2$bipy)BDur] (**87**) suitable for diffraction analysis were obtained. However, all attempts to isolate analytically pure samples of **87** were unsuccessful.

Single crystals of **87** suitable for X-ray diffraction analysis were obtained from a saturated pentane/toluene solution of pure **87** at –30 ºC. The product crystallizes in the triclinic space group *P-1* and its geometry resembles that of **86**. All the corresponding bond lengths and angles are similar to compound **86**, again suggesting the +3 oxidation state of boron.

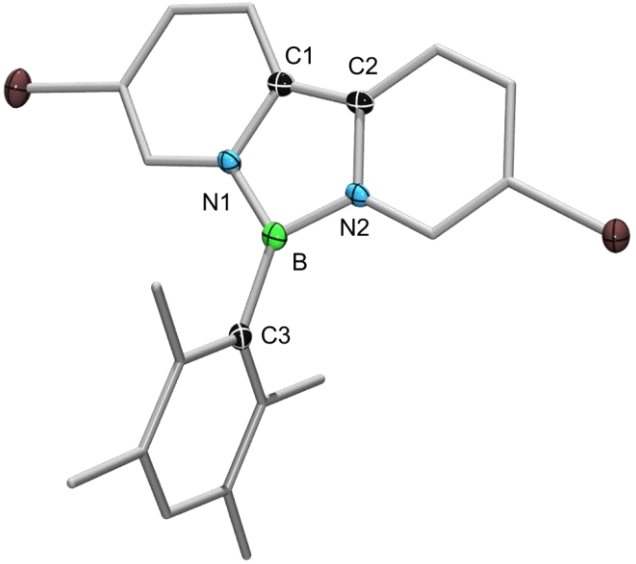

Figure 40. Molecular structure of **87**. Ellipsoids drawn at the 50% probability level. Hydrogen atoms and the ellipsoids of some carbon atoms are not shown for clarity. Relevant bond lengths [Å] and angles [º]: C1-C2: 1.382(4), B-N1: 1.438(4), B-N2: 1.447(4), N1-C1-C2: 107.9(3) N2-C2-C1: 107.9(3).

2.1.6 Reaction of [(Cp)(OC)$_2$Mn=B*t*Bu] (43) with bipyridine species (83)

The manganese borylene [(Cp)(OC)$_2$Mn=B*t*Bu] (**43**) was also allowed to react with the bipyridine ligands **81** and **83**. The reactions were carried out in C_6D_6 under similar conditions as mentioned above, under which, after 2 h at room temperature, the colors of the solutions had turned deep red. The ^{11}B NMR spectrum of both reaction mixtures revealed resonances at δ_B = 20 which represent analogous species to **82**, **86** and **87**. The ^{1}H NMR spectrum also revealed new singlets at δ_H = 0.29 for the *t*Bu substituent on boron. Unfortunately, all attempts to isolate analytically pure products remain thus far unsuccessful.

2.1.7 Reaction of [(Cp)(OC)$_2$Mn=B*t*Bu] (43) with 5,5'-bis[(trimethylsilyl)ethynyl]-2,2'-bipyridine (85)

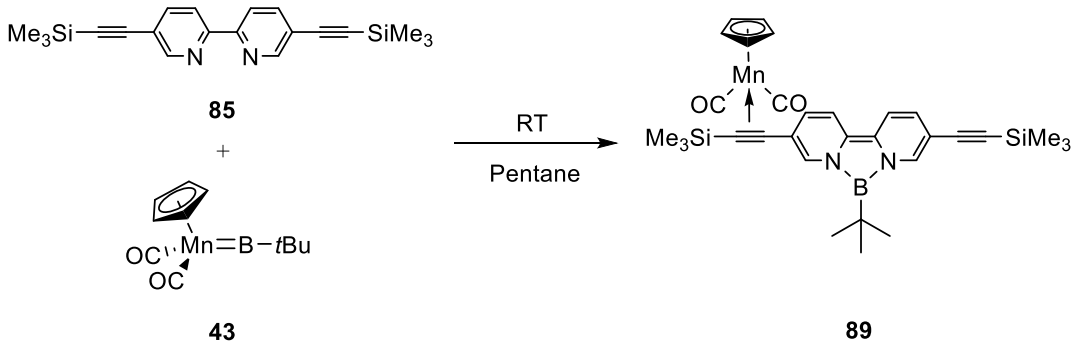

Figure 41 Synthesis of **89** from [(Cp)(OC)$_2$Mn=B*t*Bu] (**43**) and 5,5'-bis[(trimethylsilyl)ethynyl]-2,2'-bipyridine (**85**).

The bis(alkynyl)bipyridine **85** was also reacted with one equivalent of the manganese borylene complex [(Cp)(OC)$_2$Mn=B*t*Bu] (**43**). At first, the reaction was carried out in toluene solution, and was kept at –30 °C for three days. The reaction was monitored by ^{11}B NMR spectroscopy and similar results as those of **79** and **80** were observed in the ^{11}B NMR spectrum (δ_B = 23). However, no isolable product could be obtained from the mixture. Considering that **85** is highly soluble in nearly all organic solvents, the reaction was repeated using pentane as the solvent. After the reaction mixture was kept at room temperature for 12 h, dark red needle-shaped crystals precipitated from the solution. The product was characterized by ^{1}H, ^{11}B and ^{13}C NMR spectroscopy in C_6D_6 and the ^{11}B NMR spectrum shows a resonance at δ_B = 24.8, which is in the same range as that of the above-mentioned bipy-borylene (**82**, **86**, **87**) products. However, ^{1}H NMR shows an additional resonance at δ_H = 4.29 (s, 5H) ascribable to the hydrogen of a Cp ring on manganese. This was corroborated by ^{13}C NMR spectroscopy, which shows a resonance at δ_C = 233 assignable to the carbon nucleus of the CO ligands. From this evidence, the solid state structure of the product was predicted to be the one shown in **Figure 41**, which was confirmed by X-ray diffraction analysis (**Figure 42**). The constitution of **89** was further confirmed by ^{1}H, ^{11}B and ^{13}C NMR spectroscopy and elemental analysis.

Suitable single crystals were obtained from a saturated pentane solution of **89** at –30 °C. The molecule crystallized in the orthorhombic space group *Pna*2$_1$. The bridging C-C bond (1.370(3) Å) of the two pyridyl groups is similar to that of **86** (1.387(3) Å) and **87** (1.382(4) Å). Like complex **86**, the two pyridyl rings are also slightly bent towards each other. These features imply that the boron atom of **89** is in its +3 oxidation state. The C5-C6 (1.370(3) Å) distance is longer than C1-C2 (1.206(4) Å) due to the π coordination of the alkyne moiety to the manganese center. This coordination also results in a bending of the C5-C6-Si2 moiety (C5-C6-Si2: 156.8(2)°).

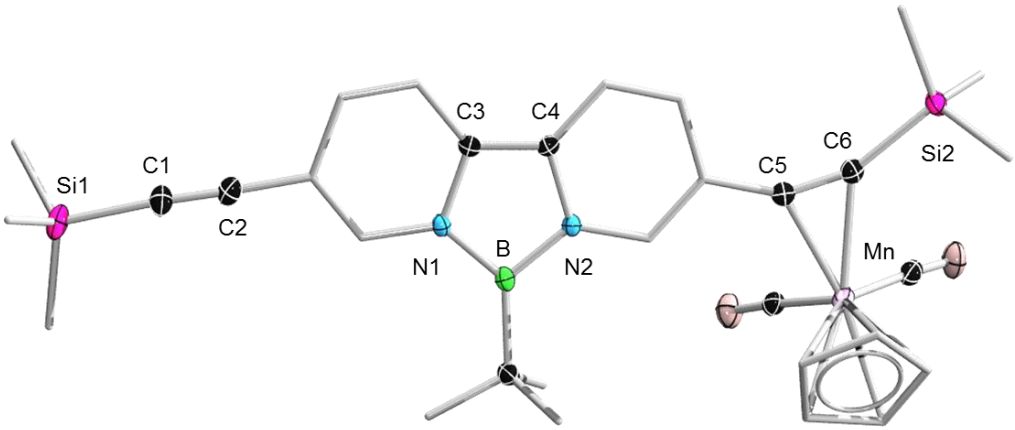

Figure 42. Molecular structure of **89**. Ellipsoids drawn at the 50% probability level. Hydrogen atoms and the ellipsoids of some carbon atoms are not shown for clarity. Relevant bond lengths [Å] and angles [°]: C1-C2: 1.206(4), B-N1: 1.454(3), B-N2: 1.454(3), C3-C4: 1.370(3), C5-C6: 1.252(4), Si1-C1: 1.836(3), Si2-C6: 1.844(3), Si1-C1-C2: 174.9(2), Si2-C6-C5: 156.8(2), N1-B-N2: 102.6(2), C3-N1-B: 109.9(2), C4-N2-B: 110.7(2).

In conclusion, we were able to synthesize boron-nitrogen analogues of the fluorenyl anion, **82**, **86**, **87** and **89**, from the reaction of bipyridines (**81**, **83** and **85**) with different borylenes (**20**, **43** and **50**). The boron atoms of these complexes are in +3 oxidation state and the bridging C-C bonds of bipyridine ligand are shortened to the

range of a C-C double bond. Similar to a previous result,[183] the central B-N-C-C-N five membered rings of these compounds have strong aromaticity. The results provide a new and direct method of synthesizing such species. Furthermore, the reaction also introduces a possible strategy to manipulate the aromaticity of a great number of macrocycles or polymers [189] featuring bipyridine units that could be applied in the fields of energy storage, catalysis and photoinduced electron transfer. Furthermore, the change of their aromatic behavior may bring new features to these materials.

2.2 Reactivity of manganese borylene complexes with elemental chalcogens to form compounds containing B=E (E = S, Se, Te) double bonds

The preparation of compounds that feature multiple bonds has significant importance in the field of synthetic chemistry and is also vital to the advancement of chemical knowledge. During the past several decades, achievements have been made in synthesizing compounds containing unusual multiple bonds between boron and many other elements, such as transition metals and a variety of main group elements, notably from groups 5-8. Interestingly, other than transition metals, which involve their d-orbitals in bonding, no complex has ever been isolated featuring a multiple bond between boron and an element heavier than the fourth period. Regarding the group 16 elements – the chalcogen family – the main problem of isolating the corresponding compounds containing boron-chalcogen multiple bonds is their tendency to undergo oligomerization. In order to prevent the compound from oligomerization, methods such as Lewis base stabilization and acid or steric protection have been applied in most investigations.[48, 79, 173-174] In fact, only a few examples of B=E complexes (E = O, S, Se) have been synthesized, while their heavier analogues containing tellurium have never been observed. Since borylene ligands are both good σ donors and π acceptors, the reaction involving transition metal borylene and elemental chalcogens may lead to the isolation of novel compounds that contain boron-chalcogen multiple bonds.

2.2.1 Reaction of [(Cp)(OC)$_2$Mn=B*t*Bu] (43) with S$_8$ in a 1:2 boron-to-sulfur ratio

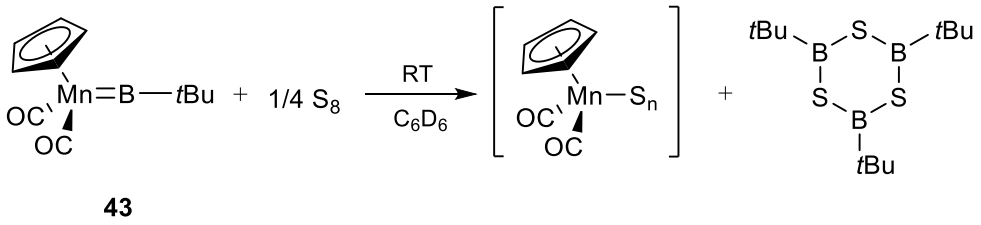

43

Figure 43. Reaction of **43** with two equivalents of sulfur.

The manganese borylene complex [(Cp)(OC)$_2$Mn=B*t*Bu] (**43**) possesses a rich reactivity which has only recently begun to be uncovered by the Braunschweig group. Among the reactions that **43** can undergo, metathesis is one of its most prominent motifs. One notable example is the reaction of [(Cp)(OC)$_2$Mn=B*t*Bu] with Ph$_3$PS, which yielded [(Cp)(OC)$_2$Mn(PPh$_3$)] and [(*t*Bu)BS]$_3$. An intermediate presumed to be [(Cp)(OC)$_2$Mn(μ^2-SB(*t*Bu))] was observed during the reaction, which features a B=S double bond on the basis of computational studies (**Figure 31**), but which could not be structurally characterized. Based on this knowledge, **43** was used to react with elemental chalcogens in order to form boron-chalcogen multiple bonds.

The reaction between compound **43** and S$_8$ was carried out in a Young NMR tube in C$_6$D$_6$, so that it could be monitored by NMR spectroscopy. After the solution had been kept at room temperature for 10 min, the solution had turned green. The ^{11}B NMR spectrum showed a new resonance at δ_B = 72 which indicated the formation of [SB(*t*Bu)]$_3$.[140] On the other hand, the green color of the solution suggested the formation of a [Mn]-S species in which sulfur is connected to the manganese moiety.[190] Hence, the reaction can be drawn as shown in **Figure 43**. However, no product could be isolated to further prove this hypothesis.

2.2.2 Reaction of [(Cp)(OC)$_2$Mn=B*t*Bu] (43) with Se and Te

Since the reaction between the manganese borylene [(Cp)(OC)$_2$Mn=B*t*Bu] and S$_8$ did not result in the formation of boron-chalcogen double bonds, heavier members of the

chalcogen family were used to further investigate the reactivity. Both reactions were carried out in C_6D_6 and were monitored by multinuclear NMR spectroscopy.

In the case of Se, a similar result was observed. The color change (orange to green) and the resonance at δ_B = 70 in the ^{11}B NMR spectrum are indicative of a similar process as in the case of the reaction with S_8. However, no pure product could be isolated to prove this hypothesis. In the case of Te, no reaction was observed at room temperature between **43** and elemental tellurium, presumably due to the lower solubility of tellurium when compared to the other chalcogens. The reaction mixture was heated and kept at 60 °C for 24 h, leading not to a similar reactivity as for S and Se, but instead to the decomposition of the manganese borylene **43**.

2.2.3 Reaction of [(Cp)(OC)$_2$Mn=B(IMe)*t*Bu] (90) with S_8 in a 1:1 boron-to-sulfur ratio

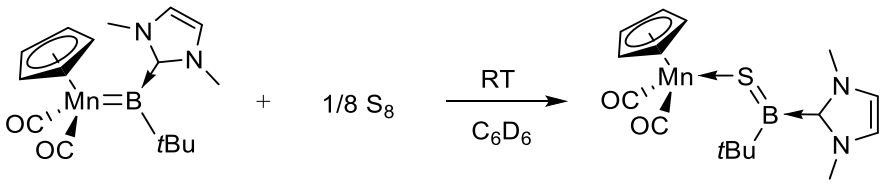

90 **91**

Figure 44. Synthesis of **91** from reaction of [(Cp)(OC)$_2$Mn=B(IMe)*t*Bu] (**90**) with S_8.

The oligomerization of compounds that contain boron-chalcogen multiple bonds can be attributed in part to the presence of an empty p orbital on the boron atom. In order to prevent this process, a base-stabilized derivative of manganese borylene [(Cp)(OC)$_2$Mn=B(IMe)*t*Bu] (IMe = *N*,*N*′-dimethylimidazol-2-ylidene) (**90**) was used to react with S_8 in a 1:1 boron-to-sulfur ratio. The reaction was carried out in C_6D_6 in a Young NMR tube at room temperature and monitored by multinuclear NMR spectroscopy. After the reaction mixture was kept at room temperature for 24 h, the ^{11}B NMR spectrum revealed a new resonance at δ_B = 67.3 replacing the one associated with the starting material (**90**: δ_B = 128.4) in the ^{11}B NMR spectrum. The resonance is in the same range as that of other compounds that contain boron-sulfur

double bonds.[140, 169] From the mixture, [(OC)$_2$Mn-S=B*t*Bu(IMe)] (**91**) was isolated as an analytically pure, moisture and air sensitive orange powder in 53% yield after workup. Interestingly, a ^{1}H NMR resonance at δ_H = 4.51 associated to a proton on a Cp ring could be observed in the spectrum, indicating that a manganese-containing moiety remained in the molecule (**Figure 44**). Additionally, the ^{13}C NMR spectrum showed a resonance at δ_C = 237 which is in accordance with the presence of CO ligands associated with the manganese moiety. The solid state structure of **91** was confirmed by X-ray diffraction analysis (**Figure 45**).

Single crystals suitable for X-ray diffraction analysis were obtained from a saturated toluene/hexane solution of compound **91** at –30 ºC. The molecule crystallizes in the triclinic space group *P*-1. The structure displays a shorter B-S separation (1.747(3) Å) than the sum of the covalent radii of boron and sulfur (~1.87 Å). In addition, this distance is much shorter than the corresponding bonds in tricoordinate boron compounds containing a B-S interaction that feature single bond character.[163, 169, 191] Indeed, the B-S distance of **91** is statistically identical to that of [HC(CMe)$_2$(NAr)$_2$B=S] (Ar = 2,6-Me$_2$C$_6$H$_3$) (1.741(2) Å), which indicates that it features a real boron-chalcogen double bond.[48] Moreover, the relatively long Mn-S separation (2.3396(9) Å) indicates a rather weak Mn-S interaction. For these reasons, the product can be described as the acid-base adduct of [(Cp)Mn(CO)$_2$] and [(IMe)(*t*Bu)B=S], in which the Mn-S interaction is likely to be a dative covalent bond. To further study the structure of the compound, calculations based on density functional theory (DFT) were performed. At the B3LYP/def2-TZVPP level, the calculated B=S bond distance (1.741 Å) matches that of the crystal structure. The Wiberg bond index (WBI) calculated for the B-S interaction in this compound at this level is 1.69, indicating a strong double bond. Moreover, the WBI for the Mn-S bond is 0.52, suggesting a weak S→Mn dative covalent interaction. In addition, the sum of the angles around boron (359.9°) indicates the planarity of the boron atoms.

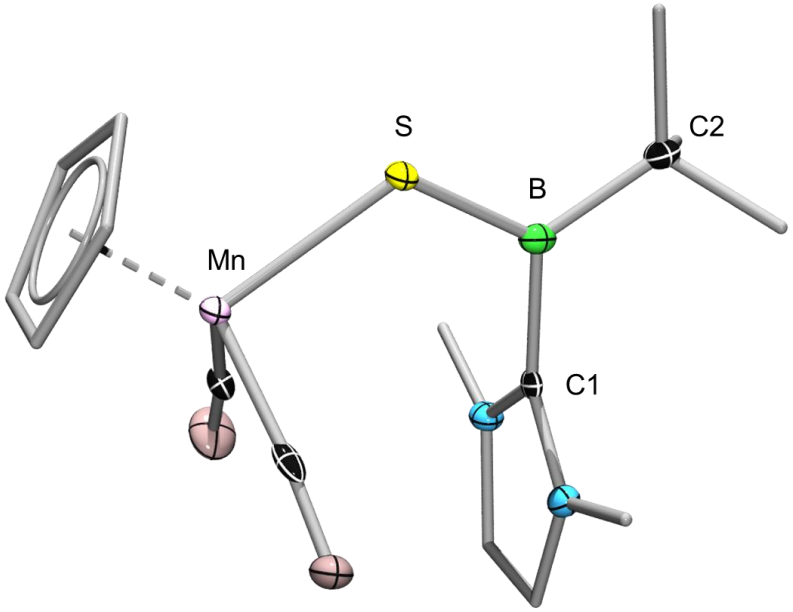

Figure 45. Molecular structure of **91**. Ellipsoids drawn at the 50% probability level. Hydrogen atoms and the ellipsoids of some carbon atoms are not shown for clarity. Relevant bond lengths [Å] and angles [º]: C1-B 1.591(5), C2-B 1.595(4), B-S 1.747(3), S-Mn 2.3396(9), S-B-C1 117.9(2), S-B-C2 123.5(2), C1-B-C2 118.5(3), B-S-Mn 121.8(1).

2.2.4 Reaction of [(Cp)(OC)$_2$Mn=B(IMe)*t*Bu] (90) with one equivalent of Se

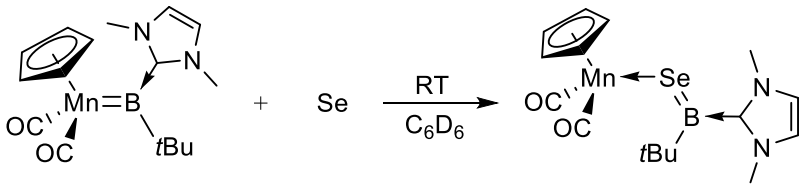

90 **92**

Figure 46. Synthesis of **92** from [(Cp)(OC)$_2$Mn=B(IMe)*t*Bu] (**90**) and elemental Se.

In order to probe the reactivity of the whole chalcogen family, a C_6D_6 solution of [(Cp)(OC)$_2$Mn=B(IMe)*t*Bu] (**90**) was treated with an equimolar amount of selenium. The reaction was carried out at room temperature in a Young NMR tube and was monitored by multinuclear NMR spectroscopy (**Figure 46**). After the solution had been kept at ambient temperature for 24 h, the color of the solution had turned from

red to green. The ^{11}B NMR spectrum revealed a new resonance at $\delta_B = 73.2$, which is in the same range as that of compound **91** ($\delta_B = 67.3$). This indicated the formation of a product that featured a similar B=E interaction as **91**. After workup, [$(OC)_2$Mn-Se=B*t*Bu(IMe)] (**92**) was isolated as an analytically pure, air and moisture sensitive violet powder in 46% yield. The constitution and solid state structure of **92** was confirmed by ^{1}H, ^{11}B and ^{13}C NMR spectroscopy and single-crystal X-ray diffraction analysis (**Figure 47**) which revealed a complex of similar structure to **91**.

Single crystals suitable for X-ray diffraction analysis were obtained by storing a saturated toluene/pentane solution at –30 ºC for 24 h. The molecule crystallizes in the triclinic space group P-1. Compared to the sum of the covalent radii of boron and selenium (~2.04 Å), the short B-Se bond length (1.882(3) Å)[163, 191-192] strongly indicates the double bond character of the B-Se interaction. Additionally, the bond length is comparable to previously reported B=Se double bonds. The B-Se distances are similar to that of [$HC(CMe)_2(NAr)_2$B=Se] (Ar = 2,6-$Me_2C_6H_3$) (1.896(4) Å),[134] which indicates that these molecules feature boron-chalcogen double bond character. The relatively long Mn-Se bond distance (2.4520(4) Å) implies a weak dative interaction between the two atoms.

Density functional theory (DFT) was also used to model **92**. At the B3LYP/def2-TZVPP level, the calculated B=Se bond distance (1.887 Å) matches that of the crystallographically-derived structure. The WBI calculated for this compound at this level is 1.69, providing strong evidence for the presence of a double bond between boron and selenium. Moreover, the WBI for the Mn-Se interaction is 0.49, suggesting a weak Se→Mn dative covalent interaction as is predicted from X-ray diffraction analysis. In addition, the sum of the angles around boron (359.9°) indicates the planarity of the boron atom.

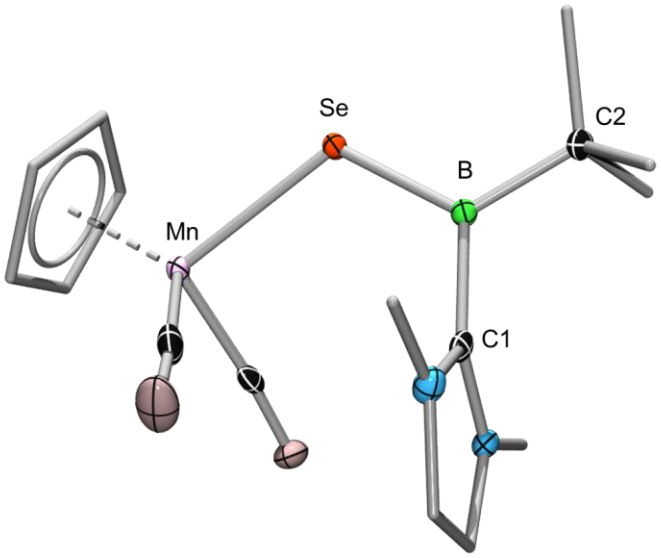

Figure 47. Molecular structure of **92**. Ellipsoids drawn at the 50% probability level. Hydrogen atoms and the ellipsoids of some carbon atoms are not shown for clarity. Relevant bond lengths [Å] and angles [º]: C1-B 1.593(4), C2-B 1.600(3), Se-B 1.882(3), Se-Mn 2.4520(4), C1-B-C2 117.8(2), Se-B-C1 118.7(2), Se-B-C2 123.4(2) Mn-Se-B 118.16(9).

2.2.5 Reaction of [(Cp)(OC)$_2$Mn=B(IMe)*t*Bu] (90) with one equivalent of Te

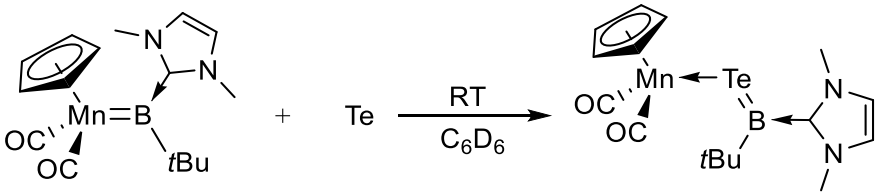

90 **93**

Figure 48. Synthesis of **93** from [(Cp)(OC)$_2$Mn=B(IMe)*t*Bu] (**90**) and elemental Te.

Since compounds featuring B=Te double bond character have never been isolated, likely due to the lower reactivity of tellurium and its compounds towards boron, we considered it to be of great significance to accomplish the synthesis of a Te analogue of **91** and **92**. Since complexes containing B=S and B=Se interactions were successfully achieved by the reaction from the manganese borylene **90** and elemental chalcogens, it seemed possible to obtain a B=Te structure through the same method.

To this end, a C_6D_6 solution of [(Cp)(OC)$_2$Mn=B(IMe)*t*Bu] (**90**) was treated with an equimolar amount of elemental tellurium. The reaction was carried out in a Young NMR tube at room temperature and was monitored by multinuclear NMR spectroscopy (**Figure 48**). After the solution had been kept at room temperature for 24 h, the color of the solution had turned from orange to dark red-violet and a new resonance at δ_B = 77.2 was observed in place of the resonance of the starting material (δ_B = 128). The signal for the new product is in the same range as the ^{11}B NMR resonances of compounds **91** (δ_B = 67.3) and **92** (δ_B = 73.2), which indicates the formation of a B=Te bond. In addition, the ^{1}H NMR spectrum also showed similar resonances to compound **91** and **92**. After workup, dark red-violet crystals of pure [(Cp)(OC)$_2$Mn-Te=B*t*Bu(IMe)] (**93**) were isolated and characterized by ^{1}H, ^{11}B, ^{13}C and ^{125}Te NMR spectroscopy. The constitution of **93** was also confirmed by elemental analysis.

Single crystals of **93** suitable for X-ray diffraction analysis were obtained from a saturated pentane/toluene solution at –30 °C. Interestingly, the solid state structure (**Figure 48**) represents one of the very few structurally characterized B-Te interactions. In fact, one can only find 31 examples of structurally authenticated B-Te bonds, 28 of which exist *endo* or *exo* to clusters and metalloclusters. Interestingly, **93** shows the shortest B-Te interaction (2.100(4) Å) ever characterized.[192-195] Therefore, **93** can be described as the first compound featuring a B=Te double bond character. Similar to compound **91** and **92**, the X-ray data of **93** shows a rather long Mn-Te interaction (2.5981(4) Å), which can be regarded as a Te-to-Mn dative covalent interaction. Furthermore, the sum of the angles around boron (360.0°) indicates its planarity.

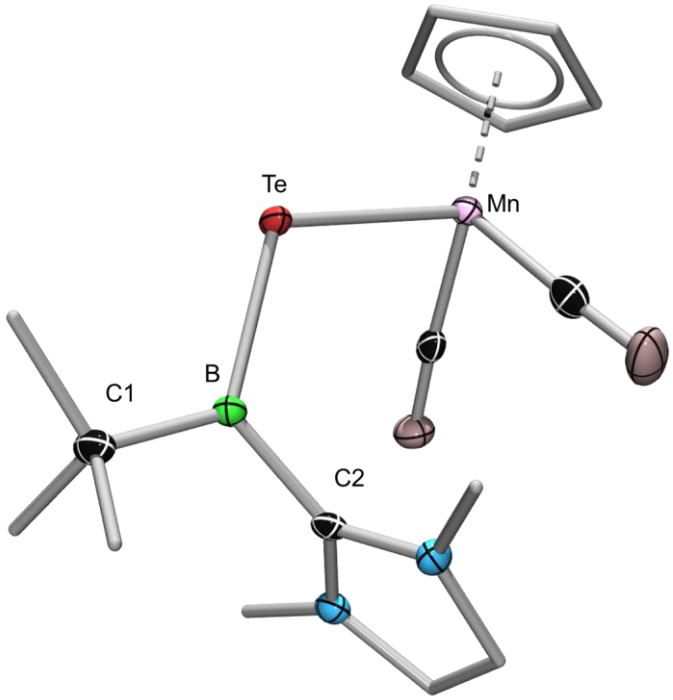

Figure 49. Molecular structure of **93**. Ellipsoids drawn at the 50% probability level. Hydrogen atoms, as well as the ellipsoids of some carbon atoms are not shown for clarity. Relevant bond lengths [Å] and angles [º]: C1-B 1.600(3), C2-B 1.584(5), Te-B 2.101(4), Mn-Te 2.5981(4), C1-B-C2 119.0(3), Te-B-C1 123.1(2), Te-B-C2 117.9(2), B-Te-Mn 116.0(1).

To further study the B=Te double bond, DFT calculations were performed to model compound **93**. At the B3LYP/def2-TZVPP level, the B=Te distance closely matched that of the crystal structure (2.107 Å). The B-Te Wiberg bond index (WBI) calculated at this level was 1.68, which provides strong evidence for the double bond nature of the B-Te interaction. On the other hand, the WBI of the Mn-Te interaction is quite low (0.49), which is consistent with a weak Te–Mn dative bond. Moreover, the presence of an occupied bonding orbital of π symmetry between the boron and chalcogen atoms was observed computationally as a natural bonding orbital (NBO) (**Figure 50**). In this case, the NBO π-orbital has a high occupancy of 1.9 electrons and is polarized towards Te (72.74%).

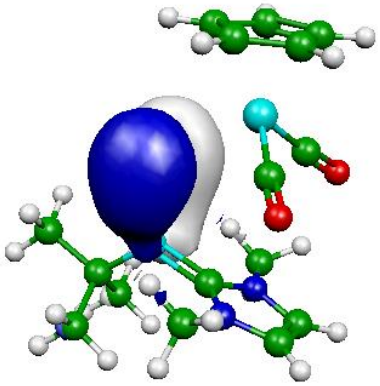

Figure 50. π-orbital of the B=Te bond of **93** depicted as an NBO.

2.2.6 Reaction of [(OC)$_5$Mo=BN(SiMe$_3$)$_2$] (20) with elemental chalcogens (S$_8$, Se, Te)

To probe the versatility of the synthetic routes to compounds featuring B=E bonds, other borylene complexes were used to react with elemental chalcogens. [(OC)$_5$Mo=BN(SiMe$_3$)$_2$] (**20**) was chosen as the borylene starting material because the boron atom in this molecule is also stabilized by a free electron pair on the adjacent nitrogen. In this case, one equivalent of elemental tellurium was added to a C_6D_6 solution of **20**. The reaction was monitored by multinuclear NMR spectroscopy and was carried out in a Young NMR tube, however, under these conditions, no reaction was observed within 24 hours. When the temperature was raised to 80 ºC a few signals could be observed by ^{11}B NMR spectroscopy, but no pure product can be isolated from the reaction. Due to the failure of the reaction with tellurium, selenium was used to react with **20** under the same conditions. However, similarly to the case of tellurium no reaction was observed at room temperature. After the mixture was heated to 60 ºC for another 24 h, the ^{11}B NMR spectrum displayed a new resonance at δ_B = 39.2. Unfortunately, all attempts to isolate the resulting product were unsuccessful. The reaction between **20** and S_8 provided a signal at δ_B = 39 in the ^{11}B NMR spectrum, indicating a similar result. Like the reaction with Se, no isolable product could be obtained.

In conclusion, we were able to isolate the first complex featuring a B=Te double bond, [(Cp)(OC)$_2$Mn-Te=B*t*Bu(IMe)] (**93**) through the reaction of base-stabilized borylene [(Cp)(OC)$_2$Mn=B(IMe)*t*Bu] (**90**) with tellurium. This unprecedented interaction has been well characterized structurally and computationally. The method was also expanded to the synthesis of complexes that feature B=S (**91**) and B=Se (**92**) double bonds. This result, a direct insertion of elemental chalcogens into a M=B bond, represents a new strategy for synthesizing boron-chalcogen multiple bonds.

2.3 Reactivity of borylenes with elemental chalcogens to form cyclic boron chalcogenide species

Organic dioxiranes (*cyclo*-O_2CR_2) and dithiiranes (*cyclo*-S_2CR_2) have significant importance as reagents and intermediates in the field of organic chemistry, for example for oxidation and chalcogen transfer reactions. Furthermore, the related inorganic cyclic dioxides and disulfides based on transition metals have attracted much attention in recent years due to their prominence in biological oxidation reactions.[196-198] However, their analogs based on main group elements remain little investigated due to the instability of such species. The first known example of this kind was reported by Akiba in 1999,[199] where a hexacoordinate phosphorus dioxirane was isolated and fully characterized. After that, phosphorus dioxiranes and silicon dioxiranes were reported successively. However, the analogues containing heavier chalcogens were not isolated until 2016, when Cui and coworkers successfully synthesized the first B-S-S three-membered cyclic dichalcogenide (**Figure 27**).[169] As for their heavier isosteres (based on selenium and tellurium), they remain unknown to this day. In fact, no ditelluriranes exist containing any main group element in the ring.

In **chapter 2.2**, the formation of compounds [(Cp)$(OC)_2$Mn-E=B*t*Bu(IMe)] (**91-93**) containing borachalcone fragment [E=BtBu(IMe)] was described through the reaction of one equivalent of elemental chalcogens with base-stabilized borylenes. From complex **93**, the borachalcone fragment could not be liberated by heating or by the addition of additional Lewis bases (PMe_3, CO). Since some chalcogens can react with manganese carbonyl compounds to form metal chalcogenides,[200] we considered it reasonable to use three or more equivalents of chalcogens to release the target fragment from the mental center. However, this reaction did not proceed as expected, but furnished a different cyclic boron chalcogenide instead. The details of these reactions will be discussed in this chapter.

2.3.1 Reaction of [(Cp)(OC)$_2$Mn=B(IMe)*t*Bu] (90) with S_8 in a 1:3 boron-to-sulfur ratio

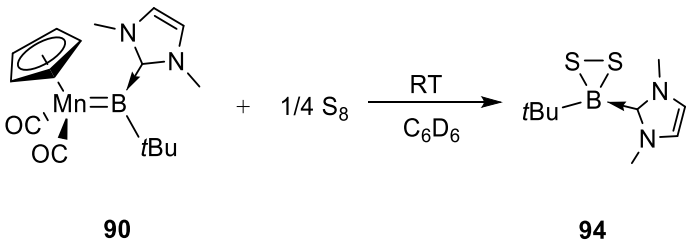

90 **94**

Figure 51. Synthesis of **94** from [(Cp)(OC)$_2$Mn=B(IMe)*t*Bu] (**90**) and three equivalents of S_8.

S_8 was added to a C_6D_6 solution of [(Cp)(OC)$_2$Mn=B(IMe)*t*Bu] (**90**) in a Young NMR tube at ambient temperature, corresponding to a 1:3 boron-to-sulfur ratio, and the reaction was monitored by multinuclear NMR spectroscopy (**Figure 51**). After 12 hours at room temperature, the ^{11}B NMR spectrum of the green mixture featured new resonances at δ_B = 67.3 and –2.9. While the former is the same as that of compound [(Cp)(OC)$_2$Mn-S=B*t*Bu(IMe)] (**91**), the new peak at δ_B = –2.9 is in the range of a tetracoordinate boron species. To allow the reaction to reach completion, the mixture was kept at room temperature for 12 more hours, after which the resonance for the starting material (δ_B = 130) had completely disappeared. After workup, [*cyclo*-SSB*t*Bu(IMe)] (**94**) was isolated as yellow crystals in low yield (19%). The low yield may be due to the high reactivity of the new dichalcogenide species, which could lead to a ring-expansion product (BS_n). A similar phenomenon was described in Cui's work, in which the formation of boron-sulfur BS_n (n = 4, 6) polycycles was reported. The ^{1}H and ^{13}C NMR spectra showed resonances for all the corresponding protons in the structure shown in **Figure 51**. The constitution was also confirmed by elemental analysis.

To further investigate the solid state structure of **94**, single crystals suitable for X-ray diffraction analysis were obtained from a saturated pentane/toluene solution of **94**. The molecule crystallizes in the triclinic space group P-1. The B-S (1.922(2) Å,

1.921(2) Å) and S-S (2.0946(4) Å) distances (**Figure 52**) of the molecule are very similar to those reported by Cui (B-S = 1.877(2) Å, 1.886(2) Å; S-S = 2.1004(8) Å),[169] which suggests a similar bonding situation. The dihedral angle of the three-membered ring and the B-C1-C2 plane is 88.8° which indicates that they are perpendicular to each other.

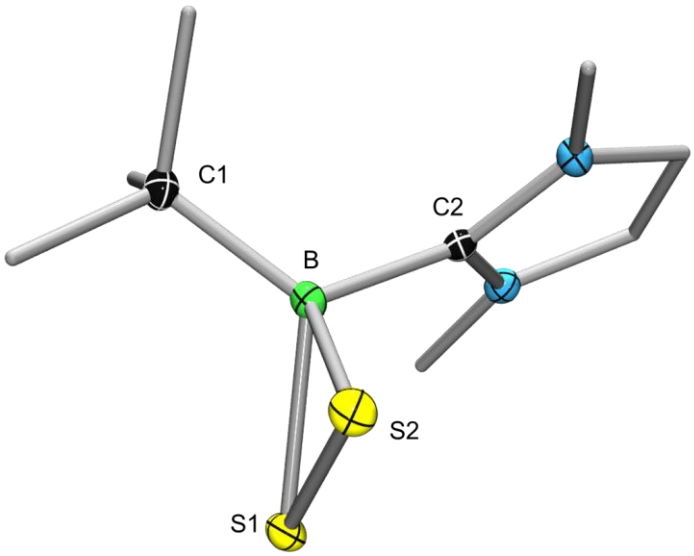

Figure 52. Molecular structure of **94**. Ellipsoids drawn at the 50% probability level. Hydrogen atoms and the ellipsoids of some carbon atoms are not shown for clarity. Relevant bond lengths [Å] and angles [º]: C1-B 1.614(2), C2-B 1613(3), S1-B 1.922(2), S2-B 1.921(2), C1-B-C2 118.4(1), S1-B-S2 66.06(6).

2.3.2 Reaction of [(Cp)(OC)$_2$Mn=B(IMe)*t*Bu] (90) with an excess of Se (gray)

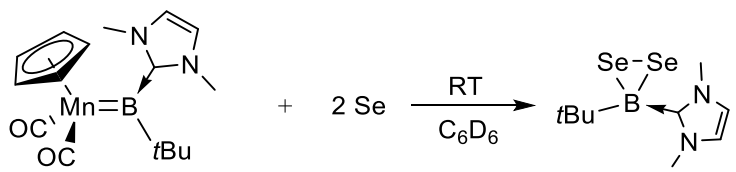

90 **95**

Figure 53. Synthesis of **95** from [(Cp)(OC)$_2$Mn=B(IMe)*t*Bu] (**90**) and three equivalents of Se.

Compound **90** was also reacted with excess Se. Gray selenium (3 equiv.) was added to a C_6D_6 solution of **90** in a Young NMR tube and the mixture was kept at room temperature (**Figure 54**). After 24 h, the ^{11}B NMR spectrum of the mixture displayed a new resonance at $\delta_B = -2.9$, with the signal associated with the starting material having completely disappeared. After workup, [*cyclo*-SeSeB*t*Bu(IMe)] **95** was isolated as violet crystals in high yield (80%) and a ^1H NMR spectrum showed corresponding resonances for all of the protons of the expected structure. The ^{77}Se NMR resonance of **95** was found to be at $\delta_{Se} = 250$. The constitution was further confirmed by elemental analysis and the solid state structure was authenticated through single-crystal X-ray diffraction analysis. All the experimental evidence confirmed that **95** is the first isolated compound to feature a B-Se-Se three-membered ring.

Single crystals suitable for X-ray diffraction analysis were obtained from a saturated toluene/pentane solution of **95**. It crystallizes in the triclinic space group P-1 and the solid state structure of the compound is shown in **Figure 54**. The B-Se distances (2.074(2) and 2.072(2) Å) lie in the expected range for a B-Se single bond, and are similar to known compounds containing B-Se single bonds (1.960 – 2.13 Å).[163, 191-192] The B-Se distance is significantly elongated compared to **92** (B=Se: 1.882(3) Å). As in compound **94**, the B-Se-Se plane is perpendicular to the B-C1-C2 plane, with a dihedral angle of 88.25°.

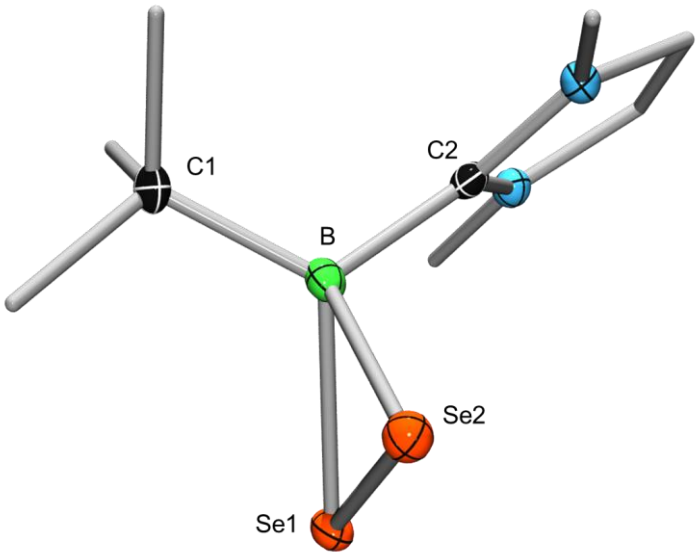

Figure 54. Molecular structure of **95**. Ellipsoids drawn at the 50% probability level. Hydrogen atoms and the ellipsoids of some carbon atoms are not shown for clarity. Relevant bond lengths [Å] and angles [°]: C1-B 1.6183(3), C2-B 1.609(4), Se1-B 2.074(2), Se2-B 2.076(2), Se1-Se2 2.3556(3), C1-B-C2 119.1(2), Se1-B-Se2 69.18(8).

2.3.3 Reaction of [(Cp)(OC)$_2$Mn=B(IMe)*t*Bu] (90) with an excess of Te

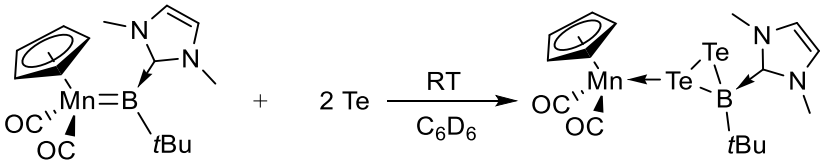

90 **96**

Figure 55. Synthesis of **96** from [(Cp)(OC)$_2$Mn=B(IMe)*t*Bu] (**90**) and three equivalents of Te.

Due to the successful synthesis of cyclic dichalcogenides [*cyclo*-SSB*t*Bu(IMe)] (**94**) and [*cyclo*-SeSeB*t*Bu(IMe)] (**95**), we reacted the base-stabilized borylene **90** with elemental tellurium in order to form a BTe$_2$ heterocycle. To this end, three equivalents of Te were added to a C$_6$D$_6$ solution of **90** in a Young NMR tube and the reaction was

monitored by multinuclear NMR spectroscopy (**Figure 55**). Compared to S and Se in the two reactions mentioned above, Te is found to be less reactive at ambient temperature and longer reaction times are needed. Indeed, after 24 h at room temperature, a resonance at δ_B = 77.2 in the ^{11}B NMR spectrum corresponds to the main product and was identified as [(Cp)(OC)$_2$Mn-Te=B*t*Bu(IMe)] (**93**). A small peak at δ_B = –1.99, however, was also observed, which is in the same range as those of [*cyclo*-SeSeB*t*Bu(IMe)] (**94**) and [*cyclo*-SSB*t*Bu(IMe)] (**95**). The mixture was kept at room temperature for a longer time (120 h in total) for the starting material to fully convert to the target cyclic boron ditellurium. After workup, [(Cp)(OC)$_2$Mn{κ^1-*cyclo*-TeTeB(*t*Bu)(IMe)}] (**96**) was isolated as pure dark-violet crystals in moderate yield (46%). Consistent with the fact that the boraditellurirane fragment remains coordinated to the manganese center, the ^{1}H NMR spectrum showed a characteristic resonance at δ_H = 4.23, which is associated with the Cp ligand on manganese [(Cp)Mn(CO)$_2$]. This indicates that the manganese moiety remains in the molecule. On the other hand, the ^{1}H NMR spectrum showed two sets of signals for symmetrical protons in the IMe ligand: NCHCHN (δ_H = 5.80, 5.69) and N(CH$_3$)$_2$ (δ_H = 3.70, 3.17) and a signal at δ_C = 235 in its ^{13}C NMR spectrum provide more evidence for the remaining Mn moiety. These facts clearly indicate a structural difference from **94** and **95**, which do not contain the manganese moiety. The constitution of **96** was further confirmed by elemental analysis.

Single crystals of **96** suitable for X-ray diffraction analysis were obtained from saturated toluene/pentane solution. The complex crystallizes in the monoclinic space group $P2_1/c$. As is predicted from multinuclear NMR spectra, the manganese moiety [(Cp)Mn(CO)$_2$] is still connected to one tellurium in the BTe$_2$ ring in this molecule. The B-Te distances (2.333(2) Å and 2.296 (3) Å) are significantly longer than in **93** (2.100(4) Å), which is consistent with the presence of a B-Te single bond. This is also consistent with an authentic B-Te single bond (2.360(3) Å) reported by Braunschweig.[192] The Te-Mn bond length (2.5476(8) Å) is comparable to that of **93** (2.5981(4) Å), corresponding to a similar Te→Mn coordination interaction. Therefore,

it is reasonable to identify this compound as a datively-bound acid-base adduct of [(Cp)Mn(OC)$_2$] and [*cyclo*-TeTeB*t*Bu(IMe)] (**Figure 56**). In this case, this intriguing [*cyclo*-TeTeB*t*Bu(IMe)] ligand represents the first example of a three-membered cyclic ditelluride of a main group element. The molecule was also studied computationally, calculations indicating near-unity WBIs across the whole B-Te-Te cycle, the calculated bond orders being consistent with single covalent bonding (B-Te = 0.8942, B-Te2 = 0.9957, Te1-Te2 = 0.8722).

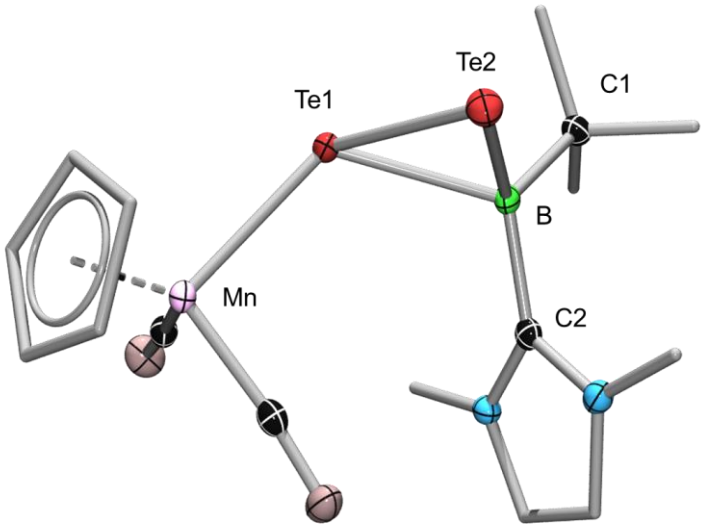

Figure 56. Molecular structure of **96**. Ellipsoids drawn at the 50% probability level. Hydrogen atoms and the ellipsoids of some carbon atoms are not shown for clarity. Relevant bond lengths [Å] and angles [º]: C1-B 1.692(3), C2-B 1.598(3), Te2-B 2.296(3), Te1-B 2.333(2), Mn-Te1 2.5476(8), C1-B-C2 116.1(2), Te1-B-Te2 73.02(7), Mn-Te1-B 119.39(6).

2.3.4 Reaction of [(Cp)(OC)$_2$Mn{κ^1-*cyclo*-TeTeB(*t*Bu)(IMe)}] (96) with PMe$_3$

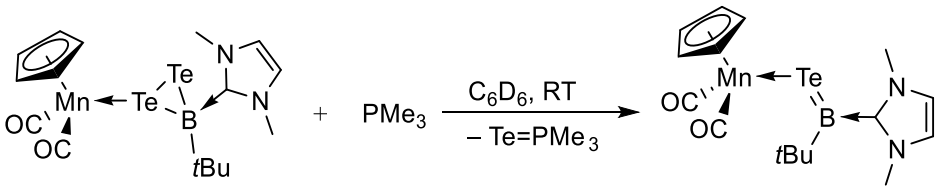

96 **93**

Figure 57. Reaction of **96** with PMe$_3$ to form [(Cp)(OC)$_2$Mn-Te=B*t*Bu(IMe)] (**93**).

In contrast to [*cyclo*-SSB*t*Bu(IMe)] (**94**) and [*cyclo*-SeSeB*t*Bu(IMe)] (**95**), the manganese moiety [(Cp)Mn(CO)$_2$] is still connected to the three-membered ring in compound **96**. In attempts to liberate the B-Te-Te ligand from the metal moiety, PMe$_3$ was reacted with **96** (**Figure 57**). To a Young NMR tube, one equivalent of PMe$_3$ was added to a C_6D_6 solution of **96**. The reaction was carried out at room temperature and monitored by multinuclear NMR spectroscopy. After 12 h, the ^{11}B NMR spectrum showed a new resonance at δ_B = 77.3, which is similar to that of [(Cp)(OC)$_2$Mn-Te=B*t*Bu(IMe)] (**93**) and the color of the solution changed from dark violet to dark red. After workup, [(Cp)(OC)$_2$Mn-Te=B*t*Bu(IMe)] (**93**) was isolated as a dark red crystalline solid. Moreover, the ^{1}H and ^{13}C NMR spectra of the pure compound showed similar resonances as **93**. In conclusion, PMe$_3$ had removed one tellurium atom from **96**, leading to the generation of **93**.

2.3.5 Reaction of [*cyclo*-SSB*t*Bu(IMe)] (94) with PMe$_3$

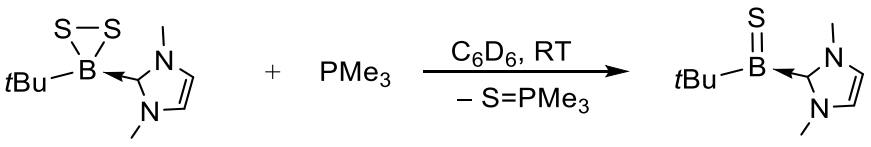

94 **97**

Figure 58. Synthesis of **97** from [*cyclo*-SSB*t*Bu(IMe)] and PMe$_3$.

Due to the result described in **2.3.5**, we assumed that it would be promising to use

Lewis bases to abstract the S or Se from compounds [*cyclo*-SSB*t*Bu(IMe)] (**94**) and [*cyclo*-SeSeB*t*Bu(IMe)] (**95**) to achieve the formation of metal-free borachalcones [E=B*t*Bu(IMe)] (E = S, Se). To this end, 1.2 equivalents of PMe_3 were added to a solution of **94** in a Young NMR tube (**Figure 58**). The reaction mixture was kept at room temperature and monitored by multinuclear NMR spectroscopy. After 30 min at room temperature, the ^{11}B NMR resonance of the starting material (δ_B = –7.8) was completely replaced by a new resonance at δ_B = 66.4. This resonance is similar to that of **91**, which suggests a boron atom in a similar bonding environment. In this case, however, the borachalcone cannot be bound to a metal center, because the starting material does not contain a [(Cp)Mn(CO)$_2$] moiety. Additionally, the ^{31}P NMR spectrum shows a resonance at δ_P = 27.2, which indicates the formation of S=PMe_3. This fact indicates that PMe_3 has abstracted one sulfur atom from the BS_2 heterocycle. The workup was carried out at –30 ºC due to the possible oligomerization side reaction. [S=B*t*Bu(IMe)] (**97**) was isolated as white crystals in moderate yield (62%). Its constitution was confirmed by ^1H, ^{11}B and ^{13}C NMR spectroscopy and elemental analysis.

Compound **97** crystallizes in the monoclinic space group *P2$_1$/c* from a saturated toluene/pentane solution at –30 ºC, and its solid state structure is shown in **Figure 59**. The B-S distance (1.739(2) Å) is nearly the same as that of **91** (1.747(3) Å), indicating the double bond nature of the B-S interaction. The boron atom is coordinated in a planar fashion, with its sum of angles being close to 360°.

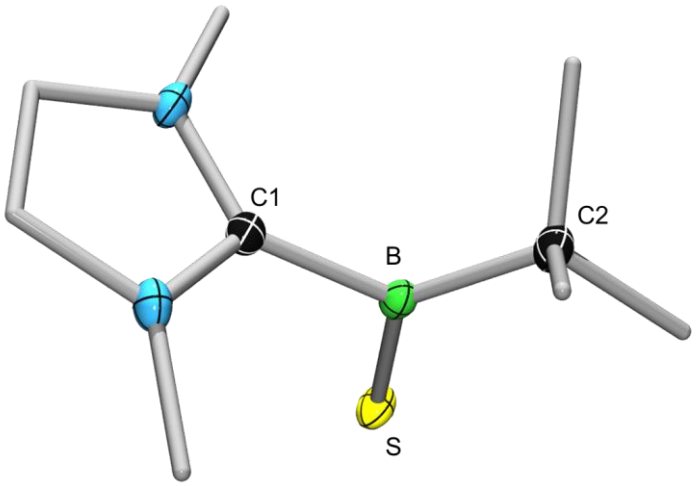

Figure 59. Molecular structure of **97**. Ellipsoids drawn at the 50% probability level. Hydrogen atoms and the ellipsoids of some carbon atoms are not shown for clarity. Relevant bond lengths [Å] and angles [º]: C1-B 1.609(2), C2-B 1.599(3), S-B 1.739(2), C1-B-C2 116.7(1), S-B-C1 115.1(1), S-B-C2 128.2.

Interestingly, even though **97** is stable in the solid state at room temperature, changes in the ^{11}B NMR spectrum could be observed at room temperature upon dissolution in toluene. To investigate this transformation further, a C_6D_6 solution of **97** was added to a Young NMR tube and the solution was monitored by multinuclear NMR spectroscopy. The mixture was heated to 60 ºC, leading to the total consumption of the starting material within 24 h. At the same time, a much high field shifted resonance from ^{11}B NMR spectrum (δ_B = –4.6) appeared, which indicated the formation of a four-coordinated boron species. After workup, [*cyclo*-{(IMe)(*t*Bu)B-S-B(IMe)(*t*Bu)-S}] (**98)** was isolated as a white powder. Single-crystal X-ray diffraction analysis allowed elucidation of the structure of **98** as a dimer of the borasulfone **97** (**Figure 61**).

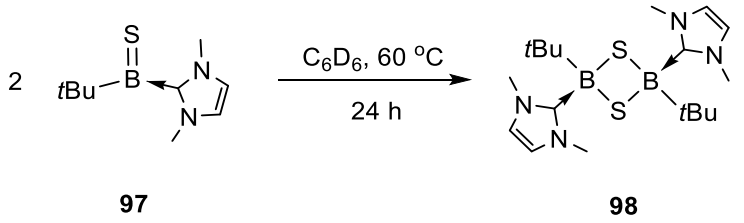

97 **98**

Figure 60. Synthesis of **98** via thermal dimerization of [S=B*t*Bu(IMe)] (**97**).

Single crystals suitable for X-ray diffraction analysis were obtained from a saturated toluene solution of **98** at room temperature. The molecule crystallizes in the triclinic space group P-1 and its solid state structure clearly shows the formation of a four-membered ring from the dimerization of **97**. According to the data, the two boron and two sulfur atoms in the four-membered ring are coplanar, with a B-S-B-S torsion angle of 0.0°. Moreover, the dihedral angles between the two B-C-C planes and the four-membered ring are near 90° (both 88.5°), which indicates that the B-C-C planes are perpendicular to the four-membered ring.

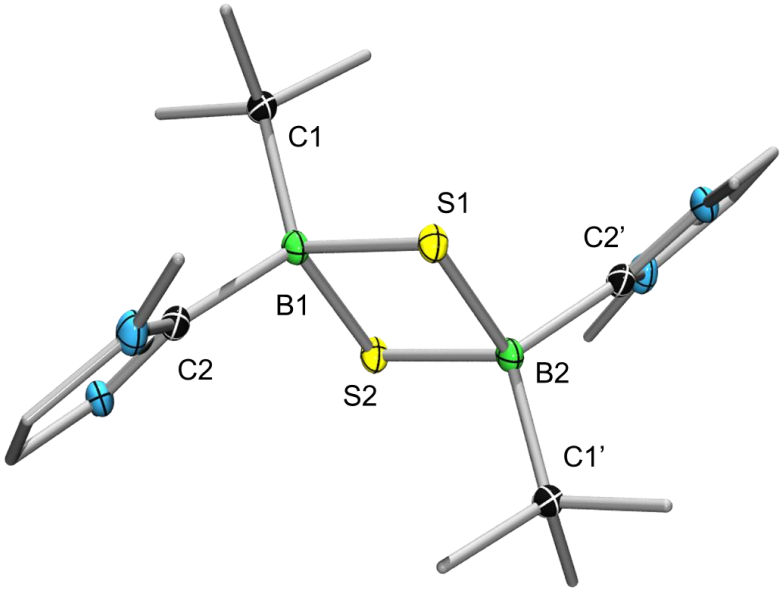

Figure 61. Molecular structure of **98**. Ellipsoids drawn at the 50% probability level. Hydrogen atoms and the ellipsoids of some carbon atoms are not shown for clarity. Relevant bond lengths [Å] and angles [°]: C1-B1=C1'-B2 1.648(3), C2-B1=C2'-B2 1.647(4), B1-S1=B2-S2 1.955(3), B1-S2=B2-S1 1.947(3), C1-B1-C2=C1'-B2-C2' 112.4(2), S1-B1-S2=S1-B2-S2 94.5(1), B1-S1-B2=B1-S2-B2 85.5(1).

2.3.6 Reaction of [*cyclo*-SeSeB*t*Bu(IMe)] (95) with PMe_3

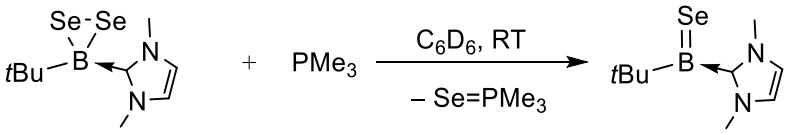

95 **99**

Figure 62. Synthesis of **99** from [*cyclo*-SeSeB*t*Bu(IMe)] (**95**) and PMe_3.

Similarly to **94**, PMe_3 can also abstract a selenium atom from [*cyclo*-SeSeB*t*Bu(IMe)] (**95**) and lead to the formation of a metal-free borachalcone. The reaction was carried out under same conditions as described in **chapter 2.3.4** and monitored by multinuclear NMR spectroscopy (**Figure 62**). It can be observed from the ^{11}B NMR spectrum that the resonance of **95** (δ_B = –2.9) was replaced by a new resonance at δ_B = 73.5 after 20 min at room temperature. To prevent dimerization, all workup

procedures were carried out at –30 ºC. After purification, [Se=B*t*Bu(IMe)] (**99**) was isolated as a pure white crystalline solid and the constitution of the compound was confirmed by ^{1}H, ^{11}B and ^{13}C NMR spectroscopy and elemental analysis. The solid state structure of **99** was confirmed by X-ray diffraction analysis. Single crystals suitable for X-ray diffraction analysis were obtained from a saturated toluene/pentane solution of pure **99** at –30 ºC (**Figure 63**). The molecule crystallizes in the monoclinic space group $P2_1/n$. The B-Se bond length (1.873(5) Å) is the same as **92** (1.882(3) Å) within experimental uncertainty, which indicates the double bond nature of the B=Se interaction.

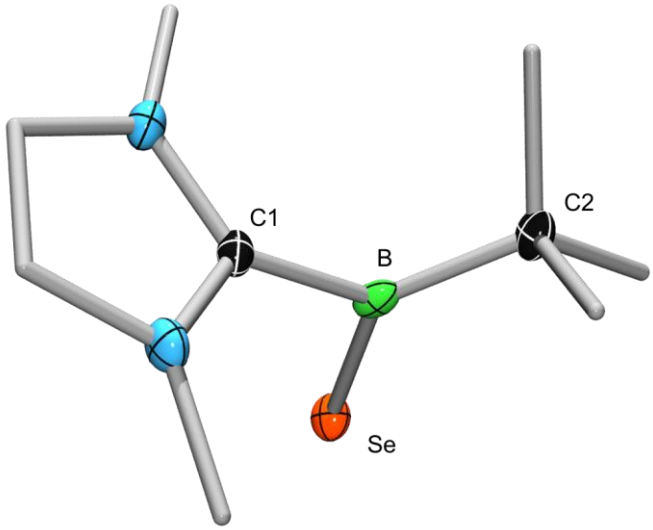

Figure 63. Molecular structure of **99**. Ellipsoids drawn at the 50% probability level. Hydrogen atoms and the ellipsoids of some carbon atoms are not shown for clarity. Relevant bond lengths [Å] and angles [º]: C1-B 1.601(5), C2-B 1.588(7), Se-B 1.873(5), C1-B-C2 117.6(3), C1-B-Se 114.4(3), C2-B-Se 128.0(3).

Compound **99** can also dimerize to form a four-membered ring, but at a much slower rate. Full conversion requires 24 h at elevated temperature (60 ºC) (**Figure 64**). From the ^{11}B NMR spectrum, a resonance at δ_B = –13.6 is found to replace the signal at δ_B = 73.5, corresponding to the starting material. After workup, [*cyclo*-{(IMe)(*t*Bu)B-Se-B(IMe)(*t*Bu)-Se}] (**100**) was isolated as a white powder.

Single crystals suitable for X-ray diffraction analysis were obtained under the same conditions as for compound **98** (**Figure 65**). The molecule crystallizes in the triclinic space group P-1. Like **98**, the four-membered ring of **100** is also coplanar and perpendicular to the two B-C-C planes.

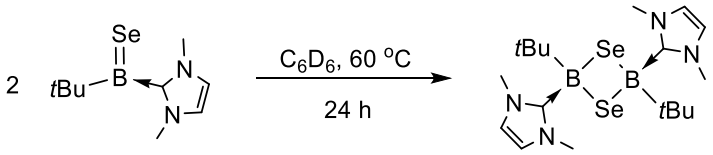

99 **100**

Figure 64. Synthesis of **100** by the dimerization of [Se=B*t*Bu(IMe)] (**99**).

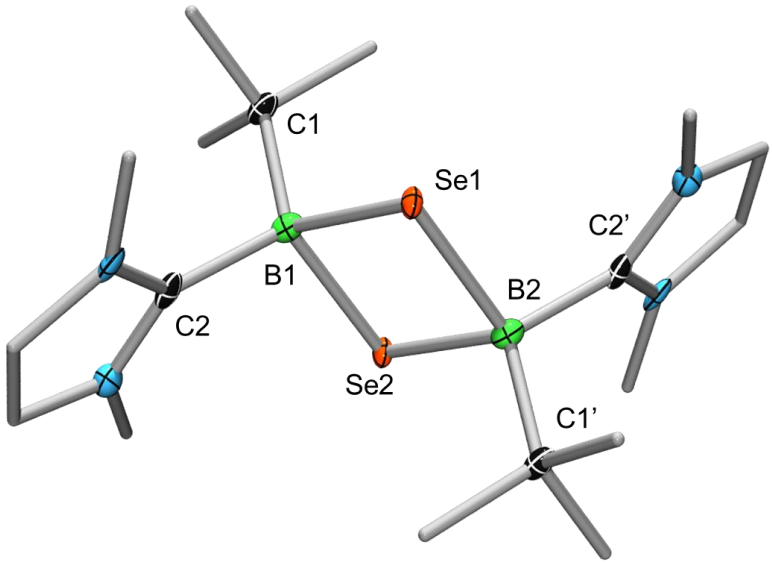

Figure 65. Molecular structure of **100**. Ellipsoids drawn at the 50% probability level. Hydrogen atoms and the ellipsoids of some carbon atoms are not shown for clarity. Relevant bond lengths [Å] and angles [º]: C1-B1=C1'-B2 1.643(9), C2-B1=C2'-B2 1.64(1), B1-Se1=B2-Se2=B1-Se2=B2-Se1 2.09(1), C1-B1-C2=C1'-B2-C2' 112.8(7), Se1-B1-Se2=Se1-B-Se2 93.9(4), B1-Se1-B2=B1-Se2-B2 86.1(4).

In conclusion, we were able to isolate complexes that feature B-E-E (**94**, **95** and **96**) (E = S, Se and Te) cycles by addition of an excess of chalcogens to [(Cp)(OC)$_2$Mn=B(IMe)*t*Bu] (**90**). In contrast to the reaction with Te, **94** and **95** are spontaneously released from the metal center as metal-free cyclic boron

dichalcogenides. In the case of tellurium, the three-membered ring unit remains connected to [(Cp)Mn(CO)$_2$] as a donor ligand. Furthermore, one chalcogen can be liberated from the three-membered cycles (**94** and **95**) by PMe_3 and forms metal-free borachalcone species (**97** and **99**) (with B=E bonds), which slowly dimerize to four-membered cycles (**98** and **100**). This study highlights the potential of hypovalent boron compounds, especially transition metal borylene complexes, to function as the starting point for unusual and innovative chalcogen chemistry.

2.4 Reactivity of borylene complexes with B-E-E (E = S, Se, Te) cyclic boron dichalcogenides

The first isolated five-membered heterocyclic boron chalcogenides $R_2B_2S_3$ date back to 1964 and were reported by Schmidt and Siebert.[161] Since then, other five-membered heterocyclic B_2S_3 rings (**Figure 27**) featuring different substituents have been synthesized by different groups.[201-203] In 1986, Nöth and Rattay reported the preparation of a phenyl-substituted B_2S_2 four-membered ring (**Figure 27**).[162] In the case of selenium, few examples that feature four- or five-membered boron-containing rings have been reported. The first cyclic B_2Se_2 (**Figure 27**) was isolated in 1985 by Nöth and coworkers.[204] Most recently, Braunschweig and coworkers have reported the synthesis of four-membered B_2E_2 (E=S, Se) rings by reacting a tetrameric cyanoborylene species with elemental chalcogens.[163]

However, in all of the aforementioned cases, the heterocyclic rings are symmetrically substituted molecules. With the aim of providing deeper chemical knowledge and to open new chemical space, it is of great importance to discover a synthetic route for unsymmetrical analogues of these heterocyclic systems. In **chapter 2.3**, the synthesis of several B-E-E three-membered cyclic boron dichalcogenide compounds is mentioned. In this case, borylenes were considered to be potential reagents to react with these boron dichalcogenides to form unsymmetrical heterocyclic boron chalcogen compounds of the form cyclo-RB_2E_nR' (n = 2 or 3 and $R \neq R'$).

2.4.1 Reaction of [*cyclo*-SSB*t*Bu(IMe)] (94) with [(OC)$_5$Mo=BN(SiMe$_3$)$_2$] (20)

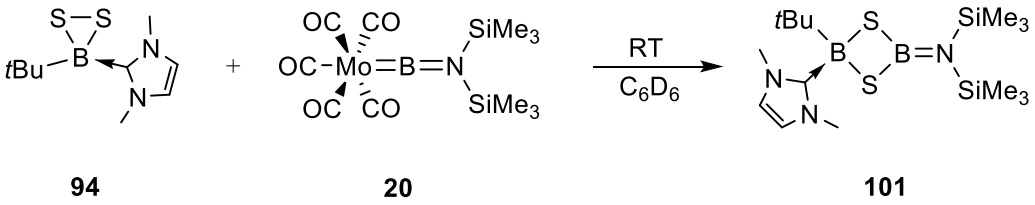

94 **20** **101**

Figure 66. Synthesis of **101** from [*cyclo*-SSB*t*Bu(IMe)] (**94**) with [(OC)$_5$Mo=BN(SiMe$_3$)$_2$] (**20**).

With the aim of synthesizing unsymmetrical boron-chalcogen heterocyclic rings, [*cyclo*-SSB*t*Bu(IMe)] (**94**) was first reacted with [(OC)$_5$Mo=BN(SiMe$_3$)$_2$] (**20**). To this end, one equivalent of **20** was added to a C_6D_6 solution of **90** in a Young NMR tube (**Figure 66**). The reaction was carried out at room temperature and monitored by multinuclear NMR spectroscopy. After 8 h, the ^{11}B NMR spectrum revealed two new resonances (δ_B: = –6.1 and 49.8) along with the disappearance of the starting materials (δ_B = –7.8 and 91). Compared to the borylene compound **20** (δ_B = 91), the new ^{11}B NMR resonance at δ_B = 49.8 is strongly upfield shifted, which is consistent with the formation of a new tricoordinate boron species. On the other hand, the resonance at δ_B = –6.1, which is slightly downfield shifted than that of compound **94** (δ_B = –7.8), indicates the formation of a tetracoordinate boron center similar to that of **94**. After workup, [*cyclo*-{(*t*Bu)(IMe)B-S-B(N(SiMe$_3$)$_2$)-S)}] (**101**) was isolated as colorless crystals and the ^{1}H and ^{13}C NMR spectra displayed all relevant signals in the expected range. The constitution of **101** was also confirmed by HRMS.

In order to further confirm the structure of the **101**, single crystals suitable for X-ray diffraction analysis were obtained from a saturated toluene/pentane solution at –30 °C (**Figure 67**). The molecule crystallizes in the triclinic space group P-1. The B-S bond lengths are in the typical range of B-S single bonds. However, compared to the symmetrical B-S four-membered ring compound **98**, this molecule shows different B-S bond lengths to the two different boron centers. From the data we can see that the

B-S bonds to the tetracoordinate boron atom B1 (B1-S1: 1.990(3) Å, B1-S2: 1.998(4) Å) are much longer than the B-S bonds to B2 (B2-S1: 1.844(4) Å, B2-S2: 1.855(3) Å). Compared to those of the starting material **94**, the corresponding B-S bonds are slightly elongated. The torsion angle of B1-S1-S2-B2 is –0.4(2)°, which indicates that the four atoms in the four-membered ring of **101** are coplanar. On the other hand, the dihedral angle between the B1-C1-C2 and B1-S1-S2-B2 planes is ca. 89°, indicating that they are mutually perpendicular. This compound additionally represents the first example of a B-E-B-E cycle with an unsymmetrical substitution pattern.

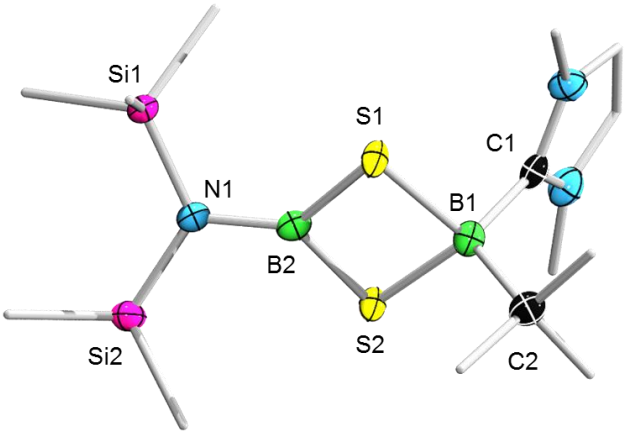

Figure 67. Molecular structure of **101**. Ellipsoids drawn at the 50% probability level. Hydrogen atoms and the ellipsoids of some carbon atoms are not shown for clarity. Relevant bond lengths [Å] and angles [º]: B1-S1 1.990(3), B1-S2 1.998(4), B2-S1 1.844(4), B2-S2 1.855(3), S1-B1-S2 104.0(2), S1-B2-S2 94.0(2), B2-S1-B1 80.8(2), 81.2(2).

2.4.2 Reaction of [*cyclo*-SSB*t*Bu(IMe)] (94) with [(Cp)(OC)$_2$Mn=B*t*Bu] (43)

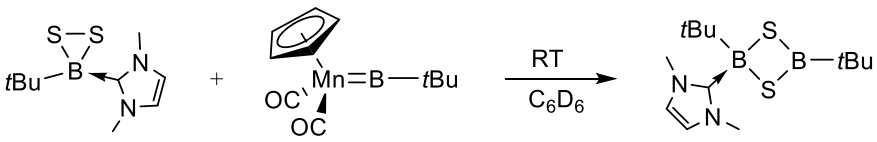

94 **43** **102**

Figure 68. Synthesis of **102** from [*cyclo*-SSB*t*Bu(IMe)] (**94**) with [(Cp)(OC)$_2$Mn=B*t*Bu] (**43**).

The success in synthesizing the unsymmetrical species **101** motivated us to extend this synthetic method to other targets. In order to introduce boron atoms with different substituents, other borylene complexes were reacted with the boradithiirane [*cyclo*-SSB*t*Bu(IMe)] (**94**). Thereby, a C_6D_6 solution of manganese borylene **43** was treated with one equivalent of **90** in a Young NMR tube. The reaction was carried out at room temperature and monitored by multinuclear NMR spectroscopy. As in the synthesis of compound **101**, the ^{11}B NMR spectrum revealed new resonances at δ_B = – 3.6 and 72.9, replacing the signals of the starting materials (δ_B = –7.8 and 144). Through a similar workup process to **101**, [*cyclo*-{(*t*Bu)(IMe)B-S-B(*t*Bu)-S}] (**102**) was obtained as a white powder, which was determined to be an analytically pure product. The ^1H NMR spectrum of **101** showed two singlets at δ_H = 1.46 (s, 9H, C*H*$_3$-B*t*Bu) and 1.27 (s, 9H, C*H*$_3$-B(IMe)*t*Bu) revealing a 1:1 ratio corresponding to two inequivalent *t*Bu groups. Furthermore, the resonances at δ_H = 5.23 (s, 2H, NC*H*C*H*N) and 3.34 (s, 6H, N-C*H*$_3$) assignable to the IMe ligand also indicated the predicted constitution of **102**. The constitution was also confirmed by high-resolution mass spectroscopy (HRMS; calcd. [M^+ –*t*Bu]: *m/z* = 239.1014; found: *m/z* = 239.1001 [M^+ – *t*Bu]). However, the solid state structure could not be confirmed by X-ray diffraction analysis as all attempts to isolate suitable single crystals were unsuccessful.

2.4.3 Reaction of [*cyclo*-SSB*t*Bu(IMe)] (94) with [(OC)$_5$Cr=BTp] (22)

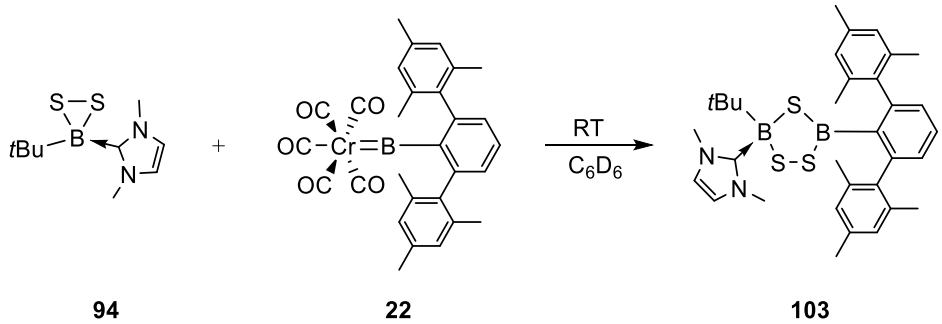

94 22 103

Figure 69. Synthesis of **103** from the reaction of [*cyclo*-SSB*t*Bu(IMe)] (**94**) with [(OC)$_5$Cr=BTp] (**22**).

Continuing this study, one equivalent of [(OC)$_5$Cr=BTp] (Tp = 2,6-bis(2,4,6-trimethylphenyl)phenyl) (**22**) was added to a C_6D_6 solution of **90** in a Young NMR tube. The reaction was performed at room temperature and monitored by multinuclear NMR spectroscopy. After 24 h, the ^{11}B NMR spectrum showed two new resonances at δ_B = 7.8 and 66.2, which were in the same range as those associated with compound **101**. After workup, [*cyclo*-{(*t*Bu)(IMe)B-SS-B(Tp)-S}] (**103**) was obtained as colorless needles. Although ^{1}H NMR spectroscopy showed appropriate signals for all of the hydrogen atoms of the substituents at boron, HRMS analysis revealed a molecular formula for the product which was consistent with the presence of a five-membered ring containing three sulfur atoms instead of a four-membered ring as in **102**. In order to further confirm the structure of the product, single crystals suitable for X-ray diffraction analysis were obtained from a saturated THF/pentane solution of **103**. From these, the solid state structure of **103** was elucidated (**Figure 69**), confirming the five-membered ring feature of **103**. However, the quality of the data was not sufficient for detailed discussion of structural parameters for this molecule.

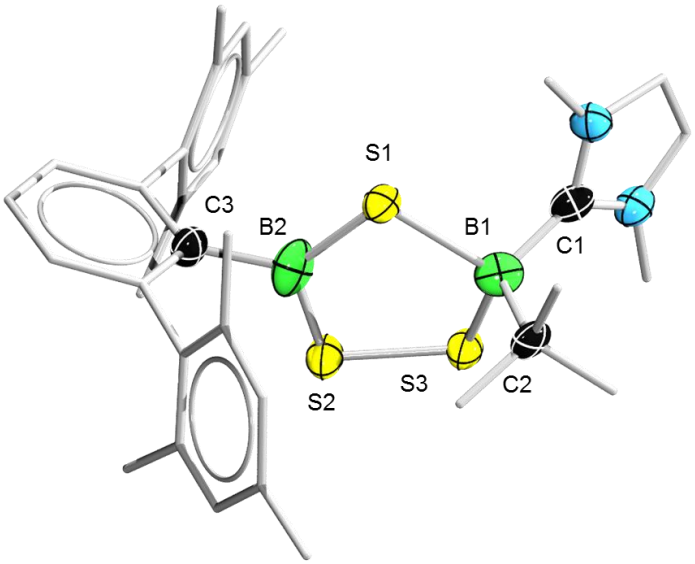

Figure 70. Molecular structure of **103**. Ellipsoids drawn at the 50% probability level. Hydrogen atoms and the ellipsoids of some carbon atoms are not shown for clarity. The quality of the diffraction data was not sufficient for detailed discussion of structural parameters.

2.4.4 Reaction of [*cyclo*-SSB*t*Bu(IMe)] (94) with cyanoborylene [(cAAC)B(CN)]$_4$ (104)

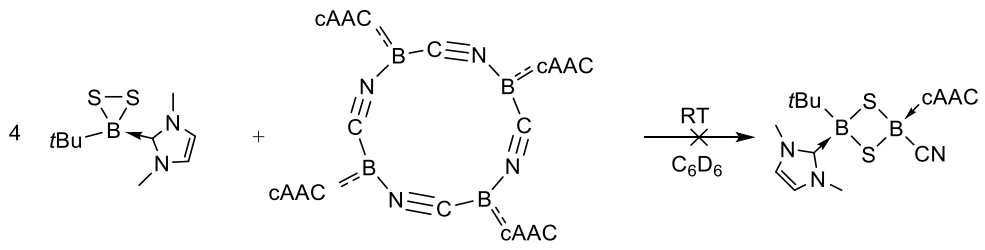

94 **104**

Figure 71. The reaction between [*cyclo*-SSB*t*Bu(IMe)] **94** and [(cAAC)B(CN)]$_4$ (cAAC = 1-(2,6-di*i*sopropylphenyl)-3,3,5,5-tetramethylpyrrolidine-2-ylidene) (**104**).

In 2018, the group of Braunschweig reported a reaction of a tetrameric cyanoborylene [(cAAC)B(CN)]$_4$ (**104**) with sulfur to form a four-membered B-S-B-S ring. Since this reaction bore similarities with the reactivity of transition metal borylenes, we used **104** in a reaction with **94** (4:1 equiv.). The reaction was carried out at room temperature and monitored by multinuclear NMR spectroscopy. After 24 h, the ^{11}B NMR spectrum showed several new resonances at around δ = 0 and all attempts to isolate any pure products were unsuccessful.

2.4.5 Reaction of [*cyclo*-SeSeB*t*Bu(IMe)] (95) with [(OC)$_5$Mo=BN(SiMe$_3$)$_2$] (20)

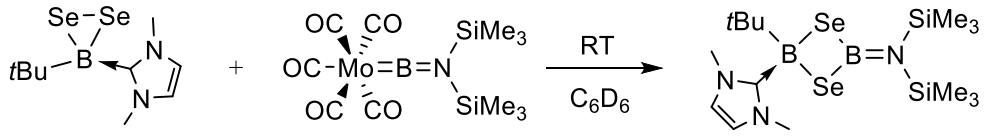

95 **20** **105**

Figure 72. Synthesis of **105** from the reaction of [*cyclo*-SeSeB*t*Bu(IMe)] (**95**) with [(OC)$_5$Mo=BN(SiMe$_3$)$_2$] (**20**).

Extending this chemistry to boron selenides, [*cyclo*-SeSeB*t*Bu(IMe)] (**95**) was combined with various borylene complexes with the goal of synthesizing

unsymmetrical heterocyclic boron chalcogen compounds. First, **95** was reacted with one equivalent of [(OC)$_5$Mo=BN(SiMe$_3$)$_2$] (**20**) in a Young NMR tube. After 24 h at room temperature, the color of the solution had changed from violet to light yellow. The ^{11}B NMR spectrum revealed new resonances at δ_B = –13.4 and 46.7, which are in the same range as those of [*cyclo*-{(*t*Bu)(IMe)B-S-B(N(SiMe$_3$)$_2$)-S)}] (**101**), and thus fit well to a Se analogue thereof. Moreover, both ^{1}H and ^{13}C NMR spectra showed appropriate signals for the corresponding nuclei. After workup, compound **105** was isolated as pure colorless crystals in a moderate yield (52%). The constitution of **105** was further confirmed by HRMS.

Single crystals suitable for X-ray diffraction analysis were obtained from a saturated toluene/pentane solution of **105,** which allowed us to confirm the four-membered B-Se-B-Se heterocyclic structure of **105**. The molecule crystallizes in the monoclinic space group P2$_1$/n. It shows similar unsymmetrical features as **104**, which has different B-Se bond lengths within the four-membered ring. The atoms of the four-membered ring are also coplanar (B1-Se1-Se2-B2: 6.2(2)°). Moreover, compared to **95**, the corresponding B-Se bonds are slightly elongated. A slight pyramidalization of the N(SiMe$_3$)$_2$ group, as well as dihedral angles of *ca.* 35° between this group and the B$_2$Se$_2$ ring, and a B-N bond distance of 1.442(7) Å (longer than 1.3549(18) Å in **20**), suggest only a small amount of N-to-B π donation.

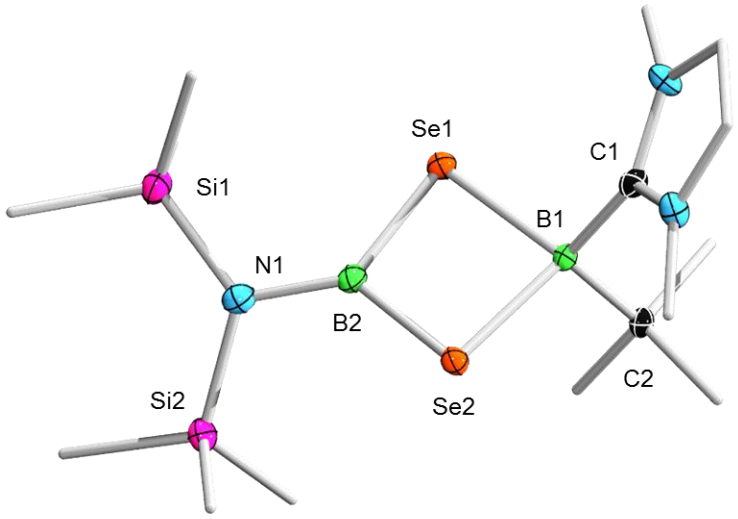

Figure 73. Molecular structure of **105**. Ellipsoids drawn at the 50% probability level. Hydrogen atoms and the ellipsoids of some carbon atoms are not shown for clarity. Relevant bond lengths [Å] and angles [º]: B1-Se1 2.116(5), B1-Se2 2.112(5), B2-Se1 1.957(5), B2-Se2 1.958(5), Se1-B1-Se2 92.8(2), B1-Se2-B2 81.7(2), Se2-B2-Se1 102.9(2), B2-Se1-B1 81.8(2), B1-Se1-Se2-B2 6.2(2).

2.4.6 Reaction of [*cyclo*-SeSeB*t*Bu(IMe)] (95) with [(Cp)(OC)$_2$Mn=B*t*Bu] (43)

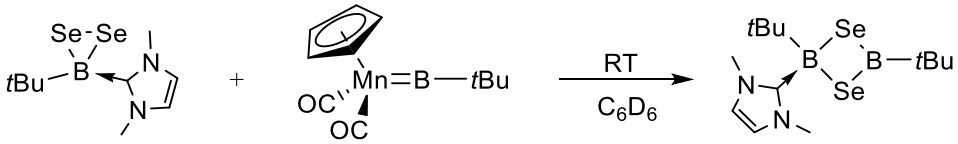

95 **43** **106**

Figure 74. Synthesis of **106** from reaction of [*cyclo*-SeSeB*t*Bu(IMe)] (**95**) with [(Cp)(OC)$_2$Mn=B*t*Bu] (**43**).

Next, one equivalent of manganese borylene complex **43** was treated with a C_6D_6 solution of diselenirane **95** in a Young NMR tube. The reaction was carried out at room temperature and monitored by multinuclear NMR spectroscopy. Similar to the reaction described in section **2.4.2**, the ^{11}B NMR spectrum showed new resonances at δ_B = –10.8 and 77.5, replacing the signals for the starting materials (δ_B = –2.9 and

144.1). Through same workup protocol as for **102**, a white powder was obtained, which was characterized as pure **106** [*cyclo*-{(*t*Bu)(IMe)B-Se-B(*t*Bu)-Se}] (**106**) (36% yield). All attempts to grow single crystals suitable for X-ray diffraction analysis were unsuccessful. Therefore, the solid state structure of **106** cannot be confirmed. However, the ^{1}H NMR spectra showed resonances at δ_H = 5.29 (s, 2H, NC*H*C*H*N), 3.30 (s, 6H, N-CH_3), 1.44 (s, 9H, CH_3-B*t*Bu), 1.34 (s, 9H, CH_3-B(IMe)*t*Bu) revealing a 1:1:1 ratio of IMe and two equivalents *t*Bu groups. The constitution was also confirmed by HRMS (calcd. [M^+ – *t*Bu]: *m/z* = 334.9903; found: *m/z* = 334.9886 [M^+ – *t*Bu]).

2.4.7 Reaction of [*cyclo*-SeSeB*t*Bu(IMe)] (95) with [(OC)$_5$Cr=BTp] (22)

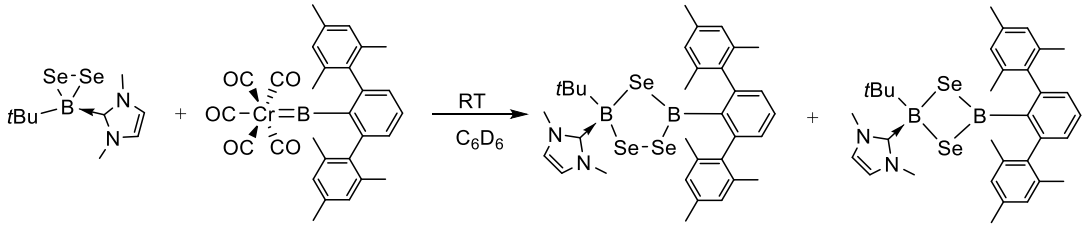

95 **22** **107** **107^b**

Figure 75. Synthesis of **107** from [*cyclo*-SeSeB*t*Bu(IMe)] and [(OC)$_5$Cr=BTp] (**22**).

A chromium borylene complex (**22**) with a bulky substitutent at boron was utilized in a reaction with diselenirane **95** to probe the versatility of this synthetic method. Equimolar amounts of compounds **95** and **22** were dissolved in C_6D_6 and were introduced to a Young NMR tube. The reaction was carried out at room temperature and monitored by multinuclear NMR spectroscopy. After 24 h, the ^{11}B NMR spectrum revealed new signals at δ_B = 6.2 and 72.1, which are reminiscent of [*cyclo*-{(*t*Bu)(IMe)B-SS-B(Tp)-S}] (**103**). After workup, [*cyclo*-{(*t*Bu)(IMe)B-SeSe-B(Tp)-Se}] (**107**) was isolated as a white powder in low yield (21.7%). Unlike the above-mentioned compounds, **107** is poorly soluble in C_6D_6. Therefore, deuterated THF (C_4D_8O) was used as a solvent for all NMR measurements.

Data from ^{1}H, ^{11}B and ^{13}C NMR spectroscopy and HRMS were consistent with the expected formula of **107**.

To further confirm the solid state structure of **107**, single crystals suitable for X-ray diffraction analysis were obtained from a saturated THF/pentane solution of **107**. The molecule crystallizes in the triclinic space group P-1. In the solid state, **107** is structurally comparable to the three previously reported examples of crystallographically characterized BSeBSeSe non-cluster five-membered rings. Interestingly, it represents, to the best of our knowledge, the first example of such a cycle with an unsymmetrical substitution pattern. The planar sp^2-hybridized TpB site features B-Se distances (1.919(5) and 1.921(4) Å) that are close to those reported by Nöth and coworkers[204] in a symmetrical five-membered ring of selenium and sp^2 boron. On the other hand, on the *t*Bu(IMe)B side of **107**, the bond distances (2.115(4) and 2.106(4) Å) are related to those found in triselena-1,3-diborolanes with sp^3 boron atoms. The five-membered BSeBSeSe ring is not coplanar and shows a slightly twisted geometry.

More interestingly, an analogous structure of **107** bearing a BSeBSe four-membered ring [*cyclo*-{(*t*Bu)(IMe)B-SeSe-B(Tp)}] (**107b**) was observed from this reaction. However, only a few crystals of it were obtained, which allowed us to determine its solid state structure and confirm its existence (**Figure 76**). The complex existed in the mother liquid after the crystallization of **107**. The molecule crystallized in the monoclinic space group $P2_1/n$. Compared to those of **107**, all the B-Se bond lengths are slightly elongated. Like **101** and **105**, the atoms of the four-membered ring are nearly coplanar, with a dihedral angle close to 0° (1.2(2)°). The isolation of pure 107b for further characterizations failed for the crystals were stuck in some brown oily side product.

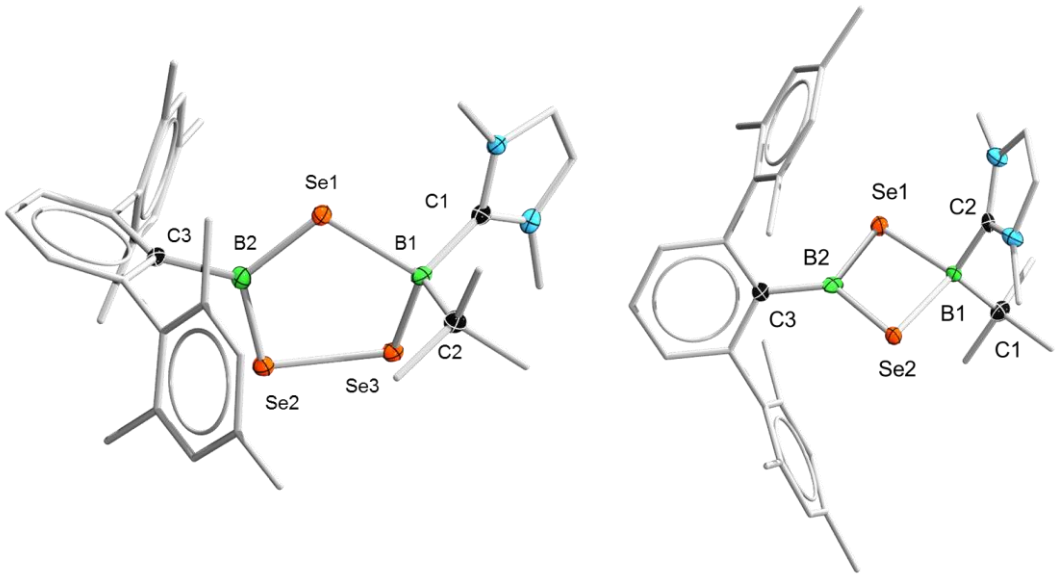

Figure 76 Molecular structures of **107** (left) and **107^{b}** (right). Ellipsoids drawn at the 50% probability level. Hydrogen atoms and the ellipsoids of some carbon atoms are not shown for clarity. Relevant bond lengths [Å] and angles [º] for **107**: B1-Se1 2.115(4), B2-Se1 1.919(5), B1-Se3 2.106(4), B2-Se2 1.921(4), Se2-Se3 2.3280(6), Se1-B2-Se2 119.4(3), Se1-B1-Se3 105.4(2), B1-Se1-B2 105.5(2), B1-Se3-Se2 102.7(1), Se3-Se2-B2 100.7(2); for **107^{b}**: B1-Se1 2.128(4), B2-Se1 1.924(4), B1-Se2 2.128(4), B2-Se2 1.932(4), Se1-B1-Se2 92.7(2), Se1-B2-Se2 105.6(2), B1-Se1-B2 81.1(2), B1-Se2-B2 80.6(2).

2.4.8 Reaction of [*cyclo*-SeSeB*t*Bu(IMe)] (95) with cyanoborylene tetramer [(cAAC)B(CN)]$_4$ (104)

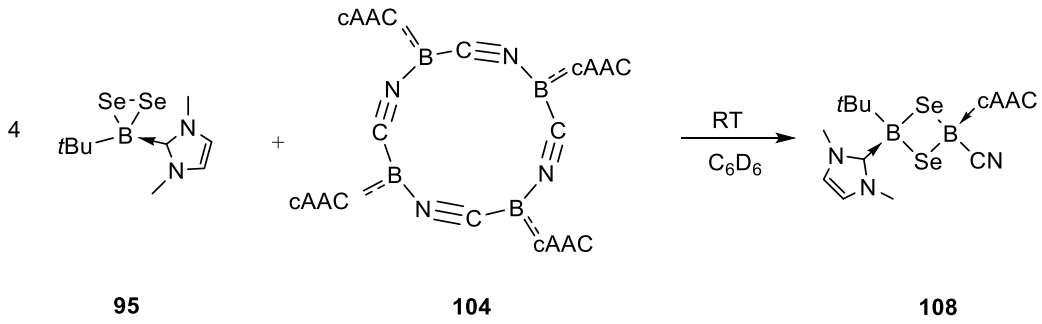

95 **104** **108**

Figure 77. Synthesis of **108** from reaction of [*cyclo*-SeSeB*t*Bu(IMe)] with [(cAAC)B(CN)]$_4$ (**104**).

The macrocyclic complex [*cyclo*-((cAAC)BCN)$_4$] (**104**) was previously shown to be a source of the monomeric borylene [(cAAC)BCN] in its reaction with Lewis bases.[163] Therefore, four equivalents of [*cyclo*-SeSeB*t*Bu(IMe)] (**95**) were added to a C_6D_6 solution of **95** in a Young NMR tube. The reaction was carried out at room temperature and was monitored by NMR spectroscopy. After 24 h at room temperature, the solution had turned from red to green and new resonances at δ_B = –9.5 and –32.8 indicated the formation of a new cyclic species related to compounds **101-103** and **105-107**. It is however trivial to assign the former to the *t*Bu(IMe)B group by comparison to the results described above, while the latter is similar to the signals of both isomers of the previously reported [*cyclo*-((cAAC)NCBSe)] (δ_B = –31.8 and –33.5). After workup, pure [*cyclo*-{(*t*Bu)(IMe)B-Se-B(cAAC)(CN)-Se}] (**108**) was isolated as red crystals in relatively low yield (34.2%). The constitution of **108** was confirmed by HRMS and ^{1}H, ^{11}B and ^{13}C NMR spectroscopy, as is shown in **Figure 76**. This compound is the first of the series herein reported to feature two unsymmetrically substituted sp^3-hybridized boron atoms.

To further confirm the solid state structure of the compound, single crystals suitable for X-ray diffraction analysis were obtained from a saturated toluene/pentane solution of **108**. Because both boron atoms in this molecule are sp^3-hybridized, the B-Se distances on the two different sides do not show large differences, in contrast to the aforementioned *cyclo*-BSe$_n$B compounds. Rather surprisingly, and in contrast with other 1,3-diselena-2,4-diboretes, **108** adopts a significantly bent butterfly structure in the solid state. This is clearly a result of the unsymmetrical substitution of the two boron atoms, which induces a large difference between the two faces of the cycle. The B-Se bond distances are slightly shorter on the (cAAC)(NC)B side (2.067(1) and 2.079(2) Å) than the *t*Bu(IMe)B side (2.114(1) and 2.114(2) Å).

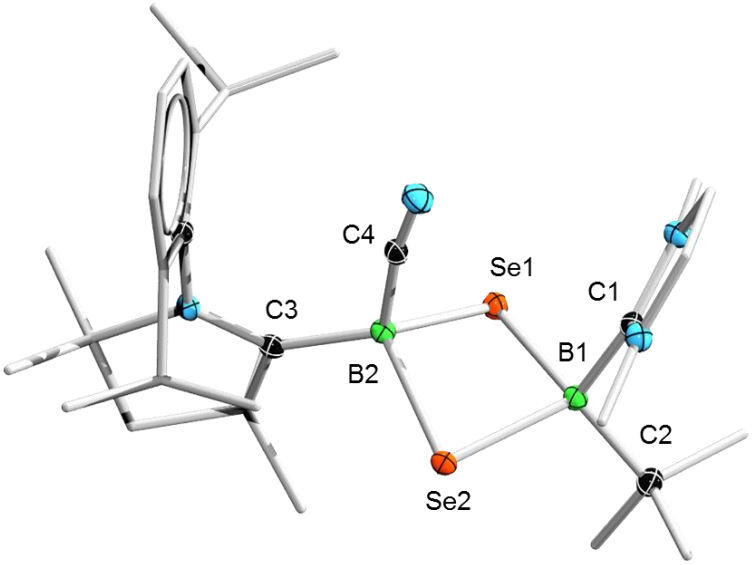

Figure 78. Molecular structure of **108**. Ellipsoids drawn at the 50% probability level. Hydrogen atoms and the ellipsoids of some carbon atoms are not shown for clarity. Relevant bond lengths [Å] and angles [º]: B1-Se1 2.111(7), B1-Se22.113.5(5), B2-Se1 2.068(6), B2-Se2 2.079(7), B1-Se1-B2 80.7(2), Se1-B1-Se2 93.8(3), B1-Se2-B2 80.4(2), Se1-B2-Se2 96.1(3).

2.4.9 Reaction of [(Cp)(OC)$_2$Mn{κ^1-*cyclo*-TeTeB(*t*Bu)(IMe)}] (96) with borylene complexes

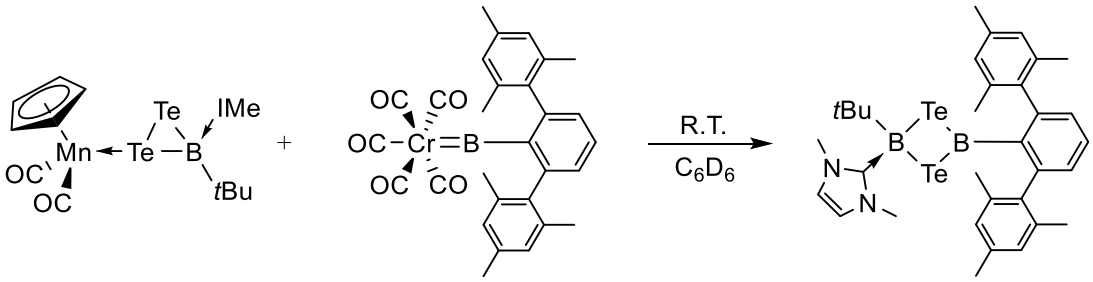

96 **22** **109**

Figure 79. Synthesis of **109** from reaction of [(Cp)(OC)$_2$Mn{κ^1-*cyclo*-TeTeB(*t*Bu)(IMe)}] (**96**) with chromium borylene (**22**).

Considering the successful isolation of B_2Se_2 and B_2Se_3 heterocycles, we set out to extend this chemistry to the synthesis of tellurium analogues of these unsymmetrical

rings. To this end, a number of different borylenes were used to react with [(Cp)(OC)$_2$Mn{κ^1-*cyclo*-TeTeB(*t*Bu)(IMe)}] (**96**). All the reactions were carried out at room temperature and were monitored by multinuclear NMR spectroscopy. For the reactions of **96** with [(OC)$_5$Mo=BN(SiMe$_3$)$_2$] (**20**) and [(Cp)(OC)$_2$Mn=B*t*Bu] (**43**), new species with ^{11}B resonances around δ_B = –32.1 were observed. However, all attempts to obtain pure compound from these mixtures led to the decomposition of the new species and no pure product could be isolated. In the case of the reaction of **93** with the cyanoborylene [(cAAC)B(CN)]$_4$ (**104**), no change in the ^{11}B NMR spectrum was observed after 48 h at room temperature. Raising the temperature to 60 °C led only to decomposition of the starting materials. Lastly, bulky chromium borylene complex **22** was reacted with the boraditellurirane **96**. The reaction was carried out using equimolar amounts of each reagent in C_6D_6 at room temperature. After 24 h at room temperature, the solution had changed from dark violet to brown and three new signals (δ_B = 81.4, 61.1 and –33.0) were observed in the ^{11}B NMR spectrum. The resonances at δ_B = 61.1 and –33.0 were assigned to the expected B_2Te_2 four-membered ring product. After workup, [*cyclo*-{(*t*Bu)(IMe)B-TeTe-B(Tp)}] (**109**) was isolated as a yellow crystalline solid in low yield (24%) and characterized by ^{1}H, ^{11}B and ^{13}C NMR spectroscopy and HRMS. However, the side-product with a signal at δ_B = 81.4 was not successfully isolated. Compared to compounds **101-108** the ^{11}B resonance for the *t*Bu(IMe)B is shifted to significantly higher field. To the best of our knowledge, **109** represents the first example of such a four-membered B_2Te_2 ring.

The solid state structure of the compound was elucidated from single crystals suitable for X-ray diffraction analysis that were obtained from a saturated toluene/pentane solution of **109**. The Tp substituent is rotated approximatively 15° from perpendicularity with the B_2E_2 cycle. Interestingly, the B-Te distances are different for both boron centers. Indeed, the TpB2-Te bonds are shorter (2.153(2) and 2.139(2) Å) than the corresponding *t*Bu(IMe)B1-Te distances (2.358(2) and 2.331(2) Å), likely owing to Te-to-B π donation that is not present in the case of the sp^3-hybridized B1.

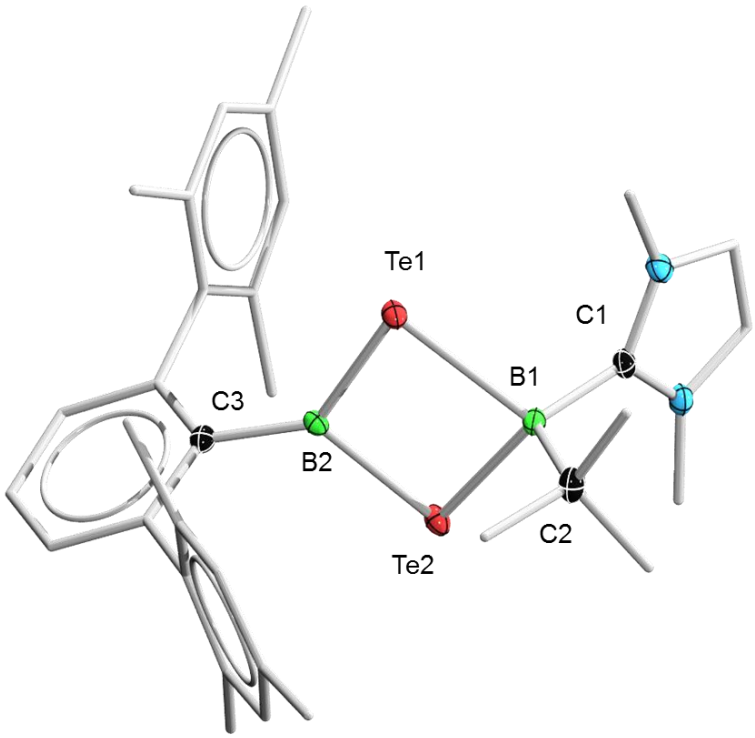

Figure 80. Molecular structure of **109**. Ellipsoids drawn at the 50% probability level. Hydrogen atoms and the ellipsoids of some carbon atoms are not shown for clarity. Relevant bond lengths [Å] and angles [º]: B1-Te1 2.358(2), B1-Te2 2.331(2), B2-Te1 2.153(2), B2-Te2 2.139(2), B1-Te1-B2 82.38(9), Te1-B1-Te2 91.23(9), B1-Te-B2 83.33(9), Te1-B2-Te2 102.7(1).

In conclusion, unsymmetrical four- or five-membered cyclic boron chalcogenides were synthesized from the reaction of boradichalcogeniranes (**94**, **95** and **96**) and borylenes (**20**, **22**, **43** and **104**). This direct insertion of borylenes into the E-E bonds (E = Te, Se and S) of boradichalcogeniranes provides an unprecedented synthetic route to unsymmetrically substituted 1,3-dichalcogena-2,4-diboretes and 1,2,4-dichalcogena-3,5-diborolanes. The synthesis of heterocycles featuring unsymmetrical boron centers in sp^2-sp^3 and sp^3-sp^3 hybridization combinations fills the previous paucity of methods for the synthesis of such unsymmetrical compounds. This approach will provide us with a useful platform to study the properties and applications of these unusual heterocycles.

2.5 Reactivity of $[(OC)_5Mo{=}BN(SiMe_3)_2]$ (20) with $[Cp_2WH_2]$ (110)

A major method to access new transition metal borylenes is through borylene transfer reactions (**Figure 12**).[115-119] These transfer reactions are mainly carried out with group 6 transition metal borylene complexes under photolytic or thermal conditions. It is known that an orbital of the metallocene dihydride complexes $[Cp_2MH_2]$ (M = Mo or W) is occupied by a lone electron pair,[205] thus an investigation into whether a borylene ligand can be transferred to the mental center is intriguing. Indeed, $[Cp_2W(CO)]$ can be synthesized by reacting $[Cp_2WCl_2]$ and Na/Hg under an atmosphere of CO (a borylene analogue).[206] Considering this, we were interested in synthesizing novel borylene complexes of the form $[Cp_2W{=}B\{N(SiMe_3)_2\}]$ by directly transferring a borylene ligand from $[(OC)_5Mo{=}BN(SiMe_3)_2]$ **(20)** to $[Cp_2WH_2]$ (**110**).

2.5.1 Reaction of $[Cp_2WH_2]$ (110) with one equivalent of $[(OC)_5Mo{=}BN(SiMe_3)_2]$ (20)

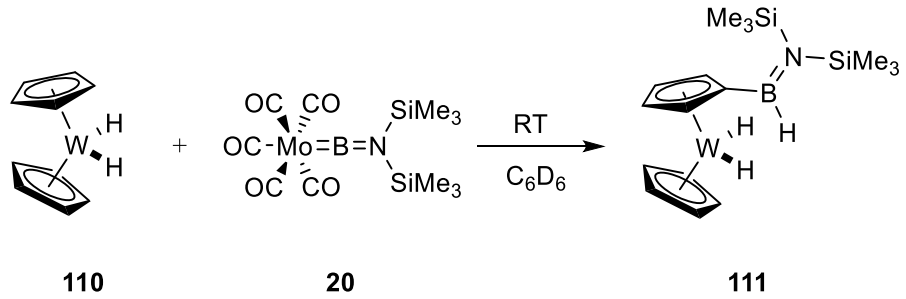

110 **20** **111**

Figure 81. Synthesis of **111** from reaction of $[Cp_2WH_2]$ (**110**) with $[(OC)_5Mo{=}BN(SiMe_3)_2]$ (**20**).

To achieve borylene transfer, $[(OC)_5Mo{=}BN(SiMe_3)_2]$ (**20**) was added to a C_6D_6 solution of an equimolar amount of $[Cp_2WH_2]$ (**110**) in a Young NMR tube (**Figure 81**). The reaction was carried out at room temperature and monitored by multinuclear NMR spectroscopy. After 24 h, the solution had changed from light yellow to brown. From the ^{11}B NMR spectrum, a new resonance at $\delta_B = 39.6$ was observed in place of that of precursor **20** ($\delta_B = 91$). This implied the formation of a tricoordinate boron species other than a tungsten terminal borylene (W=B), which normally has a boron signal in a different range ($\delta_B = 91$). Instead of the singlet signal associated with a Cp ligand ($\delta_H = 4.3$), the ^1H NMR spectrum showed a set of new resonances in the range of δ_B = 3-5, the multiplicities of which indicated the formation of several C-H activation products. A broad ^{11}B NMR signal at $\delta_B = 5.2$ also suggested the formation of a B-H bond. Due to the fact that the product has a high solubility in all organic solvents applied, the crude product had to be recrystallized from pentane several times for purification and $[CpWH_2(\eta^5\text{-}C_5H_4\{BHN(SiMe_3)_2\})]$ (**111**) was isolated as a light-yellow solid. Because of the difficult workup procedure, only moderate yields (27.5%) were achieved for this reaction. The compound was found to be sensitive to air and moisture, both in solution and in the solid state. The constitution of **111** in solution was confirmed by ^1H, ^{11}B and ^{13}C NMR spectroscopy and HRMS (**Figure 81**). The ^{11}B-decoupled ^1H NMR spectrum showed a sharpening of the broad signal at

δ_H = 5.2, which provides further evidence for the presence of a B-H bond.

To further confirm the solid state structure of the compound, single crystals suitable for X-ray diffraction analysis were obtained from a saturated pentane solution at –30 °C. The molecule crystallizes in the triclinic space group P-1 (**Figure 82**). The sums of the angles around boron (360.0°) and nitrogen (361.9°) indicate the planar coordination geometries for both atoms. The B-C bond distance is in the expected range for a boron-carbon single bond (1.54(1) Å) and the B-N bond length (1.44(1) Å) is much longer than in the borylene starting material **20** (1.355(2) Å). This elongation of the B-N interaction suggests a decrease of the π donation from nitrogen to boron, probably due to donation to boron from the Cp ring.

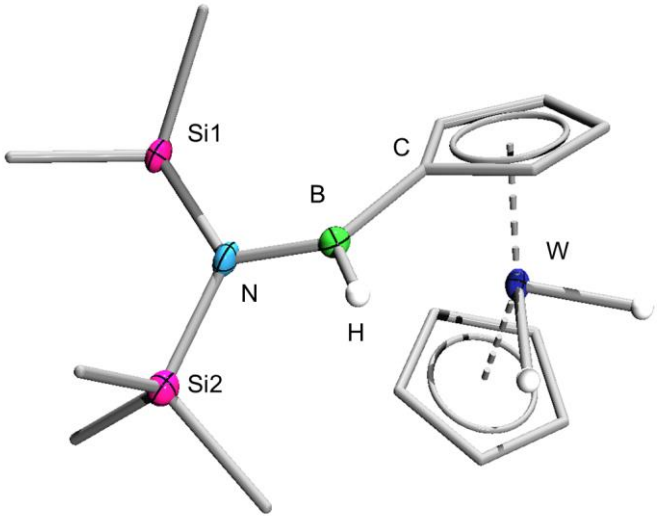

Figure 82. Molecular structure of **111**. Ellipsoids drawn at the 50% probability level. Hydrogen atoms and the ellipsoids of some carbon atoms are not shown for clarity. Relevant bond lengths [Å] and angles [º]: C-B 1.54(1), B-N 1.44(1), N-Si1 1.758(6), N-Si2 1.764(5), C-B-H 114.1, N-B-H 114.2, N-B-C 131.7(7), B-N-Si1 123.9(5), 111.3(5), Si-N-Si5 123.8(3).

2.5.2 Reaction of [Cp$_2$WH$_2$] (110) with two equivalents of [(OC)$_5$Mo=BN(SiMe$_3$)$_2$] (20)

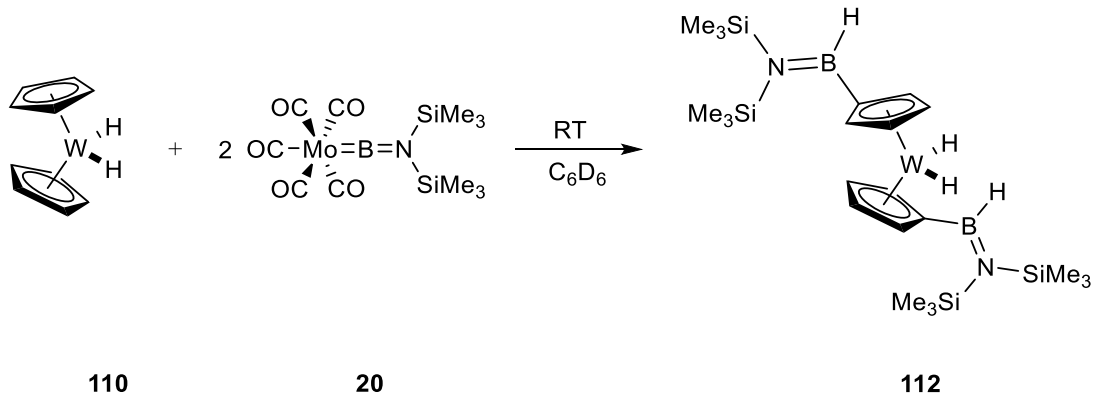

110 **20** **112**

Figure 83. Synthesis of **112** from reaction of [Cp$_2$WH$_2$] (**110**) with two equivalents of [(OC)$_5$Mo=BN(SiMe$_3$)$_2$] (**20**).

According to the in situ ^{1}H NMR spectrum of the reaction described in **2.5.1**, a number of C-H activation products of **110** were observed as side products of the reaction. In order to produce these side products more selectively, different stoichiometries was utilized in the reaction between **110** and **20**. First, two equivalents of **110** were added to a C_6D_6 solution of **20** (**Figure 83**). The reaction was carried out at room temperature and was monitored by multinuclear NMR spectroscopy. After 48 h, the ^{11}B NMR spectrum of the mixture showed a new resonance (δ_B = 41.3) in the same range as that of [CpWH$_2$(η^5-C$_5$H$_4${BHN(SiMe$_3$)$_2$})] (**111**), which indicated the insertion of a borylene moiety into the C-H bond. In the ^{1}H NMR spectrum, two resonances were observed at δ_H = 4.91 and 4.23, of equal intensity, indicating the formation of a double C-H activation product. [WH$_2$(η^5-C$_5$H$_4${BHN(SiMe$_3$)$_2$}$_2$)] (**112**) was isolated by keeping the pentane solution of the crude product at –30 ºC in an open vial (in a glovebox), which led to the formation of yellow crystals of **112** upon slow evaporation of the solvent. The constitution of **112** was confirmed by ^{1}H, ^{11}B and ^{13}C NMR spectroscopy and HRMS. Similar to compound **111**, the ^{1}H{^{11}B} NMR spectrum of **112** showed the sharpening of the signal at δ_H = 5.12, indicating the presence of a B-H bond.

Single crystals suitable for X-ray diffraction analysis were obtained from a saturated pentane solution of **112** at –30 ºC, which allowed us to elucidate its solid state structure. The molecule crystallized in the monoclinic space group P2(1)/n (**Figure 84**). As in compound **111**, the sum of the angles around boron (360.0°) and nitrogen (359.8°) indicated the planar coordination geometries for both atoms. The two boron-centered planes are also slightly bent towards the tungsten center. As expected, the two B-N bonds are also elongated (B1-N1 = 1.433 Å; B2-N2 = 1.439 Å) compared to the borylene starting material **20** (1.355(2) Å).

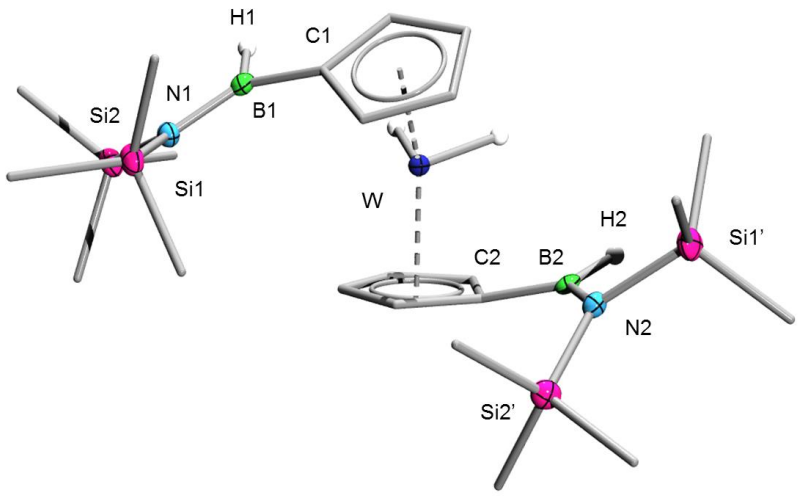

Figure 84. Molecular structure of **112**. Ellipsoids drawn at the 50% probability level. Hydrogen atoms and the ellipsoids of some carbon atoms are not shown for clarity. Relevant bond lengths [Å] and angles [º]: C1-B1 1.547(4), B1-N1 1.433(4), C2-B2 1.554(4), B2-N2 1.439(4), C1-B1-N1 128.8(2), C1-B1-H1 114(1), N1-B1-H1 118(1), C2-B2-N2 129.3(3), C2-B2-H2 111(1), N2-B2-H2 119(1), Si1-N1-B1 123.6(2), Si2-N1-B1 114.4(2), Si1-N1-Si2 121.6(1), Si1'-N2-B2 115.5(2), Si2'-N2-B2 122.4(2), Si1'-N2-Si2' 121.9(1).

2.5.3 Reaction of $[Cp_2WH_2]$ (110) with three equivalents of $[(OC)_5Mo{=}BN(SiMe_3)_2]$ (20)

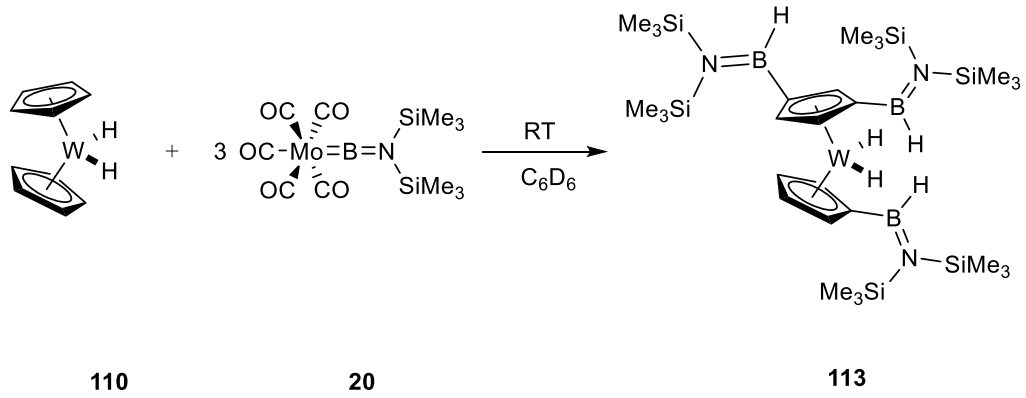

110 **20** **113**

Figure 85. Synthesis of **113** from $[Cp_2WH_2]$ (**110**) and three equivalents of $[(OC)_5Mo{=}BN(SiMe_3)_2]$ (**20**).

Having successfully isolated complexes **111** and **112**, the stoichiometry of **110** to **20** was changed to 1:3 in order to assess the possibility of performing multiple C-H activations of **110**. Thus, three equivalents of $[(OC)_5Mo{=}BN(SiMe_3)_2]$ (**20**) were added to a C_6D_6 solution of **110** at room temperature (**Figure 85**). After 48 h, the ^{11}B NMR spectrum showed a broad peak at $\delta_B = 41.3$, which indicated the formation of species similar to **111** and **112**. However, residual $[(OC)_5Mo{=}BN(SiMe_3)_2]$ (**20**) (δ_B = 91) could still be observed in the spectrum. The ^1H NMR spectrum showed a new set of peaks in the range of $\delta_H = 3.5\text{-}5.5$, including resonances that could be assigned to compounds **111** and **112**. In order to drive the reaction to completion, the temperature was increased to 60 ºC. After 24 h at this temperature, the ^{11}B NMR spectrum showed the total consumption of the starting material, however, the ^1H NMR spectrum still showed signals for single, double and quadruple C-H activation products. A number of different methods were used to isolate the triple C-H activation product $[(\eta^5\text{-}C_5H_3\{BHN(SiMe_3)_2\}_2)WH_2(\eta^5\text{-}C_5H_4\{BHN(SiMe_3)_2\})]$ (**113**) from the mixture, but no pure sample could be obtained. The formation of the tris-C-H activation product **113** was confirmed by HRMS (HRMS ($C_{28}H_{66}B_3N_3Si_6W$): calcd.: *m/z* = 829.3655; found: *m/z* = 829.3627).

2.5.4 Reaction of $[Cp_2WH_2]$ (110) with five equivalents of $[(OC)_5Mo{=}BN(SiMe_3)_2]$ (20)

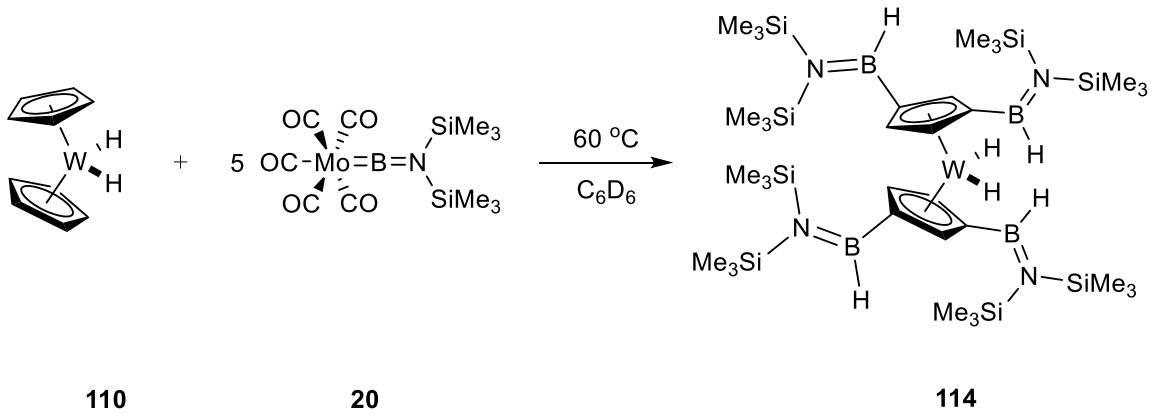

110 **20** **114**

Figure 86. Synthesis of **114** from reaction of $[Cp_2WH_2]$ (**110**) with five equivalents of $[(OC)_5Mo{=}BN(SiMe_3)_2]$ (**20**).

Even though the attempts to isolate the triple C-H activation product **113** were not successful, the ^{1}H NMR spectrum indicated the partial formation of a quadruple C-H activation product. Consequently, we treated **110** with five equivalents of compound **20** in C_6D_6 (**Figure 86**). The reaction was carried out at 60 °C and was monitored by multinuclear NMR spectroscopy. After 96 h, the color of the solution had changed to brown and the ^{11}B NMR spectrum showed the same resonance as observed for **111**, **112** and **113** (δ_B: = 41.3). The ^{1}H NMR spectrum showed two resonances at δ_H = 4.80 and 4.89 with an intensity ratio of 2:1, consistent with the activation of C-H bonds at the 3,3'-positions of the boron-substituted Cp rings in **112** by two equivalents of the molybdenum borylene **20**. The mixture was dried under vacuum at room temperature and dissolved in pentane. The solution was kept at –30 °C in an open vial to slowly evaporate the pentane solvent with side-product crystallized and separated stepwise. The process was repeated three times and the pure $[WH_2(\eta^5\text{-}C_5H_3\{BHN(SiMe_3)_2\}_2)_2]$ (**114**) was isolated as a brown oil. The constitution of **114** was indicated by ^{1}H, ^{11}B and ^{13}C NMR spectroscopy. A sharpened ^{1}H{^{11}B} resonance at δ_H = 5.42 indicated the formation of B-H bonds. The constitution of **114** was further confirmed by HRMS ($C_{34}H_{84}B_4N_4Si_8W$, calcd.: *m/z* = 1000.4731; found: *m/z* = 1000.4754). Unfortunately,

due to its high solubility in nearly all organic solvents applied, all attempts to obtain single crystals suitable for X-ray diffraction analysis of **114** were unsuccessful.

In conclusion, a direct insertion of a borylene into the C-H bond of [Cp_2WH_2] (**110**) was carried out in the reaction with [$(OC)_5Mo{=}BN(SiMe_3)_2$] (**20**). Interestingly, up to four C-H bonds of **110** can be activated by treatment with **20** in different stoichiometries. The resulting complexes **111** and **112** were fully characterized, including their solid state structures, while the formation of complexes **113** and **114** was only confirmed spectroscopically. The result is consistent with previous examples of activation of C-H bonds by borylene species (**Figure 22**) but under milder conditions.[149-151] Although the difficulty in synthesizing precursor **20** and the low yield make the reaction presented herein unfeasible as a practical method for C-H activation, it provides an alternative concept for the synthesis of borylated organic species.

2.6 Reactivity of borylene complexes with Lewis acids ($GaCl_3$, $InBr_3$)

In 2013, the group of Braunschweig reported the 1,2 addition of Au and Cl to a Mn=B bond from the reaction of gold(I) compound [(Ph_3P)AuCl] and [(Cp)$(OC)_2$Mn=B*t*Bu] (**43**).[207] One year later, the same group discovered the first 1,2-additions of main-group compounds across metal-boron double bonds. In this research, borylene complex [$(OC)_5$Mo=BN$(SiMe_3)_2$] (**20**) was reacted with $GaCl_3$, resulting in a chlorogallation reaction which led to the formation of a highly unusual Mo-B-Ga-Cl rhombus.[208] Given the aforementioned results, we were interested in the reaction of manganese borylene [(Cp)$(OC)_2$Mn=B*t*Bu] with Lewis acids of group 13 elements such as BCl_3, $GaCl_3$ and $InBr_3$.

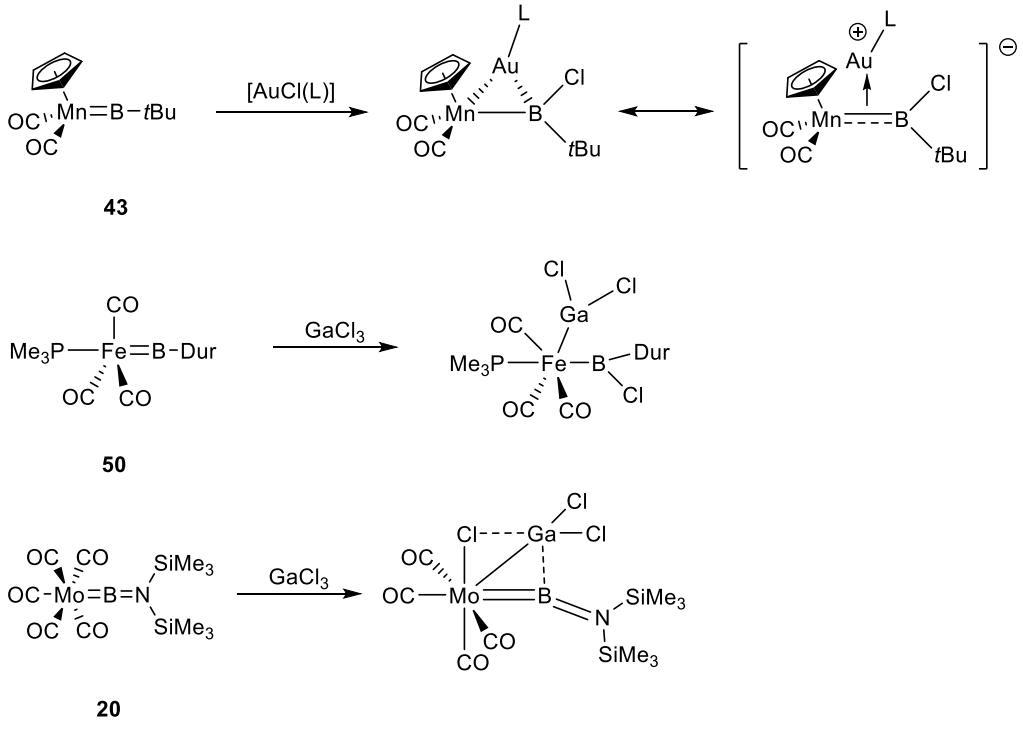

Figure 87. Reactions of terminal borylenes with Lewis acids.

2.6.1 Reaction of [(Cp)(OC)$_2$Mn=B*t*Bu] (43) with GaCl$_3$ (115)

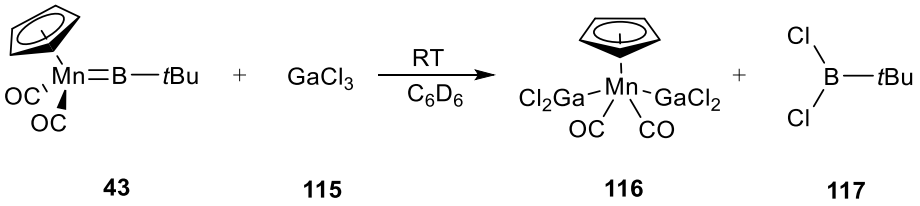

Figure 88. Synthesis of **116** from reaction of [(Cp)(OC)$_2$Mn=B*t*Bu] (**43**) with GaCl$_3$ (two equivalents).

In order to probe the reactivity of **43** with GaCl$_3$, one equivalent of GaCl$_3$ was added to a solution of [(Cp)(OC)$_2$Mn=B*t*Bu] (**43**) in a Young NMR tube. The reaction was monitored by multinuclear NMR spectroscopy (**Figure 88**). After 30 min at room temperature, the color of the solution had turned orange and a yellow precipitate formed gradually. The ^{11}B NMR spectrum revealed a new resonance at δ_B = 64, which was consistent with the signal of Cl$_2$B*t*Bu (**117**). After workup, pure [(Cp)(OC)$_2$Mn(GaCl$_2$)$_2$] (**116**) was obtained as a yellow solid. However, further NMR characterization of **116** failed due to its insolubility in all available organic solvents. The composition of the complex was confirmed by elemental analysis, which is consistent with the formula C$_7$H$_5$Ga$_2$Cl$_4$MnO$_2$ and is shown in **Figure 88**. However, no suitable single crystals can be isolated to further confirm the solid state structure of **116** due to its poor solubility.

2.6.2 Reaction of [(Cp)(OC)$_2$Mn=B*t*Bu] (43) with GaCl$_3$ (115) in Tetrahydrofuran (THF)

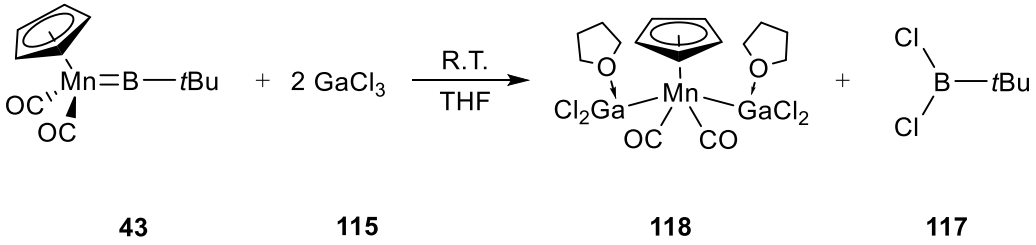

43 **115** **118** **117**

Figure 89. Synthesis of **118** from reaction of [(Cp)(OC)$_2$Mn=B*t*Bu] (**43**) with GaCl$_3$ in THF.

Since the solubility of [(Cp)(OC)$_2$Mn(GaCl$_2$)$_2$] (**116**) was poor in all organic solvents, the reaction was attempted directly in THF, which is a more polar solvent than benzene (**Figure 89**). A THF solution of GaCl$_3$ was slowly added to a THF solution of [(Cp)(OC)$_2$Mn=B*t*Bu] (**43**) and the mixture was kept at room temperature. After 12 h, colorless crystals appeared in the solution and pure [(Cp)(OC)$_2$Mn{Ga(THF)Cl$_2$}$_2$] (**118**) was obtained as colorless crystals after workup. The solid state structure of **118** was determined by single-crystal X-ray diffraction analysis and is shown in **Figure 90**. However, its solubility was still so low that the constitution of **118** could only be confirmed by elemental analysis, and not by NMR spectroscopy.

The molecule crystallized in the monoclinic space group *P*2$_1$. The Mn-Ga distances (Mn-Ga1: 2.391(2) Å, Mn-Ga2: 2.398(2) Å) are shorter than the few known examples containing Mn-Ga bonds ((Cp*)$_2$Ga{Mn(CO)}$_5$: 2.548(1) Å,[209] ArGaCl{Mn(CO)$_5$}: 2.495(4) Å[210]).

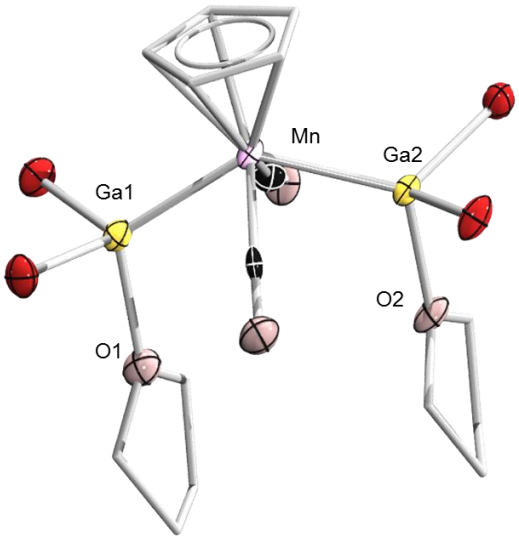

Figure 90. Molecular structure of **118**. Ellipsoids drawn at the 50% probability level. Hydrogen atoms and the ellipsoids of some carbon atoms are not shown for clarity. Relevant bond lengths [Å] and angles [º]: Mn-Ga1: 2.391(2), Mn-Ga2: 2.398(2), O1-Ga1: 2.04(2), O2-Ga2: 2.022(6), Mn-Ga1-Cl1: 118.5(1), Mn-Ga1-Cl2: 117.8(1), Cl1-Ga1-Cl2: 106.7(1), Mn-Ga2-Cl3: 119.7(1), Mn-Ga2-Cl4: 118.6(1), Cl3-Ga2-Cl4: 105.5(1).

2.6.3 Reaction of $[(Cp)(OC)_2Mn(GaCl_2)_2]$ (116) with Lewis bases (PMe_3, Et_2O)

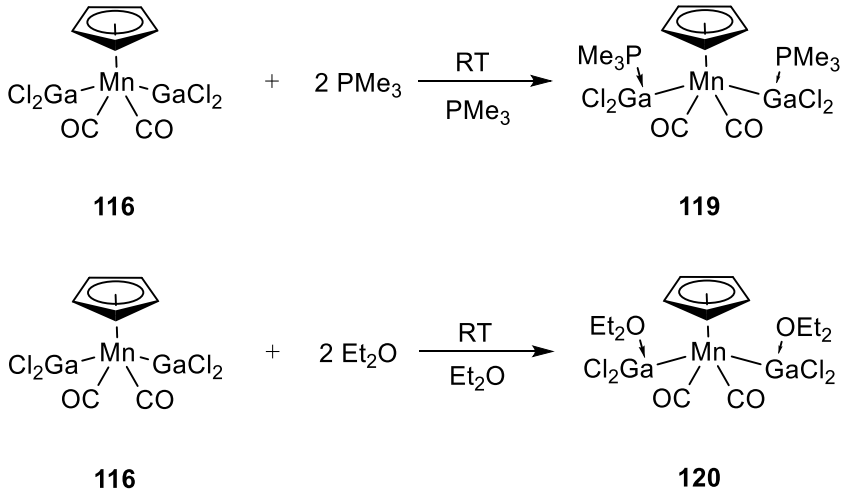

Figure 91. Synthesis of **119** and **120** from reactions of $[(Cp)(OC)_2Mn(GaCl_2)_2]$ (**116**) with Lewis bases (PMe_3, Et_2O).

Since the synthesis of [(Cp)(OC)$_2$Mn{Ga(THF)Cl$_2$}$_2$] (**118**) showed the possibility of coordinating [(Cp)(OC)$_2$Mn(GaCl$_2$)$_2$] (**116**) to Lewis bases, several reagents were used to probe the versatility of this reactivity. First, **116** was added to neat PMe$_3$ (>10 equiv.) and the mixture was kept at room temperature in a vial. After 24 h, the color of the solid had changed from yellow to white. The solid was filtered off from the solution and single crystals suitable for X-ray analysis were obtained from the mixture. The solid state structure of [(Cp)(OC)$_2$Mn{Ga(PMe$_3$)Cl$_2$}$_2$] (**119**) was revealed by X-ray diffraction analysis (**Figure 92**). Like compound **118**, PMe$_3$ was connected to gallium through a dative bond. The molecule crystallizes in the monoclinic space group $P2_1/n$. The Mn-Ga bond lengths (2.422(1) Å, 2.3888(9) Å) are also shorter than those of reported complexes that feature Mn-Ga interactions.[209-210]

Et$_2$O was also reacted with **116** under analogous conditions, giving a similar product that have a bad solubility so the constitution cannot be confirmed by NMR spectroscopy. The solid state structure of **120** was revealed by X-ray diffraction analysis and is shown in **Figure 93**. Single crystals suitable for X-ray diffraction analysis were obtained directly from the reaction mixture. The molecule crystallizes in the monoclinic space group *P*-1, and the Mn-Ga distances are in the same range as those of **118** and **119**.

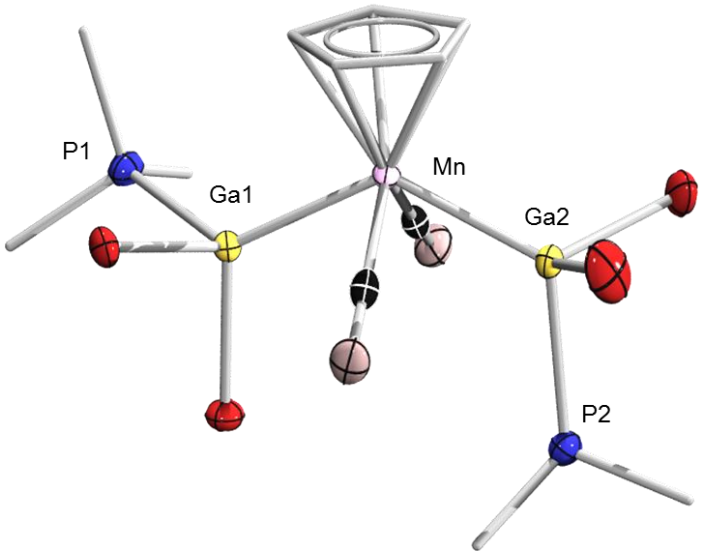

Figure 92. Molecular structure of **119**. Ellipsoids drawn at the 50% probability level. Hydrogen atoms and the ellipsoids of some carbon atoms are not shown for clarity. Relevant bond lengths [Å] and angles [º]: Mn-Ga1: 2.422(1) Å, Mn-Ga2: 2.3888(9) Å, P1-Ga1: 2.338(6), P2-Ga2: 2.402(1), Mn-Ga1-Cl1: 115.97(3), Mn-Ga1-Cl2: 117.35(3), Cl1-Ga1-Cl2: 103.07(4), Mn-Ga2-Cl3: 118.06(3), Mn-Ga2-Cl4: 115.41(3), Cl3-Ga2-Cl4: 103.90(3).

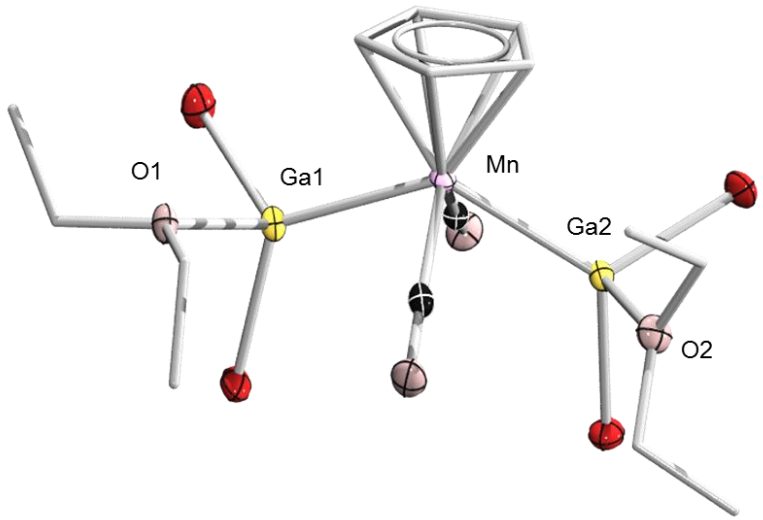

Figure 93. Molecular structure of **120**. Ellipsoids drawn at the 50% probability level. Hydrogen atoms and the ellipsoids of some carbon atoms are not shown for clarity. Relevant bond lengths [Å] and angles [º]: Mn-Ga1: 2.4096(5), Mn-Ga2: 2.3974(5), O1-Ga1: 2.023(1), O2-Ga2: 2.039(1), Mn-Ga1-Cl1: 122.18(1), Mn-Ga1-Cl2: 115.88(1), Cl1-Ga1-Cl2: 103.26(2), Mn-Ga2-Cl3: 118.76(1), Mn-Ga2-Cl4: 118.92(1), Cl3-Ga2-Cl4: 105.41(2).

2.6.4 Reaction of [(Cp)(OC)$_2$Mn=B*t*Bu] (43) with InBr$_3$ (121) in the absence and presence of DMAP.

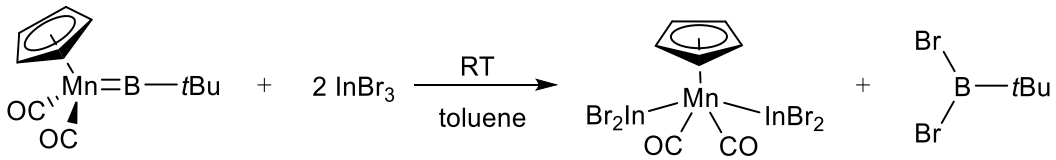

43 **121** **122** **123**

Figure 94. Synthesis of **122** from reaction of [(Cp)(OC)$_2$Mn=B*t*Bu] (**43**) with InBr$_3$.

Next, two equivalents of InBr$_3$ were added to a toluene solution of **43** in a Young NMR tube. After 24 h at room temperature, a yellow precipitate was obtained from the solution and determined to be pure [(Cp)(OC)$_2$Mn(InBr$_2$)$_2$] (**122**). The constitution was confirmed by elemental analysis. However, the structure of **122** could not be determined by single-crystal X-ray diffraction analysis due to its low solubility.

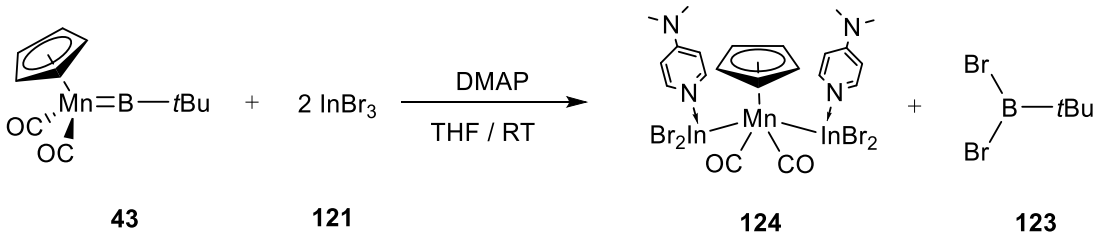

43 121 124 123

Figure 95. Synthesis of **124** from reaction of [(Cp)(OC)$_2$Mn=B*t*Bu] (**43**) with $InBr_3$ in the presence of DMAP.

To further investigate the structure of the product, 4-dimethylaminopyridine (DMAP) was used as a Lewis base in an attempt to increase the solubility of the adduct. To this end, a mixture of **43** and **121** was stirred at room temperature for 24 h and two equivalents of DMAP were subsequently added to the solution. The reaction mixture was then kept at room temperature for another 24 h (**Figure 95**). After workup, [(Cp)(OC)$_2$Mn{In(DMAP)Br$_2$}$_2$] (**124**) was isolated as colorless crystals which were suitable for X-ray diffraction analysis. The solid state structure of **124** is shown in **Figure 96**.

Compound **124** crystallized in the triclinic space group *P*-1 as colorless needles. The Mn-In distances (Mn-In1: 2.569(1), Mn-In2: 2.5638(9)) are in the typical range for Mn-In σ bonds.Similar to the aforementioned complexes **116** and **118-120**, disregarding the nitrogen donor unit, the angular sums around the In atoms (In1: 335.1°, In2: 341.5°) are less than 360°, which indicates significant pyramidalization.

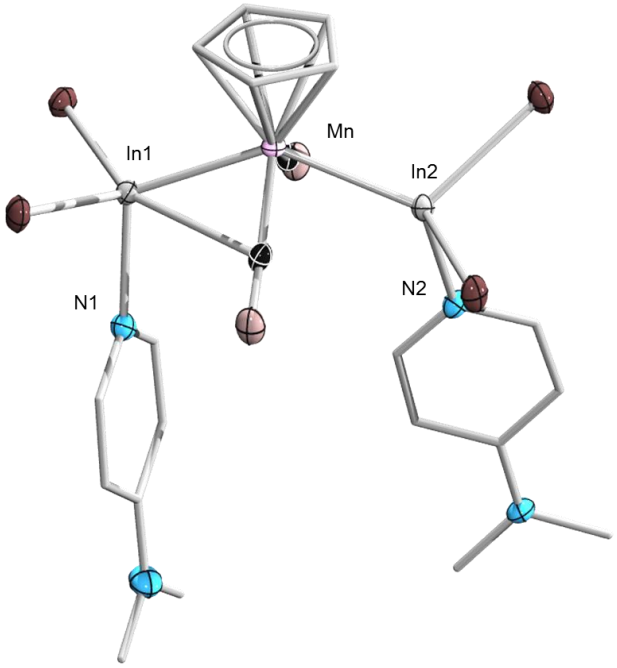

Figure 96. Molecular structure of **124**. Ellipsoids drawn at the 50% probability level. Hydrogen atoms and the ellipsoids of some carbon atoms are not shown for clarity. Relevant bond lengths [Å] and angles [º]: Mn-In1: 2.569(1), Mn-In2: 2.5638(9), N1-In1: 2.194(3), N2-In2: 2.213(3), Mn-In1-Br1: 117.57(2), Mn-In2-Br2: 117.05(2), Br1-Mn-Br2: 100.47(2), Mn-In2-Br3: 116.81(2), Mn-In2-Br4: 116.95(2), Br3-In2-Br4: 107.74(2).

In conclusion, the borylene ligand of [(Cp)(OC)$_2$Mn=B*t*Bu] (**43**) can be completely liberated in the form of [X$_2$B*t*Bu] (X = Cl or Br) by reaction with group 13 halides ($GaCl_3$ and $InBr_3$), thus leading to the isolation of [(Cp)(OC)$_2$Mn($GaCl_2$)$_2$] (**116**) and [(Cp)(OC)$_2$Mn($InBr_2$)$_2$] (**122**). The resulting complexes can further react with Lewis bases (PMe_3, THF, Et_2O, DMAP), leading to the isolation of corresponding adducts (**118**, **119**, **120** and **124**).

3. **Summary**

The research on which this thesis is based was aimed at investigating the reactivity of borylene complexes (**20**, **22**, **43**, **50**, **90**, **104**). Reactions of transition-metal borylene complexes were investigated with a range of different reagents, and products featuring novel bonding motifs were obtained accordingly. Many of these compounds were isolated as the very first examples of their kind, displaying highly unusual structural features. Moreover, thorough use of spectroscopic and structural characterization techniques helped to confirm the constitution and determine the bonding situation in these compounds.

Since the [RB:] moiety of some transition-metal borylene can be released and form base-stabilized, metal-free borylenes by addition of Lewis bases,[100, 105, 124-125, 142, 146-147] bipyridine compounds with different substitution patterns were reacted with transition-metal borylene complexes. However, the products were found to feature boron atoms in their +3 oxidation state (**Figure 97**), as confirmed by X-ray diffraction analysis. All of the products showed ^{11}B NMR resonances at around δ_B = 23 and exhibited appreciable aromaticity of the C-N-B-N-C five-membered ring. Moreover, the C-C bonds connecting the two pyridyl groups were shortened (e.g. C1-C2 = 1.387(3) Å, (**87**) *cf.* 1.488 Å in free bipy), which demonstrated the double bond character of the C-C interaction. The result also indicates that this is an effective way to reduce bipyridine species while boron (B(I)) in borylene is oxidized to B(III).

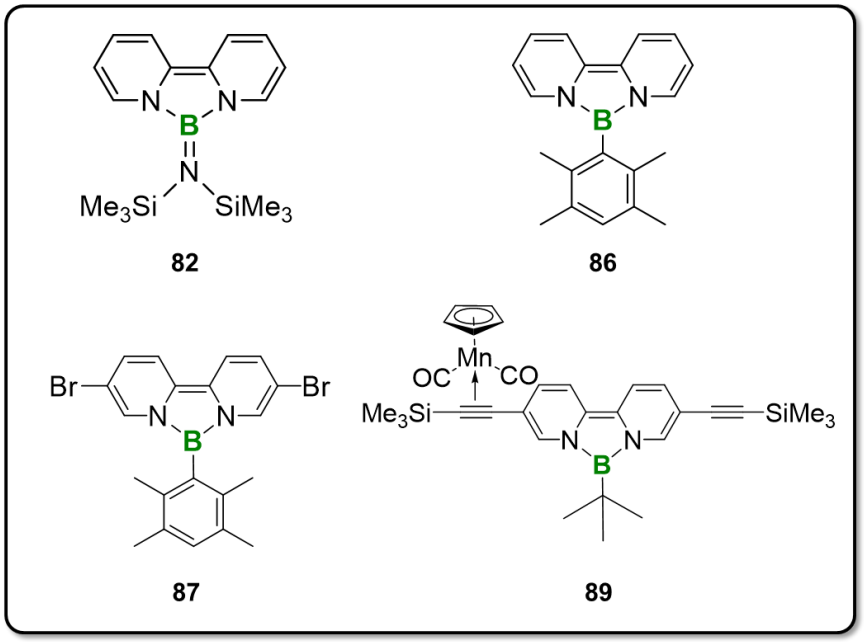

Figure 97. Complexes **82-89**.

Inspired by the known reaction of [(Cp)(OC)$_2$Mn=B*t*Bu] (**43**) with Ph$_3$P=S, which yields an intermediate complex [(Cp)(OC)$_2$Mn(μ^2-SB(*t*Bu))] featuring a B=S double bond, this work also involved investigation of the reactions of borylene complexes with elemental chalcogens E (E = S$_8$, Se, Te). Due to the unsuccessful isolation of products from the reactions between **43** and E (E = S$_8$, Se, Te), a base-stabilized borylene [(Cp)(OC)$_2$Mn=B(IMe)*t*Bu] (**90**) was instead used to react with one equivalent of these elemental chalcogens. As a result, compounds [(Cp)(OC)$_2$Mn-E=B(IMe)*t*Bu] (E = S, Se, Te) (**91-93**) that feature B=E double bonds were isolated (**Figure 98**). In these products, the [E=B(IMe)*t*Bu] moiety remains bound to the metal center through a dative bond. The constitution of these compounds was confirmed by NMR analysis and the structure was elucidated by X-ray diffraction analysis. DFT calculations were used to model these compounds and showed that the Wiberg bond indexes of the E=B (E = S, Se, Te) interactions were around 1.7, which further confirmed the double bond character of these connections. A noteworthy fact is that **93** is the first isolated compound to feature B=Te double bond character.

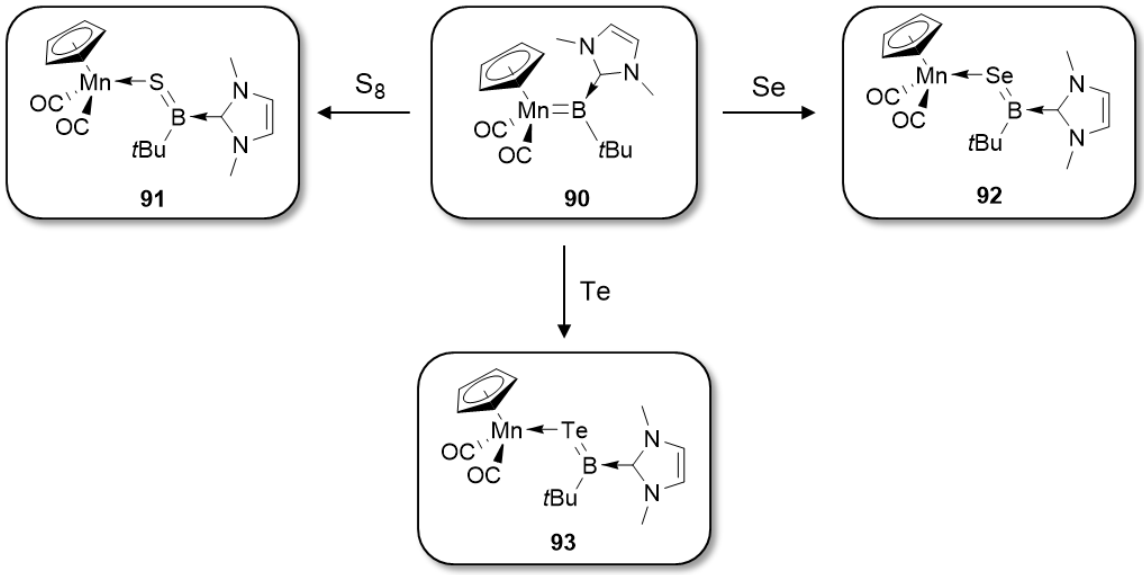

Figure 98. Synthesis of chalcogen insertion products **91-93**.

To further explore the reactions of borylene [(Cp)(OC)$_2$Mn=B*t*Bu] (**43**) with elemental chalcogens, an excess (three equivalents) of E (E = S, Se, Te) was treated with **43**. The reactions with S and Se yielded cyclic boron dichalcogenide species [*cyclo*-EEB(*t*Bu)(IMe)] (E = S, Se) (**94-95**) (**Figure 99**), which showed ^{11}B NMR resonances at around δ_B = 0. Unlike compounds **94** and **95**, which are simple metal-free B-E-E (E = **S**, **Se**) three-membered-ring-containing compounds, the reaction of **43** with Te yielded a different product [(Cp)(OC)$_2$Mn{κ^1-*cyclo*-TeTeB(*t*Bu)(IMe)}] (**96**) in which the [*cyclo*-TeTeB(*t*Bu)(IMe)] unit was connected to manganese through a dative bond. The intriguing ligand [*cyclo*-TeTeB*t*Bu(IMe)] represents the first example of a three-membered cyclic ditelluride of a main group element – an isolable analogue of the elusive ditellurirane, an isostere of a dioxirane. However, attempts to isolate the uncoordinated [TeTeB*t*Bu(IMe)] from **96** using Lewis bases such as PMe_3 led to the formation of monotellurium complex [(Cp)(OC)$_2$Mn-Te=B(IMe)*t*Bu] (**93**) by chalcogen abstraction.

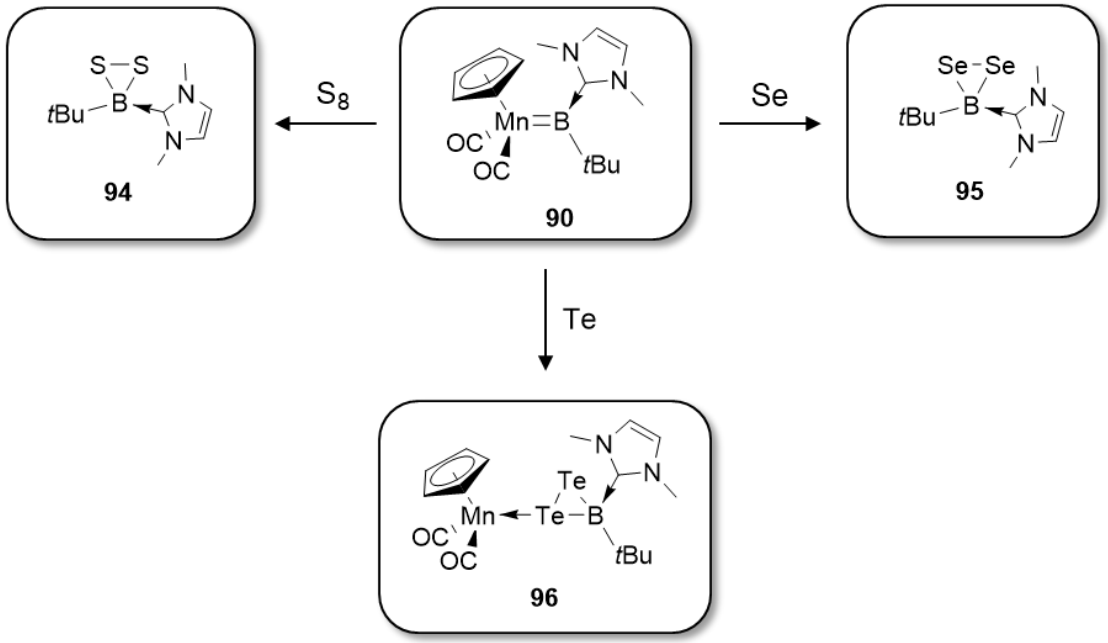

Figure 9. Synthesis of dichalcogen-containing products **94-96**.

Similarly, the reactivity of metal-free borachalcones **94** and **95** with PMe_3 resulted in the formation of [E=B*t*Bu(IMe)] (E = S, Se) (**97, 99**) at room temperature (**Figure 100**). The products showed ^{11}B NMR resonances with similar chemical shifts to those of compounds **91** and **92**. Although the complexes were stable in the solid state, they can dimerize to form B-E-E-B cyclic four-membered rings [*cyclo*-{(IMe)(*t*Bu)B-E-B(IMe)(*t*Bu)-E}] (E = S, Se) (**98**, **100**).

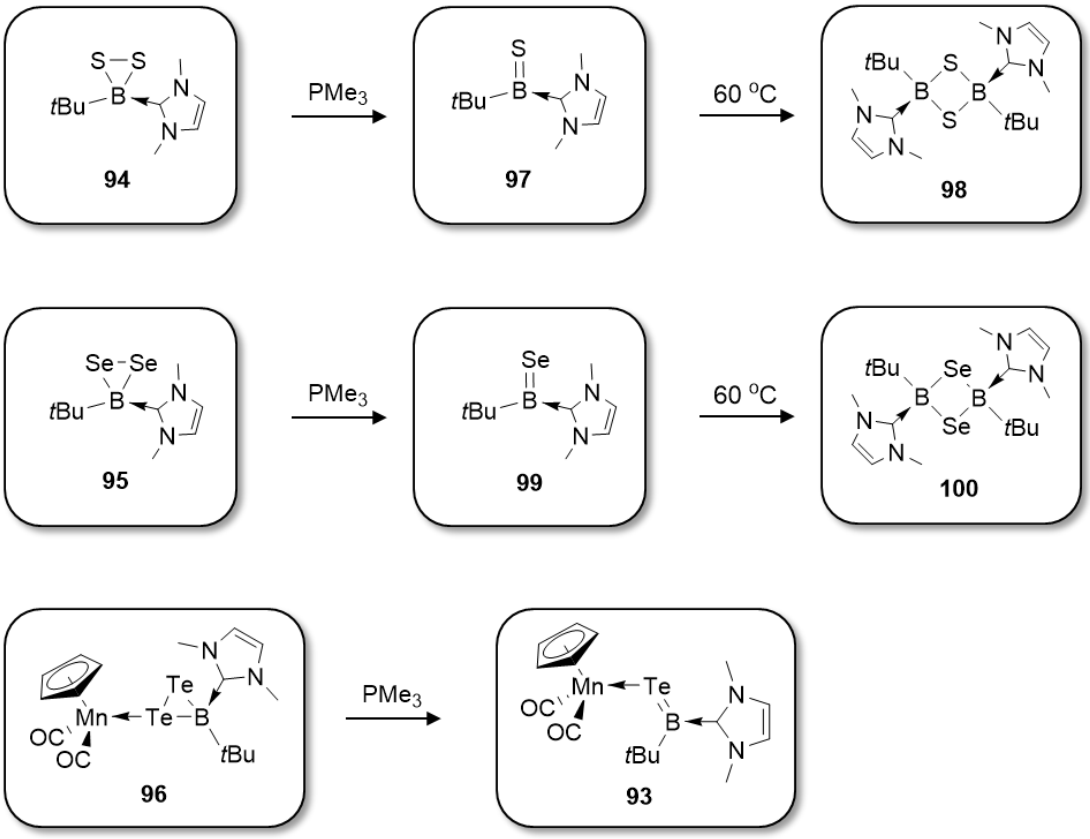

Figure 100. Synthesis of products **97-100.**

In addition to reaction with PMe_3, these cyclic boron dichalcogenide complexes were found to react with borylene complexes to form a series of four- or five-membered cyclic structures [*cyclo*-{(*t*Bu)(IMe)B-E-BR-E}] (E = S, Se, Te) or [*cyclo*-{(*t*Bu)(IMe)B-EE-BR-E}] (E = S, Se) (**101-103, 105-109**) (**Figure 101**). These compounds featured unsymmetrically substituted boron atoms and each showed two different resonances in their ^{11}B NMR spectra. The constitution of these compounds was confirmed by multinuclear NMR spectroscopy. The structures of most of these products were confirmed by single-crystal X-ray diffraction analysis.

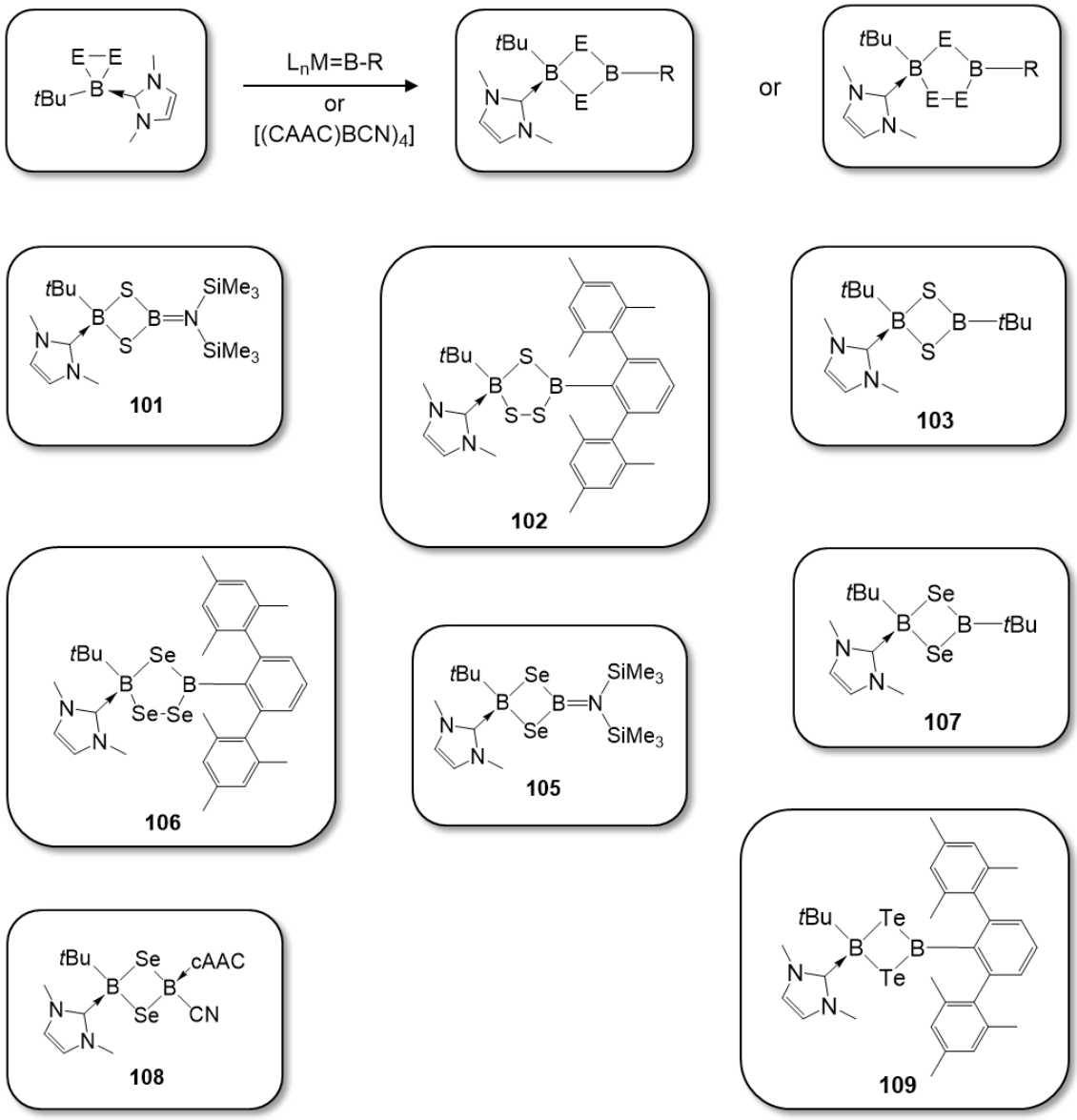

Figure 101. Synthesis of products **101-103, 105-109**.

In addition, borylene compounds showed intriguing possibilities in C-H activation reactions. Indeed, reaction of the molybdenum borylene complex $[(OC)_5Mo{=}BN(SiMe_3)_2]$ (**20**) with $[Cp_2WH_2]$ (**110**) led to the insertion of a borylene fragment into the C-H bond of the cyclopentadiene ligand. Strikingly, the borylene (**20**) was able to activate up to four C-H bonds of the cyclopentadiene ligand in **110** (**Figure 102**). Solid state structures of the mono-/bisboryl products $[CpWH_2\{\eta^5\text{-}C_5H_4(BHN(SiMe_3)_2)\}]$ (**111**) and $[WH_2(\eta^5\text{-}C_5H_4\{BHN(SiMe_3)_2\}_2)]$ (**112**) were confirmed by single-crystal X-ray diffraction analysis. However, due to

solubility issues, the tris-/tetrakisboryl products $[(\eta^5\text{-}C_5H_3\{BHN(SiMe_3)_2\}_2)WH_2(\eta^5\text{-}C_5H_4\{BHN(SiMe_3)_2\})]$ (**113**) and $[WH_2(\eta^5\text{-}C_5H_3\{BHN(SiMe_3)_2\}_2)_2]$ (**114**) could not be structurally characterized but only observed spectroscopically.

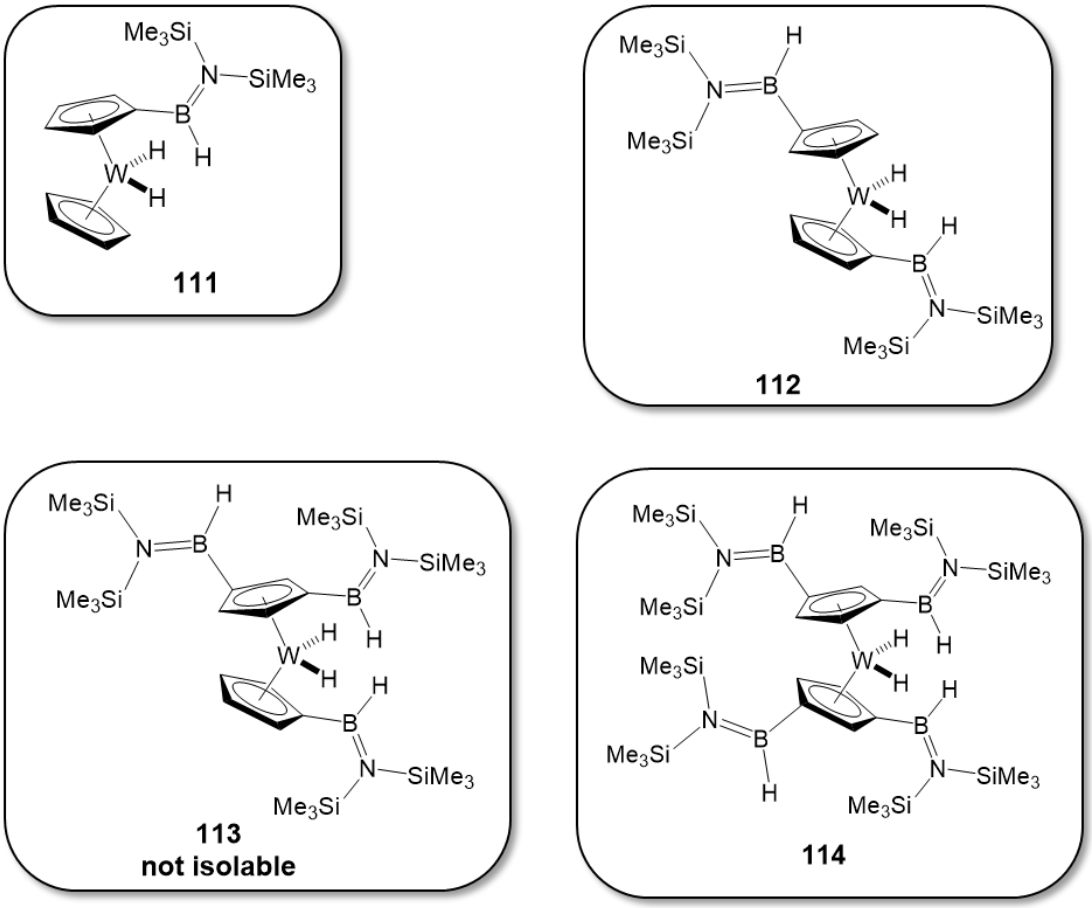

Figure 102. C-H activation products **111-114**.

Finally, the reaction of $[(Cp)(OC)_2Mn{=}B\textit{t}Bu]$ (**43**) with Lewis acids ($GaCl_3$, $InBr_3$) led to the complete elimination of the borylene moiety in the form of $Cl_2B\textit{t}Bu$ (**117**) or $Br_2B\textit{t}Bu$ (**123**). As a result, $[(Cp)(OC)_2Mn(GaCl_2)_2]$ (**116**) and $[(Cp)(OC)_2Mn(InBr_2)_2]$ (**122**) were obtained as yellow powders. Due to their low solubility, the solid state structures of **116** and **122** could not be elucidated by single-crystal X-ray diffraction analysis. In addition, the use of Lewis bases (PMe_3, THF, Et_2O, DMAP) led to adduct formation with **116** and **122** to yield $[(Cp)(OC)_2Mn(L)(ECl_2)_2]$ (E = Ga, In; L = PMe_3, THF, Et_2O, DMAP) (**117-124**). Due

to the low solubility of these compounds, their constitution could not be confirmed by NMR spectroscopy but only through by elemental analysis and single-crystal X-ray diffraction analysis.

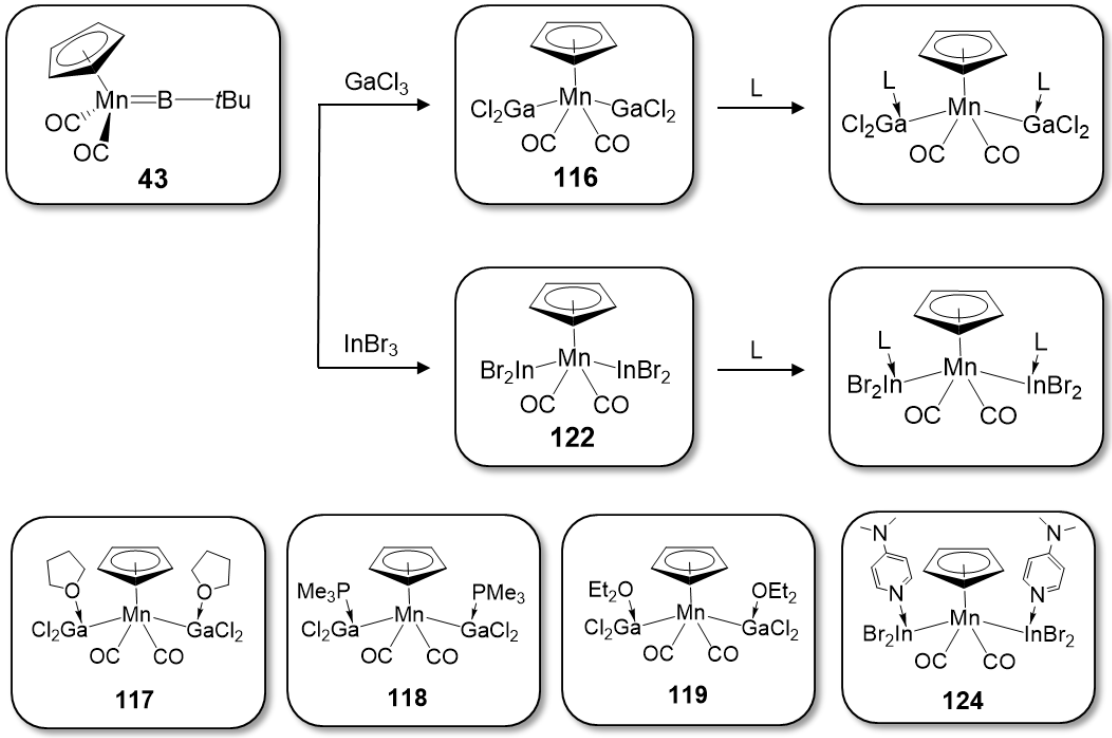

Figure 103. Synthesis of products **116-120**.

In conclusion, this project led to discovery of some novel reactivity patterns of transition metal borylene complexes (**20**, **22**, **43**, **50** and **90**) and provides new insight into the synthesis of boron-containing species. BN analogues of the fluorenyl anion complexes have been isolated previously, but their synthetic routes are not well developed. By transferring the borylene ligand to bipyridine species, we found a direct way to synthesize this species. From the reaction of base-stabilized borylene [(Cp)(OC)$_2$Mn=B(IMe)*t*Bu] (**90**) with elemental chalcogens (S_8, Se and Te), we were able to synthesize complexes containing unusual boron-chalcogen interactions. Among them, complexes featuring B=Te (**93**), B-Se-Se (**95**) and B-Te-Te (**96**) units are the first examples of their respective class. These unprecedent results highlight the potential of hypovalent boron compounds, especially transition metal borylene complexes, to function as the starting point for unusual and innovative chalcogen

chemistry. Taking this one step further, the resulting cyclic boron dichalcogenides (**94**, **95** and **96**) can in turn react with borylene complexes to form unsymmetrical heterocycles featuring boron centers in sp^2-sp^3 and sp^3-sp^3 hybridization combinations. This provides the first method for the synthesis of such unsymmetrical cyclic boron chalcogenides and will provide us with a useful platform to study the properties and applications of these unusual heterocycles. From the reaction of borylene **20** with [$CpWH_2$], we discovered the potential of activating multiple C-H bonds of aromatic systems, providing an alternative pathway for the synthesis of borylated organic species. Finally, the reaction of manganese borylene **43** with $GaCl_3$ and $InBr_3$ leads to complete elimination of the boron moiety from the metal center. This study uncovered a different reaction pathway of borylenes with group 13 halides divergent from that presented in a previous study.[208]

4. **Zusammenfassung**

Die Fragestellung der Arbeit zielte auf die Erforschung der Reaktivität von Borylenkomplexen (**20**, **22**, **43**, **50**, **90**, **104**). Reaktionen von Übergangsmetallborylen-Komplexen wurden mit einer Reihe von verschiedenen Reagenzien untersucht, deren Produkte neuartige Bindungsmotive zeigten. Viele der Verbindungen wurden als erste Beispiele ihrer Art isoliert, mit teils sehr ungewöhnlichen strukturellen Eigenschaften. Durch spektroskopische und strukturelle Charakterisierungsmethoden wurden sowohl die Konstitution der Verbindungen bestätigt als auch ihre Bindungsverhältnisse aufgeklärt.

Da die [RB:]-Einheit von einigen Übergangsmetallborylenen freigesetzt und bei der Addition von Lewisbasen basenstabilisierte, metallfreie Borylene bildet,[100, 105, 124-125, 142, 146-147] wurden verschieden substituierte Bipyridin-Verbindungen mit Übergangsmetallborylenen umgesetzt. Wie durch Röntgenbeugung gezeigt werden konnte, liegen bei den Produkten die Boratome jedoch in der Oxidationsstufe +3 vor (**Abbildung 97**). Alle Produkte zeigten ^{11}B-NMR-Signale bei ca. δ_B = 23 und wiesen eine deutliche Aromatizität im C-N-B-N-C-Fünfring auf. Zudem waren die C-C-Bindungen, welche die beiden Pyridylgruppen verbinden, verkürzt (z.B. C1-C2 = 1.387(3) Å, (**87**) vgl. mit 1.488 Å in freiem bipy), was auf einen Doppelbindungscharakter hinweist. Dieses Ergebnis deutet zudem darauf hin, dass dies ein effektiver Weg ist, um Bipyridin-Spezies zu reduzieren, während das Boratom im Borylen zu B(III) oxidiert wird.

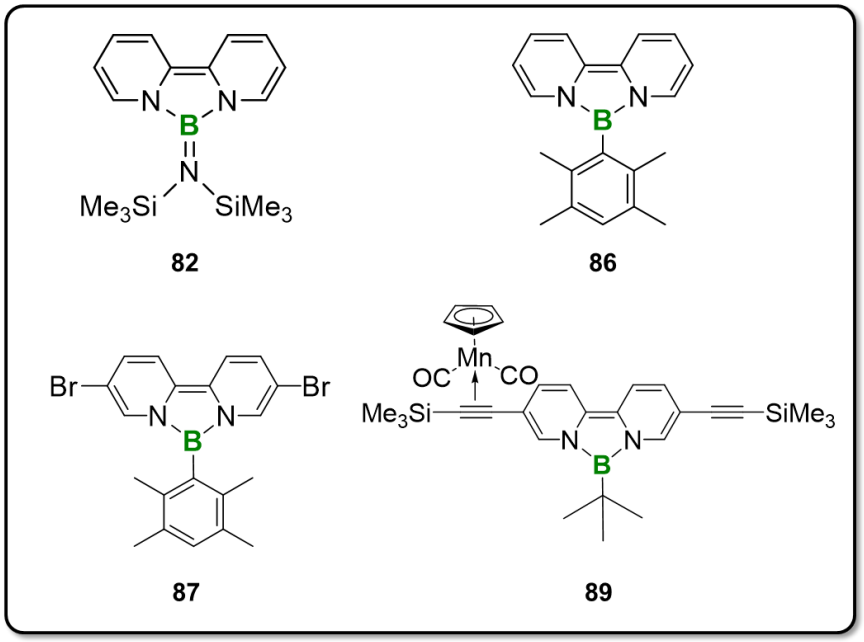

Abbildung 97. Komplexe **82-89**.

Von der bekannten Reaktion von [(Cp)(OC)$_2$Mn=B*t*Bu] (**43**) mit Ph$_3$P=S inspiriert, die zum intermediären Komplex [(Cp)(OC)$_2$Mn(μ^2-SB(*t*Bu))] mit einer B=S-Doppelbindung führt, wurden in dieser Arbeit ebenfalls Reaktionen von Borylenkomplexen mit elementaren Chalkogenen E (E = S$_8$, Se, Te) untersucht. Aufgrund der erfolglosen Isolierung von Produkten aus der Reaktion von **43** mit E (E = S$_8$, Se, Te) wurde das basenstabilisierte Borylen [(Cp)(OC)$_2$Mn=B(IMe)*t*Bu] (**90**) zur Reaktion mit jeweils einem Äquivalent der Chalkogene gebracht. Dabei konnten Verbindungen [(Cp)(OC)$_2$Mn-E=B(IMe)*t*Bu] (E = S, Se, Te) (**91-93**) isoliert werden, die eine B=E-Doppelbindung aufweisen (**Abbildung 98**). Die [E=B(IMe)*t*Bu]-Einheit bleibt in diesen Verbindungen durch eine koordinative Bindung an das Metallzentrum gebunden. Die Zusammensetzung dieser Verbindungen wurde durch NMR-Analyse bestätigt und die Strukturen durch Röntgenstrukturanalyse aufgeklärt. Mithilfe von DFT-Rechnungen wurden die Bindungsverhältnisse analysiert. Der Wiberg-Bindungsindex von 1.7 für die E=B-Wechselwirkungen (E = S, Se, Te) bestätigen weiter den Doppelbindungscharakter dieser Konnektivitäten. Eine bemerkenswerte Tatsache ist, dass **93** die erste isolierte Verbindung mit

B=Te-Doppelbindungscharakter ist.

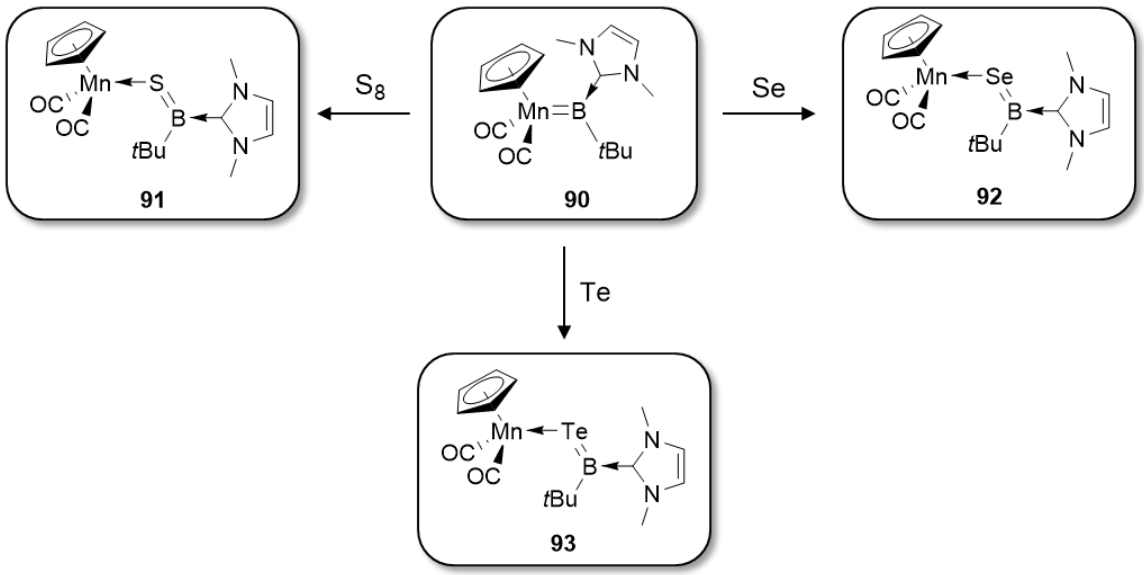

Abbildung 98. Synthese der Chalkogen-Insertionsprodukte **91-93**.

Um weitere Reaktionen des Borylens [(Cp)(OC)$_2$Mn=B*t*Bu] (**43**) mit elementaren Chalkogenen zu untersuchen, wurde **43** mit einem Überschuss (drei Äquivalente) an E (E = S, Se, Te) umgesetzt. Die Reaktionen mit S und Se führten zu cyclischen Bordichalkogenid-Spezies [*cyclo*-EEB(*t*Bu)(IMe)] (E = S, Se) (**94-95**; **Abbildung 99**) mit ^{11}B-NMR-Resonanzen bei ca. δ_B = 0. Im Gegensatz zu **94** und **95**, die einfache, metallfreie B-E-E-Dreiringe (E = S, Se) enthalten, führt die Reaktion von **43** mit Te zu einem unterschiedlichen Produkt, [(Cp)(OC)$_2$Mn{κ^1-*cyclo*-TeTeB(*t*Bu)(IMe)}] (**96**), bei welchem die [*cyclo*-TeTeB(*t*Bu)(IMe)]-Einheit über eine koordinative Bindung an das Manganatom gebunden ist. Der faszinierende Ligand [*cyclo*-TeTeB*t*Bu(IMe)] stellt das erste Beispiel eines dreigliedrigen, cyclischen Ditellurids eines Hauptgruppenelementes dar, das als isolierbares Analogon zum flüchtigen Ditelluriran, einem Isoster des Dioxirans, betrachtet werden kann. Versuche, die unkoordinierte Verbindung [TeTeB*t*Bu(IMe)] ausgehend von **96** durch Addition von Basen wie PMe$_3$ freizusetzen, schlugen fehl und führten stattdessen unter Chalkogenabstraktion zur Bildung des Monotellur-Komplexes [(Cp)(OC)$_2$Mn-Te=B(IMe)*t*Bu] (**93**).

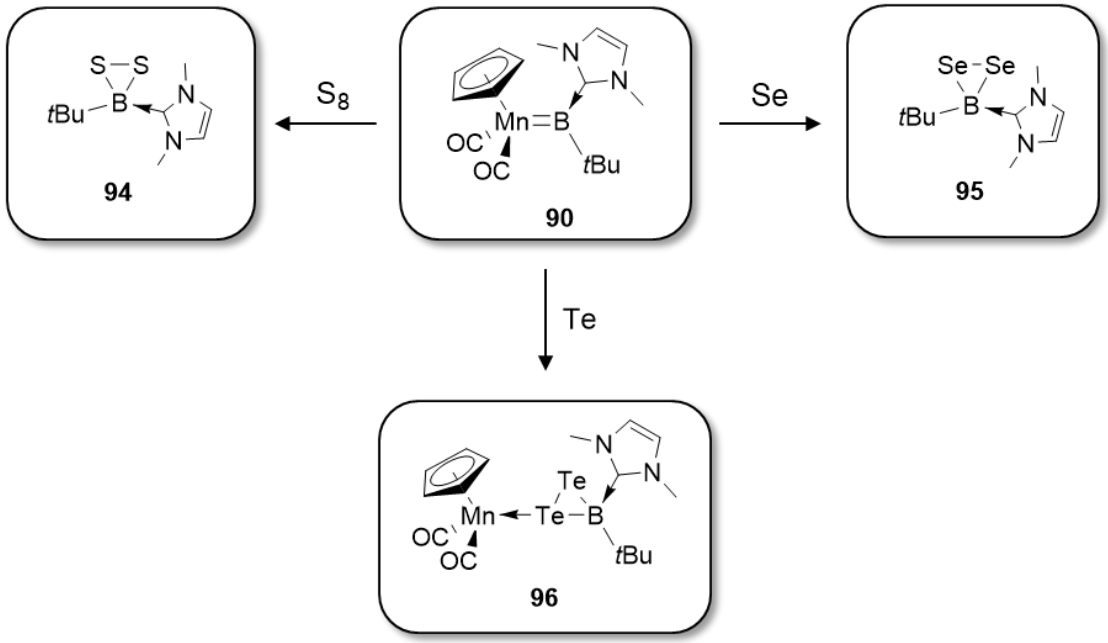

Abbildung 9. Synthese der dichalkogenhaltigen Produkte **94-96**.

In ähnlicher Weise erfolgte bei der Umsetzung der metallfreien Borchalkogene **94** und **95** mit PMe_3 bei Raumtemperatur die Bildung von [E=B*t*Bu(IMe)] (E = S, Se) (**97, 99**; **Abbildung 100**). Die Produkte zeigten ähnliche ^{11}B-NMR-chemische Verschiebungen im Vergleich zu den Verbindungen **91** und **92**. Obwohl die Komplexe im Festkörper stabil sind, können sie zu cyclischen B-E-E-B-Vierringen [*cyclo*-{(IMe)(*t*Bu)B-E-B(IMe)(*t*Bu)-E}] (E = S, Se) (**98**, **100**) dimerisieren.

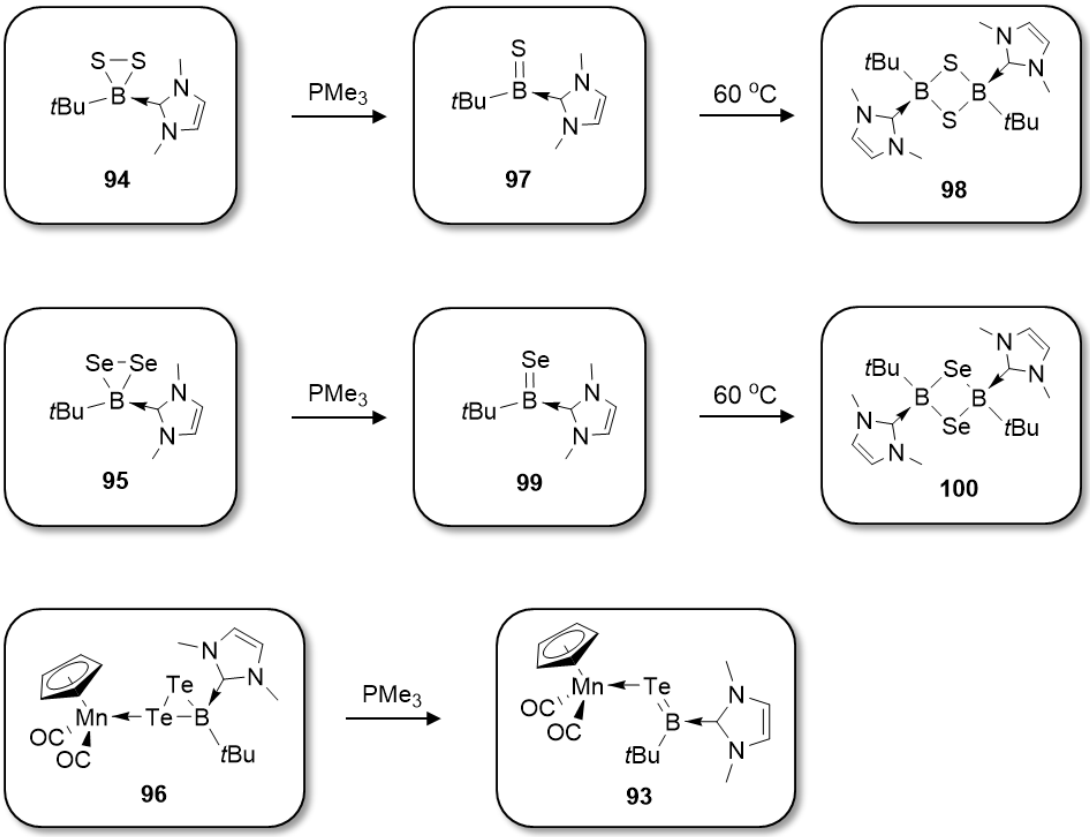

Abbildung 100. Synthese der Produkte **97-100.**

Neben der Reaktion mit PMe_3 reagierten die cyclischen Bordichalkogenid-Komplexe mit Borylenkomplexen zu einer Reihe von vier- oder fünfgliedrigen cyclischen Strukturen [*cyclo*-{(*t*Bu)(IMe)B-E-BR-E}] (E = S, Se, Te) bzw. [*cyclo*-{(*t*Bu)(IMe)B-EE-BR-E}] (E = S, Se) (**101-103, 105-109**; **Abbildung 101**). Diese Verbindungen weisen unsymmetrisch substituierte Boratome auf, die jeweils zwei unterschiedliche Resonanzen im ^{11}B-NMR-Spektrum zeigten. Die Konstitution dieser Verbindungen wurde durch multinukleare NMR-Spektroskopie bestätigt. Die Molekülstrukturen der meisten Produkte wurden zudem durch Einkristall-Röntgenstrukturanalyse bestimmt.

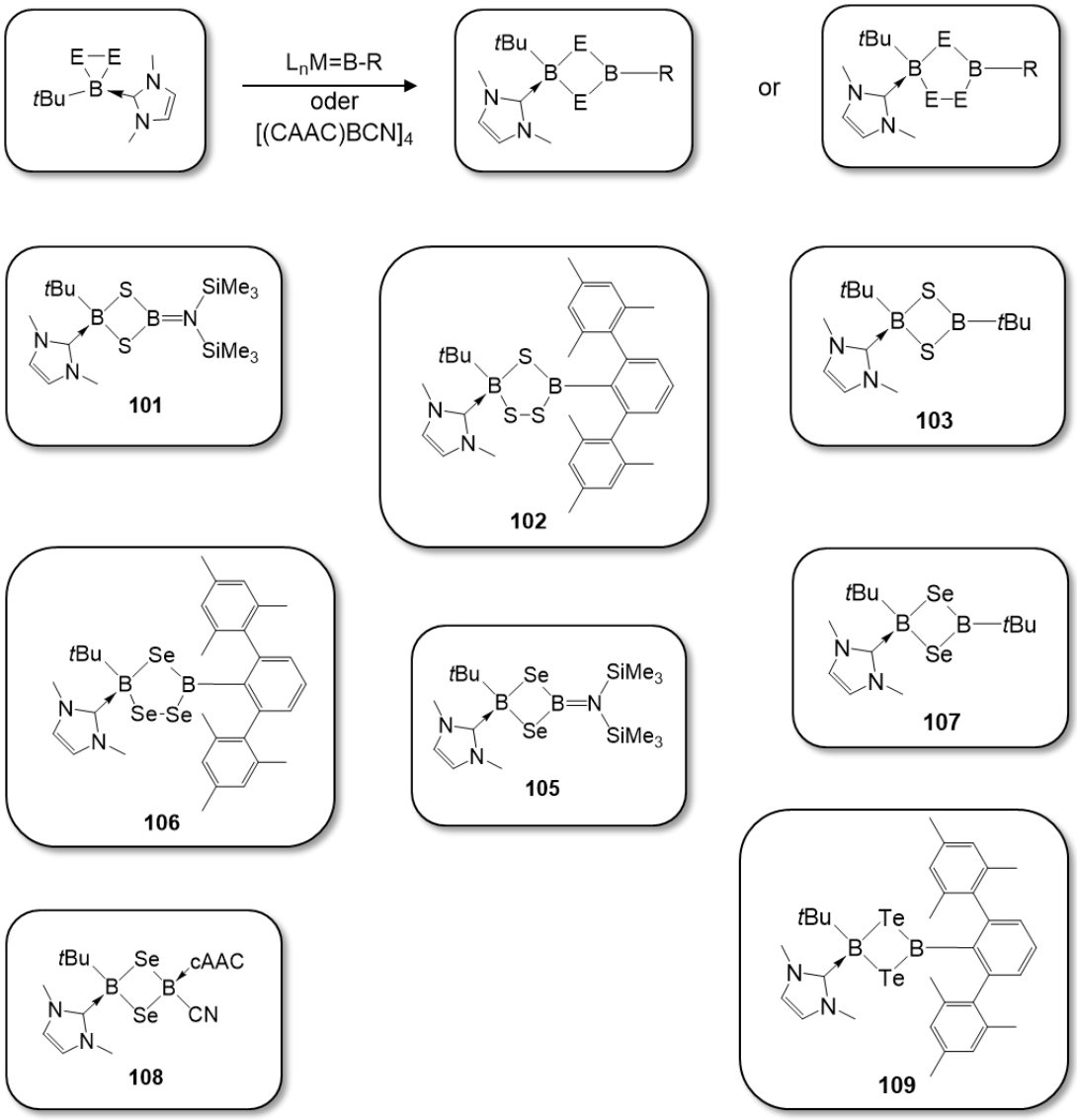

Abbildung 101. Synthese der Produkte **101-103, 105-109**.

Außerdem offenbarten die Borylen-Verbindungen vielversprechendes Potential in CH-Aktivierungsreaktionen. Die Reaktion des Molybdän-Borylenkomplexes $[(OC)_5Mo{=}BN(SiMe_3)_2]$ (**20**) mit $[Cp_2WH_2]$ (**110**) führte zur Insertion des Borylen-Fragmentes in die CH-Bindung des Cyclopentadienyl-Liganden. Verblüffenderweise war das Borylen **20** sogar imstande, bis zu vier C-H-Bindungen des Cyclopentadienyl-Liganden in **110** zu aktivieren (**Abbildung 102**). Die Strukturen der Mono- und Bisboryl-Produkte $[CpWH_2\{\eta^5\text{-}C_5H_4(BHN(SiMe_3)_2)\}]$ (**111**) bzw. $[WH_2(\eta^5\text{-}C_5H_4\{BHN(SiMe_3)_2\}_2)]$ (**112**) wurden durch

Einkristallröntgenstrukturanalyse bestätigt. Aufgrund von Löslichkeitsproblemen konnten die Tris- und Tetrakisboryl-Produkte $[(\eta^5\text{-}C_5H_3\{BHN(SiMe_3)_2\}_2)WH_2(\eta^5\text{-}C_5H_4\{BHN(SiMe_3)_2\})]$ (**113**) bzw. $[WH_2(\eta^5\text{-}C_5H_3\{BHN(SiMe_3)_2\}_2)_2]$ (**114**) nur spektroskopisch, aber nicht strukturell charakterisiert werden.

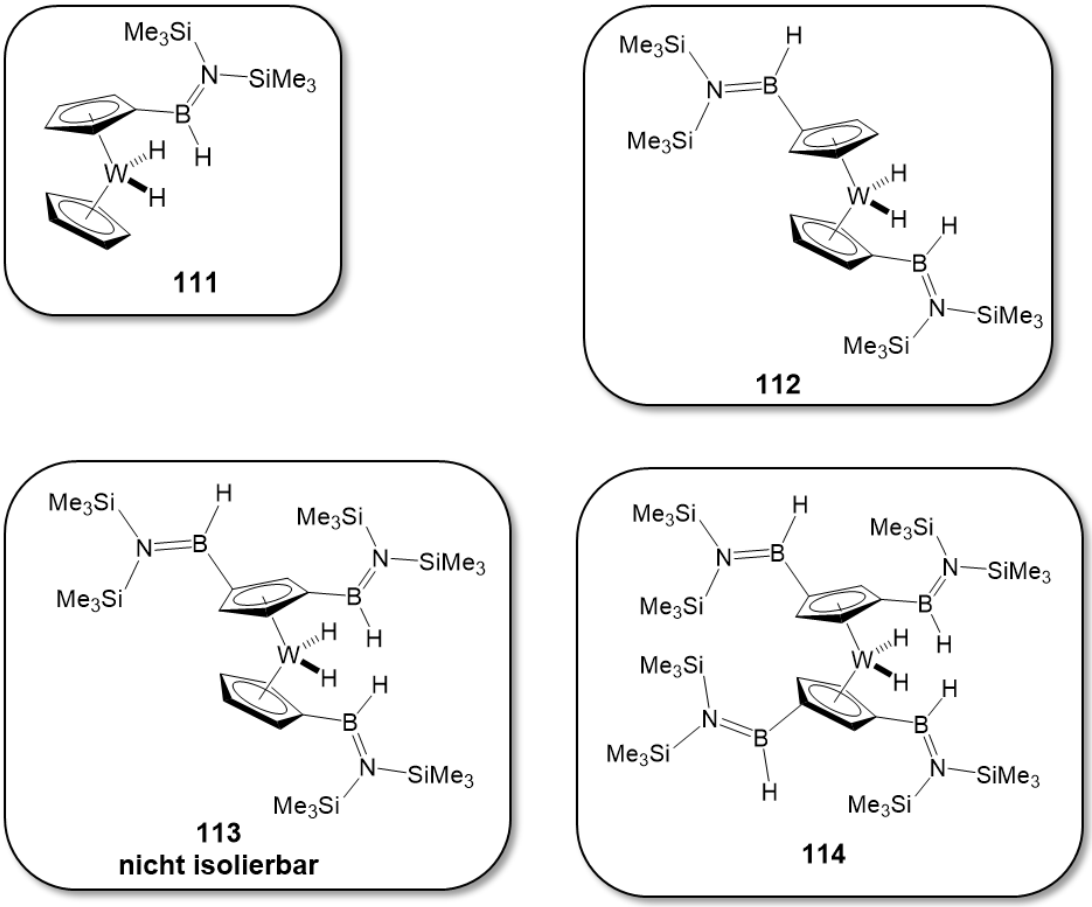

Abbildung 102. Komplexe **111-114**.

Die Reaktion von $[(Cp)(OC)_2Mn{=}B\textit{t}Bu]$ (**43**) mit Lewissäuren ($GaCl_3$, $InBr_3$) führte zur vollständigen Eliminierung der Borylen-Einheit als $Cl_2B\textit{t}Bu$ (**117**) bzw. $Br_2B\textit{t}Bu$ (**123**), wobei die Produkte $[(Cp)(OC)_2Mn(GaCl_2)_2]$ (**116**) bzw. $[(Cp)(OC)_2Mn(InBr_2)_2]$ (**122**) als gelbe Pulver erhalten wurden. Aufgrund ihrer geringen Löslichkeit konnten die Strukturen von **116** und **122** kristallographisch nicht aufgeklärt werden. Des Weiteren führte die Addition von Lewisbasen (PMe_3, THF, Et_2O, DMAP) an **116** und **122** zur Bildung der Addukte $[(Cp)(OC)_2Mn(L)(ECl_2)_2]$ (E = Ga, In; L = PMe_3, THF,

Et_2O, DMAP; **117-124**). Aufgrund der geringen Löslichkeit der Verbindungen konnte ihre Konstitution nicht durch NMR-Spektroskopie, jedoch durch Elementaranalyse und Einkristallröntgenstrukturanalyse bestätigt werden.

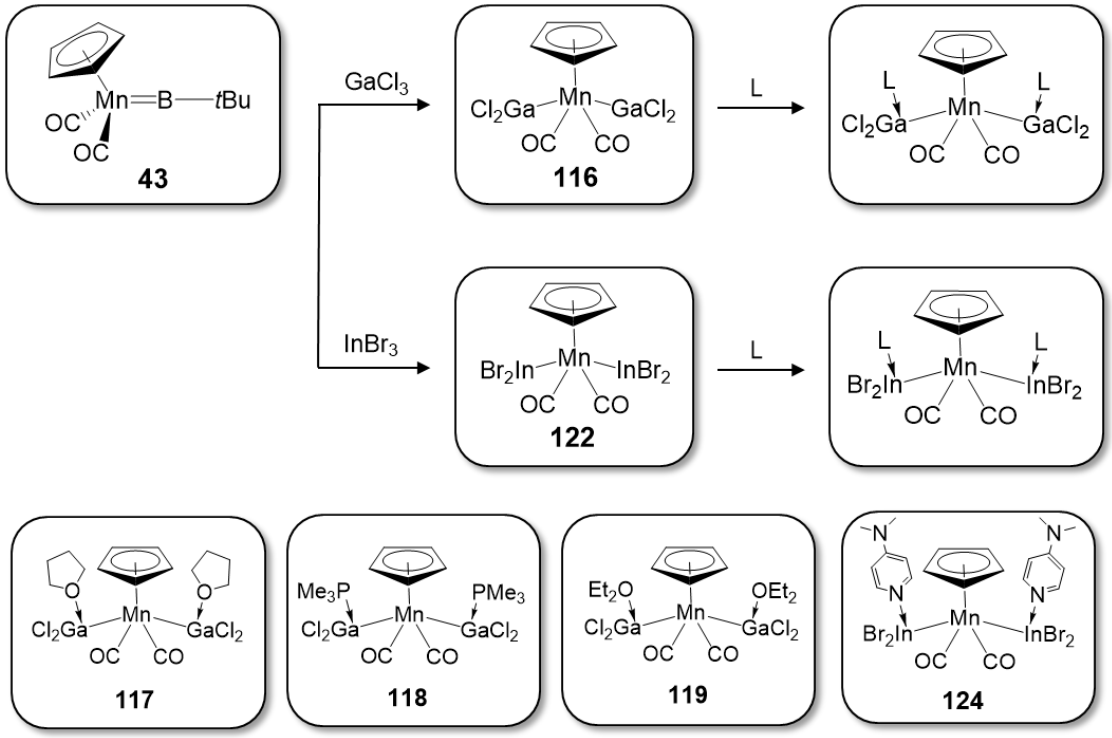

Abbildung 103. Synthese der Produkte **116-120**.

Zusammenfassend wurden in diesem Projekt neue Reaktionsmuster von Übergangsmetallborylen-Komplexen (**20**, **22**, **43**, **50** und **90**) entdeckt, die neue Einsichten in die Synthese von borhaltigen Spezies liefern. BN-analoge Verbindungen von Fluorenylanion-Komplexen wurden zwar bereits isoliert, ihre gezielte Synthese ist jedoch noch wenig entwickelt. Durch Transfer des Borylen-Liganden auf Bipyridin-Spezies konnte ein Weg gefunden werden, solche Verbindungen gezielt darzustellen. Ausgehend von der Reaktion mit elementaren Chalkogenen (S_8, Se und Te) wurden Komplexe mit ungewöhnlichen Bor-Chalkogen-Interaktionen synthetisiert, darunter Komplexe mit B=Te- (**93**), B-Se-Se- (**95**) und B-Te-Te-Interaktionen (**96**), die die ersten Beispiele ihrer Art darstellen. Diese Ergebnisse unterstreichen das Potential von hypovalenten Borverbindungen, im Besonderen Übergangsmetallborylen-Komplexen, als Ausgangspunkt zur

ungewöhnlichen Chalkogen-Chemie zu fungieren. Im Weiteren können die entsprechenden cyclischen Bor-Dichalkogenide (**94**, **95** und **96**) mit Borylenkomplexen zu unsymmetrischen Heterocyclen reagieren, in denen die Borzentren in Kombinationen aus sp^2-sp^3- und sp^3-sp^3-Hybridisierungen vorliegen. Dies stellt die erste Methode zur Darstellung von solchen unsymmetrischen Bor-Chalkogenid-Cyclen dar und ermöglicht das Studium ihrer Eigenschaften und weiteren Anwendungsmöglichkeiten. Ausgehend von der Reaktion des Borylens **20** mit [$CpWH_2$] entdeckten wir das Potential zur mehrfachen CH-Aktivierung in aromatischen Systemen, was einen alternativen Ansatz zur Synthese von borylierten, organischen Verbindungen darstellt. Schließlich gelang die vollständige Eliminierung einer Boryleneinheit vom Metallzentrum durch die Reaktion des Mangan-Borylens **43** mit $GaCl_3$ und $InBr_3$. In den Studien wurde ein alternativer Reaktionsweg von Borylenen gegenüber Gruppe-13-Halogeniden beobachtet, der sich von dem in einer bereits publizierten Arbeit unterscheidet.[208]

5. Experimental Section

5.1 General information

Due to the sensitivity of most compounds that were used in this study towards air and moisture, all manipulations were carried on under a dry argon atmosphere using standard Schlenk techniques[211] or in a argon-filled gloveboxes unless otherwise stated. All solvents were purified under argon by distillation with appropriate drying agents prior to use.[212] The pre-dried solvents were degassed by three freeze-pump cycles. C_6D_6, THF-d_8, Toluene-d_8, CD_2Cl_2 and $CDCl_3$ were degassed by three freeze-pump cycles and stored over molecular sieves.

All NMR spectra in solution were acquired on a Bruker Avance I 500 spectrometer (^{1}H: 500.1 MHz, ^{11}B: 160.5 MHz, ^{13}C: 125.8 MHz, ^{77}Se: 57.2 MHz). ^{1}H NMR and $^{13}C\{^1H\}$ NMR spectra were referenced to external TMS via residual protons of the solvent (^{1}H) or the solvent itself (^{13}C). $^{11}B\{^1H\}$ NMR spectra were referenced to external $BF_3{\cdot}OEt_2$. ^{77}Se NMR spectra were referenced to external $(CH_3)_2Se$. Infrared data were acquired on a JASCO FT/IR-6200type A apparatus. UV-vis spectra were measured on a JASCO V-660 UV-vis spectrometer at room temperature. Elemental analyses were performed on an Elementar vario MICRO cube elemental analyzer. High-resolution mass spectrometry was obtained from a Thermo Scientific Exactive Plus spectrometer.

5.2 Starting materials

The following starting materials were synthesized according to literature procedures: $[(OC)_5Mo{=}BN(SiMe_3)_2]$ (**20**),[106] 5,5'-bis[(trimethylsilyl)ethynyl]-2,2'-bipyridine (**85**),[213] 5,5'-dibromo-2,2'-bipyridine (**83**),[213] $[(Me_3P)(OC)_3Fe{=}BDur]$ (**50**),[112] $[(Cp)(OC)_2Mn{=}B\textit{t}Bu]$ (**43**),[145] $[(Cp)(OC)_2Mn{=}B(IMe)\textit{t}Bu]$ (**90**),[145] $[(OC)_5Cr{=}BTp]$ (**22**),[105] $[(cAAC)B(CN)]_4$ (**104**),[163] $[Cp_2WH_2]$ (**110**).[214]

5.3 Computational Details

Calculations were performed using the Gaussian 09 suite of programs[215] using the B3LYP functional.[216-217] The def2-tzvp[218] basis set was used for atoms. Natural charge analysis was performed using the NBO6 program as implemented in Gaussian 09.[171] The stationary points were characterized as minima by full vibration frequency calculations (no imaginary frequencies). All geometry optimizations were carried out without symmetry constraints.

5.4 Reactivity of borylene complexes with bipyridine species

5.4.1 Reaction of [(OC)$_5$Mo=BN(SiMe$_3$)$_2$] (20) with 2,2'-bipyridine (81)

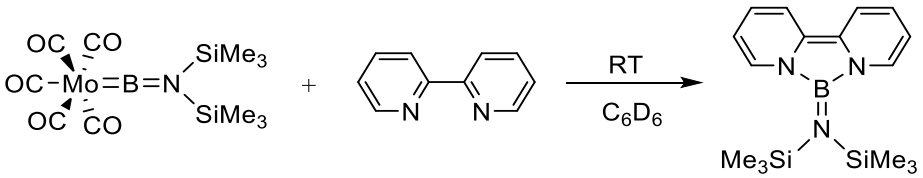

20 **81** **82**

To a solid mixture of **20** (41 mg, 0.10 mmol) and **81** (16 mg, 0.10 mmol) was added benzene (5 mL). The mixture was stirred at room temperature for 6 h and the resulting red solution was filtered through a cotton plug. The solvent of the filtrate was then evaporated under reduced pressure. The red oil was then dissolved in pentane (3 mL) and then kept at –30 ºC in an open system. The crystals that were formed during the evaporation were filtered off and the solvent of the filtrate was dried under reduced pressure to give a red oil which was treated similary three more times. **82** was obtained in this way as red oil (yield cannot be calculated).

^{1}H NMR (C_6D_6) δ = 7.51 (dt, J = 7.2, 1.2 Hz, 2H, C*H*-Bipyridine), 7.11 (dt, J = 9.2, 1.3 Hz, 2H, C*H*-Bipyridine), 6.11 (ddd, J = 9.2, 6.0, 1.1 Hz, 2H, C*H*-bipyridine), 5.99 (ddd, J = 7.2, 6.0, 1.2 Hz, 2H, C*H*-bipyridine), 0.07 (s, 18H, Si(C*H*$_3$)$_3$); ^{13}C NMR (C_6D_6) δ = 126.4 (s, *C*H-bipyridine), 118.7 (s, *C*H-bipyridine), 117.1 (s, *C*H-bipyridine), 114.0 (s, *C*H-bipyridine), 3.0 (s, Si(*C*H$_3$)$_3$); ^{11}B NMR (C_6D_6) δ = 20.0 (s).

Elemental analysis (%) calcd. data for $C_{16}H_{26}BN_3Si_2$: C 54.70, H 8.01, N 12.84. Anal. Found: C 54.53, H 7.83, N 11.50.

5.4.2 Reaction of $[(OC)_5Mo=BN(SiMe_3)_2]$ (20) with 5,5'-dibromo-2,2'-bipyridine (83)

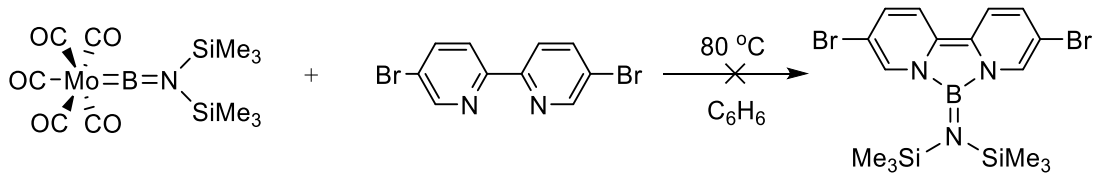

20 **83**

In a Young NMR tube, a solution of **20** (41 mg, 0.10 mmol) and **83** (31 mg, 0.10 mmol) in benzene (5 mL) was added at room temperature. The reaction was kept at room temperature and the ^{11}B NMR showed no visible change. The tube was then heated to 80 ºC. After being kept for 12 h, the ^{11}B NMR spectrum showed a small peak at $\delta_B = 20$ and the ^{1}H NMR spectrum showed many unassignable signals.

5.4.3 Reaction of $[(OC)_5Mo=BN(SiMe_3)_2]$ (20) with 5,5'-bis[(trimethylsilyl)ethynyl]-2,2'-bipyridine (85)

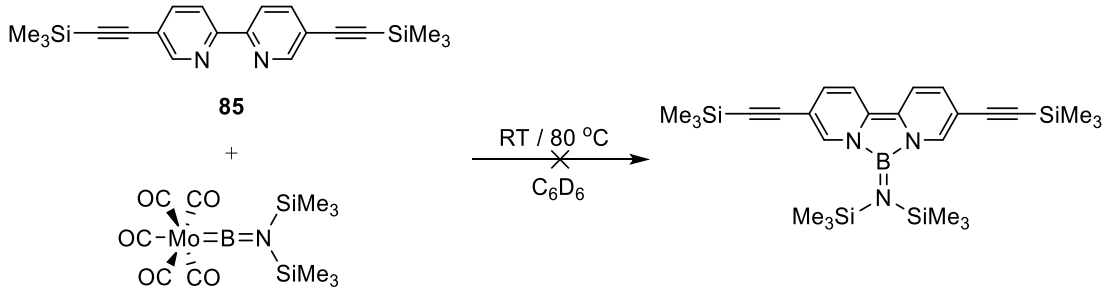

The reaction procedure was the same as in **4.4.2** and no pure product was isolated from this reaction.

5.4.4 Reaction of [(Me3P)(OC)3Fe=BDur] (50) with 2,2'-bipyridine (81)

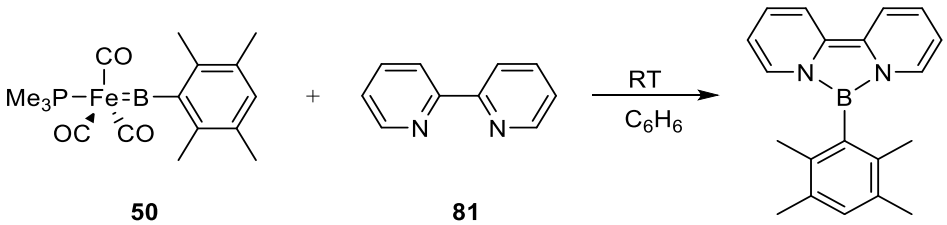

50 **81** **86**

To a solid mixture of **50** (36 mg, 0.10 mmol) and **81** (16 mg, 0.10 mmol) was added benzene (5 mL). The reaction mixture was kept at room temperature for 12 h and the dark red solution was filtered through a cotton plug. The solvent of the filtrate was evaporated at reduced pressure and the red solid was dissolved in 3 mL of pentane. The solution of the crude product was filtered and stored at –30 ºC. After 12 h, the filtrate yielded red crystals of **87** as an analytically pure product (13 mg, 43%).

^{1}H NMR (C_6D_6) δ = 7.28 (dt, *J* = 9.2, 1.2 Hz, 1H, C*H*-bipyridine), 7.19 (dt, *J* = 7.2, 1.1 Hz, 1H, C*H*-bipyridine), 7.04 (s, 1H, C*H*-Dur), 6.20 (ddd, *J* = 9.2, 6.1, 1.0 Hz, 1H), 5.93 (ddd, *J* = 7.2, 6.1, 1.2 Hz, 1H, C*H*-bipyridine, 2.16 (s, 6H, CH_3-Dur), 1.95 (s, 6H, CH_3-Dur); ^{11}B NMR (C_6D_6) δ = 23.2; ^{13}C NMR (C_6D_6) δ = 138.7 (s, *C*H-Dur), 133.5 (s, *C*H-Dur), 133.0 (s, *C*H-Dur), 118.7 (s, *C*H-Bipyridine), 114.5 (s, *C*H-bipyridine), 110.7 (s, *C*H-bipyridine), 20.1 (s, *C*H_3-Dur), 19.20 (s, *C*H_3-Dur).

Elemental analysis (%) calcd. data for $C_{20}H_{21}BN_2$: C 80.02, H 7.05, N 9.33. Anal. Found: C 79.73, H 7.69, N 8.90.

5.4.5 Reaction of [(Me3P)(OC)3Fe=BDur] (50) with 5,5'-dibromo-2,2'-bipyridine (83)

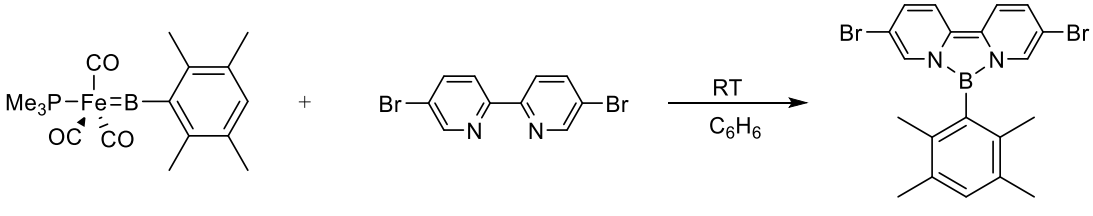

50 **83** **87**

To a solid mixture of **50** (36 mg, 0.10 mmol) and **83** (32 mg, 0.10 mmol) was added benzene (5 mL). The reaction mixture was stirred at room temperature for 12 h and the dark red solution was filtered through a cotton plug. The solvent of the filtrate was evaporated at reduced pressure and the red solid was dissolved in 3 mL of pentane. The solution of the crude product was filtered and stored at –30 ºC. After 12 h, the filtrate yielded red crystals of **87** suitable for X-ray diffraction analysis.

5.4.6 Reaction of [(Cp)(OC)$_2$Mn=B*t*Bu] (43) with 5,5'-bis[(trimethylsilyl)ethynyl]-2,2'-bipyridine (85)

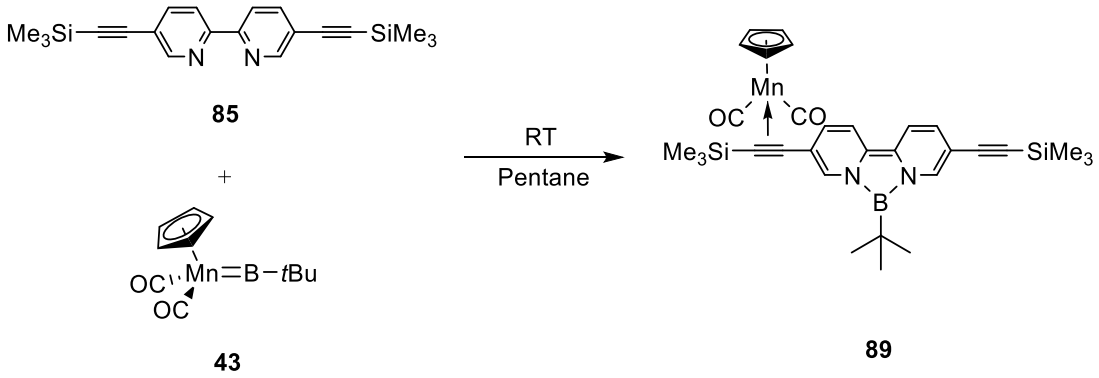

To a solid mixture of **43** (24 mg, 0.10 mmol) and **85** (35 mg, 0.10 mmol) was added pentane (5 mL). The solution was properly mixed and kept at room temperature for 12 h at which point compound **89** was isolated as dark red crystals. The solid was washed twice with 3 mL pentane at -30 ºC to yield pure **89** as a red solid in moderate yield (33.2 mg, 56%).

^{1}H NMR (C_6D_6) δ = 8.94 (s, 1H, C*H*-bipyridine), 8.37 (s, 1H, C*H*-bipyridine), 6.93 (dd, *J* = 17.2, 9.4 Hz, 2H, C*H*-bipyridine), 6.72 (d, *J* = 9.4 Hz, 1H, C*H*-bipyridine), 6.44 (d, *J* = 9.4 Hz, 1H, C*H*-bipyridine), 4.29 (s, 6H, C*H*-Cp), 1.31 (s, 9H, CH_3-*t*Bu), 0.43 (s, 9H, SiMe_3), 0.30 (s, 9H, SiMe_3); ^{11}B NMR (C_6D_6) δ = 25.3; ^{13}C NMR (C_6D_6) δ = 233.6 (CO), 135.5, 134.1, 119.8, 118.5, 118.4, 118.1, 117.4, 116.7 (*C*H-bipyridine), 106.9, 104.9, 102.0, 94.0 (*C*≡*C*), 84.9 (Cp), 32.0, 30.0 (*C*H_3-*t*Bu), 1.2, 0.2 (*C*H_3-SiMe_3).

Elemental analysis (%) calcd. data for $C_{31}H_{38}BMnN_2O_2Si_2$: C 61.83, H 6.46, N 4.73. Anal. Found: C 61.99, H 6.57, N 4.60.

5.5 Reactivity of borylenes with elemental chalcogens to form B=E (E = S, Se, Te) double bonds

5.5.1 Reaction of [(Cp)(OC)$_2$Mn=B*t*Bu] (43) with S_8

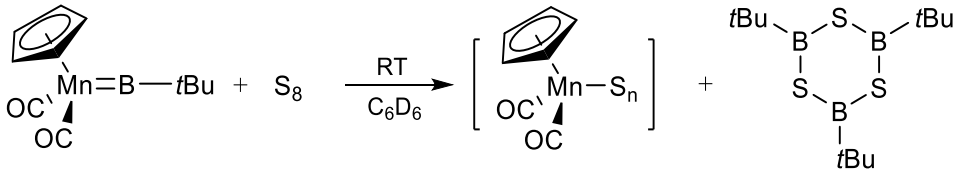

43

A benzene solution of **43** (24 mg, 0.10 mmol) and S_8 (3.2 mg, 0.013 mmol) was added to a Young NMR tube and was kept at room temperature. After 12 h, the solution had turned from light red to yellow and the ^{11}B NMR spectrum indicated the formation of [SB(tBu)]$_3$ (δ_B = 72).

5.5.2 Reaction of [(Cp)(OC)$_2$Mn=B*t*Bu] (43) with Se and Te

The reactions were carried out in a benzene solution at room temperature. No isolable product was isolated. For reaction with Se, the ^{11}B NMR spectrum showed a signal at δ_B = 70. In case of Te, no reaction was observed at room temperature between **43** and the elemental tellurium. The reaction mixture was heated and kept at 60 °C for 24 h, leading not to a similar reactivity as seen with S and Se, but instead to the decomposition of the manganese borylene **43**.

5.5.3 Reaction of [(Cp)(OC)$_2$Mn=B(IMe)*t*Bu] (90) with S_8 in a 1:1 boron-to-sulfur ratio

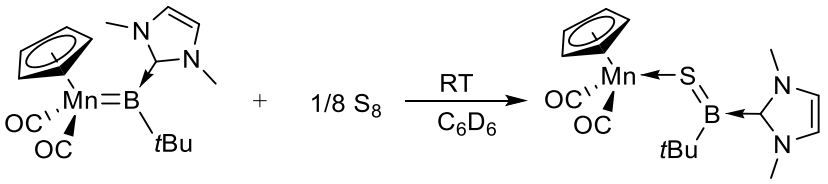

90 **91**

A solid mixture of compound **90** (68 mg, 0.20 mmol) and S_8 (6.4 mg, 0.025 mmol) was dissolved in toluene (4 mL). After stirring for 24 h, the reaction mixture was filtered through a cotton plug, which was washed with pentane (2 mL). The combined filtrate fractions were dried under reduced pressure and [(OC)$_2$Mn-S=B*t*Bu(IMe)] was crystallized from a concentrated solution of toluene to yield **91** as orange crystals (39 mg, 53%).

^{1}H NMR (C_6D_6): δ = 5.80 (s, 2H, NC*H*C*H*N), 4.51 (s, 5H, C_5H_5), 3.08 (s, 6H, N-CH_3), 1.07 (s, 9H, CH_3-*t*Bu); ^{11}B NMR (C_6D_6): δ = 67.4 (s, br); ^{13}C{^{1}H} NMR (C_6D_6): δ = 237.4 (s, *C*O), 121.5 (s, N*C*H*C*HN), 83.8 (s, C_5H_5), 36.4 (s, N-CH_3), 30.4 (s, CH_3-*t*Bu).

IR (solid): 1892 (s), 1824 (s) (*ν*CO) cm^{-1}; UV-vis (pentane): λ_1 = 427 nm; λ_2 = 257 nm.

Elemental analysis (%) calcd. data for $C_{16}H_{22}SBMnN_2O_2$: C 51.64, H 5.96, N 7.53, S: 8.61; Anal. found: C 51.50, H 6.13, N 7.61, S: 8.36.

5.5.4 Reaction of [(Cp)(OC)$_2$Mn=B(IMe)*t*Bu] (90) with one equivalent of Se

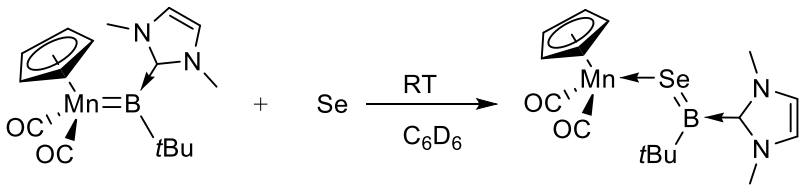

90 **92**

A solid mixture of compound **90** (68 mg, 0.20 mmol) and Se (16 mg, 0.20 mmol) was dissolved in toluene (4 mL). After stirring for 24 h, the reaction mixture was filtered through a cotton plug, which was washed with pentane (2 mL). The combined filtrate fractions were dried under reduced pressure and [$(OC)_2$Mn-Se=B*t*Bu(IMe)] was crystallized from a concentrated solution of toluene to yield **92** as orange crystals (yield: 28 mg, 46%).

^{1}H NMR (C_6D_6): δ = 5.80 (s, 2H, NC*H*C*H*N), 4.46 (s, 5H, C_5H_5), 3.08 (s, 6H, N-CH_3), 1.08 (s, 9H, CH_3-*t*Bu); ^{11}B NMR (C_6D_6): δ = 73.2 (s, br); ^{13}C{^{1}H} NMR (C_6D_6): δ = 237.6 (s, *C*O), 121.8 (s, NC*H*C*H*N), 83.1 (s, C_5H_5), 36.0 (s, N-CH_3), 29.9 (s, CH_3-*t*Bu).

IR(soild): 1886 (s), 1817 (s) (*ν*CO) cm^{-1}; UV-vis (pentane): λ_1 = 456 nm; λ_2 = 274 nm.

Elemental analysis (%) calcd. data for $C_{16}H_{22}SeBMnN_2O_2$: C 45.86, H 5.29, N 6.68; Anal. found: C 45.60, H 5.58, N 6.74.

5.5.5 Reaction of [(Cp)$(OC)_2$Mn=B(IMe*t*Bu] (90) with one equivalent of Te.

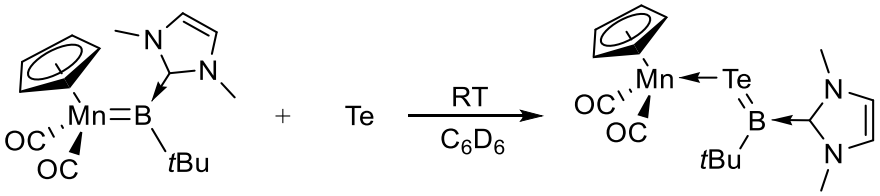

90 **93**

A solid mixture of compound **90** (68 mg, 0.20 mmol) and Te (25 mg, 0.20 mmol) was dissolved in toluene (4 mL). After stirring for 24 h, the reaction mixture was filtered through a cotton plug, which was washed with 2 mL of pentane. The combined filtrate fractions were dried under reduced pressure and [$(OC)_2$Mn-Te=B*t*Bu(IMe)] was crystallized from a concentrated solution of toluene at –30 °C to yield **93** as dark violet crystals (31 mg, 38%).

^{1}H NMR (C_6D_6): δ = 5.78 (s, 2H, NC*H*C*H*N), 4.40 (s, 5H, C_5H_5), 3.12 (s, 6H, N-CH_3), 1.07 (s, 9H, CH_3-*t*Bu); ^{11}B NMR (C_6D_6): δ = 77.2 (s, br); ^{13}C{^{1}H} NMR (C_6D_6): δ = 237.5 (s, *C*O), 122.0 (s, NC*H*C*H*N), 82.1 (s, C_5H_5), 35.1 (s, N-*C*H_3), 28.8 (s, *C*H_3-*t*Bu); ^{125}Te NMR (C_6D_6): δ 368.8 (s, br).

IR (solid): 1889 (s), 1825 (s) (ν_{CO}) cm^{-1}; UV-vis (pentane): λ_1 = 515 nm; λ_2 = 310 nm; λ_3 = 255 nm.

Elemental analysis (%) calcd. data for $C_{16}H_{22}TeBMnN_2O_2$: C 41.09, H 4.74, N 5.99; Anal. found: C 41.27, H 4.77, N 6.45.

5.6 Reactivity of borylenes with elemental chalcogens to form cyclic boron chalcogenide species

5.6.1 Reaction of [(Cp)(OC)$_2$Mn=B(IMe)*t*Bu] (90) with S$_8$ in a 1:3 boron-to-sulfur ratio

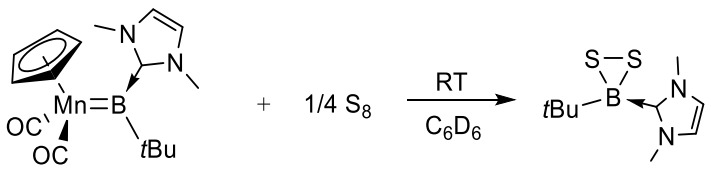

90 **94**

A solid mixture of compound **90** (68 mg, 0.20 mmol) and S_8 (19 mg, 0.075 mmol) in toluene (10 mL) was stirred for 24 h. The solution was filtered through a cotton plug and the solvent of the filtrate was removed under reduced pressure. The crude product of **94** was washed three times with 5 mL pentane and [*cyclo*-SSB*t*Bu(IMe)] was recrystallized out of a concentrated solution of toluene/pentane at –30 °C to yield **94** as yellow crystals (8 mg, 19%).

^{1}H NMR (C_6D_6): δ = 5.37 (s, 2H, NC*H*C*H*N), 3.10 (s, 6H, N-CH_3), 1.26 (s, 9H, CH_3-*t*Bu); ^{11}B NMR (C_6D_6): δ = –2.9 (s); ^{13}C{^{1}H} NMR (C_6D_6): δ = 120.0 (s,

N*C*H*C*HN), 37.0 (s, N-*C*H$_3$), 31.0 (s, *C*H$_3$-*t*Bu).

Elemental analysis (%) calcd. data for $C_9H_{17}S_2BN_2$: C 47.37, H 7.51, N 12.25. Anal. Found: C 47.84, H 7.44, N 12.69.

5.6.2 Reaction of [(Cp)(OC)$_2$Mn=B(IMe)*t*Bu] (90) with an excess of Se (gray)

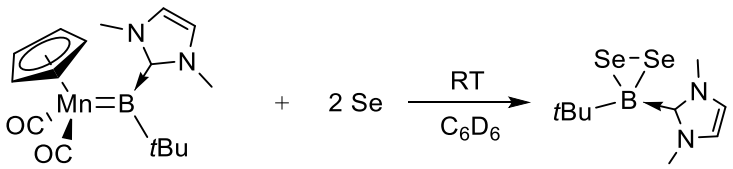

90 **95**

A solid mixture of compound **90** (68 mg, 0.20 mmol) and gray selenium (47 mg, 0.60 mmol) in toluene (10 mL) was stirred for 24 h. The unreacted selenium was filtered off through a cotton plug and the solvent was removed under reduced pressure. The crude product was washed three times with 5 mL pentane and [*cyclo*-SeSeB*t*Bu(IMe)] was recrystallized from a concentrated toluene/pentane solution at –30 ºC to yield **95** as violet crystals (51 mg, 80% yield).

^{1}H NMR (C_6D_6): δ = 5.43 (s, 2H, NC*H*C*H*N), 3.14 (s, 6H, N-C*H*$_3$), 1.33 (s, 9H, C*H*$_3$-*t*Bu); ^{11}B NMR (C_6D_6): δ = –2.9 (s); ^{13}C{^{1}H} NMR (C_6D_6): δ = 120.2 (s, N*C*H*C*HN), 37.9 (s, N-*C*H$_3$), 31.9 (s, *C*H$_3$-*t*Bu); ^{77}Se NMR (C_6D_6): δ 250.0 (s).

Elemental analysis (%) calcd. data for $C_9H_{17}Se_2BN_2$: C 32.57, H 5.32, N 8.70. Anal. Found: C 32.98, H 5.45, N 8.59.

5.6.3 Reaction of [(Cp)(OC)$_2$Mn=B(IMe)*t*Bu] (90) with an excess of Te

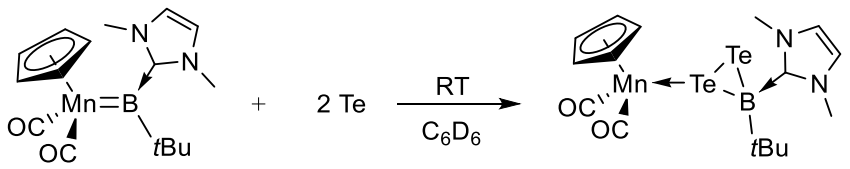

90 **96**

A solid mixture of compound **90** (68 mg, 0.20 mmol) and Te (76 mg, 0.60 mmol) in toluene (5 mL) was stirred for 120 h. The solution was filtered through a cotton plug and the solvent of the filtrate was concentrated to 2 mL under reduced pressure. 10 mL of pentane was added to the concentrated solution, and the mixture was cooled to –30 ºC to yield pure violet crystals of [(Cp)(OC)$_2$Mn{κ^1-*cyclo*-TeTeB(*t*Bu)(IMe)}] (**96**) (50 mg, 46%).

^{1}H NMR (C_6D_6): δ = 5.80 (s, 1H, NC*H*C*H*N), 5.69 (s, 1H, NC*H*C*H*N), 4.23 (s, 5H, C_5H_5), 3.70 (s, 3H, N-CH_3), 3.17 (s, 3H, N-CH_3), 1.21 (s, 9H, CH_3-*t*Bu); ^{11}B NMR (C_6D_6): δ = –1.99 (s); ^{13}C{^{1}H} NMR (C_6D_6): δ 235.5 (s, *C*O), 121.9 & 121.3 (s, NC*H*C*H*N), 84.1 (s, C_5H_5), 39.7 (s, N-*C*H$_3$), 33.0 (s, CH$_3$-*t*Bu).

Elemental analysis (%) calcd. data for $C_9H_{17}SeBN_2$: C 33.34, H 3.56, N 4.71. Anal. Found: C 33.16, H 3.87, N 4.80.

5.6.4 Reaction of [(Cp)(OC)$_2$Mn{κ^1-*cyclo*-TeTeB(*t*Bu)(IMe)}] (96) with PMe$_3$

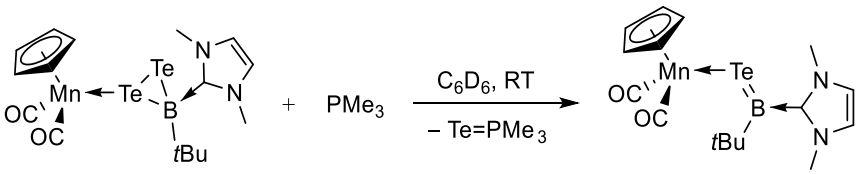

96 **93**

A C_6D_6 solution of [(Cp)(OC)$_2$Mn{κ^1-*cyclo*-TeTeB(*t*Bu)(IMe)}] (**96**) (60 mg, 0.10 mmol) and PMe$_3$ (15 mg, 0.20 mmol) was introduced to a Young NMR tube. After keeping the mixture at room temperature for 12 h, the color of the solution had turned

from dark violet to dark red.

^{1}H NMR (C_6D_6): δ = 5.78 (s, 2H, NC*H*C*H*N), 4.40 (s, 5H, C_5H_5), 3.12 (s, 6H, N-CH_3), 1.07 (s, 9H, CH_3-*t*Bu); ^{11}B NMR (C_6D_6): δ = 77.2 (s, br); ^{13}C{^{1}H} NMR (C_6D_6): δ = 237.5 (s, *C*O), 122.0 (s, N*C*H*C*HN), 82.1 (s, C_5H_5), 35.1 (s, N-*C*H_3), 28.8 (s, *C*H_3-*t*Bu); ^{125}Te NMR (C_6D_6): δ 368.8 (s, br). The signals of the product were consistent with previously characterized sample of **93**.

5.6.5 Reaction of [*cyclo*-SSB*t*Bu(IMe)] (94) with PMe_3

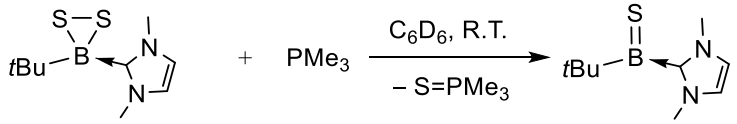

94 **97**

Compound [*cyclo*-SSB*t*Bu(IMe)] (**94**) (23 mg, 0.10 mmol) was dissolved in toluene (4 mL) and PMe_3 (15 mg, 0.20 mmol) was added to the solution. The mixture was stirred for 20 min and pentane (5 mL) was added. Then the mixture was cooled to –30 ºC and kept at this temperature overnight. [S=BtBu(IMe)] (**97**) was obtained as white crystals from a concentrated toluene/pentane solution as a pure compound (13 mg, 62%).

^{1}H NMR (toluene-d_8, 243 K): δ = 5.51 (s, 2H, NCHCHN), 2.83 (s, 6H, N-CH_3), 1.29 (s, 9H, *t*Bu); ^{11}B NMR (toluene-d_8, 243 K): δ = 66.4 (s); ^{13}C{^{1}H} NMR (toluene-d_8, 243 K): δ = 119.9 (s, NCHCHN), 35.4 (s, N-CH_3), 30.3 (s, C(CH_3)$_3$).

Elemental analysis (%) calcd. data for $C_9H_{17}SeBN_2$: C 55.12, H 8.47, N 14.28. Anal. Found: C 54.56, H 8.66, N 13.94, S 15.54.

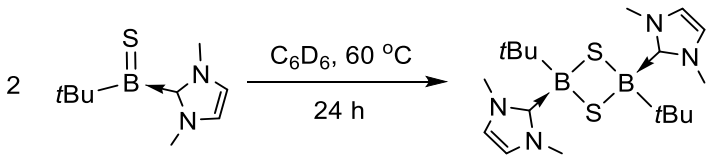

97 **98**

Compound **97** (23 mg, 0.10 mmol) was dissolved in toluene and the solution was kept at room temperature for 48 h. The solvent was removed under reduced pressure and [*cyclo*-{(IMe)(*t*Bu)B-S-B(IMe)(*t*Bu)-S}] was isolated by recrystallizing the crude product with toluene/pentane to yield **98** as a white powder (20 mg, 87%).

^{1}H NMR (toluene-d_8): δ = 5.73 (s, 4H, NC*H*C*H*N), 3.83 (s, 12H, N-CH_3), 1.18 (s, 18H, C*H*3-*t*Bu); ^{11}B NMR (toluene-d_8): δ = –4.61 (s); ^{13}C{^{1}H} NMR (toluene-d_8): δ = 120.5 (s, NCHCHN), 38.6 (s, N-*C*H_3), 29.3 (s, CH_3-*t*Bu).

Elemental analysis (%) calcd. data for $C_9H_{17}SeBN_2$: C 55.12, H 8.47, N 14.28, S 16.35. Anal. Found: C: 54.78, H 8.74, N: 13.78, S 15.87.

5.6.6 Reaction of [*cyclo*-SeSeB*t*Bu(IMe)] (95) with PMe_3

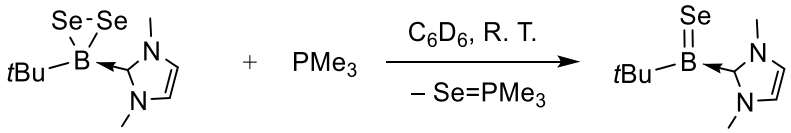

95 **99**

Compound [*cyclo*-SeSeB*t*Bu(IMe)] (**95**) (32 mg, 0.10 mmol) was dissolved in 4 mL of toluene and PMe_3 (15 mg, 0.20 mmol) was added to the solution. The mixture was stirred for 20 min and pentane (5 mL) was added. Then the mixture was cooled down to –30 °C for overnight. [Se=B*t*Bu(IMe)] (**99**) was yielded as yellow crystals from a concentrated toluene/pentane solution (15 mg, 61%).

^{1}H NMR (C_6D_6): δ = 5.52 (s, 2H, NC*H*C*H*N), 2.91 (s, 6H, N-CH_3), 1.31 (s, 9H,

C*H*$_3$-*t*Bu); ^{11}B NMR (C_6D_6): δ = 73.5 (s); ^{13}C{^{1}H} NMR (C_6D_6): δ = 120.1 (s, NC*H*C*H*N), 35.4 (s, N-*C*H$_3$), 30.0 (s, *C*H$_3$-*t*Bu).

Elemental analysis (%) calcd. data for $C_9H_{17}SeBN_2$: C 44.48, H 7.05, N 11.53. Anal. Found: C 43.96, H 7.45, N 11.24.

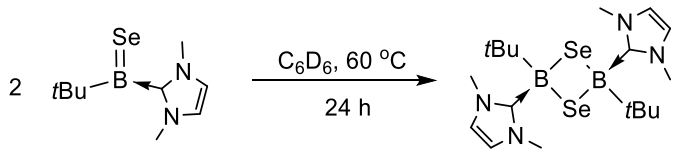

99 **100**

Compound **99** (16 mg, 0.05 mmol) was dissolved in toluene and the solution was heated to 60 ºC. After 48 h at 60 ºC, the solvent was removed under reduced pressure. [*cyclo*-{(IMe)(*t*Bu)B-Se-B(IMe)(*t*Bu)-Se}] (**100**) was isolated by recrystallizing the crude product from a saturated toluene/pentane solution (14 mg, 88%).

^{1}H NMR (C_6D_6): δ = 5.63 (s, 4H, NC*H*C*H*N), 3.80 (s, 12H, N-C*H*$_3$), 1.40 (s, 18H, C*H*$_3$-*t*Bu); ^{11}B NMR (C_6D_6): δ = –13.6 (s); ^{13}C{^{1}H} NMR (C_6D_6): δ = 120.7 (s, NC*H*C*H*N), 39.3 (s, N-*C*H$_3$), 29.83 (s, *C*H$_3$-*t*Bu).

Elemental analysis (%) calcd. data for $C_9H_{17}SeBN_2$: C 44.48, H 7.05, N 11.53. Anal. Found: C 43.96, H 7.46, N 11.24.

5.7 Reactivity of borylene complexes with B-E-E (E = S, Se, Te) cyclic boron dichalcogenides

5.7.1 Reaction of [*cyclo*-SSB*t*Bu(IMe)] (94) with [(OC)$_5$Mo=BN(SiMe$_3$)$_2$] (20)

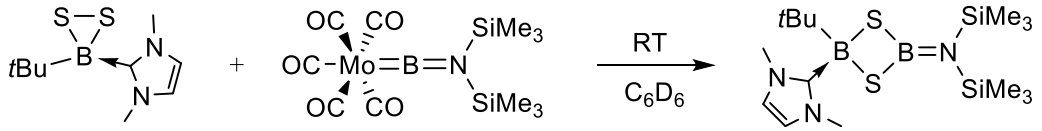

94 **20** **101**

To a solid mixture of [*cyclo*-SSB*t*Bu(IMe)] (**94**) (23 mg, 0.10 mmol) and molybdenum borylene **20** (41 mg, 0.10 mmol) was added toluene (5 mL). The mixture was stirred for 8 h. The resulting brown solution was filtered through a cotton plug and the filtrate was concentrated to 3 mL under reduced pressure. 5 mL pentane was the added to the toluene solution. The solution was then cooled to –30 ºC to yield [*cyclo*-{(*t*Bu)(IMe)B-S-B(N(SiMe$_3$)$_2$)-S)}] (**101**) as colorless crystals (15 mg, 37%).

^{1}H NMR (C_6D_6): δ = 5.39 (s, 2H, NC*H*C*H*N), 3.34 (s, 6H, N-CH_3), 1.28 (s, 9H, CH_3-*t*Bu), 0.59 (s, 18H, CH_3-SiMe$_3$); ^{11}B NMR (160 MHz, C_6D_6): δ = –6.1 (s, *B*(IMe)*t*Bu), 49.8 (s, *B*N(SiMe$_3$)$_2$); ^{13}C{^{1}H} NMR (125 MHz, C_6D_6): δ = 121.0 (s, N*C*HC*H*N), 38.6 (s, N-*C*H$_3$), 29.5 (s, *C*H$_3$-*t*Bu), 4.8 (s, *C*H$_3$-SiMe$_3$).

HRMS ($C_{15}H_{35}N_3B_2S_2Si_2$) calcd.: *m/z* = 399.1997; calcd. [M$^+$ +H]: *m/z* = 400.2075; found: *m/z* = 400.2070 [M$^+$ +H].

5.7.2 Reaction of [*cyclo*-SSB*t*Bu(IMe)] (94) with [(Cp)(OC)$_2$Mn=B*t*Bu] (43)

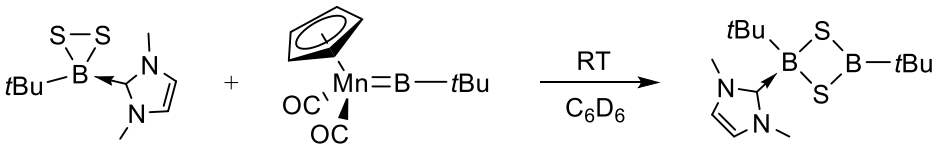

94 **43** **102**

To a solid mixture of [*cyclo*-SSB*t*Bu(IMe)] (**94**) (23 mg, 0.10 mmol) and manganese borylene **43** (24 mg, 0.10 mmol) was added toluene (5 mL). The mixture was stirred for 12 h. The resulting orange solution was filtered through a cotton plug and the filtrate was concentrated to 2 mL under reduced pressure. Pentane (5 mL) was added to the toluene solution. The solution was then cooled down to –30 ºC to yield [*cyclo*-{(*t*Bu)(IMe)B-S-B(*t*Bu)-S}] (**102**) as a white powder (10 mg, 33%).

^{1}H NMR (C_6D_6): δ = 5.23 (s, 2H, NC*H*C*H*N), 3.34 (s, 6H, N-CH_3), 1.46 (s, 9H, CH_3-B*t*Bu), 1.27 (s, 9H, CH_3-B(IMe)*t*Bu); ^{11}B NMR (160 MHz, C_6D_6): δ = –3.6 (s, *B*(IMe)*t*Bu), 72.9 (s, *B*-*t*Bu); ^{13}C{^{1}H} NMR (125 MHz, C_6D_6): δ = 121.2 (s, NC*H*C*H*N), 38.4 (s, N-*C*H_3), 29.3 (s, *C*H_3-B(IMe)*t*Bu), 28.6 (s, *C*H_3-B*t*Bu).

HRMS ($C_{13}H_{26}B_2N_2S_2$) calcd.: *m/z* = 296.1723; calcd. [M^+ – *t*Bu]: *m/z* = 239.1014; found: *m/z* = 239.1001 [M^+ – *t*Bu].

5.7.3 Reaction of [*cyclo*-SSB*t*Bu(IMe)] (94) with [(OC)$_5$Mo=BTp] (22)

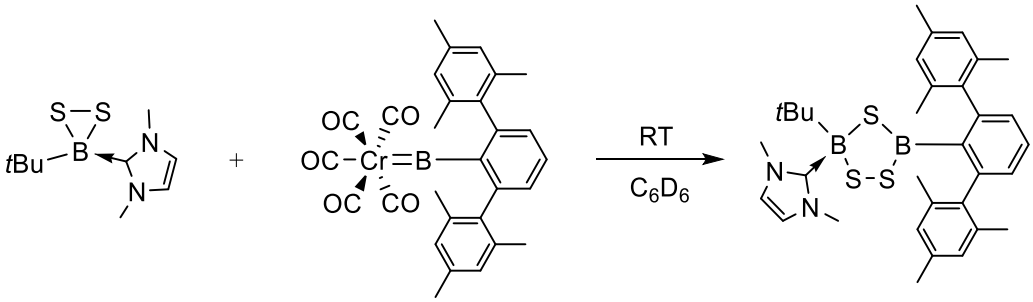

94 **22** **103**

To a solid mixture of [*cyclo*-SSB*t*Bu(IMe)] (**94**) (23 mg, 0.10 mmol) and chromium borylene (**22**) (52 mg, 0.10 mmol) was added toluene (10 mL). The mixture was stirred for 24 h. The resulting brown solution was filtered through a cotton plug and the filtrate was concentrated to 3 mL under reduced pressure. Pentane (5 mL) was added to the toluene solution. The solution was then kept at room temperature for 24 h to yield the crude product as white powder. This solid was dissolved in THF (3 mL) and pentane (3 mL) was added to the solution. The solution was cooled to –30 ºC to

yield [*cyclo*-{(*t*Bu)(IMe)B-SS-B(Tp)-S}] (**103**) as colorless crystals (13 mg, 22%).

^{1}H NMR (C_4D_8O): δ = 7.30 (t, $^{3}J_{HH}$ = 8 Hz, 1H, C*H*$_{ar}$), 7.01 (s, 2H, NC*H*C*H*N), 6.86 (d, $^{3}J_{HH}$ = 8 Hz, 2H, C*H*$_{ar}$), 6.69 (br, 4 H, C*H*$_{ar}$), 3.87 (s, 6 H, C*H*$_3$ of IMe), 2.19 (s, 6 H, C*H*$_3$ of Mes), 2.02 (d, $^{3}J_{HH}$ = 3 Hz, 12 H, C*H*$_3$ of Mes), 0.65 (s, 9 H, CH$_3$ of *t*Bu); ^{11}B NMR (160 MHz, C_4D_8O): δ = 7.7 (s, *B*(IMe)*t*Bu), 66.2 (s, *B*TpMes); ^{13}C{^{1}H} NMR (125 MHz, C_4D_8O): δ = 144.7 (*C*$_{ar}$), 140.9 (*C*$_{ar}$), 136.8 (*C*$_{ar}$), 136.2 (*C*$_{ar}$), 135.9 (*C*$_{ar}$), 128.5 (*C*H$_{ar}$), 128.0 (*C*H$_{ar}$), 127.7 (*C*H$_{ar}$), 123.6 (N*C*H*C*HN), 40.0 (N-*C*H$_3$), 31.1 (C(*C*H$_3$)$_3$), 21.6 (*C*H$_3^{ar}$), 21.5 (*C*H$_3^{ar}$), 21.1 (*C*H$_3^{ar}$).

HRMS ($C_{33}H_{42}B_2N_2S_3$) calcd.: *m/z* = 584.2696; calcd. [M$^+$ – *t*Bu]: *m/z* = 527.1986; found: *m/z* = 527.1982 [M$^+$ – *t*Bu].

5.7.4 Reaction of [*cyclo*-SSB*t*Bu(IMe)] (94) with cyanoborylene [(cAAC)B(CN)]$_4$ (104)

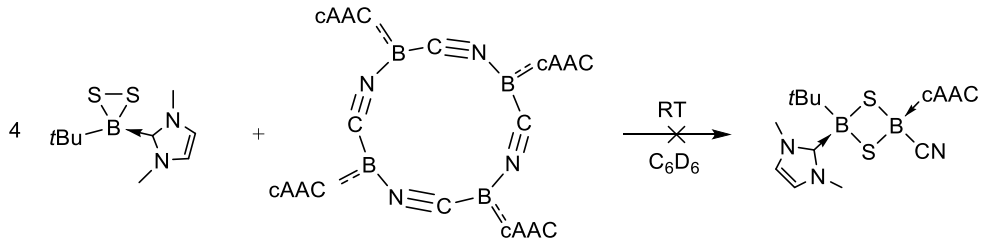

The reaction was first carried out under same conditions as in **4.7.1.** After 24 h, the ^{11}B NMR spectrum showed several new resonances around δ_B = 0 and all attempts to isolate pure compounds were unsuccessful.

5.7.5 Reaction of B-Se-Se (95) with [(OC)$_5$Mo=BN(SiMe$_3$)$_2$] (20)

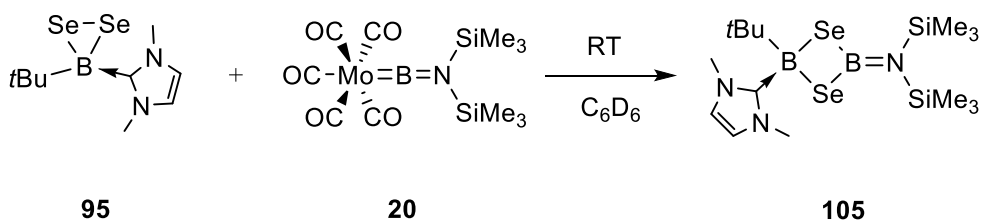

To a solid mixture of [*cyclo*-SeSeB*t*Bu(IMe)] (**95)** (32 mg, 0.10 mmol) and molybdenum borylene **20** (41 mg, 0.10 mmol) was added toluene (5 mL). The mixture was stirred for 8 h. The resulting brown solution was filtered through a cotton plug and the filtrate was concentrated to 2 mL under reduced pressure. Pentane (5 mL) was added to the toluene solution. The solution was then cooled down to –30 ºC to yield [*cyclo*-{(*t*Bu)(IMe)B-Se-BN(SiMe$_3$)$_2$}-Se)] (**105**) as colorless crystals (26 mg, 52%).

^{1}H NMR (C_6D_6): δ = 5.36 (s, 2H, NC*H*C*H*N), 3.33 (s, 6H, N-CH_3), 1.37 (s, 9H, CH_3-*t*Bu), 0.59 (s, 18H, CH_3-SiMe$_3$); ^{11}B NMR (C_6D_6): δ = –13.4 (s, *B*(IMe)*t*Bu), 46.7 (s, *B*N(SiMe$_3$)$_2$); ^{13}C{^{1}H} NMR (C_6D_6): δ = 121.2 (s, NC*H*C*H*N), 39.3 (s, N-*C*H$_3$), 30.0 (s, *C*H$_3$-*t*Bu), 5.0 (s, *C*H$_3$-SiMe$_3$); ^{77}Se NMR (C_6D_6): δ = 165.4.

HRMS ($C_{15}H_{35}B_2N_3Se_2Si_2$) calcd.: *m/z* = 495.0886; calcd. [M^+ – *t*Bu]: *m/z* = 438.0176; found: *m/z* = 438.0171 [M^+ – *t*Bu].

5.7.6 Reaction of [*cyclo*-SeSeB*t*Bu(IMe)] (95) with [(Cp)(OC)$_2$Mn=B*t*Bu] (43)

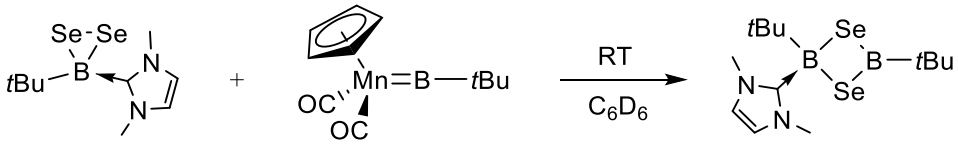

95 **43** **106**

To a solid mixture of [*cyclo*-SeSeB*t*Bu(IMe)] (**95**) (32 mg, 0.10 mmol) and manganese borylene **43** (24 mg, 0.10 mmol) was added toluene (5 mL). The mixture was stirred for 12 h. The resulting orange solution was filtered through a cotton plug and the filtrate was concentrated to 2 mL under reduced pressure. Pentane (5 mL) was the added to the toluene solution. The solution was then cooled to –30 ºC to yield [*cyclo*-{(*t*Bu)(IMe)B-Se-B(*t*Bu)-Se)}] (**106**) as a white powder (14 mg, 36%).

^{1}H NMR (500 MHz, C_6D_6): δ = 5.29 (s, 2H, NC*H*C*H*N), 3.30 (s, 6H, N-CH_3), 1.44 (s, 9H, CH_3-B*t*Bu), 1.34 (s, 9H, CH_3-B(IMe)*t*Bu); ^{11}B NMR (160 MHz, C_6D_6): δ = –10.8

(s, *B*(IMe)*t*Bu), 77.5 (s, *Bt*Bu); $^{13}C\{^{1}H\}$ NMR (125 MHz, C_6D_6): δ = 114.0 (s, NC*H*C*H*N), 31.8 (s, N-*C*H$_3$), 22.4 (s, C*H*$_3$-B(IMe)*t*Bu), 21.2 (s, C*H*$_3$-B*t*Bu), ^{77}Se NMR (C_6D_6): δ = 149.6.

HRMS ($C_{13}H_{26}B_2N_2Se_2$) calcd.: *m/z* = 392.0613; calcd. [M^+ – *t*Bu]: *m/z* = 334.9903; found: *m/z* = 334.9886 [M^+ – *t*Bu].

5.7.7 Reaction of [*cyclo*-SeSeB*t*Bu(IMe)] (95) with [(OC)$_5$Mo=BTp] (22)

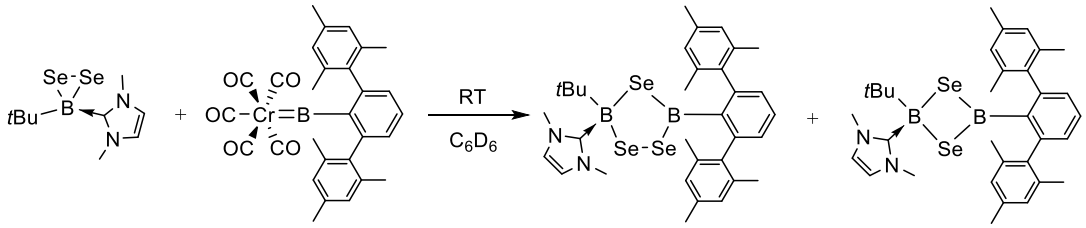

95 **22** **107** **107^b**

To a solid mixture of [*cyclo*-SeSeB*t*Bu(IMe)] (**95**) (32 mg, 0.10 mmol) and chromium borylene **22** (52 mg, 0.10 mmol) was added toluene (10 mL). The mixture was stirred for 24 h. The resulting brown solution was filtered through a cotton plug and the filtrate was concentrated to 3 mL under reduced pressure. Pentane (5 mL) was then added to the toluene solution. The resulting mixture was kept at room temperature for 24 h to yield a crude product, [*cyclo*-{(*t*Bu)(IMe)B-SeSe-B(Tp)-Se}] (**107**), as a white powder. The crude product was dissolved in THF (3 mL) and pentane (3 mL) was added to the solution. The solution was cooled to –30 ºC to yield **107** as colorless crystals. (14 mg, 22%).

^{1}H NMR (C_4D_8O): δ = 7.31 (t, $^3J_{HH}$ = 8 Hz, 1H, C*H*$_{ar}$), 7.05 (s, 2H, NC*H*C*H*N), 6.86 (d, $^3J_{HH}$ = 8 Hz, 2H, C*H*$_{ar}$), 6.71 (d, $^3J_{HH}$ = 11 Hz, 4 H, C*H*$_{ar}$), 3.89 (s, 6 H, C*H*$_3$ of IMe), 2.20 (s, 6 H, C*H*$_3$ of Mes), 2.06 (d, $^3J_{HH}$ = 9 Hz, 12 H, C*H*$_3$ of Mes), 0.68 (s, 9 H, C*H*$_3$ of *t*Bu); ^{11}B NMR (C_4D_8O): δ = 6.2 (s, *B*(IMe)*t*Bu), 72.1 (s, *B*TpMes); $^{13}C\{^{1}H\}$ NMR (C_4D_8O): δ = 143.5 (*C*$_{ar}$), 141.1 (*C*$_{ar}$), 136.6 (*C*$_{ar}$), 136.3 (*C*$_{ar}$), 136.1 (*C*$_{ar}$), 128.4 (*C*H$_{ar}$), 128.2 (*C*H$_{ar}$), 128.1 (*C*H$_{ar}$), 123.9 (NC*H*C*H*N), 40.8 (N-*C*H$_3$), 30.8

(*C*H$_3$-*t*Bu), 21.8 (*C*H$_3^{ar}$), 21.7 (*C*H$_3^{ar}$), 21.1 (*C*H$_3^{ar}$).

HRMS ($C_{33}H_{42}B_2N_2Se_3$) calcd.: *m/z* = 728.1030; calcd. [M^+ – *t*Bu]: *m/z* = 671.0325; found: *m/z* = 671.0303 [M^+ – *t*Bu].

5.7.8 Reaction of [*cyclo*-SeSeB*t*Bu(IMe)] (95) with cyanoborylene [(cAAC)B(CN)]$_4$ (104)

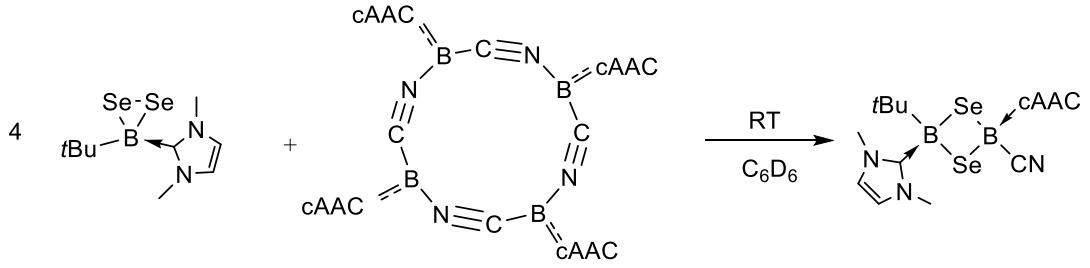

95 **104** **108**

To a solid mixture of [*cyclo*-SeSeB*t*Bu(IMe)] (**95**) (32 mg, 0.10 mmol) and cyanoborylene [(cAAC)B(CN)]$_4$ (**104**) (32 mg, 0.025 mmol) was added toluene (5 mL). The mixture was stirred for 12 h. The resulting red solution was filtered through a cotton plug and the filtrate was concentrated to 2 mL under reduced pressure. Pentane (5 mL) was the added to the toluene solution. The solution was then kept at room temperature to yield [*cyclo*-{(*t*Bu)(IMe)B-Se-B(cAAC)(CN)-Se}] (**108**) as red crystals (22 mg, 34 %).

^{1}H NMR (C_6D_6): δ = 7.18 (t, $^3J_{HH}$ = 8 Hz, 1H, C*H*$_{ar}$), 7.07 (d, $^3J_{HH}$ = 8 Hz, 2H, C*H*$_{ar}$), 5.75 (s, 2H, NC*H*C*H*N), 2.75 (sept, $^3J_{HH}$ = 7 Hz, 2H, C*H* of *i*Pr), 2.29 (s, 6H, C*H*$_3$ of *c*AAC), 1.70 (d, $^3J_{HH}$ = 7 Hz, 6H, C*H*$_3$ of *i*Pr), 1.53 (s, 2H, C*H*$_2$ of cAAC), 1.34 (s, 9H, C*H*$_3$ of *t*Bu), 1.12 (d, $^3J_{HH}$ = 7 Hz, 6H, C*H*$_3$ of *i*Pr), 0.85 (s, 6H, C*H*$_3$ of *c*AAC); ^{11}B NMR (C_6D_6): δ = –9.5 (s, *B*(IMe)*t*Bu), –32.8 (s, *B*(*c*AAC)CN); ^{13}C{^{1}H} NMR (C_6D_6): δ = 146.3 (*C*$_{ar}$), 133.6 (*C*$_{ar}$), 130.4 (*C*$_{ar}$), 129.3 (*C*H$_{ar}$), 128.6 (*C*H$_{ar}$), 125.7 (*C*$_{ar}$), 125.4 (*C*$_{ar}$), 128.1 (*C*H$_{ar}$), 121.4 (NCHCHN-IMe), 76.0 (N*C*Me$_2$), 55.0 (NC(C*H*$_3$)$_2$), 52.2 (*C*H$_2$ of cAAC), 40.8 (N*C*H$_3$-IMe), 32.5 (*C*H$_3$-*t*Bu), 30.3 (CC(*C*H$_3$)$_2$), 29.3, 28.3

(*i*Pr-*C*H), 27.4, 24.8, 22.8, 21.4 (*i*Pr-*C*H_3).

HRMS ($C_{30}H_{48}B_2N_4Se_2$) calcd.: *m/z* = 646.2396; calcd. [M^+ – *t*Bu]: *m/z* = 589.1686; found: *m/z* = 589.1671 [M^+ – *t*Bu].

5.7.9 Reaction of [(Cp)(OC)$_2$Mn{κ^1-*cyclo*-TeTeB(*t*Bu)(IMe)}] (96) with borylene complexes

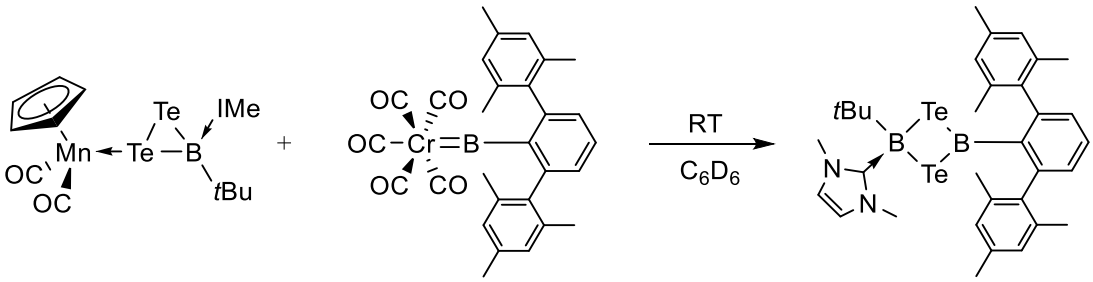

96 **22** **109**

To a solid mixture of [(Cp)(OC)$_2$Mn{κ^1-*cyclo*-TeTeB(*t*Bu)(IMe)}] (**96**) (60 mg, 0.10 mmol) and chromium borylene (**22**) (52 mg, 0.10 mmol) was added toluene (8 mL). The mixture was stirred for 12 h. The resulting dark brown solution was filtered through a cotton plug and the filtrate was concentrated to 5 mL under reduced pressure. Pentane (5 mL) was the added to the toluene solution. The solution was cooled to –30 ºC to yield [*cyclo*-{(*t*Bu)(IMe)B-TeTe-B(Tp)}] (**109)** as dark brown crystals (18 mg, 24%).

^{1}H NMR (C_6D_6): δ = 7.20 (t, $^3J_{HH}$ = 7 Hz, 1H, C*H*$_{ar}$), 6.98 (d, $^3J_{HH}$ = 7 Hz, 2H, C*H*$_{ar}$), 6.91 (s, 4H, C*H*$_{ar}$-Mes), 5.11 (s, 2H, NC*H*C*H*N), 3.01 (s, 6 H, CH_3 of IMe), 2.49 (s, 12 H, CH_3 of Mes), 2.17 (s, 6 H, CH_3 of Mes), 1.11 (s, 9 H, CH_3 of *t*Bu); ^{11}B NMR (C_6D_6): δ = –33.0 (s, *B*(IMe)*t*Bu), 61.1 (s, *B*TpMes); ^{13}C{^{1}H} NMR (C_6D_6): δ = 140.9 (*C*$_{ar}$), 140.3 (*C*$_{ar}$), 136.56 (*C*$_{ar}$), 136.0 (*C*$_{ar}$), 128.7 (*C*H$_{ar}$), 128.4 (*C*H$_{ar}$), 128.0 (*C*H$_{ar}$), 121.1 (N*C*H*C*HN), 40.0 (N-*C*H_3), 30.4 (*C*H_3-*t*Bu), 22.5 (*C*H_3^{ar}), 21.4 (*C*H_3^{ar}). ^{125}Te NMR (C_6D_6): δ = 337.7 (br).

HRMS ($C_{33}H_{42}B_2N_2Te_2$) calcd.: *m/z* = 748.1659; found: *m/z* = 748.1670 [M^+].

5.8 Reactivity of $[(OC)_5Mo{=}BN(SiMe_3)_2]$ (20) with $[Cp_2WH_2]$ (110)

5.8.1 Reaction of $[Cp_2WH_2]$ (110) with one equivalent of $[(OC)_5Mo{=}BN(SiMe_3)_2]$ (20)

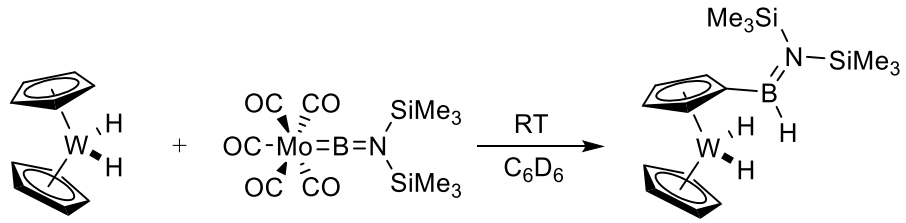

110 **20** **111**

To a solid mixture of $[Cp_2WH_2]$ (**110**) (31.6 mg, 0.10 mmol) and molybdenum borylene **20** (41 mg, 0.10 mmol) was added toluene (5 mL). The mixture was stirred for 24 h at room temperature. The resulting brown solution was filtered through a cotton plug and the solvent of the filtrate was evaporated under reduced pressure. The oily crude product was dissolved in pentane (5 mL) and the solvent was slowly evaporated at –30 ºC down to ca. 2 mL. The mixture was filtered again through a cotton plug and the filtrate was dried by evaporation. The crude product was dissolved in pentane and kept at –30 ºC to yield $[CpWH_2(\eta^5\text{-}C_5H_4\{BHN(SiMe_3)_2\})]$ (**111**) as yellow crystals (13 mg, 27%).

$^1H\{^{11}B\}$ NMR (C_6D_6): δ = 5.13 (s, 1H, *H*-B), 4.74 (s, 2H, C_BH-Cp), 4.34 (s, 5H C*H*-Cp), 3.92 (s, 2H, C_BH-Cp), 0.32 (s, 18H, Si(CH_3)$_3$), –11.16 (s, 2H, WH_2); $^{11}B\{^1H\}$ NMR (C_6D_6): δ = 39.6 (br); $^{13}C\{^1H\}$ NMR (C_6D_6): δ = 82.2, 78.1, 71.6 (C_BH-Cp), 74.7 (*C*H-Cp), 4.3 (Si(CH_3)$_3$).

HRMS ($C_{16}H_{30}BNSi_2W$) calcd.: *m/z* = 487.1519; found: *m/z* = 487.1524 [M^+].

5.8.2 Reaction of $[Cp_2WH_2]$ (110) with two equivalents of $[(OC)_5Mo{=}BN(SiMe_3)_2]$ (20)

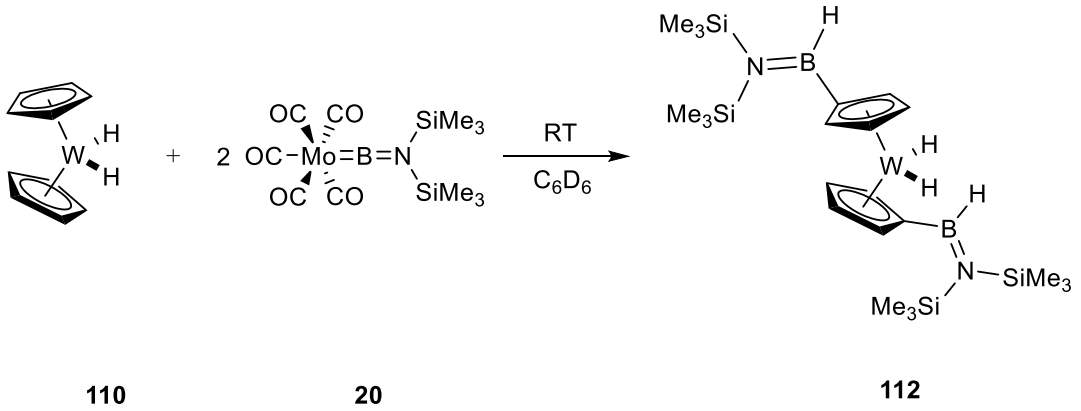

110 **20** **112**

To a solid mixture of $[Cp_2WH_2]$ (**110**) (31 mg, 0.10 mmol) and molybdenum borylene **20** (82 mg, 0.20 mmol) was added toluene (5 mL). The mixture was stirred at room temperature for 48 h. The resulting brown solution was filtered through a cotton plug and the solvent of the filtrate was evaporated under reduced pressure. The oily crude product was dissolved in pentane (5 mL) and the solvent was slowly concentrated at –30 °C down to 2 mL. The mixture was filtered again through a cotton plug and the filtrate was dried by evaporation. This procedure was repeated twice to yield $[WH_2(\eta^5\text{-}C_5H_4\{BHN(SiMe_3)_2\}_2)]$ (**112**) as yellow crystals (11 mg, 16%).

$^1H\{^{11}B\}$ NMR (C_6D_6): δ = 5.13 (br, *H*-B), 4.92 (s, 4H, C*H*-Cp), 4.23 (s, 4H, C*H*-Cp), 0.30 (s, 36H, Si(C*H*$_3$)$_3$), –10.50 (s, 2H, W*H*$_2$); $^{11}B\{^1H\}$ NMR (C_6D_6): δ = 41.3 (br); $^{13}C\{^1H\}$ NMR (C_6D_6): δ = 84.6, 80.8 (*C*H-Cp), 4.1 (Si(*C*H$_3$)$_3$).

HRMS ($C_{22}H_{48}B_2N_2Si_4W$) calcd.: *m/z* = 658.2590; found: *m/z* = 658.2600 [M^+].

5.8.3 Reaction of [Cp$_2$WH$_2$] (110) with three equivalents of [(OC)$_5$Mo=BN(SiMe$_3$)$_2$] (20)

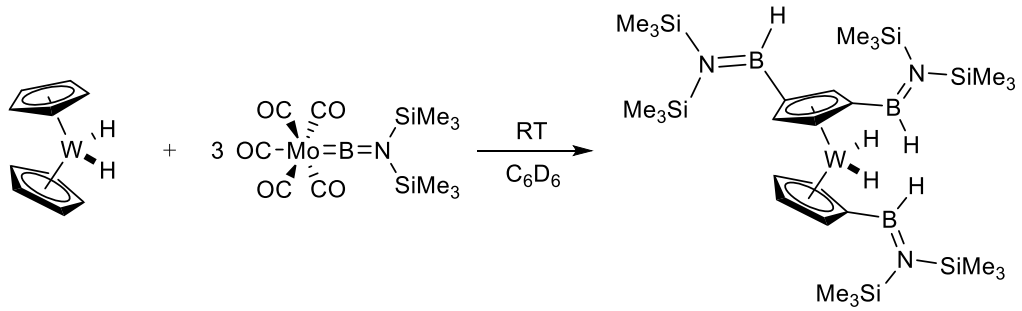

110 **20** **113**

The reaction was carried out under the same conditions as in **7.6.2**. the ^{11}B NMR showed a broad peak at δ_B = 41.3 and ^{1}H NMR spectroscopy revealed signals for multiple products instead of one unique compound. All attempts to isolate the tris-C-H activation product from the mixture failed. The composition of the product [(η^5-C$_5$H$_3${BHN(SiMe$_3$)$_2$}$_2$)WH$_2$(η^5-C$_5$H$_4${BHN(SiMe$_3$)$_2$})] (**113**) was confirmed by HRMS.

HRMS (C$_{28}$H$_{66}$B$_3$N$_3$Si$_6$W): calcd.: *m/z* = 829.3655; found: *m/z* = 829.3627 [M$^+$].

5.8.4 Reaction of [Cp$_2$WH$_2$] (110) with five equivalents of [(OC)$_5$Mo=BN(SiMe$_3$)$_2$] (20)

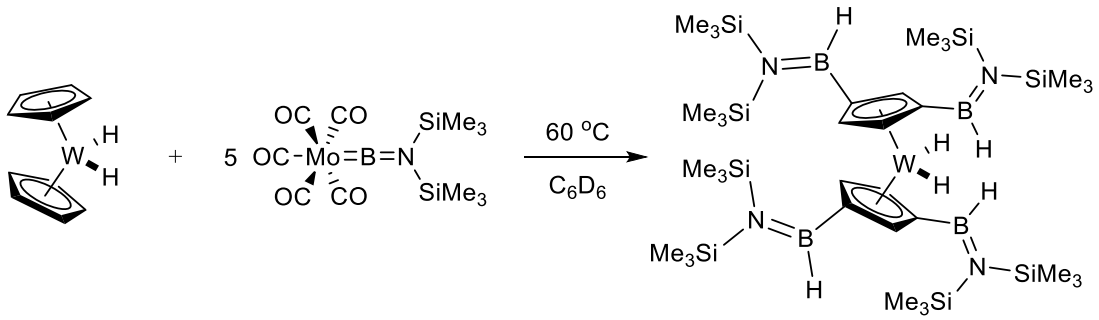

110 **20** **114**

To a solid mixture of [Cp$_2$WH$_2$] (**110**) (32 mg, 0.10 mmol) and molybdenum borylene **20** (205 mg, 0.50 mmol) was added toluene (5 mL). The mixture was stirred at 60 ºC for 96 h. The resulting brown solution was filtered through a cotton plug and the

solvent of the filtrate was evaporated under reduced pressure. The oily crude product was dissolved in pentane (5 mL) and the solvent was slowly concentrated at –30 °C to 2 mL. The mixture was filtered again through a cotton plug and the filtrate was dried by evaporation. This purification procedure was repeated twice to yield $[WH_2(\eta^5\text{-}C_5H_3\{BHN(SiMe_3)_2\}_2)_2]$ (**114**) as a brown oil (13 mg, 13%).

$^1H\{^{11}B\}$ NMR (C_6D_6): δ = 5.42 (br, *H*-B), 4.89 (s, 2H, C*H*-Cp), 4.80 (s, 4H, C*H*-Cp), 0.36 (s, 72H, Si(C*H*$_3$)$_3$), –10.87 (s, 2H, W*H*$_2$); $^{11}B\{^1H\}$ NMR (C_6D_6): δ = 43.0 (br); $^{13}C\{^1H\}$ NMR (C_6D_6): δ = 92.5, 82.5 (*C*H-Cp), 4.4 (Si(*C*H$_3$)$_3$).

HRMS ($C_{34}H_{84}B_4N_4Si_8W$) calcd.: *m/z* = 1000.4731; found: *m/z* = 1000.4754 [M^+].

5.9 Reactivity of [(Cp)(OC)$_2$Mn=B*t*Bu] (90) with Lewis acids (GaCl$_3$, InBr$_3$)

5.9.1 Reaction of [(Cp)(OC)$_2$Mn=B*t*Bu] (43) with GaCl$_3$ (115)

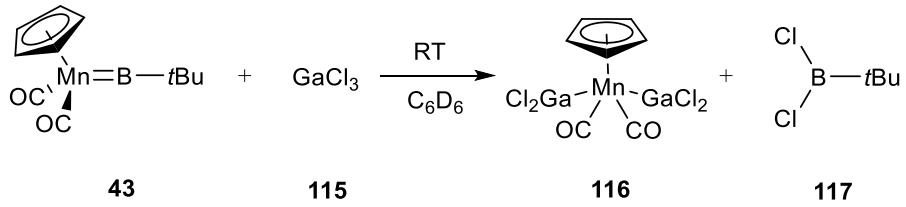

43 **115** **116** **117**

A toluene (3 mL) suspension of [(Cp)(OC)$_2$Mn=B*t*Bu] (**43**) (24 mg, 0.10 mmol) was slowly added to into a toluene (5 mL) solution of **GaCl$_3$** (35 mg, 0.20 mmol). The reaction mixture was kept at room temperature for 1 h, which led to the formation of a yellow precipitate and a color change of the solution to orange. The yellow precipitate was washed twice with toluene (5 mL) and [(Cp)(OC)$_2$Mn(GaCl$_2$)$_2$] (**116**) was obtained as a yellow powder (36 mg, 79%).

Elemental analysis (%) calcd. data for $C_7H_5Ga_2Cl_4MnO_2$: C 18.43, H 0.88; Anal. found: C 19.04, H 1.33.

5.9.2 Reaction of [(Cp)(OC)$_2$Mn=B*t*Bu] (43) with GaCl$_3$ (115) in tetrahydrofuran (THF)

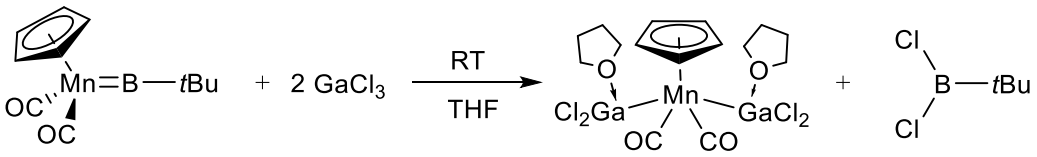

43 **115** **118** **117**

A THF suspension of [(Cp)(OC)$_2$Mn=B*t*Bu] (**43**) (24 mg, 0.10 mmol) was slowly added to to a THF solution (5 mL) of **115** (35 mg, 0.2 mmol). The reaction mixture was kept at room temperature for 1 h which led to the formation of colorless crystals formed and to a color change of the solution to orange. The crystals were washed with THF (3 mL) and [(Cp)(OC)$_2$Mn{Ga(THF)Cl$_2$}$_2$] (**118**) was isolated as colorless crystals. The structure of the product complex could only be confirmed by its solid state structure.

5.9.3 Reaction of [(Cp)(OC)$_2$Mn(GaCl$_2$)$_2$] (116) with Lewis bases (PMe$_3$, Et$_2$O)

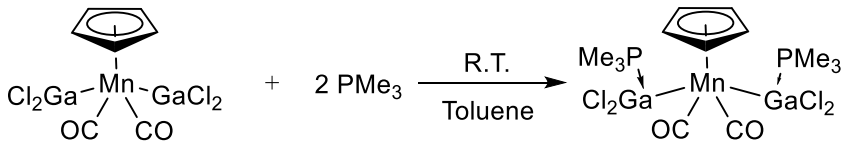

116 **119**

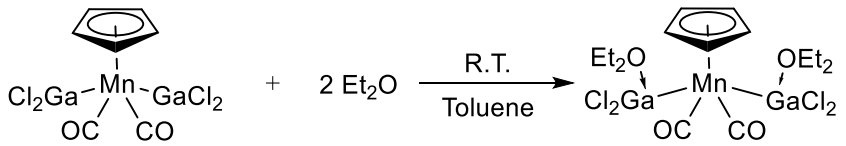

116 **120**

Compound [(Cp)(OC)$_2$Mn(GaCl$_2$)$_2$] (**116**) (46 mg, 0.1 mmol) was added to liquid PMe$_3$ (75 mg, 1.0 mmol). The mixture was stirred at room temperature for 24 h, during which time the color of the solid changed from yellow to white. The precipitate was washed by toluene (5 mL) and dried under reduced vacuum to yield

[(Cp)(OC)$_2$Mn{Ga(THF)Cl$_2$}$_2$] (**118**) as a white powder. The product complex could only be confirmed by its solid state structure.

Compound [(Cp)(OC)$_2$Mn(GaCl$_2$)$_2$] (**116**) (46 mg, 0.10 mmol) was added to 5 mL **Et$_2$O**. The mixture was stirred at room temperature for 24 h and the color of the solid had turned from yellow to white. The precipitate was washed by toluene (5 mL) and dried under reduced vacuum to yield [(Cp)(OC)$_2$Mn{Ga(PMe$_3$)Cl$_2$}$_2$] (**119**) as a white powder. The product complex could only be confirmed by its solid state structure.

5.9.4 Reaction of [(Cp)(OC)$_2$Mn(InBr$_2$)$_2$] (122) with DMAP

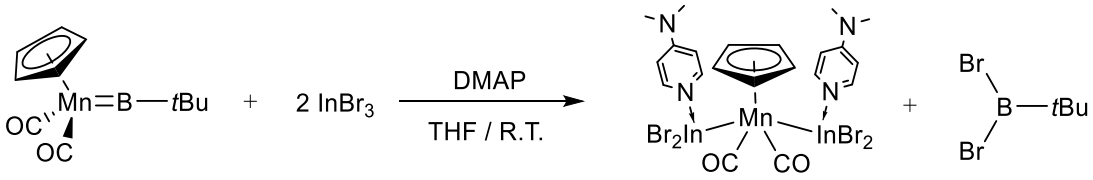

43 **121** **124** **123**

Compound [(Cp)(OC)$_2$Mn(InBr$_2$)$_2$] (**122**) (73 mg, 0.10 mmol) was added to a toluene (5 mL) solution of DMAP (24 mg, 0.20 mmol). The mixture was stirred at room temperature for 24 h. The precipitate was washed by toluene (5 mL) and dried under reduced vacuum to yield [(Cp)(OC)$_2$Mn{In(DMAP)Br$_2$}$_2$] (**124**) as a white powder. The product complex could only be confirmed by its solid state structure.

6. X-ray Structure Determination:

6.1 General

The crystal data were collected on a Bruker X8-APEX diffractometer with a CCD area detector and multi-layer mirror monochromated $Mo_{K\alpha}$ radiation. The structure was solved using direct methods, refined with the Shelx software package[172-173] and expanded using Fourier techniques. All non-hydrogen atoms were refined anisotropically. Hydrogen atoms were included in structure factor calculations. All hydrogen atoms were assigned to idealized geometric positions. Crystallographic data have been deposited with the Cambridge Crystallographic Data Center. These data can be obtained free of charge from The Cambridge Crystallographic Data Centre via www.ccdc.cam.ac.uk/data_request/cif.

6.2 Crystal data and parameters of the structure determinations

Table 1. Crystal data and parameters for compounds **86**, **87** and **89**.

	86	**87**	**89**
Empirical formula	$C_{23}H_{26}BBr_2N_2$	$C_{20}H_{21}BN_2$	$C_{31}H_{38}BMnN_2O_2Si_2$
Formula weight ($g \cdot mol^{-1}$)	501.09	300.20	592.56
Temperature (K)	100(2)	100(2)	100(2)
Radiation, λ (Å)	$Mo_{K\alpha}$ 0.71073	$Mo_{K\alpha}$ 0.71073	$Mo_{K\alpha}$ 0.71073
Crystal system	Triclinic	Monoclinic	Orthorhombic
Space group	$P\ \bar{1}$	$P2_1/c$	$Pna2_1$
a (Å)	8.1816(11)	13.136(6)	8.6532(3)
b (Å)	8.9308(19)	7.531(3)	22.5848(8)
c (Å)	15.083(3)	17.643(7)	16.0117(6)
α (°)	97.738(12)	90	90
β (°)	96.113(13)	109.810(18)	90
γ (°)	92.433(11)	90	90
Volume ($Å^3$)	1084.1(3)	1642.1(12)	3129.18(19)
Z	2	4	4
Calculated density ($Mg \cdot m^{-3}$)	1.535	1.214	1.258
Absorbtion coefficient (mm^{-1})	3.750	0.070	0.528
F(000)	506	640	1248
Theta range for collection	2.305 to 26.019°	2.449 to 26.366°	2.521 to 26.020°
Reflections collected	24731	16223	36026
Independent reflections	4106	3350	6038
Minimum/maximum transmission	0.6442/0.7457	0.5357/0.7457	0.6779/0.7456
Refinement method	Full-matrix least-squares on F^2	Full-matrix least-squares on F^2	Full-matrix least-squares on F^2
Data / parameters / restrains	4106 / 258 / 0	3350 / 212 / 0	6038 / 361 / 1
Goodness-of-fit on F^2	1.050	1.037	1.047
Final R indices [I>2σ(I)]	$R_1 = 0.0334$, $wR^2 = 0.0714$	$R_1 = 0.0587$, $wR^2 = 0.1272$	$R_1 = 0.0237$, $wR^2 = 0.0573$
R indices (all data)	$R_1 = 0.0479$, $wR^2 = 0.0762$	$R_1 = 0.1003$, $wR^2 = 0.1429$	$R_1 = 0.0253$, $wR^2 = 0.0583$
Maximum/minimum residual electron density ($e \cdot Å^{-3}$)	0.985 / –0.681	0.302 / –0.337	0.237 / –0.288

Table 2. Crystal data and parameters for compounds **91**, **92** and **93**.

	91	**92**	**93**
Empirical formula	$C_{16}H_{22}BMnN_2O_2S$	$C_{16}H_{22}BMnN_2O_2Se$	$C_{16}H_{22}BMnN_2O_2Te$
Formula weight ($g \cdot mol^{-1}$)	372.16	419.06	467.70
Temperature (K)	296(2)	100(2)	100(2)
Radiation, λ (Å)	$Mo_{K\alpha}$ 0.71073	$Mo_{K\alpha}$ 0.71073	$Mo_{K\alpha}$ 0.71073
Crystal system	Triclinic	Triclinic	Triclinic
Space group	$P\ \bar{1}$	$P\ \bar{1}$	$P\ \bar{1}$
a (Å)	7.7306(11)	7.9000(7)	8.058(2)
b (Å)	9.1643(12)	9.9308(8)	10.053(5)
c (Å)	13.4761(18)	12.9035(12)	12.691(7)
α (°)	78.351(3)	98.508(3)	97.22(3)
β (°)	87.427(3)	97.979(3)	99.097(17)
γ (°)	70.058(3)	113.182(2)	111.929(15)
Volume ($Å^3$)	878.7(2)	898.47(14)	922.2(7)
Z	2	2	2
Calculated density ($Mg \cdot m^{-3}$)	1.407	1.549	1.684
Absorbtion coefficient (mm^{-1})	0.879	2.769	2.275
F(000)	388	424	460
Theta range for collection	2.412 to 26.022°	2.288 to 26.021°	2.230 to 26.019°
Reflections collected	12009	34589	33610
Independent reflections	3458	3544	3632
Minimum/maximum transmission	0.4655/0.7456	0.4482/0.7455	0.4448/0.6468
Refinement method	Full-matrix least-squares on F^2	Full-matrix least-squares on F^2	Full-matrix least-squares on F^2
Data / parameters / restrains	3458 / 213 / 0	3544 / 213 / 0	3632 / 213 / 0
Goodness-of-fit on F^2	1.027	1.068	1.126
Final R indices [I>2σ(I)]	$R_1 = 0.0460$, $wR^2 = 0.0989$	$R_1 = 0.0287$, $wR^2 = 0.0678$	$R_1 = 0.0246$, $wR^2 = 0.0620$
R indices (all data)	$R_1 = 0.0667$, $wR^2 = 0.1074$	$R_1 = 0.0394$, $wR^2 = 0.0732$	$R_1 = 0.0302$, $wR^2 = 0.0652$
Maximum/minimum residual electron density ($e \cdot Å^{-3}$)	0.659 / –0.601	0.591 / –0.734	0.669 / –1.130

Table 3. Crystal data and parameters for compounds **94**, **95** and **96**.

	94	**95**	**96**
Empirical formula	$C_9H_{17}BN_2S_2$	$C_9H_{17}BN_2Se_2$	$C_{16}H_{22}BMnN_2O_2Te_2$
Formula weight ($g \cdot mol^{-1}$)	228.17	321.97	595.30
Temperature (K)	100(2)	100(2)	100(2)
Radiation, λ (Å)	$Mo_{K\alpha}$ 0.71073	$Mo_{K\alpha}$ 0.71073	$Mo_{K\alpha}$ 0.71073
Crystal system	Triclinic	Triclinic	Monoclinic
Space group	$P\ \bar{1}$	$P\ \bar{1}$	$P2_1/c$
a (Å)	6.4382(20)	6.587(2)	9.0510(13)
b (Å)	9.070(3)	9.123(3)	9.9167(12)
c (Å)	10.891(3)	11.052(4)	21.724(4)
α (°)	75.737(8)	76.48(3)	90
β (°)	77.099(8)	77.86(3)	90.139(7)
γ (°)	74.734(19)	74.261(19)	90
Volume ($Å^3$)	586.0(3)	613.8(4)	1949.9(5)
Z	2	2	4
Calculated density ($Mg \cdot m^{-3}$)	1.293	1.742	2.028
Absorbtion coefficient (mm^{-1})	0.418	5.989	3.620
F(000)	244	316	1128
Theta range for collection	1.958 to 26.017°	1.919 to 26.022°	2.781 to 26.020°
Reflections collected	34550	14936	76700
Independent reflections	2304	2422	3821
Minimum/maximum transmission	0.6943/0.7456	0.0503/0.1035	0.2757/0.4034
Refinement method	Full-matrix least-squares on F^2	Full-matrix least-squares on F^2	Full-matrix least-squares on F^2
Data / parameters / restrains	2304 / 132 / 0	2422 / 132 / 0	3821 / 222 / 0
Goodness-of-fit on F^2	1.069	1.057	1.197
Final R indices [I>2σ(I)]	$R_1 = 0.0275$, $wR^2 = 0.0664$	$R_1 = 0.0217$, $wR^2 = 0.0551$	$R_1 = 0.0166$, $wR^2 = 0.0382$
R indices (all data)	$R_1 = 0.0306$, $wR^2 = 0.0681$	$R_1 = 0.0241$, $wR^2 = 0.0563$	$R_1 = 0.0168$, $wR^2 = 0.0383$
Maximum/minimum residual electron density ($e \cdot Å^{-3}$)	0.380 / –0.341	0.513 / –0.482	0.363 / –0.392

Table 4. Crystal data and parameters for compounds **97**, **98** and **99**.

	97	**98**	**99**
Empirical formula	$C_9H_{17}BN_2S$	$C_{18}H_{34}B_2N_4S_2$	$C_9H_{17}BN_2Se$
Formula weight ($g \cdot mol^{-1}$)	196.11	392.23	243.01
Temperature (K)	100(2)	100(2)	100(2)
Radiation, λ (Å)	Mo_K 0.71073	Mo_K 0.71073	Mo_K 0.71073
Crystal system	Monoclinic	Triclinic	Monoclinic
Space group	$P2_1/n$	$P\bar{1}$	$P2_1/n$
a (Å)	12.364(3)	8.0243(20)	12.404(7)
b (Å)	7.522(3)	8.053(3)	7.679(4)
c (Å)	12.850(3)	9.721(4)	12.800(7)
α (°)	90	105.103(9)	90
β (°)	109.438(10)	104.95(2)	108.23(4)
γ (°)	90	106.457(18)	90
Volume ($Å^3$)	1127.0(6)	543.0(3)	1157.9(11)
Z	4	1	4
Calculated density ($Mg \cdot m^{-3}$)	1.156	1.199	1.394
Absorbtion coefficient (mm^{-1})	0.246	0.255	3.202
F(000)	424	212	496
Theta range for collection	1.980 to 26.005°	2.324 to 26.010°	1.996 to 26.020°
Reflections collected	26141	13340	11282
Independent reflections	2216	2137	2281
Minimum/maximum transmission	0.5847/0.7455	0.6716/0.7456	0.3044/0.5867
Refinement method	Full-matrix least-squares on F^2	Full-matrix least-squares on F^2	Full-matrix least-squares on F^2
Data / parameters / restrains	2216 / 123 / 0	2137 / 123 / 0	2281 / 123 / 0
Goodness-of-fit on F^2	1.056	1.173	1.031
Final R indices [I>2σ(I)]	$R_1 = 0.0394$, $wR^2 = 0.1053$	$R_1 = 0.0387$, $wR^2 = 0.0904$	$R_1 = 0.0370$, $wR^2 = 0.0810$
R indices (all data)	$R_1 = 0.0459$, $wR^2 = 0.1105$	$R_1 = 0.0431$, $wR^2 = 0.0928$	$R_1 = 0.0559$, $wR^2 = 0.0877$
Maximum/minimum residual electron density ($e \cdot Å^{-3}$)	0.422 / –0.205	0.386 / –0.231	0.844 / –0.752

Table 5. Crystal data and parameters for compounds **100**, **101** and **105**.

	100	**101**	**105**
Empirical formula	$C_{18}H_{34}B_2N_4Se_2$	$C_{35}H_{82}B_4N_6S_4Si_4$	$C_{15}H_{35}B_2N_3Se_2Si_2$
Formula weight ($g \cdot mol^{-1}$)	486.03	870.90	493.18
Temperature (K)	100(2)	100(2)	100(2)
Radiation, λ (Å)	$Mo_{K\alpha}$ 0.71073	$Mo_{K\alpha}$ 0.71073	$Mo_{K\alpha}$ 0.71073
Crystal system	Triclinic	Triclinic	Monoclinic
Space group	$P\ \bar{1}$	$P\ \bar{1}$	$P2_1/n$
a (Å)	8.085(2)	9.1005(10)	11.500(5)
b (Å)	8.208(3)	11.8019(13)	12.544(6)
c (Å)	9.845(3)	12.4035(13)	16.944(7)
α (°)	108.77(2)	80.466(3)	90
β (°)	100.22(2)	84.795(3)	109.60(2)
γ (°)	108.10(2)	86.977(4)	90
Volume ($Å^3$)	559.3(3)	1307.4(2)	2302.8(18)
Z	1	1	4
Calculated density ($Mg \cdot m^{-3}$)	1.443	1.106	1.423
Absorbtion coefficient (mm^{-1})	3.315	0.303	3.319
F(000)	248	474	1008
Theta range for collection	2.297 to 26.021°	1.671 to 26.019°	1.885 to 26.017°
Reflections collected	2185	19417	27381
Independent reflections	2185	5150	4531
Minimum/maximum transmission	0.2081/0.4305	0.5432/0.7456	0.3432/0.5256
Refinement method	Full-matrix least-squares on F^2	Full-matrix least-squares on F^2	Full-matrix least-squares on F^2
Data / parameters / restrains	2185 / 124 / 0	5150 / 266 / 45	4531 / 228 / 0
Goodness-of-fit on F^2	1.483	1.016	1.020
Final R indices [I>2σ(I)]	$R_1 = 0.0526$, $wR^2 = 0.1699$	$R_1 = 0.0621$, $wR^2 = 0.1655$	$R_1 = 0.0394$, $wR^2 = 0.0848$
R indices (all data)	$R_1 = 0.0549$, $wR^2 = 0.1708$	$R_1 = 0.0701$, $wR^2 = 0.1725$	$R_1 = 0.0668$, $wR^2 = 0.0956$
Maximum/minimum residual electron density ($e \cdot Å^{-3}$)	2.772 / –1.285	2.752 / –0.512	0.671 / –0.519

Table 6. Crystal data and parameters for compounds **107**, **108** and **109**.

	107	**108**	**109**
Empirical formula	$C_{33}H_{42}B_2N_2Se_{2.96}$	$C_{30}H_{48}B_2N_4Se_2$	$C_{33}H_{42}B_2N_2Te_2$
Formula weight ($g \cdot mol^{-1}$)	722.39	644.26	743.50
Temperature (K)	100(2)	100(2)	100(2)
Radiation, λ (Å)	$Mo_{K\alpha}$ 0.71073	$Mo_{K\alpha}$ 0.71073	$Mo_{K\alpha}$ 0.71073
Crystal system	Triclinic	Triclinic	Triclinic
Space group	$P\ \bar{1}$	$P\ \bar{1}$	$P\ \bar{1}$
a (Å)	8.6416(7)	9.2253(4)	8.8783(8)
b (Å)	13.4779(11)	13.3449(5)	13.1076(11)
c (Å)	14.6575(12)	14.4581(6)	14.7911(13)
α (°)	75.409(3)	107.0150(10)	73.716(2)
β (°)	77.096(3)	93.8670(10)	75.160(3)
γ (°)	85.540(3)	90.0350(10)	83.313(2)
Volume ($Å^3$)	1610.0(2)	1697.77(12)	1595.3(2)
Z	2	2	2
Calculated density ($Mg \cdot m^{-3}$)	1.490	1.260	1.548
Absorbtion coefficient (mm^{-1})	3.412	2.201	1.853
F(000)	730	668	736
Theta range for collection	1.469 to 26.022°	1.829 to 25.682°	1.475 to 26.022°
Reflections collected	36493	33910	26498
Independent reflections	6330	6448	6279
Minimum/maximum transmission	0.4400/0.5629	0.3446/0.4915	0.5918/0.7456
Refinement method	Full-matrix least-squares on F^2	Full-matrix least-squares on F^2	Full-matrix least-squares on F^2
Data / parameters / restrains	6330 / 397 / 116	6448 / 357 / 0	6279 / 363 / 0
Goodness-of-fit on F^2	1.089	1.036	1.030
Final R indices [I>2σ(I)]	$R_1 = 0.0378$, $wR^2 = 0.0848$	$R_1 = 0.0186$, $wR^2 = 0.0447$	$R_1 = 0.0203$, $wR^2 = 0.0532$
R indices (all data)	$R_1 = 0.0549$, $wR^2 = 0.0905$	$R_1 = 0.0202$, $wR^2 = 0.0455$	$R_1 = 0.0239$, $wR^2 = 0.0559$
Maximum/minimum residual electron density ($e \cdot Å^{-3}$)	0.823 / –0.663	0.352 / –0.226	1.024 / –0.323

Table 7. Crystal data and parameters for compounds **111**, **112** and **118**.

	111	**112**	**118**
Empirical formula	$C_{16}H_{30}BNSi_2W$	$C_{22}H_{48}B_2N_2Si_4W$	$C_{15}H_{21}Cl_4Ga_2MnO_4$
Formula weight ($g \cdot mol^{-1}$)	487.25	462.80	601.50
Temperature (K)	100(2)	296(2)	117(2)
Radiation, λ (Å)	$Mo_{K\alpha}$ 0.71073	$Mo_{K\alpha}$ 0.71073	$Mo_{K\alpha}$ 0.71073
Crystal system	Triclinic	Monoclinic	Monoclinic
Space group	$P\ \bar{1}$	$P2_1/n$	$P2_1$
a (Å)	9.1544(9)	12.0424(6)	7.971(2)
b (Å)	13.250(2)	8.8836(5)	16.389(4)
c (Å)	17.443(3)	31.4360(15)	8.2515(18)
α (°)	99.524(8)	90	90
β (°)	102.213(5)	90.468(3)	93.405(12)
γ (°)	106.236(4)	90	90
Volume ($Å^3$)	1927.7(5)	3362.9(3)	1076.0(4)
Z	4	6	2
Calculated density ($Mg \cdot m^{-3}$)	1.679	1.371	1.857
Absorbtion coefficient (mm^{-1})	6.111	3.593	3.578
F(000)	960	1419	596
Theta range for collection	2.281 to 26.371°	1.296 to 26.021°	2.768 to 26.372°
Reflections collected	7942	118525	4295
Independent reflections	7942	6624	4295
Minimum/maximum transmission	0.640151/0.709053	0.5811/0.7455	0.624342/0.745431
Refinement method	Full-matrix least-squares on F^2	Full-matrix least-squares on F^2	Full-matrix least-squares on F^2
Data / parameters / restrains	7942 / 406 / 138	6624 / 354 / 23	4295 / 284 / 328
Goodness-of-fit on F^2	1.079	1.061	1.099
Final R indices [I>2σ(I)]	$R_1 = 0.0347$, $wR^2 = 0.0526$	$R_1 = 0.0220$, $wR^2 = 0.0470$	$R_1 = 0.0384$, $wR^2 = 0.0819$
R indices (all data)	$R_1 = 0.0495$, $wR^2 = 0.0577$	$R_1 = 0.0266$, $wR^2 = 0.0484$	$R_1 = 0.0445$, $wR^2 = 0.0857$
Maximum/minimum residual electron density ($e \cdot Å^{-3}$)	0.927 / –1.029	0.772 / –1.026	0.734 / –0.645

Table 8. Crystal data and parameters for compounds **119**, **120** and **121**.

	119	**120**	**121**
Empirical formula	$C_{17}H_{33}Cl_4Ga_2MnO_3P_2$	$C_{15}H_{25}Cl_4Ga_2MnO_4$	$C_{30}H_{34}Br_4In_2MnN_4O_2$
Formula weight ($g \cdot mol^{-1}$)	683.55	605.53	1086.83
Temperature (K)	100(2)	100(2)	100(2)
Radiation, λ (Å)	$Mo_{K\alpha}$ 0.71073	$Mo_{K\alpha}$ 0.71073	$Mo_{K\alpha}$ 0.71073
Crystal system	Monoclinic	Triclinic	Triclinic
Space group	$P2_1/n$	$P\bar{1}$	$P\bar{1}$
a (Å)	7.049(3)	7.4300(15)	8.6796(18)
b (Å)	32.121(8)	11.467(2)	13.914(4)
c (Å)	12.311(5)	13.647(2)	16.350(5)
α (°)	90	77.701(8)	105.98(2)
β (°)	94.132(19)	84.818(12)	102.202(11)
γ (°)	90	83.861(8)	99.214(12)
Volume ($Å^3$)	2780.2(18)	1126.7(4)	1804.7(9)
Z	4	2	2
Calculated density ($Mg \cdot m^{-3}$)	1.633	1.785	2.000
Absorbtion coefficient (mm^{-1})	2.887	3.417	6.072
F(000)	1376	604	1042
Theta range for collection	2.524 to 26.372°	2.612 to 26.021°	2.368 to 26.372°
Reflections collected	54330	43540	64515
Independent reflections	5686	4428	7363
Minimum/maximum transmission	0.5973/0.7457	0.5627/0.7457	0.5676/0.7456
Refinement method	Full-matrix least-squares on F^2	Full-matrix least-squares on F^2	Full-matrix least-squares on F^2
Data / parameters / restrains	5686 / 308 / 162	4428 / 239 / 0	7363 / 380 / 0
Goodness-of-fit on F^2	1.068	1.074	1.056
Final R indices [I>2σ(I)]	$R_1 = 0.0312$, $wR^2 = 0.0636$	$R_1 = 0.0148$, $wR^2 = 0.0375$	$R_1 = 0.0254$, $wR^2 = 0.0683$
R indices (all data)	$R_1 = 0.0434$, $wR^2 = 0.0670$	$R_1 = 0.0155$, $wR^2 = 0.0378$	$R_1 = 0.0328$, $wR^2 = 0.0722$
Maximum/minimum residual electron density ($e \cdot Å^{-3}$)	0.499 / –0.590	0.362 / –0.245	1.262 / –0.662

Table 9. Crystal data and parameters for compounds **107b**.

	107b
Empirical formula	$C_{33}H_{42}B_2N_2Se_2$
Formula weight ($g \cdot mol^{-1}$)	646.22
Temperature (K)	100(2)
Radiation, λ (Å)	$Mo_{K\alpha}$ 0.71073
Crystal system	Monoclinic
Space group	$P2_1/n$
a (Å)	12.9542(7)
b (Å)	12.1291(7)
c (Å)	20.4231(10)
α (°)	90
β (°)	90.590(2)
γ (°)	90
Volume ($Å^3$)	3208.8(3)
Z	4
Calculated density ($Mg \cdot m^{-3}$)	1.338
Absorbtion coefficient (mm^{-1})	2.328
F(000)	1328
Theta range for collection	2.501 to 25.681°
Reflections collected	43396
Independent reflections	6084
Minimum/maximum transmission	0.6010/0.7456
Refinement method	Full-matrix least-squares on F^2
Data / parameters / restrains	6084 / 363 / 0
Goodness-of-fit on F^2	1.018
Final R indices [I>2σ(I)]	R_1 = 0.0384, wR^2 = 0.0731
R indices (all data)	R_1 = 0.0792, wR^2 = 0.0858
Maximum/minimum residual electron density ($e \cdot Å^{-3}$)	0.587 / –0.509

7. **Bibliography**

Uncategorized References

[1] R. Thompson, in: R.J. Brotherton, H. Steinberg (Eds.), *Progress in Boron Chemistry*, Pergamon, Oxford, **1970**, 173–230.

[2] H. Nöth, G. Schmid, *Angew. Chem. Int. Ed. Engl.* **1963**, *2*, 623-623.

[3] R. T. Baker, D. W. Ovenall, J. C. Calabrese, S. A. Westcott, N. J. Taylor, I. D. Williams, T. B. Marder, *J. Am. Chem. Soc.* **1990**, *112*, 9399-9400.

[4] J. R. Knorr, J. S. Merola, *Organometallics* **1990**, *9*, 3008-3010.

[5] K. Burgess, M. J. Ohlmeyer, *Chem. Rev.* **1991**, *91*, 1179-1191.

[6] D. Männig, H. Nöth, *Angew. Chem. Int. Ed. Engl.* **1985**, *24*, 878-879.

[7] H. Wadepohl, *Angew. Chem. Int. Ed. Engl.* **1997**, *36*, 2441-2444.

[8] I. Beletskaya, A. Pelter, *Tetrahedron* **1997**, *53*, 4957-5026.

[9] H. Chen, S. Schlecht, T. C. Semple, J. F. Hartwig, *Science* **2000**, *287*, 1995-1997.

[10] J.-Y. Cho, M. K. Tse, D. Holmes, R. E. Maleczka, M. R. Smith, *Science* **2002**, *295*, 305-308.

[11] G. A. Chotana, M. A. Rak, M. R. Smith, *J. Am. Chem. Soc.* **2005**, *127*, 10539-10544.

[12] D. N. Coventry, A. S. Batsanov, A. E. Goeta, J. A. Howard, T. B. Marder, R. N. Perutz, *Chem. Commun.* **2005**, 2172-2174.

[13] C. M. Crudden, D. Edwards, *Eur. J. Org. Chem.* **2003**, *2003*, 4695-4712.

[14] J. F. Hartwig, K. S. Cook, M. Hapke, C. D. Incarvito, Y. Fan, C. E. Webster, M. B. Hall, *J. Am. Chem. Soc.* **2005**, *127*, 2538-2552.

[15] T. Ishiyama, N. Miyaura, *J. Synth. Org. Chem Jpn.* **1999**, *57*, 503-511.

[16] T. Ishiyama, N. Miyaura, *J. Organomet. Chem.* **2000**, *611*, 392-402.

[17] T. Ishiyama, N. Miyaura, *J. Organomet. Chem.* **2003**, *680*, 3-11.

[18] T. B. Marder, N. C. Norman, *Top. Catal.* **1998**, *5*, 63-73.

[19] I. A. Mkhalid, D. N. Coventry, D. Albesa-Jove, A. S. Batsanov, J. A. Howard, R. N. Perutz, T. B. Marder, *Angew. Chem. Int. Ed.* **2006**, *45*, 489-491.

[20] D. W. Stephan, *Org. Biomol. Chem.* **2008**, *6*, 1535-1539.

[21] D. W. Stephan, *Dalton Trans.* **2009**, 3129-3136.

[22] D. W. Stephan, G. Erker, *Angew. Chem. Int. Ed.* **2010**, *49*, 46-76.

[23] H. Braunschweig, T. Herbst, D. Rais, F. Seeler, *Angew. Chem. Int. Ed.* **2005**, *44*, 7461-7463.

[24] C. D. Entwistle, T. B. Marder, *Angew. Chem. Int. Ed.* **2002**, *41*, 2927-2931.

[25] C. D. Entwistle, T. B. Marder, *Chem. Mater.* **2004**, *16*, 4574-4585.

[26] H. Braunschweig, C. Kollann, D. Rais, *Angew. Chem. Int. Ed.* **2006**, *45*, 5254-5274.

[27] G. Bouhadir, A. Amgoune, D. Bourissou, *Adv. Organomet. Chem.,* **2010**, *58*, 1-107.

[28] H. Braunschweig, R. D. Dewhurst, *Dalton Trans.* **2011**, *40*, 549-558.

[29] J. Bauer, H. Braunschweig, R. D. Dewhurst, K. Radacki, *Chem. Eur. J.* **2013**, *19*, 8797-8805.

[30] S. Aldridge, D. L. Coombs, *Coord. Chem. Rev.* **2004**, *248*, 535-559.

[31] G. J. Irvine, M. G. Lesley, T. B. Marder, N. C. Norman, C. R. Rice, E. G. Robins, W. R. Roper, G. R. Whittell, L. J. Wright, *Chem. Rev.* **1998**, *98*, 2685-2722.

[32] H. Braunschweig, *Adv. Organomet. Chem.* **2004**, *51*, 163-192.

[33] H. Braunschweig, R. D. Dewhurst, V. H. Gessner, *Chem. Soc. Rev.* **2013**, *42*, 3197-3208.

[34] H. Braunschweig, C. Kollann, F. Seeler, *Struct. Bond.* **2008**, *130*, 1–27.

[35] H. Braunschweig, D. Rais, *Heteroat. Chem.* **2005**, *16*, 566-571.

[36] D. Vidovic, G. A. Pierce, S. Aldridge, *Chem. Commun.* **2009**, 1157-1171.

[37] C. Boehme, J. Uddin, G. Frenking, *Coord. Chem. Rev.* **2000**, *197*, 249-276.

[38] Y. Chen, G. Frenking, *J. Chem. Soc., Dalton Trans.* **2001**, 434-440.

[39] A. W. Ehlers, E. J. Baerends, F. M. Bickelhaupt, U. Radius, *Chem. Eur. J.* **1998**, *4*, 210-221.

[40] C. L. Macdonald, A. H. Cowley, *J. Am. Chem. Soc.* **1999**, *121*, 12113-12126.

[41] K. K. Pandey, D. G. Musaev, *Organometallics* **2009**, *29*, 142-148.

[42] U. Radius, F. M. Bickelhaupt, A. W. Ehlers, N. Goldberg, R. Hoffmann, *Inorg. Chem.* **1998**, *37*, 1080-1090.

[43] J. Uddin, C. Boehme, G. Frenking, *Organometallics* **2000**, *19*, 571-582.

[44] J. Uddin, G. Frenking, *J. Am. Chem. Soc.* **2001**, *123*, 1683-1693.

[45] B. Wrackmeyer, *Angew. Chem. Int. Ed.* **1999**, *38*, 771-772.

[46] L. Xu, Q. Li, Y. Xie, R. B. King, H. F. Schaefer III, *Inorg. Chem.* **2009**, *49*, 1046-1055.

[47] D. Shriver, *J. Am. Chem. Soc.* **1963**, *85*, 3509-3510.

[48] H. Wang, J. Zhang, H. Hu, C. Cui, *J. Am. Chem. Soc.* **2010**, *132*, 10998-10999.

[49] H. Braunschweig, C. Kollann, *Z. Naturforsch. B* **1999**, *54*, 839-842.

[50] H. Braunschweig, T. Wagner, *Chem. Ber.* **1994**, *127*, 1613-1614.

[51] H. Braunschweig, T. Wagner, *Z. Naturforsch. B* **1996**, *51*, 1618-1620.

[52] G. Parshall, *J. Am. Chem. Soc.* **1964**, *86*, 361-364.

[53] J. Grobe, R. Martin, *Z. Anorg. Allg. Chem.* **1992**, *607*, 146-152.

[54] A. F. Hill, G. R. Owen, A. J. White, D. J. Williams, *Angew. Chem. Int. Ed.* **1999**, *38*, 2759-2761.

[55] M. R. S. Foreman, A. F. Hill, P. White, D. J. Williams, *Organometallics* **2004**, *23*, 913-916.

[56] H. Braunschweig, R. D. Dewhurst, A. Schneider, *Chem. Rev.* **2010**, *110*, 3924-3957.

[57] M. Sircoglou, S. Bontemps, G. Bouhadir, N. Saffon, K. Miqueu, W. Gu, M. Mercy, C.-H. Chen, B. M. Foxman, L. Maron, *J. Am. Chem. Soc.* **2008**, *130*, 16729-16738.

[58] D. J. Mihalcik, J. L. White, J. M. Tanski, L. N. Zakharov, G. P. A. Yap, C. D. Incarvito, A. L. Rheingold, D. Rabinovich, *Dalton Trans.* **2004**, 1626-1634.

[59] I. R. Crossley, M. R. S.-J. Foreman, A. F. Hill, A. J. P. White, D. J. Williams, *Chem. Commun.* **2005**, 221-223.

[60] I. R. Crossley, A. F. Hill, A. C. Willis, *Organometallics* **2005**, *24*, 1062-1064.

[61] H. Braunschweig, K. Radacki, F. Seeler, G. R. Whittell, *Organometallics* **2004**, *23*, 4178-4180.

[62] H. Braunschweig, K. Radacki, F. Seeler, G. R. Whittell, *Organometallics* **2006**, *25*, 4605-4610.

[63] C. Dai, G. Stringer, J. F. Corrigan, N. J. Taylor, T. B. Marder, N. C. Norman, *J. Organomet. Chem.* **1996**, *513*, 273-275.

[64] J. F. Hartwig, X. He, *Organometallics* **1996**, *15*, 5350-5358.

[65] J. F. Hartwig, X. He, *Angew. Chem. Int. Ed. Engl.* **1996**, *35*, 315-317.

[66] J. F. Hartwig, C. N. Muhoro, X. He, O. Eisenstein, R. Bosque, F. Maseras, *J. Am. Chem. Soc.* **1996**, *118*, 10936-10937.

[67] S.-Y. Onozawa, Y. Hatanaka, T. Sakakura, S. Shimada, M. Tanaka, *Organometallics* **1996**, *15*, 5450-5452.

[68] G. Schmid, W. Petz, W. Arloth, H. Nöth, *Angew. Chem. Int. Ed. Engl.* **1967**, *6*, 696-697.

[69] Y. Segawa, Y. Suzuki, M. Yamashita, K. Nozaki, *J. Am. Chem. Soc.* **2008**, *130*, 16069-16079.

[70] Y. Segawa, M. Yamashita, K. Nozaki, *Science* **2006**, *314*, 113-115.

[71] M. Yamashita, Y. Suzuki, Y. Segawa, K. Nozaki, *J. Am. Chem. Soc.* **2007**, *129*, 9570-9571.

[72] T. Kajiwara, T. Terabayashi, M. Yamashita, K. Nozaki, *Angew. Chem. Int. Ed.* **2008**, *47*, 6606-6610.

[73] Y. Segawa, M. Yamashita, K. Nozaki, *Angew. Chem. Int. Ed.* **2007**, *46*, 6710-6713.

[74] T. Terabayashi, T. Kajiwara, M. Yamashita, K. Nozaki, *J. Am. Chem. Soc.*

2009, *131*, 14162-14163.

[75] S. Bertsch, J. Brand, H. Braunschweig, F. Hupp, K. Radacki, *Chem. Eur. J.* **2015**, *21*, 6278-6285.

[76] J. Brand, H. Braunschweig, R. D. Dewhurst, F. Hupp, K. Lang, *Eur. J. Inorg. Chem.* **2015**, *2015*, 2592-2595.

[77] J. Brand, H. Braunschweig, F. Hupp, A. K. Phukan, K. Radacki, S. S. Sen, *Angew. Chem. Int. Ed.* **2014**, *53*, 2240-2244.

[78] H. Braunschweig, K. Radacki, D. Rais, K. Uttinger, *Angew. Chem. Int. Ed.* **2006**, *45*, 162-165.

[79] H. Braunschweig, K. Radacki, A. Schneider, *Science* **2010**, *328*, 345-347.

[80] C. J. Adams, R. A. Baber, A. S. Batsanov, G. Bramham, J. P. H. Charmant, M. F. Haddow, J. A. K. Howard, W. H. Lam, Z. Lin, T. B. Marder, N. C. Norman, A. G. Orpen, *Dalton Trans.* **2006**, 1370-1373.

[81] T. Ishiyama, N. Matsuda, M. Murata, F. Ozawa, A. Suzuki, N. Miyaura, *Organometallics* **1996**, *15*, 713-720.

[82] D. Bourissou, O. Guerret, F. P. Gabbai, G. Bertrand, *Chem. Rev.* **2000**, *100*, 39-92.

[83] P. Timms, *J. Am. Chem. Soc.* **1967**, *89*, 1629-1632.

[84] M. Soleilhavoup, G. Bertrand, *Angew. Chem. Int. Ed.* **2017**, *56*, 10282-10292.

[85] M. Krasowska, H. F. Bettinger, *J. Am. Chem. Soc.* **2012**, *134*, 17094-17103.

[86] M. Krasowska, M. Edelmann, H. F. Bettinger, *J. Phys. Chem. A* **2016**, *120*, 6332-6341.

[87] M. Nomoto, T. Okabayashi, T. Klaus, M. Tanimoto, *J. Mol. Struct.* **1997**, *413-414*, 471-476.

[88] P. L. Timms, *Acc. Chem. Res.* **1973**, *6*, 118-123.

[89] L. Andrews, P. Hassanzadeh, J. M. L. Martin, P. R. Taylor, *J. Phys. Chem.* **1993**, *97*, 5839-5847.

[90] H. F. Bettinger, *J. Am. Chem. Soc.* **2006**, *128*, 2534-2535.

[91] C. A. Thompson, L. Andrews, J. M. L. Martin, J. El-Yazal, *J. Phys. Chem.* **1995**, *99*, 13839-13849.

[92] W. J. Grigsby, P. P. Power, *J. Am. Chem. Soc.* **1996**, *118*, 7981-7988.

[93] A. Meller, D. Bromm, W. Maringgele, D. Böhler, G. Elter, *J. Organomet. Chem.* **1988**, *347*, 11-16.

[94] A. Meller, U. Seebold, W. Maringgele, M. Noltemeyer, G. M. Sheldrick, *J. Am. Chem. Soc.* **1989**, *111*, 8299-8300.

[95] B. Pachaly, R. West, *Angew. Chem. Int. Ed. Engl.* **1984**, *23*, 454-455.

[96] F. Dahcheh, D. Martin, D. W. Stephan, G. Bertrand, *Angew. Chem. Int. Ed.* **2014**, *53*, 13159-13163.

[97] A. D. Ledet, T. W. Hudnall, *Dalton Trans.* **2016**, *45*, 9820-9826.

[98] M. Arrowsmith, D. Auerhammer, R. Bertermann, H. Braunschweig, G. Bringmann, M. A. Celik, R. D. Dewhurst, M. Finze, M. Grüne, M. Hailmann, T. Hertle, I. Krummenacher, *Angew. Chem. Int. Ed.* **2016**, *55*, 14464-14468.

[99] H. Braunschweig, M. A. Celik, R. D. Dewhurst, K. Ferkinghoff, A. Hermann, J. O. C. Jimenez-Halla, T. Kramer, K. Radacki, R. Shang, E. Siedler, F. Weißenberger, C. Werner, *Chem. Eur. J.* **2016**, *22*, 11736-11744.

[100] H. Braunschweig, R. D. Dewhurst, F. Hupp, M. Nutz, K. Radacki, C. W. Tate, A. Vargas, Q. Ye, *Nature* **2015**, *522*, 327-330.

[101] R. Kinjo, B. Donnadieu, M. A. Celik, G. Frenking, G. Bertrand, *Science* **2011**, *333*, 610-613.

[102] D. A. Ruiz, M. Melaimi, G. Bertrand, *Chem. Commun.* **2014**, *50*, 7837-7839.

[103] H. Wang, J. Zhang, Z. Lin, Z. Xie, *Chem. Commun.* **2015**, *51*, 16817-16820.

[104] B. Blank, M. Colling-Hendelkens, C. Kollann, K. Radacki, D. Rais, K. Uttinger, G. R. Whittell, H. Braunschweig, *Chem. Eur. J.* **2007**, *13*, 4770-4781.

[105] H. Braunschweig, R. D. Dewhurst, C. Hörl, K. Radacki, C. W. Tate, A. Vargas, Q. Ye, *Angew. Chem. Int. Ed.* **2013**, *52*, 10120-10123.

[106] H. Braunschweig, C. Kollann, U. Englert, *Angew. Chem. Int. Ed.* **1998**, *37*, 3179-3180.

[107] H. Braunschweig, T. Wagner, *Angew. Chem. Int. Ed. Engl.* **1995**, *34*, 825-826.

[108] A. H. Cowley, V. Lomelí, A. Voigt, *J. Am. Chem. Soc.* **1998**, *120*, 6401-6402.

[109] M. J. Drance, J. D. Sears, A. M. Mrse, C. E. Moore, A. L. Rheingold, M. L. Neidig, J. S. Figueroa, *Science* **2019**, *363*, 1203-1205.

[110] K. K. Pandey, H. Braunschweig, A. Lledós, *Inorg. Chem.* **2011**, *50*, 1402-1410.

[111] K. K. Pandey, A. Lledós, F. Maseras, *Organometallics* **2009**, *28*, 6442-6449.

[112] H. Braunschweig, Q. Ye, K. Radacki, *Chem. Commun.* **2012**, *48*, 2701-2703.

[113] M. Nutz, B. Borthakur, C. Pranckevicius, R. D. Dewhurst, M. Schäfer, T. Dellermann, F. Glaab, M. Thaler, A. K. Phukan, H. Braunschweig, *Chem. Eur. J.* **2018**, *24*, 6843-6847.

[114] C. Pranckevicius, J. O. C. Jimenéz-Halla, M. Kirsch, I. Krummenacher, H. Braunschweig, *J. Am. Chem. Soc.* **2018**, *140*, 10524-10529.

[115] H. Braunschweig, M. Colling, C. Hu, K. Radacki, *Angew. Chem. Int. Ed.* **2003**, *42*, 205-208.

[116] H. Braunschweig, M. Colling, C. Kollann, H. G. Stammler, B. Neumann, *Angew. Chem. Int. Ed.* **2001**, *40*, 2298-2300.

[117] H. Braunschweig, M. Forster, T. Kupfer, F. Seeler, *Angew. Chem. Int. Ed.* **2008**,

47, 5981-5983.

[118] H. Braunschweig, M. Forster, K. Radacki, F. Seeler, G. R. Whittell, *Angew. Chem. Int. Ed.* **2007**, *46*, 5212-5214.

[119] H. Braunschweig, M. Forster, F. Seeler, *Chem. Eur. J.* **2009**, *15*, 469-473.

[120] S. Bertsch, H. Braunschweig, B. Christ, M. Forster, K. Schwab, K. Radacki, *Angew. Chem. Int. Ed.* **2010**, *49*, 9517-9520.

[121] H. Braunschweig, Q. Ye, A. Vargas, R. D. Dewhurst, K. Radacki, A. Damme, *Nat. Chem.* **2012**, *4*, 563-567.

[122] D. L. Coombs, S. Aldridge, C. Jones, D. J. Willock, *J. Am. Chem. Soc.* **2003**, *125*, 6356-6357.

[123] D. L. Coombs, S. Aldridge, A. Rossin, C. Jones, D. J. Willock, *Organometallics* **2004**, *23*, 2911-2926.

[124] D. L. Kays, J. K. Day, L. L. Ooi, S. Aldridge, *Angew. Chem. Int. Ed.* **2005**, *44*, 7457-7460.

[125] G. A. Pierce, D. Vidovic, D. L. Kays, N. D. Coombs, A. L. Thompson, E. D. Jemmis, S. De, S. Aldridge, *Organometallics* **2009**, *28*, 2947-2960.

[126] H. Braunschweig, K. Radacki, D. Rais, D. Scheschkewitz, *Angew. Chem. Int. Ed.* **2005**, *44*, 5651-5654.

[127] H. Braunschweig, K. Radacki, K. Uttinger, *Organometallics* **2008**, *27*, 6005-6012.

[128] H. Braunschweig, K. Radacki, K. Uttinger, *Angew. Chem. Int. Ed.* **2007**, *46*, 3979-3982.

[129] G. Alcaraz, U. Helmstedt, E. Clot, L. Vendier, S. Sabo-Etienne, *J. Am. Chem. Soc.* **2008**, *130*, 12878-12879.

[130] H. Braunschweig, M. A. Celik, R. D. Dewhurst, K. Ferkinghoff, K. Radacki, F. Weißenberger, *Chem. Eur. J.* **2016**, *22*, 8596-8602.

[131] H. Braunschweig, A. Damme, R. D. Dewhurst, H. Kelch, B. B. Macha, K. Radacki, A. Vargas, Q. Ye, *Chem. Eur. J.* **2015**, *21*, 2377-2386.

[132] H. Braunschweig, T. Herbst, D. Rais, S. Ghosh, T. Kupfer, K. Radacki, A. G. Crawford, R. M. Ward, T. B. Marder, I. Fernández, *J. Am. Chem. Soc.* **2009**, *131*, 8989-8999.

[133] H. Braunschweig, Q. Ye, K. Radacki, *Chem. Commun.* **2009**, 6979-6981.

[134] H. Braunschweig, Q. Ye, K. Radacki, T. Kupfer, *Dalton Trans.* **2011**, *40*, 3666-3670.

[135] N. L. Allinger, J. H. Siefert, *J. Am. Chem. Soc.* **1975**, *97*, 752-760.

[136] J. J. Eisch, B. Shafii, A. L. Rheingold, *J. Am. Chem. Soc.* **1987**, *109*, 2526-2528.

[137] C. Habben, A. Meller, *Chem. Ber.* **1984**, *117*, 2531-2537.

[138] C. Pues, A. Berndt, *Angew. Chem. Int. Ed. Engl.* **1984**, *23*, 313-314.
[139] P. Timms, *J. Am. Chem. Soc.* **1968**, *90*, 4585-4589.
[140] J. Bauer, H. Braunschweig, A. Damme, J. O. C. Jimenez-Halla, T. Kramer, K. Radacki, R. Shang, E. Siedler, Q. Ye, *J. Am. Chem. Soc.* **2013**, *135*, 8726-8734.
[141] H. Braunschweig, M. Burzler, K. Radacki, F. Seeler, *Angew. Chem. Int. Ed.* **2007**, *46*, 8071-8073.
[142] H. Braunschweig, K. Radacki, R. Shang, C. W. Tate, *Angew. Chem. Int. Ed.* **2013**, *52*, 729-733.
[143] M. Nutz, B. Borthakur, R. D. Dewhurst, A. Deißenberger, T. Dellermann, M. Schäfer, I. Krummenacher, A. K. Phukan, H. Braunschweig, *Angew. Chem. Int. Ed.* **2017**, *56*, 7975-7979.
[144] F. R. Kreißl, K. Eberl, W. Uedelhoven, *Chem. Ber.* **1977**, *110*, 3782-3791.
[145] H. Braunschweig, T. Kramer, K. Radacki, R. Shang, E. Siedler, C. Werner, *Chem. Sci.* **2014**, *5*, 2271-2276.
[146] H. Braunschweig, Q. Ye, A. Vargas, K. Radacki, A. Damme, *Angew. Chem. Int. Ed.* **2013**, *52*, 10657-10660.
[147] H. Braunschweig, I. Krummenacher, M.-A. Légaré, A. Matler, K. Radacki, Q. Ye, *J. Am. Chem. Soc.* **2017**, *139*, 1802-1805.
[148] I. A. Mkhalid, J. H. Barnard, T. B. Marder, J. M. Murphy, J. F. Hartwig, *Chem. Rev.* **2009**, *110*, 890-931.
[149] H. Braunschweig, R. D. Dewhurst, T. Herbst, K. Radacki, *Angew. Chem. Int. Ed.* **2008**, *47*, 5978-5980.
[150] H. Braunschweig, Q. Ye, A. Damme, T. Kupfer, K. Radacki, J. Wolf, *Angew. Chem. Int. Ed.* **2011**, *50*, 9462-9466.
[151] H. Braunschweig, J. O. C. Jimenez-Halla, K. Radacki, R. Shang, *Chem. Commun.* **2015**, *51*, 16569-16572.
[152] H. Braunschweig, M. A. Celik, R. D. Dewhurst, S. Kachel, B. Wennemann, *Angew. Chem. Int. Ed.* **2016**, *55*, 5076-5080.
[153] H. R. Snyder, J. A. Kuck, J. R. Johnson, *J. Am. Chem. Soc.* **1938**, *60*, 105-111.
[154] M. A. Mehta, T. Fujinami, *Chem. Lett.* **1997**, *26*, 915-916.
[155] M. A. Mehta, T. Fujinami, *Solid State Ionics* **1998**, *113*, 187-192.
[156] M. A. Mehta, T. Fujinami, S. Inoue, K. Matsushita, T. Miwa, T. Inoue, *Electrochim. Acta* **2000**, *45*, 1175-1180.
[157] V. Benin, S. Durganala, A. B. Morgan, *J. Mater. Chem.* **2012**, *22*, 1180-1190.
[158] A. B. Morgan, J. L. Jurs, J. M. Tour, *J. Appl. Polym. Sci.* **2000**, *76*, 1257-1268.
[159] A. P. Cote, A. I. Benin, N. W. Ockwig, M. O'keeffe, A. J. Matzger, O. M. Yaghi, *Science* **2005**, *310*, 1166-1170.

[160] S. Chandra, S. Kandambeth, B. P. Biswal, B. Lukose, S. M. Kunjir, M. Chaudhary, R. Babarao, T. Heine, R. Banerjee, *J. Am. Chem. Soc.* **2013**, *135*, 17853-17861.
[161] M. Schmidt, W. Siebert, *Angew. Chem. Int. Ed. Engl.* **1964**, *3*, 637-638.
[162] H. Nöth, W. Rattay, *J. Organomet. Chem.* **1986**, *312*, 139-148.
[163] D. Auerhammer, M. Arrowsmith, R. D. Dewhurst, T. Kupfer, J. Böhnke, H. Braunschweig, *Chem. Sci.* **2018**, *9*, 2252-2260.
[164] R. Curci, L. D'Accolti, C. Fusco, *Acc. Chem. Res.* **2006**, *39*, 1-9.
[165] A. Greer, *Science* **2003**, *302*, 235-236.
[166] A. Ishii, M. Hoshino, J. Nakayama, *Pure Appl. Chem.* **1996**, *68*, 869-874.
[167] D. G. Ho, R. Gao, J. Celaje, H.-Y. Chung, M. Selke, *Science* **2003**, *302*, 259-262.
[168] Y. Xiong, S. Yao, R. Müller, M. Kaupp, M. Driess, *Nat. Chem.* **2010**, *2*, 577-580.
[169] P. Chen, C. Cui, *Chem. Eur. J.* **2016**, *22*, 2902-2905.
[170] M. Saito, N. Tokitoh, R. Okazaki, *J. Am. Chem. Soc.* **1997**, *119*, 11124-11125.
[171] D. Franz, S. Inoue, *Dalton Trans.* **2016**, *45*, 9385-9397.
[172] H. Braunschweig, R. Shang, *Inorg. Chem.* **2015**, *54*, 3099-3106.
[173] N. Tokitoh, M. Ito, R. Okazaki, *Tetrahedron Lett.* **1996**, *37*, 5145-5148.
[174] D. Vidovic, J. A. Moore, J. N. Jones, A. H. Cowley, *J. Am. Chem. Soc.* **2005**, *127*, 4566-4567.
[175] Y. Wang, H. Hu, J. Zhang, C. Cui, *Angew. Chem. Int. Ed.* **2011**, *50*, 2816-2819.
[176] M. Ahijado Salomon, T. Braun, A. Penner, *Angew. Chem. Int. Ed.* **2008**, *47*, 8867-8871.
[177] A. Del Grosso, E. R. Clark, N. Montoute, M. J. Ingleson, *Chem. Commun.* **2012**, *48*, 7589-7591.
[178] Y. K. Loh, C. C. Chong, R. Ganguly, Y. Li, D. Vidovic, R. Kinjo, *Chem. Commun.* **2014**, *50*, 8561-8564.
[179] T. Miyada, M. Yamashita, *Organometallics* **2013**, *32*, 5281-5284.
[180] A. Solovyev, S. J. Geib, E. Lacôte, D. P. Curran, *Organometallics* **2011**, *31*, 54-56.
[181] Y. Wang, M. Y. Abraham, R. J. Gilliard Jr, D. R. Sexton, P. Wei, G. H. Robinson, *Organometallics* **2013**, *32*, 6639-6642.
[182] W. Kaim, *Chem. Ber.* **1981**, *114*, 3789-3800.
[183] S. M. Mansell, C. J. Adams, G. Bramham, M. F. Haddow, W. Kaim, N. C. Norman, J. E. McGrady, C. A. Russell, S. J. Udeen, *Chem. Commun.* **2010**, *46*, 5070-5072.

[184] T. K. Wood, W. E. Piers, B. A. Keay, M. Parvez, *Chem. Commun.* **2009**, 5147-5149.

[185] S. M. Mansell, N. C. Norman, C. A. Russell, *Dalton Trans.* **2010**, *39*, 5084-5086.

[186] M. Alibadi, A. Batsanov, G. Bramham, J. Charmant, M. Haddow, L. MacKay, S. Mansell, J. McGrady, N. Norman, A. Roffey, *Dalton Trans.* **2009**, 5348-5354.

[187] P. v. R. Schleyer, C. Maerker, A. Dransfeld, H. Jiao, N. J. v. E. Hommes, *J. Am. Chem. Soc.* **1996**, *118*, 6317-6318.

[188] F. E. Kühn, M. Groarke, É. Bencze, E. Herdtweck, A. Prazeres, A. M. Santos, M. J. Calhorda, C. C. Romão, I. S. Gonçalves, A. D. Lopes, *Chem. Eur. J.* **2002**, *8*, 2370-2383.

[189] C. Kaes, A. Katz, M. W. Hosseini, *Chem. Rev.* **2000**, *100*, 3553-3590.

[190] M. Herberhold, B. Schmidkonz, *J. Organomet. Chem.* **1988**, *358*, 301-320.

[191] H. Braunschweig, T. Dellermann, W. C. Ewing, T. Kramer, C. Schneider, S. Ullrich, *Angew. Chem. Int. Ed.* **2015**, *54*, 10271-10275.

[192] H. Braunschweig, P. Constantinidis, T. Dellermann, W. C. Ewing, I. Fischer, M. Hess, F. R. Knight, A. Rempel, C. Schneider, S. Ullrich, *Angew. Chem. Int. Ed.* **2016**, *55*, 5606-5609.

[193] S. A. Batten, J. C. Jeffery, L. H. Rees, M. D. Rudd, F. G. A. Stone, *J. Chem. Soc., Dalton Trans.* **1998**, 2839-2848.

[194] G. Ferguson, J. D. Kennedy, X. L. R. Fontaine, Faridoon, T. R. Spalding, *J. Chem. Soc., Dalton Trans.* **1988**, 2555-2564.

[195] D. K. Roy, S. K. Bose, K. Geetharani, K. K. Varma Chakrahari, S. M. Mobin, S. Ghosh, *Chem. Eur. J.* **2012**, *18*, 9983-9991.

[196] A. Decker, E. I. Solomon, *Curr. Opin. Chem. Biol.* **2005**, *9*, 152-163.

[197] A. Müller, W. Jaegermann, J. H. Enemark, *Coord. Chem. Rev.* **1982**, *46*, 245-280.

[198] T. Punniyamurthy, S. Velusamy, J. Iqbal, *Chem. Rev.* **2005**, *105*, 2329-2364.

[199] M. Nakamoto, K.-y. Akiba, *J. Am. Chem. Soc.* **1999**, *121*, 6958-6959.

[200] I. V. Skabitskiy, A. A. Pasynskii, S. G. Sakharov, V. A. Grinberg, *Polyhedron* **2014**, *67*, 422-428.

[201] A. Almenningen, H. Seip, P. Vassbotn, *Acta Chem. Scand.* **1973**, *27*, 21-25.

[202] B. Krebs, *Angew. Chem. Int. Ed. Engl.* **1983**, *22*, 113-134.

[203] H. Seip, *Acta Chem. Scand* **1973**, *27*, 21.

[204] D. Männig, C. K. Narula, H. Noeth, U. Wietelmann, *Chem. Ber.* **1985**, 118, 3748-3758

[205] D. H. Harris, S. A. Keppie, M. F. Lappert, *J. Chem. Soc., Dalton Trans.* **1973**,

1653-1658.

[206] J. L. Thomas, *J. Am. Chem. Soc.* **1973**, *95*, 1838-1848.

[207] H. Braunschweig, K. Radacki, R. Shang, *Chem. Commun.* **2013**, *49*, 9905-9907.

[208] H. Braunschweig, Q. Ye, A. Vargas, R. D. Dewhurst, F. Hupp, *J. Am. Chem. Soc.* **2014**, *136*, 9560-9563.

[209] E. Leiner, M. Scheer, *J. Organomet. Chem.* **2002**, *646*, 247-254.

[210] A. H. Cowley, A. Decken, C. A. Olazabal, N. C. Norman, *Inorg. Chem.* **1994**, *33*, 3435-3437.

[211] D. F. Shriver, M. A. Drezdzon, M. A. Drezdzon, *The manipulation of air-sensitive compounds*, John Wiley & Sons, **1986**.

[212] W. L. F. Armarego, C. L. L. Chai, *Purification of laboratory chemicals* **2009**, 577-708.

[213] J.-F. Ayme, J. E. Beves, D. A. Leigh, R. T. McBurney, K. Rissanen, D. Schultz, *Nat. Chem.* **2011**, *4*, 15-20.

[214] M. L. H. Green, J. A. McCleverty, L. Pratt, G. Wilkinson, *J. Chem. Soc.* **1961**, 4854-4859.

[215] M. J. Frisch, G. W. Trucks, H. B. Schlegel, G. E. Scuseria, M. A. Robb, J. R. Cheeseman, G. Scalmani, V. Barone, B. Mennucci, G. A. Petersson, *Wallingford, CT* **2009**, *6492*.

[216] A. D. Becke, *J. Chem. Phys.* **1993**, *98*, 5648-5652.

[217] C. Lee, W. Yang, R. G. Parr, *Phys. Rev. B* **1988**, *37*, 785.

[218] F. Weigend, R. Ahlrichs, *PCCP* **2005**, *7*, 3297-3305.